

# Analytic solutions for flows in non-linear fluids



By

*Khadija Maqbool*

Department of Mathematics  
Quaid-i-Azam University  
Islamabad, Pakistan  
2010

# Analytic solutions for flows in non-linear fluids



By  
Khadija Maqbool

Supervised by  
**Dr. Tasawar Hayat**

**Department of Mathematics**  
**Quaid-i-Azam University**  
**Islamabad, Pakistan**  
**2010**

# **Analytic solutions for flows in non-linear fluids**

By

***Khadija Maqbool***

A Thesis

Submitted in the Partial Fulfillment of the  
Requirements for the Degree of  
**DOCTOR OF PHILOSOPHY**

IN  
**MATHEMATICS**

Supervised By

***Dr. Tasawar Hayat***

**Department of Mathematics  
Quaid-i-Azam University  
Islamabad, Pakistan  
2010**

# CERTIFICATE

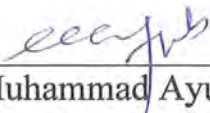
## **Analytic solutions for flows in non-linear fluids**

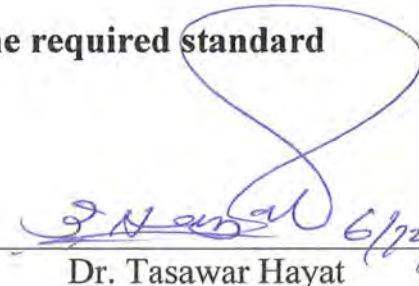
**By**


**Khadija Maqbool**

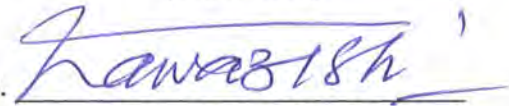
A THESIS SUBMITTED IN THE PARTIAL FULFILLMENT OF THE  
REQUIREMENTS FOR THE DEGREE OF THE DOCTOR OF  
PHILOSOPHY

**We accept this thesis as conforming to the required standard**

1.   
Prof. Dr. Muhammad Ayub  
(Chairman)

2.   
Dr. Tasawar Hayat  
(Supervisor)

3.   
Prof. Dr. Akhtar Hussain  
(External Examiner)

4.   
Prof. Dr. Nawazish Ali Shah  
(External Examiner)

**Department of Mathematics  
Quaid-i-Azam University  
Islamabad, Pakistan  
2010**



Dedicated to my family  
And  
Supervisor Dr. Tasawar Hayat

# Acknowledgement

All praise to Allah the most merciful and most benevolent who gave me knowledge, courage and confidence to accomplish the task.

First of all, I want to express my deepest gratitude to my respectable supervisor Dr. Tasawar Hayat, who guided me throughout this research work. His kind and invaluable guidance, sympathetic, professional attitude, extensive discussions, critical comments and help during my research work, especially during the weekly group meetings of the Fluid Mechanics Group (FMG) provided me with insight. He has the unique credit to keep the research spirit *vibrant* among all research students. He played a pivotal role for the entire group and his dedication and devotion to his work has won many laurels to the department, the University and the beloved homeland, PAKISTAN.

It has been an excellent learning experience for me working under his supervision. It gives me a sense of great honor for being a member of his team. Indeed, it is a matter of pride and privilege for me to be his Ph. D. student.

I am grateful to Prof. Dr. Muhammad Ayub, Chairman Department of Mathematics, Quaid-i-Azam University Islamabad for providing excellent atmosphere of research in the department.

Thanks to all teachers of the department for being a source of inspiration and motivation for me during my stay in the department. Thanks are also due to the staff of Mathematics department for their help and cooperation. At this stage I also want to pay homage to my teachers Ms. Naheed and Nighat who infused me with the spirit to learn Mathematics.

I am very thankful to the Higher Education Commission for providing me the financial support to pursue my studies and research and for the support and facilities provided to the group (FMG) and the department.

Finally, I owe my family, especially my husband and son, a great debt of gratitude for the prayers, sacrifices and efforts. The accomplishment of this task would have never been possible without the help of my seniors Dr. Masood, Dr. Rehmat, Dr. Ambreen and Dr. Rehana. I feel deeply indebted to all of them for their support. Besides these people, my friends, Maryiam, sherish, Raheela, sadia and saima have always been helpful to me. For that I am really obliged to them.

Khadija Maqbool

# Contents

|          |                                                                                  |           |
|----------|----------------------------------------------------------------------------------|-----------|
| <b>1</b> | <b>Introduction</b>                                                              | <b>7</b>  |
| 1.1      | Equations of change . . . . .                                                    | 13        |
| 1.1.1    | Continuity equation . . . . .                                                    | 13        |
| 1.1.2    | Equation of motion . . . . .                                                     | 13        |
| 1.1.3    | Energy equation . . . . .                                                        | 14        |
| 1.2      | Basic Definitions . . . . .                                                      | 15        |
| 1.2.1    | Hall effect . . . . .                                                            | 15        |
| 1.2.2    | Hartman number . . . . .                                                         | 15        |
| 1.2.3    | Reynold number . . . . .                                                         | 15        |
| 1.2.4    | Magnetic Reynold number . . . . .                                                | 15        |
| 1.2.5    | Weissenberg number . . . . .                                                     | 15        |
| 1.2.6    | Relaxation time . . . . .                                                        | 16        |
| 1.2.7    | Retardation time . . . . .                                                       | 16        |
| <b>2</b> | <b>Hall effect on the flows of generalized Oldroyd-B fluid in a porous space</b> | <b>17</b> |
| 2.1      | Mathematical formulation . . . . .                                               | 17        |
| 2.2      | Flows induced by a rigid plate . . . . .                                         | 20        |
| 2.3      | Periodic flows between two plates . . . . .                                      | 24        |
| 2.4      | Poiseuille flow . . . . .                                                        | 25        |
| 2.5      | Analytical results for a Newtonian fluid . . . . .                               | 26        |
| 2.6      | Results and discussion . . . . .                                                 | 26        |

|          |                                                                                                                                                                |            |
|----------|----------------------------------------------------------------------------------------------------------------------------------------------------------------|------------|
| <b>3</b> | <b>Influence of Hall current on the flows in a fractional generalized Burgers' fluid</b>                                                                       | <b>37</b>  |
| 3.1      | Mathematical formulation . . . . .                                                                                                                             | 37         |
| 3.2      | Flow induced by a rigid plate . . . . .                                                                                                                        | 39         |
| 3.3      | Periodic flows between two plates . . . . .                                                                                                                    | 41         |
| 3.4      | Poiseuille flow . . . . .                                                                                                                                      | 42         |
| 3.5      | Results and discussion . . . . .                                                                                                                               | 43         |
| <b>4</b> | <b>The influence of Hall current and heat transfer on the steady flow of a generalized Burgers' fluid induced by a sudden pull of eccentric rotating disks</b> | <b>57</b>  |
| 4.1      | Mathematical formulation . . . . .                                                                                                                             | 58         |
| 4.2      | Exact analytic solution . . . . .                                                                                                                              | 63         |
| 4.3      | Heat transfer analysis . . . . .                                                                                                                               | 64         |
| 4.4      | The force and torque . . . . .                                                                                                                                 | 66         |
| 4.5      | Results and discussion . . . . .                                                                                                                               | 67         |
| <b>5</b> | <b>Effects of Hall current and heat transfer on the steady flow of a fourth grade fluid</b>                                                                    | <b>78</b>  |
| 5.1      | Formulation of the problem . . . . .                                                                                                                           | 78         |
| 5.2      | Analytic solution by homotopy analysis method . . . . .                                                                                                        | 83         |
| 5.2.1    | Zeroth order deformation problem . . . . .                                                                                                                     | 83         |
| 5.2.2    | <i>m</i> th-order deformation equation . . . . .                                                                                                               | 85         |
| 5.3      | Heat transfer analysis . . . . .                                                                                                                               | 88         |
| 5.3.1    | Zeroth and <i>m</i> th order problem . . . . .                                                                                                                 | 88         |
| 5.3.2    | Solution of the <i>m</i> th order problem . . . . .                                                                                                            | 89         |
| 5.4      | Convergence of the homotopy solution . . . . .                                                                                                                 | 90         |
| 5.5      | Numerical results and discussion . . . . .                                                                                                                     | 92         |
| <b>6</b> | <b>Steady flow of a Sisko fluid under the influence of Hall current and heat transfer</b>                                                                      | <b>108</b> |
| 6.1      | Mathematical formulation . . . . .                                                                                                                             | 108        |

|          |                                                                                                                     |            |
|----------|---------------------------------------------------------------------------------------------------------------------|------------|
| 6.2      | Analytic solution by homotopy analysis method (HAM) . . . . .                                                       | 111        |
| 6.3      | Heat transfer analysis . . . . .                                                                                    | 114        |
| 6.4      | Convergence of the solution . . . . .                                                                               | 116        |
| 6.5      | Results and discussion . . . . .                                                                                    | 121        |
| <b>7</b> | <b>Simultaneous effects of heat transfer and Hall current on the flow of a<br/>Johnson-Segalman fluid</b> . . . . . | <b>138</b> |
| 7.1      | Mathematical formulation . . . . .                                                                                  | 138        |
| 7.1.1    | Analytic solution . . . . .                                                                                         | 141        |
| 7.2      | Heat transfer analysis . . . . .                                                                                    | 149        |
| 7.3      | Convergence of the solution . . . . .                                                                               | 152        |
| 7.4      | Results and discussion . . . . .                                                                                    | 154        |
| <b>8</b> | <b>Analytic solution for MHD plane and axisymmetric flow near a stagnation<br/>point</b> . . . . .                  | <b>165</b> |
| 8.1      | Mathematical formulation . . . . .                                                                                  | 166        |
| 8.2      | Solution by homotopy analysis method . . . . .                                                                      | 167        |
| 8.3      | Numerical results . . . . .                                                                                         | 171        |
| <b>9</b> | <b>Series solution for the Falkner Skan flow of the FENE-P model</b> . . . . .                                      | <b>179</b> |
| 9.1      | Mathematical formulation . . . . .                                                                                  | 179        |
| 9.1.1    | Boundary layer equations . . . . .                                                                                  | 182        |
| 9.2      | Crocco's transformation . . . . .                                                                                   | 184        |
| 9.3      | Solution by homotopy analysis method (HAM) . . . . .                                                                | 186        |
| 9.4      | Numerical results . . . . .                                                                                         | 188        |

## Preface

The Navier-Stokes equations govern the flow of a viscous fluid. There have been several fluids including polymer melt, butter, ketchup, shampoo, certain paints, drilling muds, oil and greases, clay coatings and many emulsions which cannot be described as viscous fluids. In fact such fluids have been treated as non-Newtonian fluids. Confusion over the classification of the non-Newtonian fluids stems from the difficulty of single fluid model that displays all characteristics of non-Newtonian fluids. In spite of this, these fluids can be classified into three categories (i) the differential type, (ii) the rate type, and (iii) an integral type. As a consequence of diversity in the physical structure, non-Newtonian fluids do not have a single constitutive equation. Thus many models for these fluids have been proposed and most of them being empirical or semi-empirical. In the case of three dimensional representation, the method of continuum mechanics is required. Many key questions are thus unresolved. Some of the proposed models do not agree with experiments. Hence in practical applications, empirical or semi-empirical equations have been invoked. The relevant constitutive relationships of non - Newtonian fluids give rise equations which in general are of higher order than the Navier-Stokes equations. Further, the usual no-slip boundary condition is enough for the flow in a viscous fluid. However, it may not be sufficient in the flows of non-Newtonian fluid in general. For a unique solution, one needs the extra boundary/initial condition(s).

The second grade fluid model is one of the most popular models. This is so for numerical and analytic computations thus making calculations simpler. This model is utilized to predict the normal stress effects and is incapable of showing shear thickening/shear thinning and relaxation/retardation features. Hence this thesis throws light on the flows of generalized Oldroyd-B, Burgers' and generalized Burgers', fourth grade, Sisko and Johnson-Segalman fluids. The flows of such fluids in porous space have extensive engineering applications. To be more specific, these are encountered in tissue engineering, power technology, petroleum technology etc. Hydromagnetic transport in porous space has been studied a great deal due to its importance in material processing and geophysics. Several complex phenomena are induced by magnetic fields such as Hall current. Influence of such effects on flow dynamics can be significant. In ionized gases, for example, subject to low density and strong magnetic field, the electrical conductivity

perpendicular to the magnetic field is lower due to free spiraling of electrons as well as ions about the magnetic lines of force before collisions. Thereby a current is induced which is perpendicular to the electrical and magnetic fields constituting the Hall current effects. In view of all these facts and paucity of analytic solutions in non-Newtonian fluid dynamics, this thesis runs as follows.

In chapter one survey of the relevant existing literature and basic equations are presented.

Chapter two develops the exact analytic solutions for the magnetohydrodynamic (MHD) flows of an Oldroyd-B fluid in a porous space. The fractional calculus approach is employed to describe the constitutive model of a generalized Oldroyd-B fluid. Modified Darcy's law for generalized Oldroyd-B fluid has been introduced in the mathematical formulation. The effects of Hall current are further considered. The resulting flow problems are solved by Fourier transform for fractional calculus. It is noticed that velocity increases when Hall parameter is increased. In oscillatory flows by a boundary, the velocity profiles in Oldroyd-B fluid are greater than generalized Oldroyd-B fluid when pressure gradient is absent. Such observations have been published in *Acta Mechanica* 184 (2006) 1. In chapter three, we revisit the flow problems for a fractional generalized Burgers' fluid. Comparison between the six cases is presented.

There has been much focus on the heat transfer process in non-Newtonian fluids. This is because of the fact that heat transfer in the boundary layer flows of non-Newtonian fluids is of interest in many engineering applications such as the design of thrust bearings and radial diffusers, transpiration cooling, drag reduction, thermal recovery of oil and many others. Therefore, chapter four is devoted to discuss the steady flow of a Burgers' fluid due to a sudden pull with constant velocities of eccentric rotating infinite disks with constant angular velocity. Symmetry condition is invoked. The Burgers' fluid can describe the response of materials such as asphalt that is very common in geomechanics, food product such as cheese, soil etc. The fluid is magnetohydrodynamic (MHD) in the presence of a constant magnetic field. The effect of Hall current is taken into account. Computations are carried out for velocity, temperature and torque. It is found that temperature in Burgers' fluid is less when compared with a generalized Burgers' fluid. Both velocity and temperature increase when Hall parameter increases. These results are published in *Nonlinear Dynamics* 51 (2008) 267.

Chapters five to seven look at the flow analysis of chapter four for fourth grade, Sisko



and Johnson-Segalman fluids respectively. The relevant equations are modelled and the effects of rheological parameters are particularly analyzed. Unlike the previous chapter, the series solution in these chapters has been developed by using the homotopy analysis method (HAM). Convergence of the constructed series solutions is shown explicitly. The observations of chapters five and six are accepted for publication in “**Numerical Methods for Partial Differential Equations**” and “**Zeitschrift für Naturforschung A**”, respectively. The findings of chapter seven are submitted for publication in “**Comm. Nolinear Sci. Numerical Simulation**”.

Chapter eight presents homotopy solution of a stagnation point flow problem describing the phenomena of heat and mass transfer in a viscous fluid. The fluid is conducted in the presence of a uniform applied magnetic field. The resulting partial differential equations are reduced to the ordinary differential equations. These ordinary differential equations are solved analytically. Graphs depicting the variations of pertinent parameters are made and discussed. The results of this chapter are accepted for publication in “**Comm. Nolinear Sci. Numerical Simulation**”.

Chapter nine aims to examine the boundary layer flow of a FENE-P fluid past a plate. No pressure gradient is taken into account. Crocco’s transformation has been utilized. Mathematical formulation yields a nonlinear problem which is solved by a homotopy analysis method (HAM). The skin friction coefficient is tabulated. A comparative study is made between the numerical and homotopy solutions. The conclusions of this chapter are accepted for publication in “**Int. J. Numerical Methods in fluids**”.



# Chapter 1

## Introduction

Many researchers have discussed the flow of an incompressible fluid between two eccentric rotating disks in which the stream lines are concentric circles in each plane which is parallel to a fixed plane [1]. Berker hinted on the possibility of an exact solution of the Navier-Stokes equations for flows in this direction. Some papers [3, 4] have not taken into account Berker's work [2]. A single solution for such a flow needs an extra condition. The assumed condition is that the flow be symmetric with respect to the origin. The use of this condition is subjected to the symmetric disks. In fact, if one prescribes the pressure gradient for the Navier-Stokes equations, the unknown constants are determined and one gets a unique solution. No additional condition is required for the solution of a single disk problem. Coirier [5] investigated the flow due to a disk and fluid at infinity which are rotating non-coaxially with slightly different angular velocities. Erdogan [6, 7] found exact solutions for the three dimensional Navier - Stokes equations when flow is caused by non-coaxial rotation of porous disk and a viscous fluid at infinity. He established the existence of asymptotic solutions for the velocity when the suction or blowing at the disk is uniform. He also studied flow induced by disk and a second grade fluid at infinity. Here the fluid and disk are rotating non-coaxially at a slightly different angular velocity [8]. The MHD flow and heat transfer due to eccentric rotations of a porous disk and fluid at infinity were investigated by Murthy and Ram [9]. The flow of a simple fluid in an orthogonal rheometer was studied by Rajagopal [10]. The flow considered here has similarities with that of Ekman layer. Lingwood [11] studied the stability of the family of related rotating problems. Rajagopal examined the flow of second grade fluid between rotating

parallel plates [12]. Berker [13, 14] analyzed the stability of this flow by employing energy methods also Rajagopal and Gupta [15] considered second order fluids. Mohanty looked at MHD flows between eccentric rotating disks with same angular velocities for symmetric cases when induced magnetic field is very small in comparison to an applied magnetic field. Rao and Kasiviswanathan [16] considered an extension of this type of flow to that of micropolar fluid. Other extensions are due to Rajagopal [17] for an Oldroyd-B fluid. The inertia effects between eccentric disks rotating at different speed were studied by Knight [18]. Numerical analysis of three dimensional flow between parallel plates rotating about a common axis or about distinct axes were performed by Lai et al. [19]. A one parameter family of solution is developed when the disks rotate with different angular velocities about distinct axes or a common axes [20]. Rao and Kasiviswanathan [21], in order to extend Berker's work [14] to unsteady motion, investigated the flow of a fluid between eccentric rotating disks in which the stream lines at a given instant are concentric circles in each plane parallel to a fixed plane and at each point of the plane which performs non-torsional oscillations. Berker's work was extended by Smith [22]. This was to include time dependent terms in the Navier-Stokes equations. Kasiviswanathan and Rao [23] presented the unsteady flow induced by non-coaxial rotations of disk executing non-torsional oscillations in its own plane and viscous fluid at infinity. Impulsively started unsteady flow caused by eccentric rotations of a disk and fluid at infinity was studied by Pop [24]. The flow was assumed two-dimensional and the disk and fluid at infinity are initially at rest and are impulsively started at time zero. However, the flow is supposed to be three-dimensional. The conditions for two dimensionality were considered by Erdogan [25, 26]. In continuation, Erdogan [27] studied the time-dependent Navier -Stokes equations for flow of a viscous fluid between two eccentric rotating disks performing non-torsional oscillations. The hydrodynamic flow due to an oscillating disk and viscous fluid rotating non-coaxially has also been discussed by Erdogan [28]. Hayat et al. [29] extended the Erdogan analysis to the magnetohydrodynamic situation. Siddiqui et al. [30] also found an exact solution of the unsteady flow of a second grade fluid induced by non-coaxial rotations of a porous disk and fluid at infinity in the presence of a constant magnetic field applied in the transverse direction. Hayat et al. [31] further considered periodic flows generated by general periodic oscillations of disk and viscous fluid exhibiting non-coaxial rotation.

The study of non-Newtonian fluids by rotating plates and disks has vast applications in industry and technology. To be more specific, a perturbation method was utilized in the study of the flow of a Reiner-Rivlin fluid between rotating parallel plates by Srivastava [32]. Then investigations of the flow between two disks of a Reiner-Rivlin fluid in which one disk was stationary and other rotating was carried out by Bhatnagar [33]. Reiner [34] introduced this model in order to describe the behavior of wet sand and the model was considered as an adequate model, at one time, for rheological characteristics. This model is not capable of describing normal stress differences or shear thickening/shear thinning effects. The flow of a fluid of order two due to rotating disks about an axis was dealt with by Bhatnagar and Zago [35]. The flow analysis of fourth-order fluid and a special subclass of models of K-BKZ type between two eccentric rotating disks were conducted by Kaloni and Siddiqui [36] and Dupont and Crochet [37]. The flow of the Wagner and Currie models were looked at by Rajagopal et al. [38]. The Currie, Wagner as well as the model with algebraically explicit complex viscosity function were examined by Zhang and Goddard [39]. The flows of Wagner and Currie models were studied by Bower et al. [40] and Dai et al. [41]. An exact solution for an Oldroyd-B fluid was given by Rajagopal [42]. Also an exact solution for a mixture of two incompressible Newtonian fluids was found by Gogus [43]. Granular materials flow was analyzed by Rajagopal et al. [44]. Rajagopal and Wineman [45] discussed the flow of electrorheological materials. The MHD effect on the Ekman layer over an infinite horizontal plate at rest relative to an electrically liquid which is rotating with uniform angular velocity about a vertical axis has been studied by Gupta [46]. Then Erkmann [47] included the induced magnetic field for this problem. Thereafter, this problem was examined by Rao [48] and Ersoy [49] for a second grade fluid as well as an Oldroyd-B fluid. Exact solutions for MHD flows of micropolar fluids were given by Kasiviswanthan and Gandhi [50]. Numerical simulation for MHD flow due to non-coaxial rotations of porous disk and third grade fluid was presented by Hayat et al. [51]. Ersoy [52] also investigated unsteady flow induced by a sudden pull of eccentric rotating disks. Rajagopal [53] made a review of the flows of viscous and non-Newtonian fluids between parallel disks rotating about a common axis.

The magnetohydrodynamic transport in porous space has been studied a great deal because of its applications in materials processing, astrophysics and geophysics etc. Several complex

phenomena are engendered by magnetic fields such as Hall currents, ionslip effects, Ohmic heating, Alfvén waves in plasmas etc. [54]. Influence of such effects on flow and temperature can be significant. Porous media are often utilized material fabrication applications. A large amount of work on steady and transient aspects of hydromagnetic convective flows in Darcian regimes that are viscous dominated and having Reynolds number less than ten have been examined. The magneto convective flow in a Darcian porous medium channel was discussed by Rao [55]. The transient hydromagnetic natural convection flow together with Hall effects in a Darcian regime was analytically treated in Ram [56]. Ram then extended this to study the mass transfer effects in [57]. Ram together with Takhar investigated the Hall effects on natural MHD convection in a Darcian porous medium [58]. The hydromagnetic natural convection flow over an isothermal conical body to a nonhomogeneous porous medium has been looked at by Kafoussias [59]. Heat generation and Hall current Darcian hydromagnetic convection were reported in [60]. By using a state space technique Ezzat and Zakaria [61] studied the oscillating hydromagnetic flow of viscoelastic fluid occupying a Darcian porous medium. In a recent study, Kamal [62] discussed the transient one-dimensional magneto convective heat and mass transfer through a Darcian porous medium adjacent to an infinite vertical porous plate. They used Laplace transform and state space approaches. Analytical solutions and the discussion on the structure of the different boundary layers for hydromagnetic convection, boundary layer heat transfer through a Darcian porous medium in a rotating plate channel were seen by Krishna et al. [63]. The magnetohydrodynamic transient natural convection flow of a coupled stress fluid filling a Darcian porous medium with relaxation effects was considered in [64] by employing the state space method. By using a perturbation approach, Beg et al. [65] studied the oscillatory hydromagnetic convection in a Darcian porous regime. The group approach was used to study the transient hydromagnetic convection boundary layer flow in a Darcian porous regime in [66]. In magneto fluids engineering systems, Joule and viscous dissipation effects can be significant. Ohmic heating manifests itself when kinetic energy is dissipated in the flow due to retardation by magnetic field. Viscous heating, Joule heating as well as inertial porous drag effects on forced magneto convection boundary layers over a nonisothermal horizontal cylinder in porous media were considered by El-Amin [67]. The MHD natural convection with heat and mass transfer and Joule and viscous and heat were numerically examined by Chen [68]. Attempts of MHD Couette

flows without taking into account porous medium effects were analyzed by Soundalgeker [69] and with the transient nature due to Attia [70]. The extension of [70] in considering the effects of Darcian porous media were looked at in Beg et al. [71]. In [71] an induced magnetic field is neglected and network simulation technique is used to solve the underlying equations. There were other researchers who discussed the Hall effects in magnetohydrodynamics. An exact analysis of a generalized MHD steady Couette flow with Hall current was carried out by Soundalgeker and Uplekar [72]. Unsteady hydromagnetic free convection flow taking into account Hall current was studied by Singh and Raptis [73]. The Hall effect on the hydromagnetic flow of a viscous fluid ionized gas between two parallel plates was dealt by Sato and Sherman [74]. Krishna and Rao [75] provided the analysis of Hall current on unsteady MHD boundary layer flow. Nagy and Demendy [76] consider general wall conditions on Hartman flow under the effects of coriolis force and Hall current. Ray and Mazumder [77] made an investigation for the flow of an electrically conducting falling liquid film over a smooth vertical surface taking Hall effects into account. Takhar et al. [78] discussed the MHD flow over a moving plate in a rotating fluid with magnetic field, Hall currents and free stream velocity. Megahed et al. [79] examined the heat and mass transfer analysis along a semi-infinite vertical flat plate under the combined buoyancy force effects of thermal and species diffusion in the presence of a strong nonuniform magnetic field and Hall currents are taken into account. Rotating flow of a second grade fluid on an infinite oscillating plate is investigated by T. Hayat et al. [80]. The effect of Hall current on unsteady free convection flows of MHD viscous incompressible fluids along infinite vertical porous plate in uniform magnetic fields inclined to the plates was researched by Sattar [81]. Watanabe [82] studied the effects of Hall currents on a magnetohydrodynamic boundary layer flow over a continuous moving semi-infinite flat plate. The situation when the liquid was permeated by a uniform transverse magnetic field with small magnetic Reynolds number was looked at. Aboul-Hassan and Attia [83] discussed the Hall effect on the steady flow generated by a rotating disk. Hayat et al. [84] studied the Hall effects on the hydromagnetic oscillatory flow of a second grade fluid. In [85] Hayat et al. extended the work of Ersoy [54] for the effects of Hall current and heat transfer.

Literature survey witnesses that equation of non-Newtonian fluids in general are of higher order and more complicated in comparison to the Navier -Stokes equations. Even the governing



equation for simplest subclass of non-Newtonian fluids namely the second grade is third order which is one order higher than the second order Navier-Stokes equations. The ignorance of nonlinearity in the Navier-Stokes equation does not lower the order whereas in the case of second grade fluids the order is reduced by leaving out higher order nonlinearities. An additional boundary condition may be needed for a second order fluid. For initial boundary value problem, there is also needed extra initial condition(s) in flows of non-Newtonian fluid. Rajagopal [86] gave a critical review on existence and uniqueness as well as boundary conditions. Rajagopal and Gupta [87] examined the flow of second grade fluid passed a porous plate. Augmentation of the boundary condition is employed in ref. [87]. Similar results have been presented by Rajagopal and Kaloni [88]. These authors investigated the flow in the annular region between two porous rotating cylinders. This work shows that the non-uniqueness of the solution as a result of insufficiency of the no-slip condition in a bounded domain. To circumvent this, researchers have added a suitable boundary condition. The flow in an annular region between two porous rotating cylinders was investigated by Fosdick and Berstein [89]. One of the constants in the solution was set to be zero by them without any reason. In the work [90] Frater studied the asymptotic suction flow. He showed that the perturbation expansion in terms of the coefficient of the higher order derivative of the equation may give wrong results. This is due to looking at singular perturbation problems as regular ones. In [91] non perturbation were used. As only two of the coefficients can be obtained by the no-slip conditions, Frater imposed an extra condition, viz the solution must tend to the Newtonian value as coefficient of the higher order derivative tends to zero. The perturbation approach does not give correct result under certain condition [91]. Rajgopal [92] presented a review of these points. Ariel [93] discussed the stagnation point flow of a second grade fluid . He [?] also examined the stagnation point in an elastico-viscous fluid towards a moving plate. The flow of an elastico-viscous fluid near a rotating disk was studied by Ariel in ref. [94]. Steady flow of a second grade fluid bounded between two parallel porous walls was presented in an investigation [95]. Several other works [?, 96–98, 100–107, 110–122] in the field have analyzed the steady and unsteady flows of non-Newtonian fluids under varied conditions.

## 1.1 Equations of change

Fluid motion is described through mass, momentum and energy conservations. By such equations one can access that how mass, momentum and energy change with respect to the position and time.

### 1.1.1 Continuity equation

By law of mass conservation, the total mass of the fluid within an arbitrary volume will increase only because of net influx of the fluid across the bounding surface. In mathematical form this may put as follows.

$$\frac{d}{dt} \int_{V_1} \rho dV_1 = - \int_S (\mathbf{n} \cdot \rho \mathbf{V}) dS, \quad (1.1)$$

where  $V_1$  is the volume and  $\mathbf{V}$  is the velocity.

Invoking Gauss's Divergence theorem

$$\int_{V_1} \left[ \frac{\partial \rho}{\partial t} + (\nabla \cdot \rho \mathbf{V}) \right] dV_1 = 0. \quad (1.2)$$

For arbitrary volume  $V_1$  we have

$$\frac{\partial \rho}{\partial t} + (\nabla \cdot \rho \mathbf{V}) = 0. \quad (1.3)$$

The above equation is known as continuity equation.

### 1.1.2 Equation of motion

According to the law of conservation of momentum "the total momentum of the fluid within the arbitrary volume will increase because of net influx of momentum across the bounding surface both by bulk flow and by molecular motions and because of the external force of gravity acting on the fluid".

In mathematical notation we can express as

$$\frac{d}{dt} \int_{V_1} \rho \mathbf{V} dV_1 = - \int_S (\mathbf{n} \cdot \rho \mathbf{V} \mathbf{V}) dS - \int_S (\mathbf{n} \cdot \boldsymbol{\tau}) dS + \int_{V_1} \rho \mathbf{g} dV_1. \quad (1.4)$$

Employing Gauss's result one have

$$\int_{V_1} \frac{\partial}{\partial t} \rho \mathbf{V} dV_1 = - \int_{V_1} [(\nabla \cdot \rho \mathbf{V} \mathbf{V}) + (\nabla \cdot \boldsymbol{\tau}) - \rho \mathbf{g}] dV_1, \quad (1.5)$$

Since volume is arbitrary so integrand taken to be zero i.e.

$$\frac{\partial (\rho \mathbf{V})}{\partial t} + (\mathbf{V} \cdot \nabla) (\rho \mathbf{V}) = -\nabla \cdot \boldsymbol{\tau} + \rho \mathbf{g}. \quad (1.6)$$

The above equation of motion states that mass time acceleration of a fluid element equals the sum of pressure, viscous and gravitational forces acting on the element.

### 1.1.3 Energy equation

It states that the temperature of a fluid element changes as it moves along with the fluid because of heat conduction and heat production by the viscous heating.

Mathematically we can write

$$\rho \frac{de}{dt} = \boldsymbol{\tau} \cdot \mathbf{L} - \nabla \cdot \mathbf{q} + \rho r, \quad (1.7)$$

in which  $e$  is the internal energy per unit mass,  $\mathbf{q}$  is heat flux vector.

By using the following Fourier law of heat conduction

$$\mathbf{q} = -\kappa \nabla T,$$

equation (1.7) becomes

$$\rho C_p \frac{dT}{dt} = \mathbf{T} \cdot \mathbf{L} + \kappa \nabla^2 T + \rho r, \quad (1.8)$$

where  $T$  is the temperature,  $r$  is radial heating,  $C_p$  is the specific heat and  $\kappa$  is the thermal conductivity.



## 1.2 Basic Definitions

### 1.2.1 Hall effect

when current carrying conductor is placed in a magnetic field, then electric field is produced which is normal or perpendicular to the direction of the current and the magnetic field. This phenomena is known as the Hall effect and the field produced is Hall field. Note that

$$R_H = -\frac{\mu_e}{en_e},$$
$$\mathbf{E}_H = -\frac{\mu_e}{en_e}(\mathbf{J} \times \mathbf{H})$$

$R_H$  is the Hall coefficient and  $\mathbf{E}_H$  is the Hall field.

### 1.2.2 Hartman number

It is the measure of ratio of the magnetic body forces to the viscous forces.

$$M = \frac{\sigma B_0^2}{\rho},$$

where  $\sigma$  is the electrical conductivity,  $\rho$  is the fluid density and  $B_0$  is constant applied magnetic field.

### 1.2.3 Reynold number

It is the ratio of the inertial to the viscous forces i.e  $R = UL/\nu$ ,  $U$ ,  $L$  and  $\nu$  are the fluid velocity, length scale and kinematic viscosity respectively.

### 1.2.4 Magnetic Reynold number

A dimensionless number used to compare the transport of magnetic lines of force in a conducting fluid to the leakage of such lines from the fluid equal to the charecteristic lengthof the fluid times the fluid velocity divided by the magnetic diffusivity.

### 1.2.5 Weissenberg number

It is the ratio of relaxation time to the specific process time.

### 1.2.6 Relaxation time

It is the time in which a system relaxes under certain changes in external condition. In particular it measures the time dependent response of a system to a well defined external simulation.

### 1.2.7 Retardation time

A time refers to a time scale for the build up of stress in a fluid.

## Chapter 2

# Hall effect on the flows of generalized Oldroyd-B fluid in a porous space

This chapter develops exact analytical solutions for the magnetohydrodynamic (MHD) flows of generalized Oldroyd-B fluid through a porous space. Mathematical development involves modified Darcy's law for fractional viscoelastic fluid with Hall effect. Three fundamental flows are considered. These are the flow induced by the rigid plate, periodic flow between two plates and Poiseuille flow. The analytic solutions are obtained with the help of Fourier transform for fractional calculus. The results are deduced for viscous fluid as the limiting cases. Graphical results are depicted for the emerging parameters and discussed.

### 2.1 Mathematical formulation

The fundamental equations governing the magnetohydrodynamic (MHD) flow of an incompressible fluid in a porous medium are

$$\rho \frac{d\mathbf{V}}{dt} = -\nabla p + \text{div}\mathbf{S} + \mathbf{J} \times \mathbf{B} + \mathbf{r}, \quad (2.1)$$

$$\text{div}\mathbf{V} = 0. \quad (2.2)$$

In Eqs. (2.1) and (2.2),  $\mathbf{V} = (u, v, w)$  is the velocity field,  $\rho$  is the fluid density,  $p$  is the hydrostatic pressure and  $r$  is the Darcy resistance in an Oldroyd-B fluid .

Since we are interested in the generalized Oldroyd-B fluid, its constitutive equation for an extra stress tensor  $\mathbf{S}$  can be written as

$$\left(1 + \lambda^\alpha \frac{D^\alpha}{Dt^\alpha}\right) \mathbf{S} = \mu \left(1 + \lambda_r^\beta \frac{D^\beta}{Dt^\beta}\right) \mathbf{A}_1, \quad (2.3)$$

where  $\mu$  is the dynamic viscosity and  $\lambda$  and  $\lambda_r$  are the relaxation and retardation times,  $\alpha$  and  $\beta$  are fractional calculus parameters such that  $0 \leq \alpha \leq \beta \leq 1$ . For  $\alpha > \beta$  the relaxation fraction is increasing, which is generally not possible and requires that  $\alpha \leq \beta$ .

The first Rivlin-Ericksen tensor is defined by

$$\mathbf{A}_1 = \nabla \mathbf{V} + (\nabla \mathbf{V})^T, \quad (2.4)$$

where  $\nabla$  is the gradient operator, the superscript  $T$  indicates the matrix transpose and

$$\frac{D^\alpha \mathbf{S}}{Dt^\alpha} = \frac{\partial^\alpha \mathbf{S}}{\partial t^\alpha} + (\mathbf{V} \cdot \nabla) \mathbf{S} - (\nabla \mathbf{V}) \mathbf{S} - \mathbf{S} (\nabla \mathbf{V})^T, \quad (2.5)$$

$$\frac{D^\beta \mathbf{A}_1}{Dt^\beta} = \frac{\partial^\beta \mathbf{A}_1}{\partial t^\beta} + (\mathbf{V} \cdot \nabla) \mathbf{A}_1 - (\nabla \mathbf{V}) \mathbf{A}_1 - \mathbf{A}_1 (\nabla \mathbf{V})^T, \quad (2.6)$$

in which  $\partial^\alpha / \partial t^\alpha$  shows the fractional derivative of order  $\alpha$  with respect to  $t$  and satisfies the following expression

$$\frac{\partial^\alpha f(t)}{\partial t^\alpha} = \frac{1}{\Gamma(1-\alpha)} \frac{d}{dt} \int_0^t (t-\xi)^{-\alpha} f(\xi) d\xi, \quad 0 < \alpha < 1. \quad (2.7)$$

Here  $\Gamma(\cdot)$  is Gamma function. We here point out the following limiting cases:

- When  $\alpha = \beta = 1$ , equation (2.3) holds for an ordinary Oldroyd-B fluid.
- For  $\lambda = 0$  we recover generalized second grade fluid.
- The generalized Maxwell fluid situation is retained for  $\lambda_r = 0$ .
- The classical Navier-Stokes fluid can be deduced for  $\lambda = \lambda_r = 0$  and  $\alpha = \beta = 1$ .

The Maxwell's equations are

$$\operatorname{div}\mathbf{B} = 0, \quad \operatorname{curl}\mathbf{B} = \mu_m\mathbf{J}, \quad \operatorname{curl}\mathbf{E} = -\frac{\partial\mathbf{B}}{\partial t}, \quad (2.8)$$

where  $\mathbf{J}$  is the current density,  $\mathbf{B}$  is the total magnetic field so that  $\mathbf{B} = \mathbf{B}_0 + \mathbf{b}$ ,  $\mathbf{B}_0$  and  $\mathbf{b}$  are the applied and induced magnetic fields, respectively,  $\mu_m$  is the magnetic permeability and  $\mathbf{E}$  is the electric field. There is no consideration of an applied or polarization voltage so that  $\mathbf{E} = \mathbf{0}$  and the induced magnetic field is negligible so that total magnetic field  $\mathbf{B} = (0, 0, B_0)$  where  $\mathbf{B}_0$  is an applied magnetic field. In the presence of Hall current, we have

$$\mathbf{J} + \frac{\omega_e\tau_e}{B_0}(\mathbf{J} \times \mathbf{B}_0) = \sigma \left[ \mathbf{E} + \mathbf{V} \times \mathbf{B}_0 + \frac{1}{en_e} \nabla p_e \right]. \quad (2.9)$$

In the above expression,  $\omega_e$  is the cyclotron frequency of electrons,  $\tau_e$  is the electron collision time,  $\sigma$  is the electrical conductivity,  $e$  is the electron charge,  $n_e$  is the number density of electrons and  $p_e$  is the electron pressure. Equation (2.9) does not include the ion-slip and thermoelectric effects.

In porous medium, the pressure drop and velocity in an Oldroyd-B fluid [49] satisfy the following expression

$$\left(1 + \lambda \frac{\partial}{\partial t}\right) \nabla p = -\frac{\mu}{k_1} \left(1 + \lambda_r \frac{\partial}{\partial t}\right) \mathbf{V}_D,$$

and the above expression in a generalized Oldroyd-B fluid is of the form

$$\left(1 + \lambda^\alpha \frac{\partial^\alpha}{\partial t^\alpha}\right) \nabla p = -\frac{\mu}{k_1} \left(1 + \lambda_r^\beta \frac{\partial^\beta}{\partial t^\beta}\right) \mathbf{V}_D, \quad (2.10)$$

where  $k_1$  is the permeability of the porous medium,  $\mathbf{V}_D$  is the Darcian velocity, which is related to the usual (i.e. volume averaged over a volume element consisting of fluid only in the pores) velocity  $\mathbf{V}$  by  $\mathbf{V}_D = \phi_1 \mathbf{V}$  and  $\phi_1$  is the porosity of the medium. Moreover, the pressure gradient in equation (2.10) also measures the resistance to flow in the bulk of the porous medium and  $r$  is a measure of the flow resistance offered by the solid matrix. Thus  $r$  through equation (2.10) satisfies

$$\left(1 + \lambda^\alpha \frac{\partial^\alpha}{\partial t^\alpha}\right) \mathbf{r} = -\frac{\mu\phi_1}{k_1} \left(1 + \lambda_r^\beta \frac{\partial^\beta}{\partial t^\beta}\right) \mathbf{V}. \quad (2.11)$$

The velocity field and stress are defined as

$$\mathbf{V} = \begin{pmatrix} u \\ 0 \\ 0 \end{pmatrix}, \quad \mathbf{S} = \begin{pmatrix} s_{xx} & s_{xy} & s_{xz} \\ s_{yx} & s_{yy} & s_{yz} \\ s_{zx} & s_{zy} & s_{zz} \end{pmatrix}, \quad (2.12)$$

where  $u$  is the velocity in the  $x$ -direction.

Now Eq. (2.3) yields

$$\left(1 + \lambda^\alpha \frac{\partial^\alpha}{\partial t^\alpha}\right) s_{xx} - 2\lambda^\alpha s_{xy} \frac{\partial u}{\partial y} = -2\mu\lambda_r^\beta \left(\frac{\partial u}{\partial y}\right)^2, \quad (2.13)$$

$$\left(1 + \lambda^\alpha \frac{\partial^\alpha}{\partial t^\alpha}\right) s_{xy} - \lambda^\alpha s_{yy} \frac{\partial u}{\partial y} = \mu \left(1 + \lambda_r^\beta \frac{\partial^\beta}{\partial t^\beta}\right) \frac{\partial u}{\partial y}, \quad (2.14)$$

and

$$s_{xz} = s_{yz} = s_{yy} = s_{zz} = 0. \quad (2.15)$$

Using equation (2.12), the continuity equation (2.2) is satisfied identically and Eq. (2.1) finally gives

$$\begin{aligned} \left(1 + \lambda^\alpha \frac{\partial^\alpha}{\partial t^\alpha}\right) \frac{\partial u}{\partial t} &= -\frac{1}{\rho} \left(1 + \lambda^\alpha \frac{\partial^\alpha}{\partial t^\alpha}\right) \frac{\partial p}{\partial x} + \nu \left(1 + \lambda_r^\beta \frac{\partial^\beta}{\partial t^\beta}\right) \frac{\partial^2 u}{\partial y^2} \\ &\quad - \frac{\nu\phi_1}{k_1} \left(1 + \lambda_r^\beta \frac{\partial^\beta}{\partial t^\beta}\right) u - \frac{\sigma B_0^2}{\rho(1-i\phi)} \left(1 + \lambda^\alpha \frac{\partial^\alpha}{\partial t^\alpha}\right) u, \end{aligned} \quad (2.16)$$

where  $\phi = \omega_e \tau_e$  indicates the Hall parameter and  $\nu$  denotes the kinematic viscosity.

## 2.2 Flows induced by a rigid plate

Let us consider the flow of a generalized Oldroyd-B fluid over an infinite rigid plate at  $y = 0$ . The fluid medium is porous. The fluid motion is set up from rest and at time  $t = 0^+$ , the plate is making periodic oscillation of the form  $f(t)$  having period  $T_0$ . Due to shear effects, the fluid over the plate is gradually disturbed. Neglecting pressure gradient equation (2.16) reduces to

$$\left(1 + \lambda^\alpha \frac{\partial^\alpha}{\partial t^\alpha}\right) \frac{\partial u}{\partial t} = \nu \left(1 + \lambda_r^\beta \frac{\partial^\beta}{\partial t^\beta}\right) \frac{\partial^2 u}{\partial y^2} - \frac{\nu\phi_1}{k_1} \left(1 + \lambda_r^\beta \frac{\partial^\beta}{\partial t^\beta}\right) u - \frac{\sigma B_0^2}{\rho(1-i\phi)} \left(1 + \lambda^\alpha \frac{\partial^\alpha}{\partial t^\alpha}\right) u. \quad (2.17)$$

The boundary conditions for the problem are

$$u(0, t) = Uf(t), \quad t > 0, \quad (2.18)$$

$$u \rightarrow 0 \quad \text{as} \quad y \rightarrow \infty, \quad (2.19)$$

where

$$f(t) = \sum_{k=-\infty}^{\infty} a_k e^{ik\omega_0 t}, \quad (2.20)$$

and the Fourier series coefficients  $\{a_k\}$  are given by the following expression

$$a_k = \frac{1}{T_0} \int_{T_0} f(t) e^{-ik\omega_0 t},$$

in which  $\omega_0 = 2\pi/T_0$  is the non-zero fundamental frequency.

We are interested in dimensionless form of the system by defining the following non-dimensional variables

$$\begin{aligned} u^* &= \frac{u}{U}, \quad y^* = \frac{y}{(\nu/U)}, \quad t^* = \frac{t}{(\nu/U^2)}, \quad \omega_0^* = \frac{\omega_0}{(U^2/\nu)}, \\ \lambda^* &= \frac{\lambda}{(\nu/U^2)}, \quad \lambda_r^* = \frac{\lambda_r}{(\nu/U^2)}, \quad M^2 = \frac{\sigma B_0^2}{(\rho^2 U^2/\mu)}, \quad \frac{1}{K} = \frac{\phi_1}{k_1 (U^2/\nu^2)}, \end{aligned} \quad (2.21)$$

in which asterik on a variable designates its dimensionless form.

In view of Eq. (2.21), Eq. (2.17) reduces to the following dimensionless form

$$\left(1 + \lambda^\alpha \frac{\partial^\alpha}{\partial t^\alpha}\right) \frac{\partial u}{\partial t} = \left(1 + \lambda_r^\beta \frac{\partial^\beta}{\partial y^\beta}\right) \frac{\partial^2 u}{\partial y^2} - \frac{1}{K} \left(1 + \lambda_r^\beta \frac{\partial^\beta}{\partial t^\beta}\right) u - \frac{M^2}{1 - i\phi} \left(1 + \lambda^\alpha \frac{\partial^\alpha}{\partial t^\alpha}\right) u, \quad (2.22)$$

where asterik are omitted for clarity.

The dimensionless boundary conditions are given by

$$u(0, t) = \sum_{k=-\infty}^{\infty} a_k e^{ik\omega_0 t}, \quad t > 0, \quad (2.23)$$

$$u \rightarrow 0 \quad \text{as} \quad y \rightarrow \infty. \quad (2.24)$$

We will find the solution of the governing dimensionless problem by Fourier transform treatment. Hence the Fourier transform pair is defined as follows:

$$\psi(y, \omega) = \int_{-\infty}^{\infty} u(y, t) e^{-i\omega t} dt, \quad (2.25)$$

$$u(y, t) = \frac{1}{2\pi} \int_{-\infty}^{\infty} \psi(y, \omega) e^{i\omega t} d\omega \quad (2.26)$$

and the Fourier transform of the fractional derivative is [124–126]

$$\int_{-\infty}^{\infty} \frac{D^\beta}{Dt^\beta} [u(y, t)] e^{-i\omega t} dt = (i\omega)^\beta \psi(y, \omega), \quad (2.27)$$

where

$$(i\omega)^\beta = |\omega|^\beta e^{i\beta\pi/2 \text{sign}\omega} = |\omega|^\beta \left( \cos \frac{\beta\pi}{2} + i \text{sign}\omega \sin \frac{\beta\pi}{2} \right)$$

and sign is the signum function.

Applying the Fourier transform to equations (2.22)-(2.24), solving the resulting transformed problem and making use of equation (2.26) and property of delta function, one has

$$u(y, t) = \sum_{k=-\infty}^{\infty} a_k e^{-m_k y + i(k\omega_0 t - n_k y)}, \quad (2.28)$$

where

$$m_k = \sqrt{\frac{\sqrt{L_r^2 + L_i^2} + L_r}{2}}, \quad n_k = \sqrt{\frac{\sqrt{L_r^2 + L_i^2} - L_r}{2}}, \quad (2.29)$$



$$L_r = \frac{1}{K} + \left[ \frac{M^2 \left\{ (1 + \lambda^\alpha |k\omega_0|^\alpha \cos \frac{\alpha\pi}{2}) (1 + \lambda_r^\beta |k\omega_0|^\beta \cos \frac{\beta\pi}{2}) \right\} + \lambda^\alpha \lambda_r^\beta |k\omega_0|^{\alpha+\beta} (\text{sign} k\omega_0)^2 \sin \frac{\alpha\pi}{2} \sin \frac{\beta\pi}{2}}{-\text{sign} k\omega_0 \{M^2 \phi + k\omega_0 (1 + \phi^2)\} \left\{ \begin{array}{l} \lambda^\alpha |k\omega_0|^\alpha \sin \frac{\alpha\pi}{2} (1 + \lambda_r^\beta |k\omega_0|^\beta \cos \frac{\beta\pi}{2}) \\ -\lambda_r^\beta |k\omega_0|^\beta \sin \frac{\beta\pi}{2} (1 + \lambda^\alpha |k\omega_0|^\alpha \cos \frac{\alpha\pi}{2}) \end{array} \right\}}{(1 + \phi^2) \left\{ (1 + \lambda_r^\beta |k\omega_0|^\beta \cos \frac{\beta\pi}{2})^2 + (\lambda_r^\beta |k\omega_0|^\beta \text{sign} k\omega_0 \sin \frac{\beta\pi}{2})^2 \right\}} \right],$$

$$L_i = \left[ \frac{\{M^2 \phi + k\omega_0 (1 + \phi^2)\} \left\{ (1 + \lambda^\alpha |k\omega_0|^\alpha \cos \frac{\alpha\pi}{2}) (1 + \lambda_r^\beta |k\omega_0|^\beta \cos \frac{\beta\pi}{2}) \right\} + \lambda^\alpha \lambda_r^\beta |k\omega_0|^{\alpha+\beta} (\text{sign} k\omega_0)^2 \sin \frac{\alpha\pi}{2} \sin \frac{\beta\pi}{2}}{-M^2 \text{sign} k\omega_0 \left\{ \begin{array}{l} \lambda^\alpha |k\omega_0|^\alpha \sin \frac{\alpha\pi}{2} (1 + \lambda_r^\beta |k\omega_0|^\beta \cos \frac{\beta\pi}{2}) \\ -\lambda_r^\beta |k\omega_0|^\beta \sin \frac{\beta\pi}{2} (1 + \lambda^\alpha |k\omega_0|^\alpha \cos \frac{\alpha\pi}{2}) \end{array} \right\}}{(1 + \phi^2) \left\{ (1 + \lambda_r^\beta |k\omega_0|^\beta \cos \frac{\beta\pi}{2})^2 + (\lambda_r^\beta |k\omega_0|^\beta \text{sign} k\omega_0 \sin \frac{\beta\pi}{2})^2 \right\}} \right].$$

It is worth pointing out here that equation (2.28) is a result corresponding to general periodic oscillation of a plate. As a special case of this oscillation, the flow field is obtained by an appropriate choice of the Fourier coefficients  $\{a_k\}$  which give rise to different plate oscillations. For example, the flow fields  $u_j$  ( $j = 1 - 5$ ) caused by the five oscillations  $\exp(i\omega_0 t)$ ,  $\cos \omega_0 t$ ,  $\sin \omega_0 t$ ,  $\left\{ \begin{array}{l} 1, \quad |t| < T_1, \\ 0, \quad T_1 < |t| < T_0/2 \end{array} \right\}$ ,  $\sum_{k=-\infty}^{\infty} \delta(t - kT_0)$  are given by

$$u_1(y, t) = \exp(-m_1 y + i(\omega_0 t - n_1 y)), \quad (2.30)$$

$$u_2(y, t) = \frac{1}{2} [\exp(-m_1 y + i(\omega_0 t - n_1 y)) + \exp(-m_{-1} y - i(\omega_0 t + n_{-1} y))], \quad (2.31)$$

$$u_3(y, t) = \frac{1}{2i} [\exp(-m_1 y + i(\omega_0 t - n_1 y)) - \exp(-m_{-1} y - i(\omega_0 t + n_{-1} y))], \quad (2.32)$$

$$u_4(y, t) = \sum_{k=-\infty}^{\infty} \frac{\sin k\omega_0 T_1}{k\pi} \exp(-m_k y + i(k\omega_0 t - n_k y)), \quad k \neq 0, \quad (2.33)$$

$$u_5(y, t) = \frac{1}{T_0} \sum_{k=-\infty}^{\infty} \exp(-m_k y + i(k\omega_0 t - n_k y)). \quad (2.34)$$

### 2.3 Periodic flows between two plates

Let us consider oscillating flows in the domain  $0 \leq y \leq h$ . The lower plate at  $y = 0$  oscillates with a velocity  $Uf(t)$ , while the upper plate at  $y = h$  is kept stationary. We seek the situation when there is no pressure gradient and the flow is entirely driven due to oscillation of the lower plate. Thus the governing problem consists of equations (2.22), (2.23) and the following boundary condition

$$u(h, t) = 0. \quad (2.35)$$

Here we define the following variables in order to make the governing problem dimensionless

$$\begin{aligned} u^* &= \frac{u}{U}, \quad y^* = \frac{y}{h}, \quad t^* = \frac{t}{(h^2/\nu)}, \quad \omega_0^* = \frac{\omega_0}{(\nu/h^2)}, \\ \lambda^* &= \frac{\lambda}{(h^2/\nu)}, \quad \lambda_r^* = \frac{\lambda_r}{(h^2/\nu)}, \quad M^2 = \frac{\sigma B_0^2}{(\mu/h^2)}, \quad \frac{1}{K} = \frac{\phi_1}{(k_1/h^2)}. \end{aligned} \quad (2.36)$$

In terms of the above dimensionless variables, the arising problem after ignoring the asterisks takes the following form:

$$\left(1 + \lambda^\alpha \frac{\partial^\alpha}{\partial t^\alpha}\right) \frac{\partial u}{\partial t} = \left(1 + \lambda_r^\beta \frac{\partial^\beta}{\partial t^\beta}\right) \frac{\partial^2 u}{\partial y^2} - \frac{1}{K} \left(1 + \lambda_r^\beta \frac{\partial^\beta}{\partial t^\beta}\right) u - \frac{M^2}{1 - i\phi} \left(1 + \lambda^\alpha \frac{\partial^\alpha}{\partial t^\alpha}\right) u, \quad (2.37)$$

$$u(0, t) = \sum_{k=-\infty}^{\infty} a_k e^{ik\omega_0 t}, \quad t > 0, \quad (2.38)$$

$$u(1, t) = 0. \quad (2.39)$$

Adopting the procedure of previous section, the resulting solutions can be represented as follows:

$$u(y, t) = \sum_{k=-\infty}^{\infty} a_k \frac{\sinh \beta_k (1-y)}{\sinh \beta_k} e^{ik\omega_0 t}, \quad (2.40)$$

$$u_1(y, t) = \frac{\sinh \beta_1 (1-y)}{\sinh \beta_1} e^{i\omega_0 t}, \quad (2.41)$$

$$u_2(y, t) = \frac{1}{2} \left[ \frac{\sinh \beta_1 (1-y)}{\sinh \beta_1} e^{i\omega_0 t} + \frac{\sinh \beta_{-1} (1-y)}{\sinh \beta_{-1}} e^{-i\omega_0 t} \right], \quad (2.42)$$

$$u_3(y, t) = \frac{1}{2i} \left[ \frac{\sinh \beta_1 (1-y)}{\sinh \beta_1} e^{i\omega_0 t} - \frac{\sinh \beta_{-1} (1-y)}{\sinh \beta_{-1}} e^{-i\omega_0 t} \right], \quad (2.43)$$

$$u_4(y, t) = \sum_{k=-\infty}^{\infty} \frac{\sin k\omega_0 T_1}{k\pi} \frac{\sinh \beta_k (1-y)}{\sinh \beta_k} e^{ik\omega_0 t}, \quad k \neq 0, \quad (2.44)$$

$$u_5(y, t) = \frac{1}{T_0} \sum_{k=-\infty}^{\infty} \frac{\sinh \beta_k (1-y)}{\sinh \beta_k} e^{ik\omega_0 t}, \quad (2.45)$$

where

$$\beta_k^2 = (m_k + in_k)^2.$$

## 2.4 Poiseuille flow

This section deals with the flow between two infinite stationary plates separated by a distance  $2h$ . The flow induced is due to imposition of periodic pressure gradient of the form

$$\frac{\partial p}{\partial x} = -\rho Q_0 e^{i\omega_0 t}. \quad (2.46)$$

The flow is governed by equation (2.16) and the boundary conditions given below

$$u(\pm h, t) = 0. \quad (2.47)$$

Solving Eq. (2.16) and using boundary conditions (2.47), we obtain the velocity

$$u(y, t) = Q_0 \left[ \frac{\left\{ 1 + \lambda^\alpha |\omega_0|^\alpha \left( \cos \frac{\alpha\pi}{2} + i \operatorname{sign} \omega_0 \sin \frac{\alpha\pi}{2} \right) \right\} (\cosh \beta^* y - \cosh \beta^*) e^{i\omega_0 t}}{\beta^{*2} \left\{ 1 + \lambda_r^\beta |\omega_0|^\beta \left( \cos \frac{\beta\pi}{2} + i \operatorname{sign} \omega_0 \sin \frac{\beta\pi}{2} \right) \right\} \cosh \beta^*} \right], \quad (2.48)$$

$$\beta^* = \beta_k|_{k=1}.$$

## 2.5 Analytical results for a Newtonian fluid

For this section, the MHD results for the Newtonian fluid with Hall effect in a porous medium can be deduced by taking  $\lambda = \lambda_r = 0$  in all the previous three sections. Moreover, the results for MHD Newtonian fluid with Hall current in a non-porous medium can be taken by choosing  $\lambda = \lambda_r = 0 = \phi_1$  or  $\lambda = \lambda_r = 0$  and  $K \rightarrow \infty$ . For  $\phi = 0$ , the results hold in absence of Hall current. When  $M = 0$  (i.e.  $B_0 = 0$ ), the results of hydrodynamic fluid are achieved.

When  $\lambda = \lambda_r = M = \phi_1 = 0$  then Eqs. (2.31), (2.42) and (2.48) respectively give

$$u(y, t) = e^{-\sqrt{\frac{\omega_0}{2}} y} \cos\left(\omega_0 t - \sqrt{\frac{\omega_0}{2}} y\right), \quad (2.42)$$

$$u(y, t) = \text{Re} \left[ \frac{\sinh\left\{(1+i)\sqrt{\frac{\omega_0}{2}}(1-y)\right\} e^{i\omega_0 t}}{\sinh(1+i)\sqrt{\frac{\omega_0}{2}}}\right], \quad (2.43)$$

$$u(y, t) = \frac{2Q_0}{\omega_0} \left[ \frac{\cosh(1+i) - \cosh(1+i)y}{2i \cosh(1+i)} \right] e^{i\omega_0 t}. \quad (2.44)$$

It should be noted that the above solutions are similar to the existing results. This provides confidence that the derived solutions here are correct.

## 2.6 Results and discussion

In this section, we present various results obtained from the flows analyzed in this investigation. We interpret these results with respect to the variation of emerging parameters of interest. Special attention has been paid to two kinds of fluids namely an Oldroyd-B fluid (when  $\alpha = \beta = 1$ ) and a generalized Oldroyd-B fluid (when  $0 < \alpha < \beta < 1$ ). The effects of magnetic parameter  $M$ , Hall parameter  $\phi$  and the permeability of porous medium  $K$  have been studied when  $\lambda = 2$ ,  $\lambda_r = 1$ ,  $\omega_0 = 0$  and  $t = 0.5$  are fixed.

Figures 2.1 to 2.6 are prepared for flow induced by a rigid plate and Figures 2.7 to 2.12 for periodic flow between two plates when the oscillation is of the type  $\cos \omega_0 t$ . Figures 2.13 to 2.18 display Poiseuille flow when the pressure gradient is also of the form  $\cos \omega_0 t$ . The effects of magnetic parameter  $M$  and porosity parameter  $K$  are specifically shown in Figures 2.1–2.18 in an Oldroyd-B fluid and a generalized Oldroyd-B fluid in the presence as well as in the absence

of Hall parameter  $\phi$  and by keeping the values of other parameters fixed. These Figures indicate that an increase in the values of magnetic parameter  $M$  tend to reduce the velocity profiles monotonically due to the effect of magnetic force against the direction of the flow for various types of fluids. It is further noted that velocity in generalized Oldroyd-B fluid is greater when compared with an Oldroyd-B fluid. The effect of  $M$  in an Oldroyd-B and generalized Oldroyd-B fluid is also opposite to that of  $K$ .

The sketched Figures also elucidate the influence of Hall parameter  $\phi$  on the velocity profiles with fixed values of other parameters. As expected, the velocity increases with increasing  $\phi$  for examined fluids. This has the effect of reducing effective conductivity by increasing  $\phi$ . In other words this is quite well in agreement with the fact that the magnetic damping force on velocity decreases.

It is also noted that when the flow is driven by the oscillation of the boundary, the velocity profiles in an Oldroyd-B fluid are larger than those in a generalized Oldroyd-B fluid. However, the situation is quite reverse when the flow is driven by the adverse pressure gradient. In this situation, the velocity profiles in a generalized Oldroyd-B fluid are larger in magnitude than that of an Oldroyd-B fluid. Finally, the analytical results for generalized second grade fluid, Oldroyd-B fluid and generalized Maxwell fluid can be obtained as the limiting cases of this study by choosing  $\lambda = 0$ ,  $\alpha = \beta = 1$  and  $\lambda_r = 0$  respectively.

Furthermore the present analytical results for  $\alpha = \beta = 1$ ,  $K \rightarrow \infty$  and  $M = 0 = \lambda$  reduce to that in the case of second grade fluid.

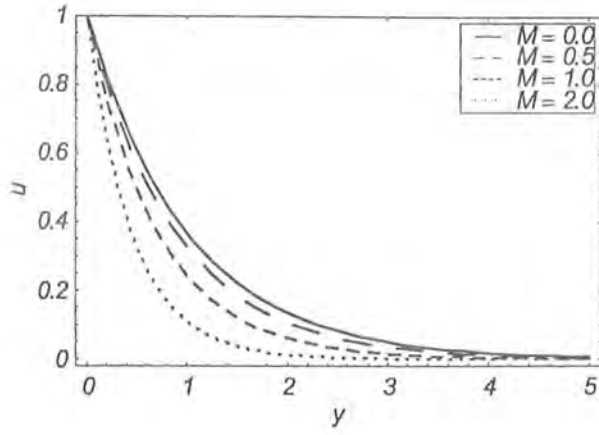


Figure 2.1: Velocity profile (flow induced by a rigid plate) of an Oldroyd-B fluid for various values of magnetic parameter  $M$  when  $K = 1$  and  $\phi = 0$ .

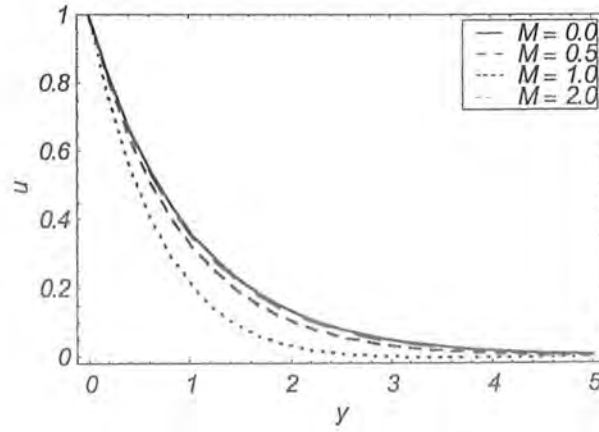


Figure 2.2: Velocity profile (flow induced by a rigid plate) of an Oldroyd-B fluid for various values of magnetic parameter  $M$  when  $K = 1$  and  $\phi = 2$ .

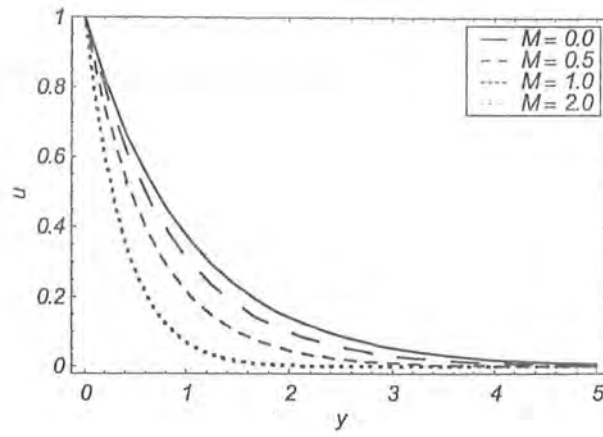


Figure 2.3: Velocity profile (flow induced by a rigid plate) of generalized Oldroyd-B fluid for various values of magnetic parameter  $M$  when  $K = 1$  and  $\phi = 0$ .

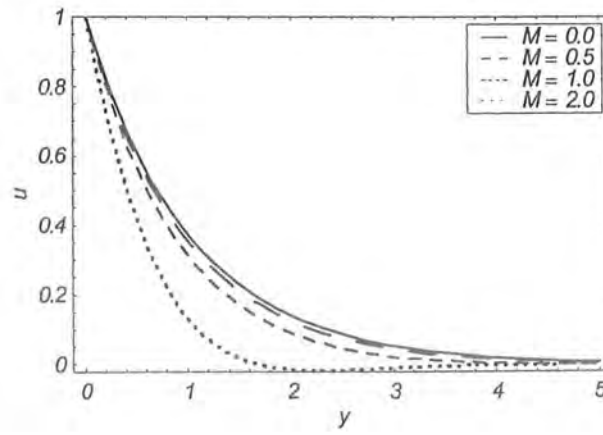


Figure 2.4: Velocity profile (flow induced by a rigid plate) of generalized Oldroyd-B fluid for various values of magnetic parameter  $M$  when  $K = 1$  and  $\phi = 2$ .

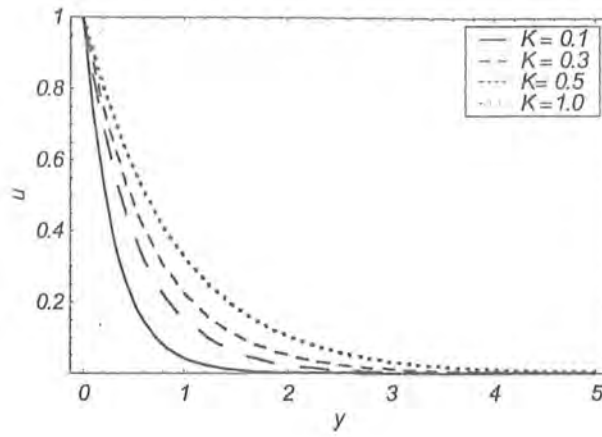


Figure 2.5: Velocity profile (flow induced by a rigid plate) of an Oldroyd-B fluid for various values of porosity parameter  $K$  when  $M = 1$  and  $\phi = 2$ .

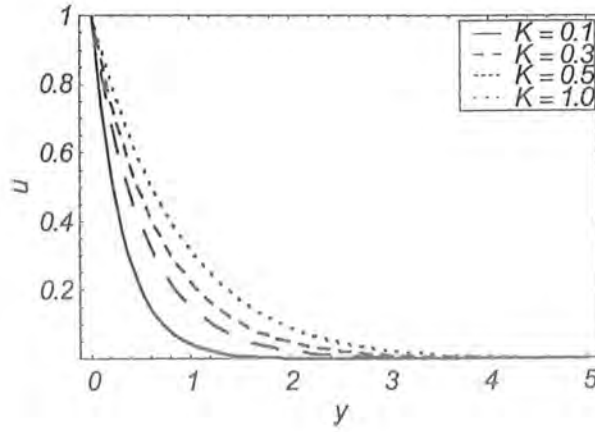


Figure 2.6: Velocity profile (flow induced by a rigid plate) of generalized Oldroyd-B fluid for various values of porosity parameter  $K$  when  $M = 1$  and  $\phi = 2$ .



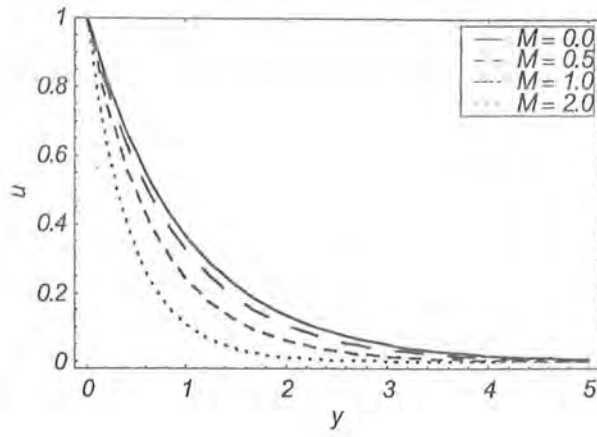


Figure 2.7: Velocity profile (periodic flow between two plates) of an Oldroyd-B fluid for various values of magnetic parameter  $M$  when  $K = 1$  and  $\phi = 0$ .

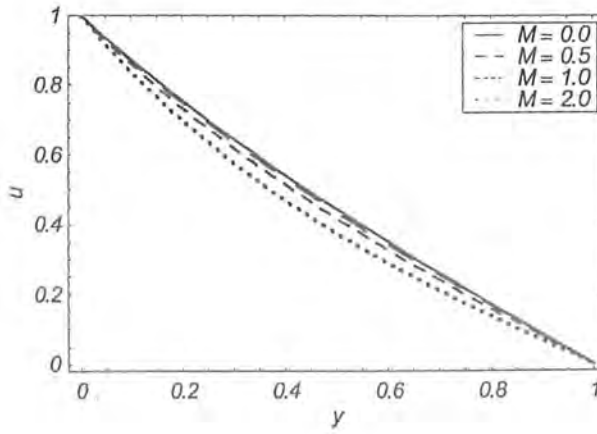


Figure 2.8: Velocity profile (periodic flow between two plates) of the generalized Oldroyd-B fluid for various values of magnetic parameter  $M$  when  $K = 1$  and  $\phi = 0$ .

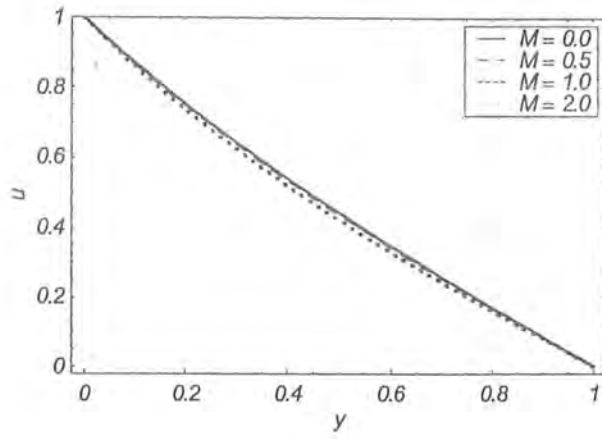


Figure 2.9: Velocity profile (periodic flow between two plates) of an Oldroyd-B fluid for various values of magnetic parameter  $M$  when  $K = 1$  and  $\phi = 2$ .

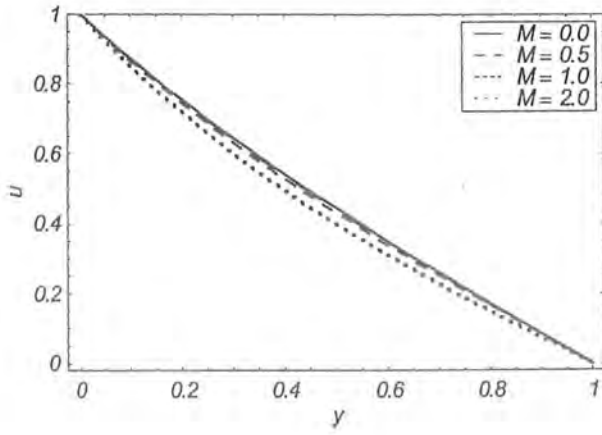


Figure 2.10: Velocity profile (periodic flow between two plates) of generalized Oldroyd-B fluid for various values of magnetic parameter  $M$  when  $K = 1$  and  $\phi = 2$ .

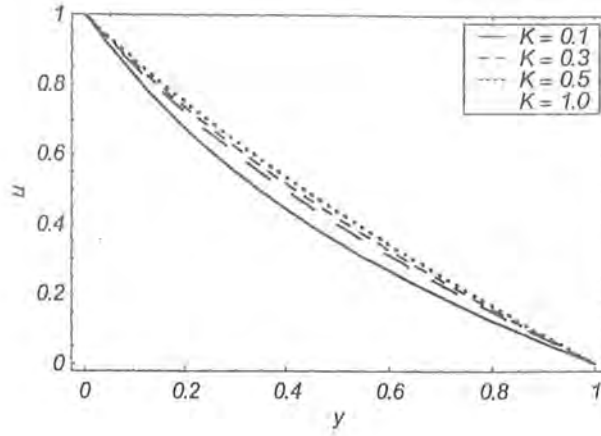


Figure 2.11: Velocity profile (periodic flow between two plates) of an Oldroyd-B fluid for various values of porosity parameter  $K$  when  $M = 1$  and  $\phi = 2$ .

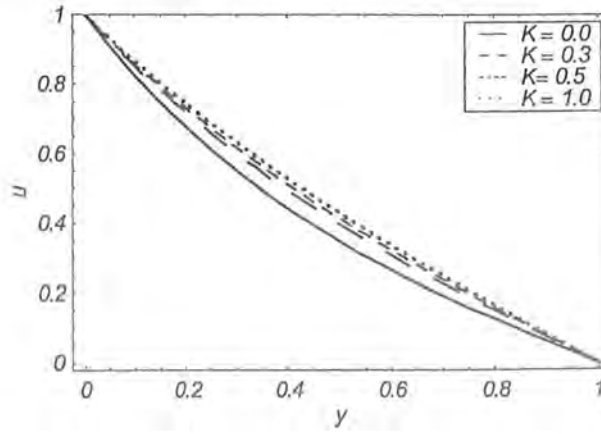


Figure 2.12: Velocity profile (periodic flow between two plates) of generalized Oldroyd-B fluid for various values of porosity parameter  $K$  when  $M = 1$  and  $\phi = 2$ .

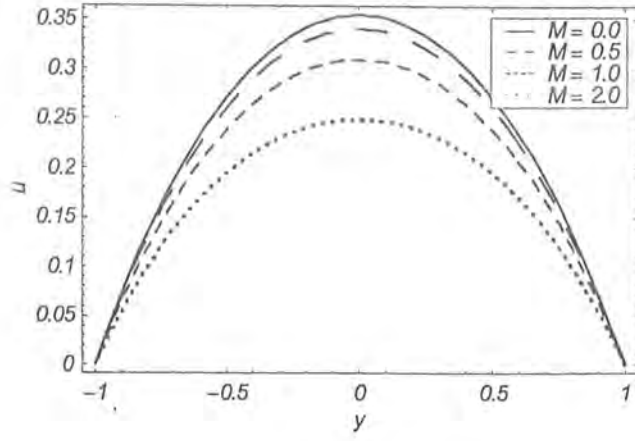


Figure 2.13: Velocity profile (Poiseuille flow) of Oldroyd-B fluid for various values of magnetic parameter  $M$  when  $K = 1$  and  $\phi = 0$ .

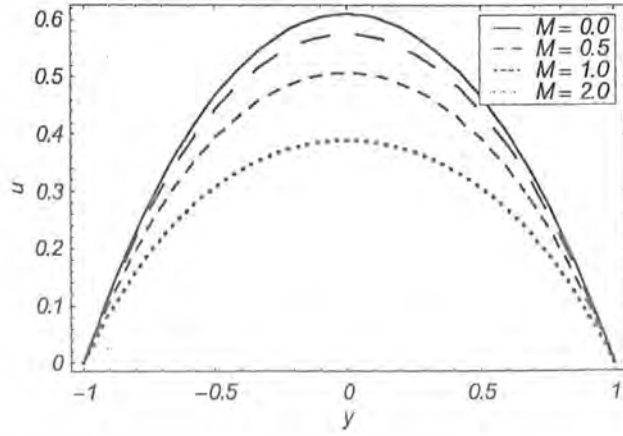


Figure 2.14: Velocity profile (Poiseuille flow) of generalized Oldroyd-B fluid for various values of magnetic parameter  $M$  when  $K = 1$  and  $\phi = 0$ .

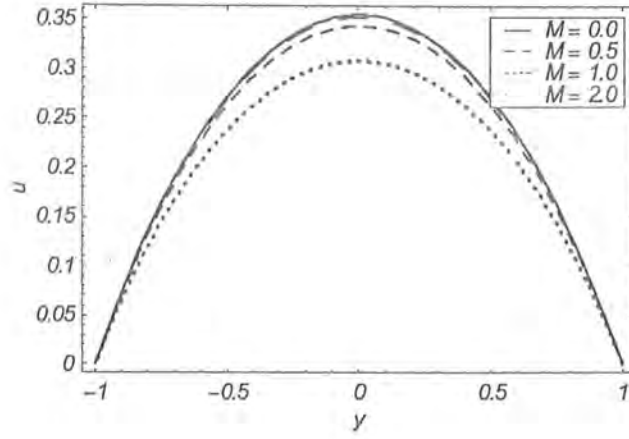


Figure 2.15: Velocity profile (Poiseuille flow) of an Oldroyd-B fluid for various values of magnetic parameter  $M$  when  $K = 1$  and  $\phi = 2$ .

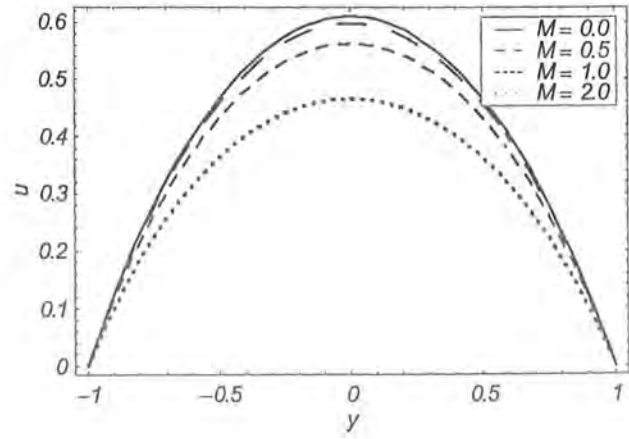


Figure 2.16: Velocity profile (Poiseuille flow) of generalized Oldroyd-B for various values of magnetic parameter  $M$  when  $K = 1$  and  $\phi = 2$ .

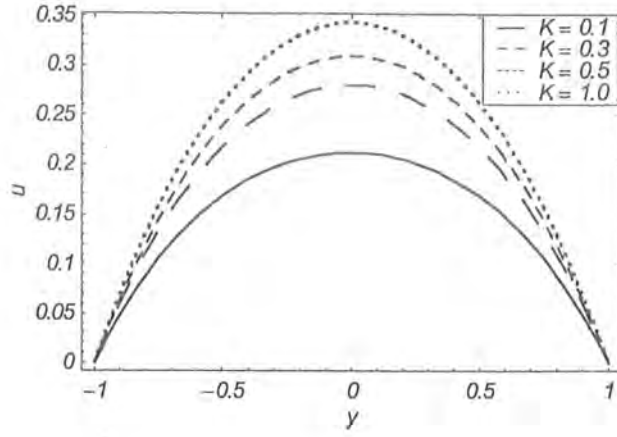


Figure 2.17: Velocity profile (Poiseuille flow) for various values of porosity parameter  $K$  for Oldroyd-B fluid when  $M = 1$  and  $\phi = 2$ .

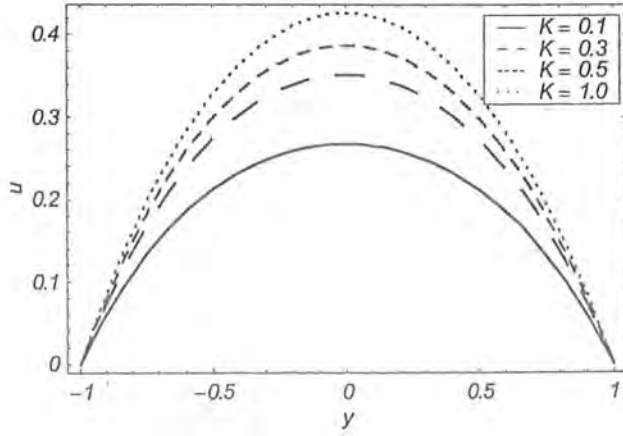


Figure 2.18: Velocity profile (Poiseuille flow) of generalized Oldroyd-B fluid for various values of porosity parameter  $K$  when  $M = 1$  and  $\phi = 2$ .

## Chapter 3

# Influence of Hall current on the flows in a fractional generalized Burgers' fluid

This chapter aims to extend the analysis of previous chapter for a fractional generalized Burgers' fluid. Closed form solutions are derived. Mathematical results are plotted for embedded flow parameters into the arising problems and discussed. A comparative study between the present and limiting cases of generalized Burgers' fluid model is also made.

### 3.1 Mathematical formulation

The constitutive equation in a fractional generalized Burgers' fluid is

$$\left(1 + \lambda_1^\alpha \frac{D^\alpha}{Dt^\alpha} + \lambda_2^{2\alpha} \frac{D^{2\alpha}}{Dt^{2\alpha}}\right) \mathbf{S} = \mu \left(1 + \lambda_3^\beta \frac{D^\beta}{Dt^\beta} + \lambda_4^{2\beta} \frac{D^{2\beta}}{Dt^{2\beta}}\right) \mathbf{A}_1, \quad (3.1)$$

where  $\mu$  is the dynamic viscosity,  $\lambda_1$  and  $\lambda_2$  are the relaxation times and  $\lambda_3$  and  $\lambda_4$  are the retardation times. Here  $\alpha$  and  $\beta$  are fractional calculus parameters such that  $0 \leq \alpha \leq \beta \leq 1$ . For  $\alpha > \beta$  relaxation fraction is increasing which is generally not possible and thus one requires that  $\alpha \leq \beta$ . The first Rivlin Ericksen tensor  $\mathbf{A}_1$  and the convected and fractional derivatives are defined in equations (2.4)-(2.6).

It is important to note that model (3.1) includes many non-Newtonian fluid models as the special cases.

- For  $\alpha = \beta = 1$ ,  $\lambda_4 = 0$  it reduces to classical Burgers' fluid. It recovers the results of fractional Burgers' fluid when  $\lambda_4 = 0$ .
- The results of generalized Oldroyd-B fluid and Oldroyd-B fluid are deduced by selecting  $\lambda_4 = \lambda_2 = 0$  and  $\alpha = \beta = 1$ ;  $\lambda_4 = \lambda_2 = 0$  respectively.
- When  $\lambda_4 = \lambda_3 = \lambda_2 = 0$ ,  $\lambda_i = 0$  ( $i = 1 - 4$ ) with  $\alpha = \beta = 1$  the model (3.1) respectively gives the Maxwell and Navier-Stokes fluid.
- The results for fractional second grade fluid can be obtained when  $\lambda_4 = \lambda_2 = \lambda_1 = 0$ .

The pressure drop and velocity in the generalized Burgers' fluid [127] are related by the following expression

$$\left(1 + \lambda_1^\alpha \frac{D^\alpha}{Dt^\alpha} + \lambda_2^{2\alpha} \frac{D^{2\alpha}}{Dt^{2\alpha}}\right) \nabla \mathbf{P} = -\frac{\mu\phi_1}{k_1} \left(1 + \lambda_3^\beta \frac{D^\beta}{Dt^\beta} + \lambda_4^{2\beta} \frac{D^{2\beta}}{Dt^{2\beta}}\right) \mathbf{V}, \quad (3.2)$$

where  $\phi_1$  and  $k_1$  denote the porosity and permeability of the porous medium respectively. Following Eq. (3.2), the expression of  $\mathbf{r}$  here is of the form

$$\left(1 + \lambda_1^\alpha \frac{D^\alpha}{Dt^\alpha} + \lambda_2^{2\alpha} \frac{D^{2\alpha}}{Dt^{2\alpha}}\right) \mathbf{r} = -\frac{\mu\phi_1}{k_1} \left(1 + \lambda_3^\beta \frac{D^\beta}{Dt^\beta} + \lambda_4^{2\beta} \frac{D^{2\beta}}{Dt^{2\beta}}\right) \mathbf{V}. \quad (3.3)$$

Making use of equation (3.1) we have

$$\left(1 + \lambda_1^\alpha \frac{D^\alpha}{Dt^\alpha} + \lambda_2^{2\alpha} \frac{D^{2\alpha}}{Dt^{2\alpha}}\right) s_{xx} - 2 \frac{\partial u}{\partial y} \left(\lambda_1^\alpha + \lambda_2^{2\alpha} \frac{D^\alpha}{Dt^\alpha}\right) s_{xy} = -2\mu \left(\lambda_3^\beta + \frac{3}{2} \lambda_4^{2\beta} \frac{D^\beta}{Dt^\beta}\right) \left(\frac{\partial u}{\partial y}\right)^2, \quad (3.4)$$

$$\left(1 + \lambda_1^\alpha \frac{D^\alpha}{Dt^\alpha} + \lambda_2^{2\alpha} \frac{D^{2\alpha}}{Dt^{2\alpha}}\right) s_{xy} = \mu \left(1 + \lambda_3^\beta \frac{D^\beta}{Dt^\beta} + \lambda_4^{2\beta} \frac{D^{2\beta}}{Dt^{2\beta}}\right) \left(\frac{\partial u}{\partial y}\right), \quad (3.5)$$

$$s_{yz} = s_{zz} = s_{yy} = s_{zx} = 0, \quad (3.6)$$

The present flow is governed by the following equations

$$\rho \frac{\partial u}{\partial t} = -\frac{\partial p}{\partial x} + \frac{\partial s_{xy}}{\partial y} - \frac{\sigma B_0^2 u}{1 - i\phi} + r, \quad (3.7)$$



$$\frac{\partial p}{\partial y} = 0. \quad (3.8)$$

The above expression indicates that  $p \neq p(y)$ .

From Eqs.(3.3),(3.5)and(3.7)one obtains

$$\begin{aligned} & \rho \left[ 1 + \lambda_1^\alpha \frac{D^\alpha}{Dt^\alpha} + \lambda_2^{2\alpha} \frac{D^{2\alpha}}{Dt^{2\alpha}} \right] \frac{\partial u}{\partial t} + \frac{\sigma B_0^2}{1 - i\phi} \left( 1 + \lambda_1^\alpha \frac{D^\alpha}{Dt^\alpha} + \lambda_2^{2\alpha} \frac{D^{2\alpha}}{Dt^{2\alpha}} \right) u \\ &= \mu \left( 1 + \lambda_3^\beta \frac{D^\beta}{Dt^\beta} + \lambda_4^{2\beta} \frac{D^{2\beta}}{Dt^{2\beta}} \right) \frac{\partial^2 u}{\partial y^2} - \frac{\mu \phi_1}{k_1} \left( 1 + \lambda_3^\beta \frac{D^\beta}{Dt^\beta} + \lambda_4^{2\beta} \frac{D^{2\beta}}{Dt^{2\beta}} \right) u. \end{aligned} \quad (3.9)$$

For non-dimensionalization, we now proceed to use Eq. (2.21) and the following quantities

$$\lambda_1^* = \frac{\lambda_1 U^2}{\nu}, \quad \lambda_2^* = \frac{\lambda_2 U^4}{\nu^2}, \quad \lambda_3^* = \frac{\lambda_3 U^2}{\nu}, \quad \lambda_4^* = \frac{\lambda_4 U^4}{\nu^2}. \quad (3.10)$$

### 3.2 Flow induced by a rigid plate

The non-dimensional problem in this case is of the form

$$\begin{aligned} & \left( 1 + \lambda_1^\alpha \frac{D^\alpha}{Dt^\alpha} + \lambda_2^{2\alpha} \frac{D^{2\alpha}}{Dt^{2\alpha}} \right) \frac{\partial u}{\partial t} + \frac{M^2}{1 - i\phi} \left( 1 + \lambda_1^\alpha \frac{D^\alpha}{Dt^\alpha} + \lambda_2^{2\alpha} \frac{D^{2\alpha}}{Dt^{2\alpha}} \right) u \\ &+ \frac{1}{K} \left( 1 + \lambda_3^\beta \frac{D^\beta}{Dt^\beta} + \lambda_4^{2\beta} \frac{D^{2\beta}}{Dt^{2\beta}} \right) u = \left( 1 + \lambda_3^\beta \frac{D^\beta}{Dt^\beta} + \lambda_4^{2\beta} \frac{D^{2\beta}}{Dt^{2\beta}} \right) \frac{\partial^2 u}{\partial y^2}, \end{aligned} \quad (3.11)$$

$$u(0, t) = \sum_{k=-\infty}^{k=\infty} a_k e^{ik\omega_0 t}, \quad (3.12)$$

$$u(\infty, t) = 0. \quad (3.13)$$

By Fourier transform treatment the problem in the  $\omega$ -plane reduces to

$$\frac{d^2 \Psi}{dy^2} - (\xi + i\eta)^2 \Psi = 0, \quad (3.14)$$

$$\begin{aligned} \Psi(0, \omega) &= \sum_{k=-\infty}^{k=\infty} 2\pi a_k \delta(\omega - k\omega_0), \\ \Psi(\infty, \omega) &= 0, \end{aligned} \quad (3.15)$$

where

$$(\xi + i\eta)^2 = \frac{(x_1x_2 + y_1y_2) + i(x_2y_1 - x_1y_2)}{x_2^2 + y_2^2} + \frac{1}{K},$$

$$\begin{aligned} x_1 = & -\frac{M^2}{1 + \phi^2} \left( 1 + |k\omega_0|^\alpha \lambda_1^\alpha \cos \frac{\alpha\pi}{2} + |k\omega_0|^{2\alpha} \lambda_2^{2\alpha} \cos \alpha\pi \right) \\ & + \left( \frac{\phi M^2}{1 + \phi^2} \right) \left( |k\omega_0|^\alpha \lambda_1^\alpha \sin \frac{\alpha\pi}{2} + |k\omega_0|^{2\alpha} \lambda_2^{2\alpha} \sin \alpha\pi \right) \text{sign}(k\omega_0) \\ & - \left( |k\omega_0|^\alpha \lambda_1^\alpha \cos \frac{\alpha\pi}{2} + |k\omega_0|^{2\alpha} \lambda_2^{2\alpha} \cos \alpha\pi \right), \end{aligned}$$

$$\begin{aligned} y_1 = & \left( \frac{-\phi M^2}{1 + \phi^2} \right) \left( 1 + |k\omega_0|^\alpha \lambda_1^\alpha \cos \frac{\alpha\pi}{2} + |k\omega_0|^{2\alpha} \lambda_2^{2\alpha} \cos \alpha\pi \right) - k\omega_0 \\ & + \left( 1 + \frac{M^2}{1 + \phi^2} \right) \left( 1 + |k\omega_0|^\alpha \lambda_1^\alpha \cos \frac{\alpha\pi}{2} + |k\omega_0|^{2\alpha} \lambda_2^{2\alpha} \cos \alpha\pi \right) \text{sign}(k\omega_0), \end{aligned}$$

$$x_2 = 1 + |k\omega_0|^\beta \lambda_3^\beta \cos \frac{\beta\pi}{2} + |k\omega_0|^{2\beta} \lambda_4^{2\beta} \cos \beta\pi,$$

$$y_2 = \left( |k\omega_0|^\beta \lambda_3^\beta \sin \frac{\beta\pi}{2} + |k\omega_0|^{2\beta} \lambda_4^{2\beta} \sin \beta\pi \right) \text{sign}(k\omega_0).$$

The solution of problem consisting of Eqs. (3.14) and (3.15) is

$$u(y, t) = \sum_{k=-\infty}^{k=\infty} a_k e^{-\xi_k y + i(k\omega_0 t - \eta_k y)}, \quad (3.16)$$

where

$$\xi_k = \sqrt{\frac{\sqrt{L_r^2 + L_i^2} + L_r}{2}},$$

$$\eta_k = \sqrt{\frac{\sqrt{L_r^2 + L_i^2} - L_r}{2}},$$

$$L_r = \frac{(x_1x_2 + y_1y_2)}{x_2^2 + y_2^2} + \frac{1}{K},$$

$$L_i = \frac{(x_2y_1 - x_1y_2)}{x_2^2 + y_2^2}.$$

Now our interest lies in finding the velocity fields corresponding to the oscillations defined below.

| Oscillations                                                             | Fourier coefficients                                       |
|--------------------------------------------------------------------------|------------------------------------------------------------|
| $f(t)$                                                                   | $a_k$                                                      |
| i) $e^{i\omega_0 t}$                                                     | $a_1 = 1$ and $a_k = 0$ otherwise                          |
| ii) $\cos \omega_0 t$                                                    | $a_1 = a_{-1} = \frac{1}{2}$ and $a_k = 0$ otherwise       |
| iii) $\sin \omega_0 t$                                                   | $a_1 = -a_{-1} = \frac{1}{2i}$ and $a_k = 0$ otherwise     |
| iv) $\begin{cases} 1, &  t  < T_1 \\ 0, & T_1 <  t  < T_0/2 \end{cases}$ | $a_0 = 2T_1/T_0$ , $a_k = \sin \frac{k\omega_0 T_1}{k\pi}$ |
| v) $\sum_{k=-\infty}^{\infty} \delta(t - kT_0)$                          | $a_k = \frac{1}{T_0}$ for all $k$ ,                        |

(3.17)

The expressions of resulting velocity fields are

$$u_1(y, t) = e^{-\xi_1 y + i(\omega_0 t - \eta_1 y)}, \quad (3.18)$$

$$u_2(y, t) = \frac{1}{2} \left[ e^{-\xi_1 y + i(\omega_0 t - \eta_1 y)} + e^{-\xi_{-1} y - i(\omega_0 t + \eta_{-1} y)} \right], \quad (3.19)$$

$$u_3(y, t) = \frac{1}{2i} \left[ e^{-\xi_1 y + i(\omega_0 t - \eta_1 y)} - e^{-\xi_{-1} y - i(\omega_0 t + \eta_{-1} y)} \right], \quad (3.20)$$

$$u_4(y, t) = \frac{1}{\pi} \sum_{k=-\infty}^{\infty} \sin \frac{k\omega_0 T_1}{k} e^{\xi_k y + i(\omega_0 t - \eta_k y)}, \quad k \neq 0, \quad (3.21)$$

$$u_5(y, t) = \frac{1}{T_0} e^{-\xi_k y + i(\omega_0 t - \eta_k y)}. \quad (3.22)$$

### 3.3 Periodic flows between two plates

The non-dimensional problem here is expressed as

$$\begin{aligned} & \left[ 1 + \lambda_1^\alpha \frac{D^\alpha}{Dt^\alpha} + \lambda_2^{2\alpha} \frac{D^{2\alpha}}{Dt^{2\alpha}} \right] \frac{\partial u}{\partial t} + \frac{M^2}{1 - i\phi} \left( 1 + \lambda_1^\alpha \frac{D^\alpha}{Dt^\alpha} + \lambda_2^{2\alpha} \frac{D^{2\alpha}}{Dt^{2\alpha}} \right) u \\ & + \frac{1}{K} \left( 1 + \lambda_3^\beta \frac{D^\beta}{Dt^\beta} + \lambda_4^{2\beta} \frac{D^{2\beta}}{Dt^{2\beta}} \right) u = \left( 1 + \lambda_3^\beta \frac{D^\beta}{Dt^\beta} + \lambda_4^{2\beta} \frac{D^{2\beta}}{Dt^{2\beta}} \right) \frac{\partial^2 u}{\partial y^2}, \end{aligned} \quad (3.23)$$

$$\begin{aligned}
u(0, t) &= \sum_{k=-\infty}^{\infty} a_k e^{ik\omega_0 t}, \quad t > 0, \\
u(1, t) &= 0, \quad \text{for all } t
\end{aligned} \tag{3.24}$$

and the resulting velocity fields are

$$u(y, t) = \sum_{k=-\infty}^{\infty} a_k \frac{\sinh \gamma_k (1-y)}{\sinh \gamma_k} e^{ik\omega_0 t}, \tag{3.25}$$

$$u_1(y, t) = \frac{\sinh \gamma_1 (1-y)}{\sinh \gamma_1} e^{i\omega_0 t}, \tag{3.26}$$

$$u_2(y, t) = \frac{1}{2} \left[ \frac{\sinh \gamma_1 (1-y)}{\sinh \beta_1} e^{i\omega_0 t} + \frac{\sinh \gamma_{-1} (1-y)}{\sinh \beta_{-1}} e^{-i\omega_0 t} \right], \tag{3.27}$$

$$u_3(y, t) = \frac{1}{2i} \left[ \frac{\sinh \gamma_1 (1-y)}{\sinh \gamma_1} e^{i\omega_0 t} - \frac{\sinh \gamma_{-1} (1-y)}{\sinh \gamma_{-1}} e^{-i\omega_0 t} \right], \tag{3.28}$$

$$u_4(y, t) = \sum_{k=-\infty}^{\infty} \frac{\sin k\omega_0 T_1}{k\pi} \frac{\sinh \gamma_k (1-y)}{\sinh \gamma_k} e^{ik\omega_0 t}, \quad k \neq 0, \tag{3.29}$$

$$u_5(y, t) = \frac{1}{T_0} \sum_{k=-\infty}^{\infty} \frac{\sinh \gamma_k (1-y)}{\sinh \gamma_k} e^{ik\omega_0 t}, \tag{3.30}$$

where

$$\gamma_k^2 = (\xi_k + i\eta_k)^2.$$

### 3.4 Poiseuille flow

The solution of Eq. (3.9) alongwith conditions (2.46) and (2.47) is

$$u(y, t) = Q_0 \frac{\left\{ \begin{aligned} &1 + \lambda_1^\alpha |\omega_0|^\alpha \left( \cos \frac{\alpha\pi}{2} + i \operatorname{sign} \omega_0 \sin \frac{\alpha\pi}{2} \right) \\ &+ \lambda_2^{2\alpha} |\omega_0|^{2\alpha} \left( \cos \alpha\pi + i \operatorname{sign} \omega_0 \sin \alpha\pi \right) \end{aligned} \right\} \times (\cosh \gamma^* y - \cosh \gamma^*) e^{i\omega_0 t}}{\gamma^{*2} \left\{ \begin{aligned} &1 + \lambda_3^\beta |\omega_0|^\beta \left( \cos \frac{\beta\pi}{2} + i \operatorname{sign} \omega_0 \sin \frac{\beta\pi}{2} \right) \\ &+ \lambda_4^{2\beta} |\omega_0|^{2\beta} \left( \cos \beta\pi + i \operatorname{sign} \omega_0 \sin \beta\pi \right) \end{aligned} \right\} \cosh \gamma^*}, \tag{3.31}$$

$$\gamma^* = \gamma_k|_{k=1}$$

### 3.5 Results and discussion

Table 3.1: Velocities at  $y = 1/2$  when the flow of fractional generalized Burgers' fluid is produced by a rigid plate.

| Types of the fluid | Rheological parameter                                            | $u(y, t), \phi = 0$ | $u(y, t), \phi = 2$ |
|--------------------|------------------------------------------------------------------|---------------------|---------------------|
| Newtonian          | $\lambda_i = 0 \quad (i = 1 - 4)$                                | 0.479321            | 0.699011            |
| Maxwell            | $\lambda_i = 0 \quad (i = 2 - 4), \lambda_1 = 2$                 | 0.368084            | 0.697365            |
| Second grade       | $\lambda_1 = \lambda_2 = \lambda_4 = 0, \lambda_3 = 1.5$         | 0.516043            | 0.720708            |
| Oldroyd-B          | $\lambda_1 = 2, \lambda_2 = \lambda_4 = 0, \lambda_3 = 1.5$      | 0.416278            | 0.707905            |
| Burger's           | $\lambda_1 = 2, \lambda_2 = 1, \lambda_4 = 0, \lambda_3 = 1.5$   | 0.408554            | 0.712404            |
| Generalized-Burger | $\lambda_1 = 2, \lambda_2 = 1, \lambda_4 = 0.5, \lambda_3 = 1.5$ | 0.407047            | 0.711337            |

Table 3.2: Velocities at  $y = 1/2$  when the flow of fractional generalized Burgers' fluid is produced between two plates.

| Types of the fluid | Rheological parameter                                            | $u(y, t), \phi = 0$ | $u(y, t), \phi = 2$ |
|--------------------|------------------------------------------------------------------|---------------------|---------------------|
| Newtonian          | $\lambda_i = 0 \quad (i = 1 - 4)$                                | 0.396106            | 0.432768            |
| Maxwell            | $\lambda_i = 0 \quad (i = 2 - 4), \lambda_1 = 2$                 | 0.383785            | 0.431392            |
| Second grade       | $\lambda_1 = \lambda_2 = \lambda_4 = 0, \lambda_3 = 1.5$         | 0.400399            | 0.433825            |
| Oldroyd-B          | $\lambda_1 = 2, \lambda_2 = \lambda_4 = 0, \lambda_3 = 1.5$      | 0.387297            | 0.432115            |
| Burger's           | $\lambda_1 = 2, \lambda_2 = 1, \lambda_4 = 0, \lambda_3 = 1.5$   | 0.386772            | 0.432475            |
| Generalized-Burger | $\lambda_1 = 2, \lambda_2 = 1, \lambda_4 = 0.5, \lambda_3 = 1.5$ | 0.386489            | 0.432417            |

Table 3.3: Velocities at  $y = 1/2$  when the flow of fractional generalized Burgers' fluid is produced between two plates due to oscillating pressure gradient.

| Types of the fluid | Rheological parameter                                            | $u(y, t), \phi = 0$ | $u(y, t), \phi = 2$ |
|--------------------|------------------------------------------------------------------|---------------------|---------------------|
| Newtonian          | $\lambda_i = 0 \quad (i = 1 - 4)$                                | 0.210496            | 0.254813            |
| Maxwell            | $\lambda_i = 0 \quad (i = 2 - 4), \lambda_1 = 2$                 | 0.260184            | 0.341175            |
| Second grade       | $\lambda_1 = \lambda_2 = \lambda_4 = 0, \lambda_3 = 1.5$         | 0.194183            | 0.232894            |
| Oldroyd-B          | $\lambda_1 = 2, \lambda_2 = \lambda_4 = 0, \lambda_3 = 1.5$      | 0.25084             | 0.324288            |
| Burger's           | $\lambda_1 = 2, \lambda_2 = 1, \lambda_4 = 0, \lambda_3 = 1.5$   | 0.251671            | 0.330089            |
| Generalized-Burger | $\lambda_1 = 2, \lambda_2 = 1, \lambda_4 = 0.5, \lambda_3 = 1.5$ | 0.252193            | 0.31191             |

A comparison of the different types of fluid when velocities are produced by the rigid plate, between two oscillating plates and due to Poiseuille flow are also given in the tables. Graphs are included only for classical generalized Burgers' fluid and fractional generalized Burgers' fluid. The effect of various emerging parameters especially Hartman number  $M$ , Hall parameter  $\phi$ , porosity parameter  $K$  and fractional parameters  $\alpha$  and  $\beta$  of the generalized Burgers' fluid on the velocity profile are investigated.

From Tables 3.1 and 3.2 it is important to note that second grade fluid has the maximum velocity in the presence as well as in the absence of Hall parameter when compared with other fluids whereas Maxwell fluid has minimum. In Table 3.3 it is shown that velocity is maximum for the Maxwell fluid and minimum for the second grade fluid in the presence and absence of Hall current. It is anticipated from Tables 3.1-3.3 that velocity in the presence of Hall current is greater when compared with the absence of Hall current.

Figures 3.1-3.5 are prepared to show the effect of increasing Hartman number  $M$  for the velocity in classical generalized Burgers' ( $\alpha = \beta = 1$ ) fluid and fractional generalized Burgers' fluid ( $\alpha = 0.5, \beta = 0.8$ ) produced by the oscillation of the rigid plate in the absence as well as in the presence of Hall parameter  $\phi$ . The values of the other parameters are kept fixed ( $\lambda_1 = 2, \lambda_2 = 1, \lambda_3 = 1.5$  are  $\lambda_4 = 0.5$ ). These Figures show that an increase in Hartman number  $M$  decreases the velocity profile monotonically. This is due to the effect of magnetic force against the direction of flow. The velocity profile increases if we increase porosity parameter  $K$ .

Figures 3.8-3.12 show the behavior of the velocity produced between two plates for the classical and fractional generalized Burgers' fluid. It is seen that velocity decreases by increasing the Hartman number  $M$  while it increases if we increase the porosity parameter  $K$ .

Figures 3.15-3.19 describe the variation of the velocity produced by the imposition of periodic pressure gradient in the  $x$ - direction. It is noted that velocity in generalized Burgers' fluid and fractional generalized Burgers' fluid decreases with an increase of Hartman number  $M$  in the absence and presence of Hall parameter  $\phi$ . The velocity increases with an increase in porosity parameter  $K$ .

From Figures (3.6), (3.7), (3.13), (3.14), (3.20) and (3.21) we note that velocity profiles have opposite effects on both fractional parameters  $\alpha$  and  $\beta$  in all three cases.

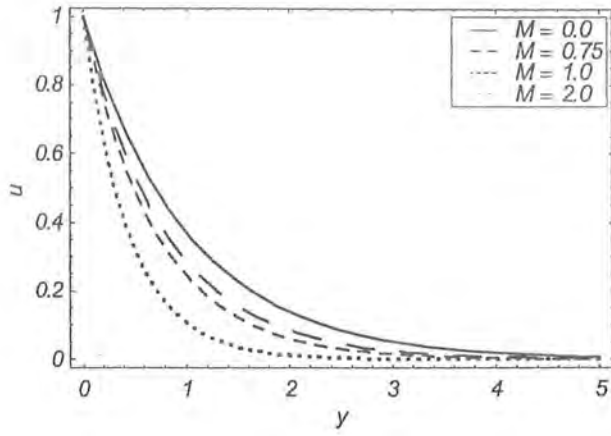


Figure 3.1: Velocity profile  $u(y, t)$  (flow induced by rigid plate) in classical generalized Burgers' fluid for different values of Hartman number  $M$  when  $\phi = 0$ .

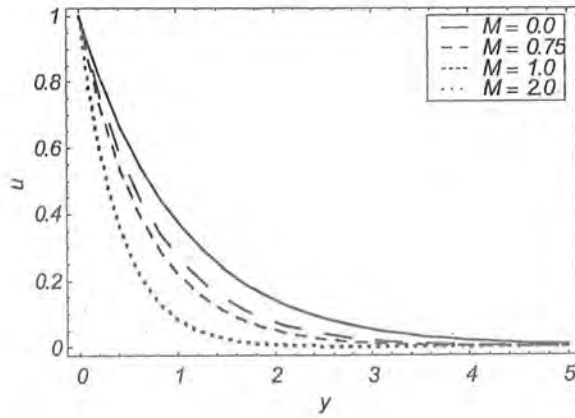


Figure 3.2: Velocity profile  $u(y, t)$  (flow induced by rigid plate) in fractional generalized Burgers' fluid for different values of Hartman number  $M$  when  $\phi = 0$ .



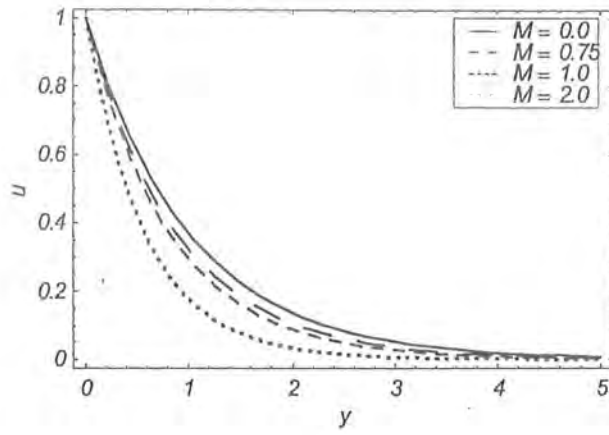


Figure 3.3: Velocity profile  $u(y, t)$  (flow induced by rigid plate) in classical generalized Burgers' fluid for different values of Hartman number  $M$  when  $\phi = 2$ .

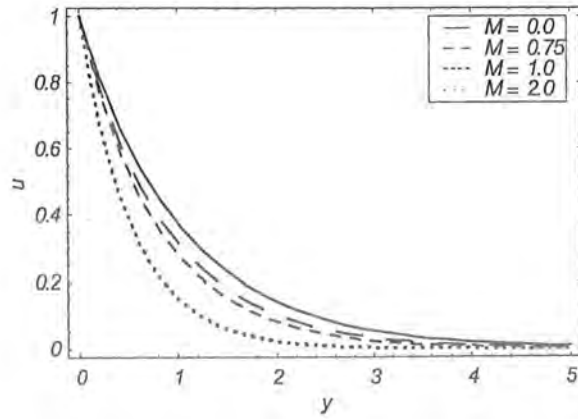


Figure 3.4: Velocity profile  $u(y, t)$  (flow induced by rigid plate) in fractional generalized Burgers' fluid for different values of Hartman number  $M$  when  $\phi = 2$ .

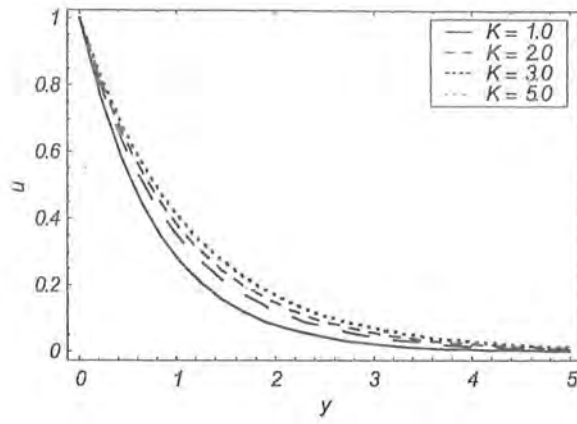


Figure 3.5: Velocity profile  $u(y, t)$  (flow induced by rigid plate) in fractional generalized Burgers' fluid for different values of porosity parameter  $K$  when  $\phi = 2$ .

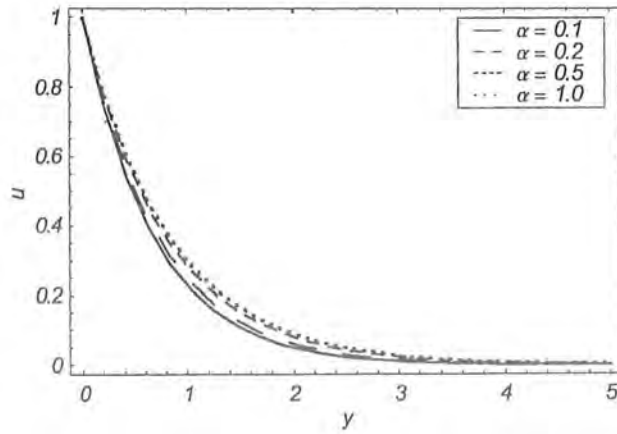


Figure 3.6: Effect of fractional parameter  $\alpha$  on the velocity profile (flow induced by rigid plate) in fractional generalized Burgers' fluid when  $\phi = 2$ .

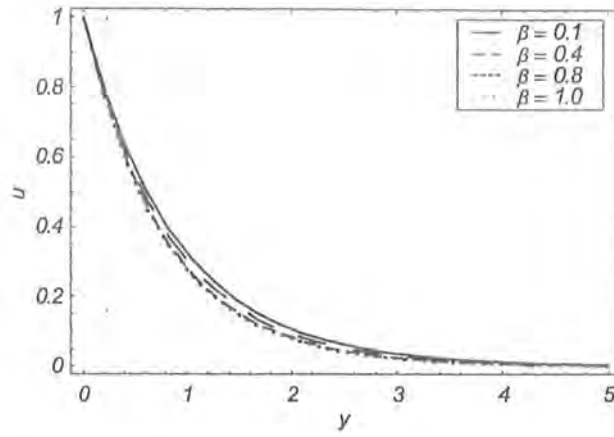


Figure 3.7: Effect of fractional parameter  $\beta$  on the velocity profile (flow induced by rigid plate) in fractional generalized Burgers' fluid when  $\phi = 2$ .

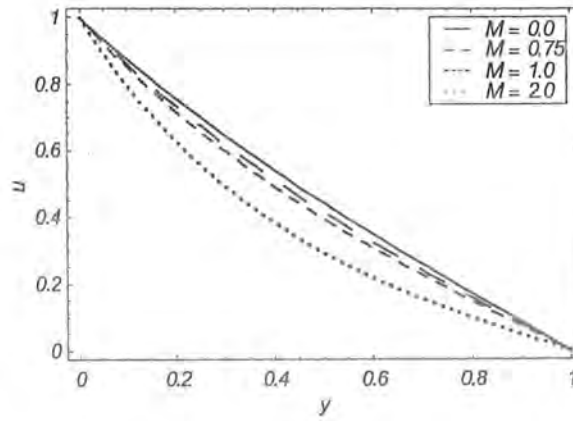


Figure 3.8: Velocity profile  $u(y,t)$  (periodic flow between two plates) in classical generalized Burgers' fluid for different values of Hartman number  $M$  when  $\phi = 0$ .

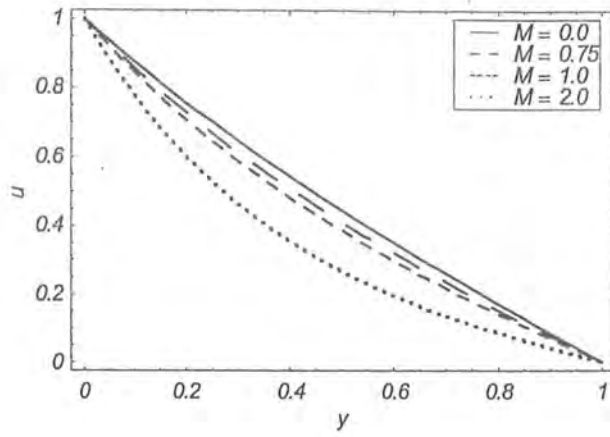


Figure 3.9: Velocity profile  $u(y, t)$  (periodic flow between two plates) in fractional generalized Burgers' fluid for different values of Hartman number  $M$  when  $\phi = 0$ .

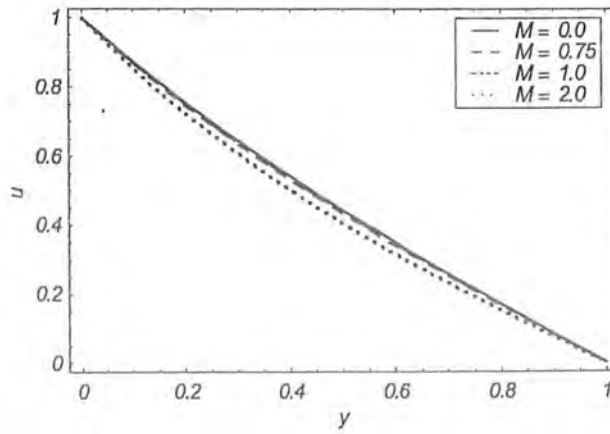


Figure 3.10: Velocity profile  $u(y, t)$  (periodic flow between two plates) in classical generalized Burgers' fluid for different values of Hartman number  $M$  when  $\phi = 2$ .

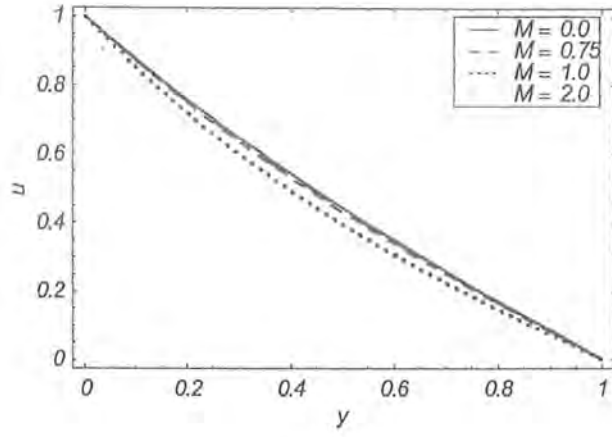


Figure 3.11: Velocity profile  $u(y, t)$  (periodic flow between two plates) in fractional generalized Burgers' fluid for different values of Hartman number  $M$  when  $\phi = 2$ .

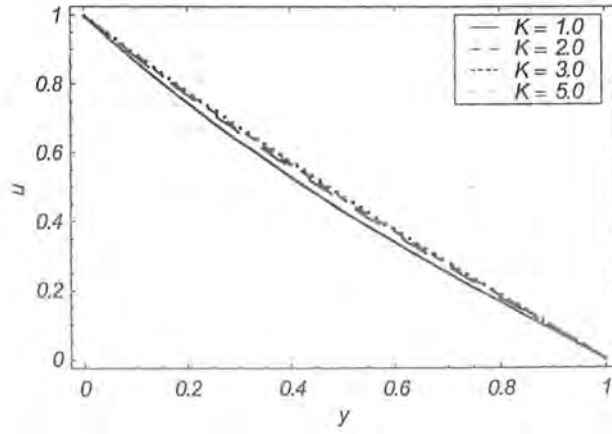


Figure 3.12: Velocity profile  $u(y, t)$  (periodic flow between two plates) in fractional generalized Burgers' fluid for different values of porosity parameter  $K$  when  $\phi = 2$ .

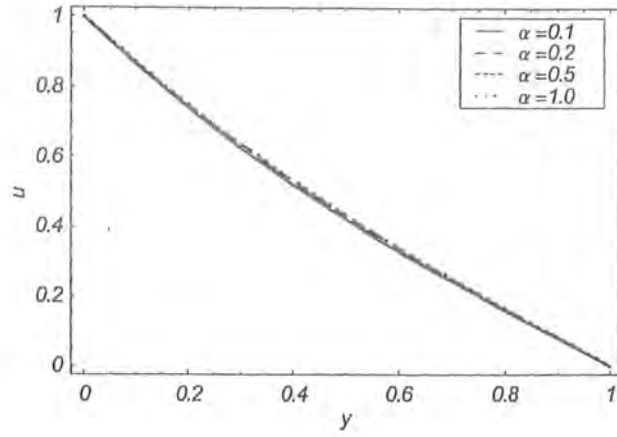


Figure 3.13: Effect of fractional parameter  $\alpha$  on the velocity profile (periodic flow between two plates) in fractional generalized Burgers' fluid when  $\phi = 2$ .

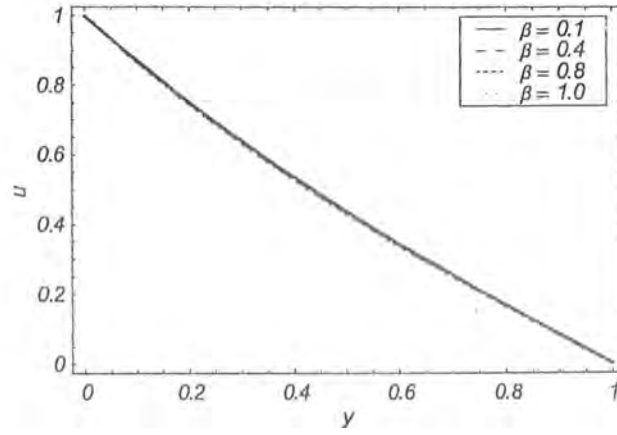


Figure 3.14: Effect of fractional parameter  $\beta$  on the velocity profile (periodic flow between two plates) in fractional generalized Burgers' fluid when  $\phi = 2$ .

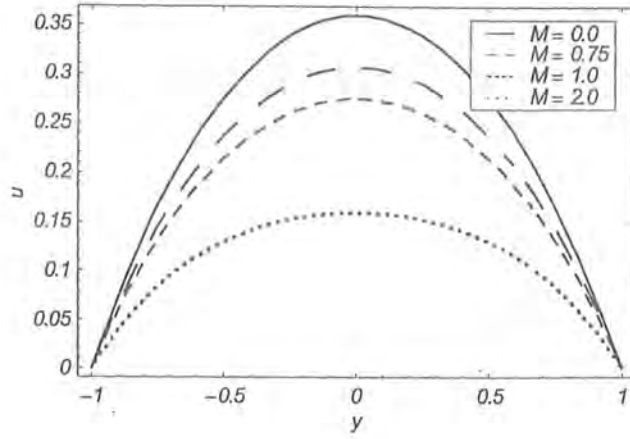


Figure 3.15: Velocity profile  $u(y,t)$  (Poiseuille flow) in classical generalized Burgers' fluid for different values of Hartman number  $M$  when  $\phi = 0$ .

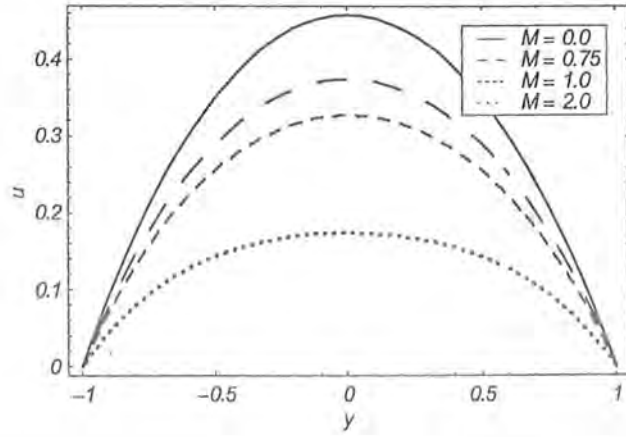


Figure 3.16: Velocity profile  $u(y,t)$  (Poiseuille flow) in fractional generalized Burgers' fluid for different values of Hartman number  $M$  when  $\phi = 0$ .

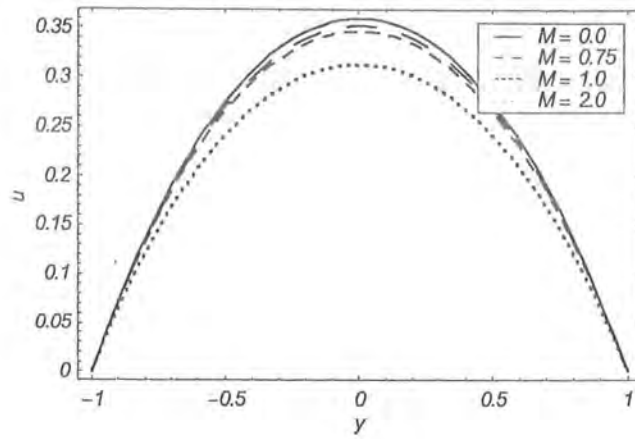


Figure 3.17: Velocity profile  $u(y, t)$  (Poiseuille flow) in classical generalized Burgers' fluid for different values of Hartman number  $M$  when  $\phi = 2$ .

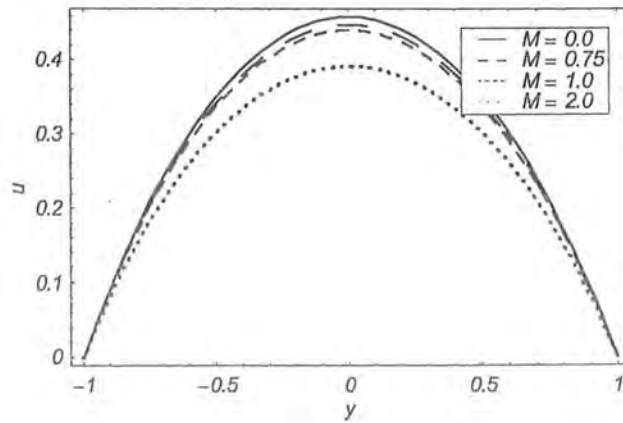


Figure 3.18: Velocity profile  $u(y, t)$  (Poiseuille flow) in fractional generalized Burgers' fluid for different values of Hartman number  $M$  when  $\phi = 2$ .



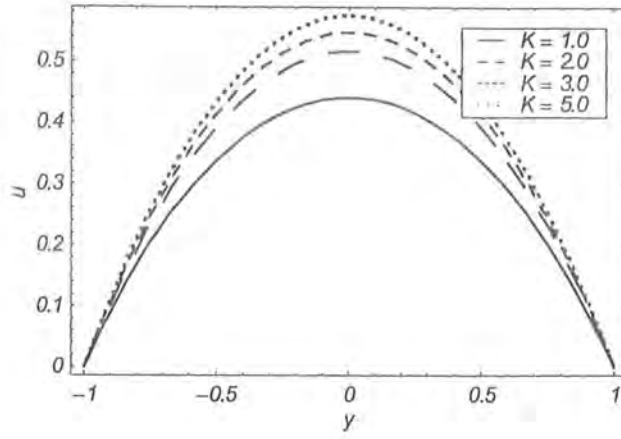


Figure 3.19: Velocity profile  $u(y, t)$  (Poiseuille flow) in fractional generalized Burgers' fluid for different values of porosity parameter  $K$  when  $\phi = 2$ .

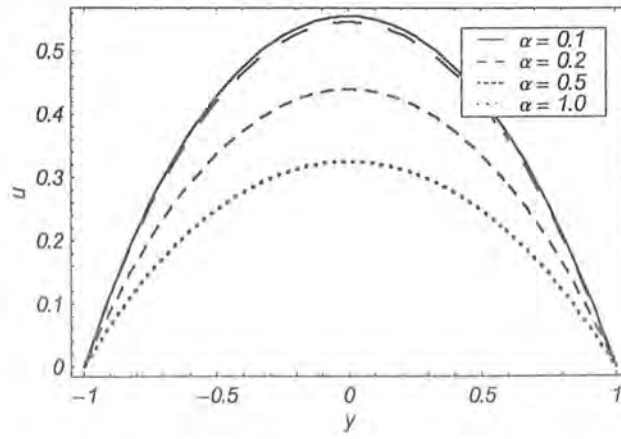


Figure 3.20: Effect of fractional parameter  $\alpha$  on the velocity profile (Poiseuille flow) in fractional generalized Burgers' fluid when  $\phi = 2$ .

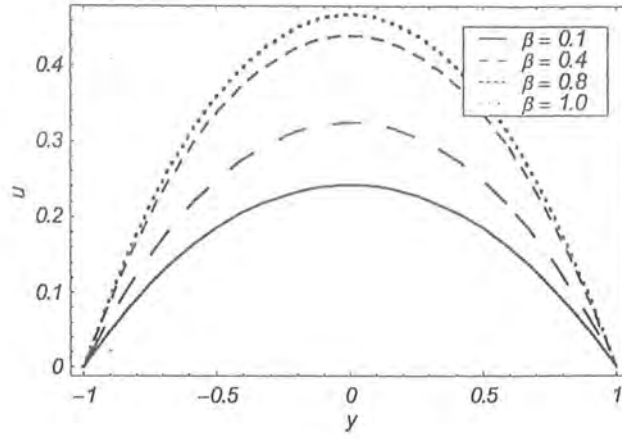


Figure 3.21: Effect of fractional parameter  $\beta$  on the velocity profile (Poiseuille flow) in fractional generalized Burgers' fluid when  $\phi = 2$ .

## Chapter 4

# The influence of Hall current and heat transfer on the steady flow of a generalized Burgers' fluid induced by a sudden pull of eccentric rotating disks

This chapter looks at the effects of Hall current and heat transfer on the magnetohydrodynamic flow of a generalized Burgers' fluid between two eccentric rotating infinite disks of different temperatures. The flow is induced by a pull with constant velocities to the disks. Induced magnetic field is neglected under the assumption of a small magnetic Reynolds number. Analytic solutions for the velocity, temperature, force and torque are constructed. The results of velocity and temperature profiles are described by displaying graphs for various physical parameters of interest.

## 4.1 Mathematical formulation

Let us consider the flow of an electrically conducting generalized Burgers' fluid between two infinite disks rotating with angular velocity  $\Omega$  about two non-coaxial axes distant  $2l$  apart. We choose a Cartesian coordinate system  $(x, y, z)$ . The  $z$ -axis is taken normal to the disks and a constant strong magnetic field is applied. No electric field is applied. The disks at  $z = h$  and  $z = -h$  are pulled with constant velocities  $U$  and  $-U$ , respectively. (See Fig. 4.1).

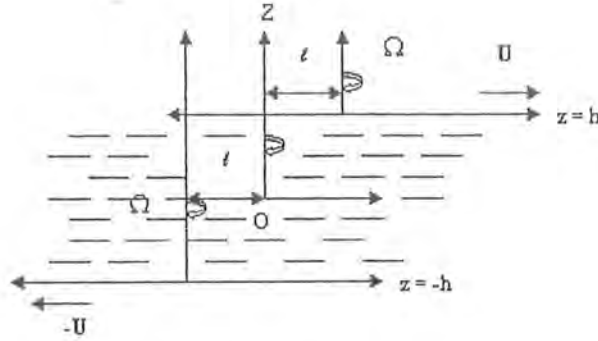


Fig. 4.1: Geometry of flow problem.

If the components of the velocity vector  $\mathbf{V}$  are given by  $u, v, w$  then the subjected boundary conditions are

$$\begin{aligned} u &= -\Omega(y-l) + U_1, & v &= \Omega x + U_2 & \text{at } z = h, \\ u &= -\Omega(y+l) - U_1, & v &= \Omega x - U_2 & \text{at } z = -h. \end{aligned} \quad (4.1)$$

The above conditions suggest a velocity distribution of the form

$$u = -\Omega y + f(z), \quad v = \Omega x + g(z), \quad (4.2)$$

which together with an incompressibility condition ( $\text{div} \mathbf{V} = 0$ ) leads to  $w = 0$ .

The Cauchy stress tensor  $\mathbf{T}$  in a generalized Burgers' fluid is [128]

$$\mathbf{T} = -p\mathbf{I} + \mathbf{S}, \quad (4.3)$$

$$\mathbf{S} + \lambda_1 \frac{D\mathbf{S}}{Dt} + \lambda_2 \frac{D^2\mathbf{S}}{Dt^2} = \mu \left( 1 + \lambda_3 \frac{D}{Dt} + \lambda_4 \frac{D^2}{Dt^2} \right) \mathbf{A}_1, \quad (4.4)$$

in which  $\mathbf{S}$  is an extra stress tensor,  $-p\mathbf{I}$  the indeterminate spherical stress,  $\mathbf{A}_1$  the first Rivlin Ericksen tensor,  $\mu$  the dynamic viscosity,  $\lambda_i$  ( $i = 1, 2$ ) the relaxation time and  $\lambda_i$  ( $i = 3, 4$ ) the retardation times and

$$\frac{D\mathbf{S}}{Dt} = \frac{d\mathbf{S}}{dt} - \mathbf{L}\mathbf{S} - \mathbf{S}\mathbf{L}^T, \quad (4.5)$$

is the upper convected time derivative and  $D^2\mathbf{S}/Dt^2 = D/Dt(D\mathbf{S}/Dt)$ . In Eq. (4.5),  $\mathbf{L}$  is the velocity gradient,  $d/dt$  is the material time derivative and  $\lambda_1 > \lambda_3$ .

Invoking equations (2.4) and (4.2) in equation (4.3) we obtain

$$\begin{aligned} S_{xx} + 2\lambda_1 (\Omega S_{xy} - S_{xz}f') - 2\Omega\lambda_2 (\Omega(S_{xx} - S_{yy})) \\ + f' S_{yz} + g' S_{zx} = -2\mu (\lambda_3 f' + 3\Omega\lambda_4 g') f', \end{aligned} \quad (4.6)$$

$$\begin{aligned} S_{xy} - \lambda_1 (\Omega(S_{xx} - S_{yy}) + f' S_{yz} + g' S_{zx}) \\ - \lambda_2 \Omega (4\Omega S_{xy} + 3 (g' S_{yz} - f' S_{zx})) \\ = \mu (3\Omega\lambda_4 ((f')^2 - (g')^2) - 2\lambda_3 f' g'), \end{aligned} \quad (4.7)$$

$$\begin{aligned} S_{yy} - 2\lambda_1 (\Omega S_{xy} + S_{yz}g') + 2\Omega\lambda_2 (\Omega(S_{xx} - S_{yy})) \\ + f' S_{yz} + 2g' S_{zx} = -2\mu (\lambda_3 g' - 3\Omega\lambda_4 f') g', \end{aligned} \quad (4.8)$$

$$\begin{aligned} S_{xz} - \lambda_1 (f' S_{zz} - \Omega S_{yz}) - \lambda_2 \Omega^2 S_{xz} \\ = \mu (f' + \lambda_3 \Omega g' - \lambda_4 \Omega^2 f'), \end{aligned} \quad (4.9)$$

$$\begin{aligned} S_{yz} - \lambda_2 \Omega (\Omega S_{yz} - f' S_{zz}) - \lambda_1 \Omega S_{xz} \\ = \mu (g' - \lambda_3 \Omega f' - \lambda_4 \Omega^2 g'), \end{aligned} \quad (4.10)$$

$$S_{zz} = 0, \quad (4.11)$$

where primes indicate differentiation with respect to  $z$ .

One can solve equations (4.6) to (4.11) to derive the following expressions

$$S_{xx} = 2\mu \frac{(b_1 f'^2 + b_2 g'^2 + b_3 f'g')}{c\alpha_1\alpha_2}, \quad (4.12)$$

$$S_{yy} = -2\mu \frac{(c_1 f'^2 + c_2 g'^2 + c_3 f'g')}{c\alpha_1\alpha_2}, \quad (4.13)$$

$$S_{xy} = \mu \frac{(a_1 f'^2 + a_2 g'^2 + a_3 f'g')}{c\alpha_1}, \quad (4.14)$$

$$S_{xz} = \mu \frac{af' + b\Omega g'}{c}, \quad (4.15)$$

$$S_{yz} = \mu \frac{ag' - b\Omega f'}{c}, \quad (4.16)$$

whence

$$a = (1 - \lambda_2\Omega^2)(1 - \lambda_4\Omega^2) + \lambda_1\lambda_3\Omega^2,$$

$$b = (1 - \lambda_2\Omega^2)\lambda_3 - \lambda_1(1 - \lambda_4\Omega^2), \quad c = (1 - \lambda_2\Omega^2)^2 + \lambda_1^2\Omega^2,$$

$$a_1 = a\{2\lambda_1^2\Omega - 3\lambda_2\Omega(1 - 4\lambda_2\Omega^2)\} - b\{4\lambda_1\lambda_2\Omega^2 + \lambda_1(1 - 4\lambda_2\Omega^2)\} \\ + c\Omega\{2\lambda_1\lambda_3 + 3\lambda_4(1 - 4\lambda_2\Omega^2)\},$$

$$a_2 = -a\{2\lambda_1^2\Omega - 3\lambda_2\Omega(1 - 4\lambda_2\Omega^2)\} + b\{6\lambda_1\lambda_2\Omega^2 + \lambda_1(1 - 4\lambda_2\Omega^2)\} \\ + c\Omega\{2\lambda_1\lambda_3 - 3\lambda_4(1 - 4\lambda_2\Omega^2)\},$$

$$a_3 = 2b\{2\lambda_1^2\Omega - 3\lambda_2\Omega(1 - 4\lambda_2\Omega^2)\} + 2a\{5\lambda_1\lambda_2\Omega^2 + \lambda_1(1 - 4\lambda_2\Omega^2)\} \\ - 2c\{6\lambda_1\lambda_4\Omega^2 + \lambda_3(1 - 4\lambda_2\Omega^2)\},$$

$$b_1 = (1 - 2\lambda_2\Omega^2)\{\lambda_1(a\alpha_1 - a_1\Omega) - \alpha_1(b\lambda_2\Omega + c\lambda_3)\} - 2\lambda_2\Omega^3(a_1\lambda_1 + b\lambda_2\alpha_1),$$

$$b_2 = (1 - 2\lambda_2\Omega^2)\Omega(b\alpha_1\lambda_2 - a_2\lambda_1) + 4\alpha_1\lambda_2\Omega^2(c\lambda_3 + b\lambda_2\Omega),$$

$$b_3 = (1 - 2\lambda_2\Omega^2)\{\lambda_1(b\alpha_1 - a_3\Omega) + \alpha_1\Omega(2a\lambda_2 - 3c\lambda_4)\} \\ + 2\alpha_1\lambda_2\Omega^2(b\lambda_1 + 3a\lambda_2\Omega) - 2\lambda_2\Omega^3(3c\alpha_1\lambda_4 + a_3\lambda_1),$$

$$c_1 = (1 - 2\lambda_2\Omega^2)\{\lambda_1a_1 + b\alpha_1\lambda_2\}\Omega - 2\lambda_2\Omega^2\{\lambda_1(a\alpha_1 - a_1\Omega) - \alpha_1(b\lambda_2\Omega + c\lambda_3)\},$$

$$c_2 = -2\alpha_1(1 - 2\lambda_2\Omega^2)\{\lambda_3c + b\lambda_2\Omega\} - 2\lambda_2\Omega^3\{b\lambda_2\alpha_1 - a_2\lambda_1\},$$

$$c_3 = (1 - 2\lambda_2\Omega^2)\{(3c\lambda_4a_1 + a_3\lambda_1)\Omega - \alpha_1(3a\lambda_2\Omega + b\lambda_1)\} \\ - 2\lambda_2\Omega^2\{2\lambda_2a\alpha_1\Omega - 3ca_1\lambda_4\Omega + \lambda_1(b\alpha_1 - a_3\Omega)\},$$

$$\alpha_1 = (1 - 4\lambda_2\Omega^2)^2 + 4\lambda_1^2\Omega^2, \quad \alpha_2 = (1 - 2\lambda_2\Omega^2)^2 - 4\lambda_2^2\Omega^2.$$

On putting equations (2.8), (2.9), (4.2) and (4.3) into equation (2.1) one can write

$$\frac{\partial p}{\partial x} = \rho\Omega(\Omega x + g(z)) + \frac{\partial S_{xz}}{\partial z} + \frac{\sigma B_0^2(1+i\phi)}{1+\phi^2} \left( \frac{Q}{2h} - f \right), \quad (4.17)$$

$$\frac{\partial p}{\partial y} = -\rho\Omega(-\Omega y + f(z)) + \frac{\partial S_{yz}}{\partial z} + \frac{\sigma B_0^2(1+i\phi)}{1+\phi^2} \left( \frac{P}{2h} - g \right), \quad (4.18)$$

where

$$P = \int_{-h}^h g(z) dz, \quad Q = \int_{-h}^h f(z) dz \quad (4.19)$$

and  $z$ -component of momentum equation shows that  $p \neq p(z)$ .

The version of boundary conditions (4.1) in  $f$  and  $g$  takes the form

$$f(h) = \Omega l + U_1, \quad g(h) = U_2, \quad (4.20)$$

$$f(-h) = -\Omega l - U_1, \quad g(-h) = -U_2. \quad (4.21)$$

Due to equations (4.17)-(4.19)

$$\rho\Omega g(z) + \frac{\partial S_{xz}}{\partial z} - Hf = C_1, \quad (4.22)$$

$$-\rho\Omega f(z) + \frac{\partial S_{yz}}{\partial z} - Hg = C_2, \quad (4.23)$$

$$H = \frac{\sigma B_0^2 (1 + i\phi)}{1 + \phi^2} \quad (4.24)$$

and  $C_i$  ( $i = 1, 2$ ) are the arbitrary constants of integration. Integrating Eqs. (4.17) and (4.18) we have

$$p = p_0 + \frac{1}{2}\Omega^2 (x^2 + y^2) + \left[ C_1 + \frac{HQ}{2h} \right] x + \left[ C_2 + \frac{HP}{2h} \right] y, \quad (4.25)$$

where  $p_0$  is the reference pressure. We see from above equation that non-zero values of  $C_1 + \frac{HQ}{2h}$  and  $C_2 + \frac{HP}{2h}$  would give rise to a pressure gradient between the disks with a corresponding Poiseuille type flow. In order to remove the possibility of the Poiseuille flow and at the same time to ensure the symmetry of the velocity distribution about the disk  $z = 0$ , we put

$$C_1 = -\frac{HQ}{2h}, \quad C_2 = -\frac{HP}{2h}. \quad (4.26)$$

Upon making use of Eqs. (4.17), (4.18) and (4.26) we obtain

$$\mu \frac{(a - ib\Omega)}{c} F'' - i\rho\Omega F - HF = -\frac{H(Q + iP)}{2h} \quad (4.27)$$

with

$$F = f + ig. \quad (4.28)$$

The governing equation can be put in dimensionless form

$$\begin{aligned} \Gamma''(\eta) &= \frac{\left( \frac{M^2(1+i\phi)}{1+\phi^2} + iR \right) (1 + D_1^2 + D_2^2 - 2D_1D_2)}{\left[ (1 + D_1D_3 + D_2D_4 - D_2 - D_4) + i(D_1 + D_2D_3 - D_1D_4 - D_3) \right]} \Gamma(\eta) \\ &= \frac{(1 + D_1^2 + D_2^2 - 2D_1D_2)}{\left[ (1 + D_1D_3 + D_2D_4 - D_2 - D_4) + i(D_1 + D_2D_3 - D_1D_4 - D_3) \right]} \\ &\quad \times \left( \frac{M^2(1+i\phi)}{1+\phi^2} \right) \frac{(\bar{Q} + i\bar{P})}{2hl\Omega} \end{aligned} \quad (4.29)$$

with the boundary conditions

$$\Gamma(1) = (1 + V_1 + iV_2), \quad \Gamma(-1) = -(1 + V_1 + iV_2), \quad (4.30)$$



where

$$\eta = \frac{z}{h}, \quad \Gamma = \frac{F}{\Omega l}, \quad V_1 = \frac{\Omega l}{U_1}, \quad V_2 = \frac{\Omega l}{U_2}, \quad R = \rho \Omega h^2 / \mu, \quad M^2 = \sigma B_0^2 h^2 / \mu,$$

$$D_1 = \Omega \lambda_1, \quad D_2 = \lambda_2 \Omega^2, \quad D_3 = \Omega \lambda_3, \quad D_4 = \lambda_4 \Omega^2$$

and  $R, M$  are Reynold number and Hartman number respectively.

## 4.2 Exact analytic solution

The solution of the problem for zero pressure gradient is

$$\Gamma(\eta) = (1 + V_1 + iV_2) \frac{\sinh m_1 \eta}{\sinh m_1}, \quad (4.31)$$

where

$$m_1^2 = \frac{(1 + D_1^2 + D_2^2 - 2D_1 D_2) \left( \frac{M^2(1+i\phi)}{1+\phi^2} + iR \right)}{[(1 + D_1 D_3 + D_2 D_4 - D_2 - D_4) + i(D_1 + D_2 D_3 - D_1 D_4 - D_3)]}. \quad (4.32)$$

Separating real and imaginary parts we have

$$\frac{f}{\Omega l} = \frac{\begin{pmatrix} 1 + V_1 \begin{pmatrix} \sinh \xi_1 \eta \cos \xi_2 \eta \sinh \xi_1 \cos \xi_2 \\ + \cosh \xi_1 \eta \sin \xi_2 \eta \cosh \xi_1 \sin \xi_2 \end{pmatrix} \\ -V_2 \begin{pmatrix} \cosh \xi_1 \eta \sin \xi_2 \eta \sinh \xi_1 \cos \xi_2 \\ - \sinh \xi_1 \eta \cos \xi_2 \eta \cosh \xi_1 \sin \xi_2 \end{pmatrix} \end{pmatrix}}{\Delta}, \quad (4.33)$$

$$\frac{g}{\Omega l} = \frac{\begin{pmatrix} 1 + V_1 \begin{pmatrix} \cosh \xi_1 \eta \sin \xi_2 \eta \sinh \xi_1 \cos \xi_2 \\ - \sinh \xi_1 \eta \cos \xi_2 \eta \cosh \xi_1 \sin \xi_2 \end{pmatrix} \\ -V_2 \begin{pmatrix} \sinh \xi_1 \eta \cos \xi_2 \eta \sinh \xi_1 \cos \xi_2 \\ + \cosh \xi_1 \eta \sin \xi_2 \eta \cosh \xi_1 \sin \xi_2 \end{pmatrix} \end{pmatrix}}{\Delta} \quad (4.34)$$

in which

$$\Delta = \sinh^2 \xi_1 \cos^2 \xi_2 + \cosh^2 \xi_1 \sin^2 \xi_2,$$

$$\begin{aligned}
\xi_1 &= \sqrt{\frac{(\sqrt{x_1^2 + y_1^2} + x_1)}{2} \frac{\omega}{\frac{-2}{x} \frac{-2}{y}}}, \\
\xi_2 &= \sqrt{\frac{(\sqrt{x_1^2 + y_1^2} - x_1)}{2} \frac{\omega}{\frac{-2}{x} \frac{-2}{y}}}, \\
\bar{a} &= 1 + \phi^2, \quad \omega = (1 + D_1^2 + D_2^2 - 2D_1D_2), \\
\bar{x} &= (1 + D_1D_3 + D_2D_4 - D_2 - D_4), \quad \bar{y} = (1 + D_1 + D_2D_3 - D_1D_4 - D_3), \\
x_1 &= \frac{M^2x + y(M^2\phi + R\bar{a})}{\bar{a}}, \quad y_1 = \frac{-M^2y + x(M^2\phi + R\bar{a})}{\bar{a}}. \tag{4.35}
\end{aligned}$$

### 4.3 Heat transfer analysis

In this section we discuss the heat transfer from the disks to the fluid. The energy conservation law is

$$\rho \frac{de}{dt} = \mathbf{T} \cdot \mathbf{L} - \text{div} \mathbf{q} + \rho r, \tag{4.36}$$

where  $\mathbf{q} = [-K_e \nabla \tau, (K_e \text{ being the thermal conductivity})]$  is the heat flux vector,  $\tau$  the temperature,  $r$  the radial heating (taken here to be zero) and  $e = C_p \tau$  ( $C_p$  the specific internal energy). The appropriate boundary conditions are

$$\begin{aligned}
\tau &= \tau_1 \quad \text{at } z = -h, \\
\tau &= \tau_2 \quad \text{at } z = h,
\end{aligned} \tag{4.37}$$

where  $\tau_1$  and  $\tau_2$  are the corresponding temperatures of the disks at  $z = -h$  and  $z = h$  respectively.

Equation (4.36) for the flow under consideration reduces to

$$\rho C_p \frac{d\tau}{dt} = K_e \frac{d^2\tau}{dz^2} + \frac{df}{dz} S_{xz} + \frac{dg}{dz} S_{yz}. \tag{4.38}$$

Using equations (4.15) and (4.16) and assumption of steady flow, one obtains the following from

$$\frac{d^2\theta}{d\eta^2} = -\frac{\bar{x}E_cP_r}{\omega} \left( \left( \frac{d\bar{f}}{d\eta} \right)^2 + \left( \frac{d\bar{g}}{d\eta} \right)^2 \right), \quad (4.39)$$

where  $\bar{f} = f/\Omega l$ ,  $\bar{g} = g/\Omega l$ ,  $P_r = \rho C_p \nu / K_e$  is the Prandtl number,  $E_c = (\Omega l)^2 / (\tau_1 - \tau_2) C_p$  is the Eckert number and  $\theta = \frac{\tau_1 - \tau_2}{\tau_1 - \tau_2}$  (where  $\theta$  is the dimensionless temperature). Here  $\tau_1 > \tau_2$ , so that  $E_c > 0$  (i.e. heat is transferred from disk to the fluid).

From Eq. (4.31) we have

$$\frac{d\Gamma}{d\eta} \frac{d\bar{\Gamma}}{d\eta} = \left( \frac{d\bar{f}}{d\eta} \right)^2 + \left( \frac{d\bar{g}}{d\eta} \right)^2, \quad (4.40)$$

where  $\bar{\Gamma}$  is the complex conjugate of  $\Gamma$  and Eq. (4.39) after using Eq. (4.40) gives

$$\frac{d^2\theta}{d\eta^2} = -\frac{\bar{x}E_cP_r}{\omega} \frac{\left( (1+V_1)^2 + V_2^2 \right) (\xi_1^2 + \xi_2^2)}{\cosh(2\xi_1) - \cos(2\xi_2)} (\cosh(2\xi_1\eta) + \cos(2\xi_2\eta)). \quad (4.41)$$

The relevant boundary conditions are

$$\theta(-1) = 1, \quad \theta(1) = 0. \quad (4.42)$$

The solution of equations (4.41) and (4.42) is

$$\begin{aligned} \theta(\eta) = & \frac{1}{2} - \frac{\eta}{2} + \frac{\bar{x}B_r}{\omega} \frac{\left( (1+V_1)^2 + V_2^2 \right) (\xi_1^2 + \xi_2^2)}{\cosh(2\xi_1) - \cos(2\xi_2)} \\ & \times \left[ \left\{ \frac{\cosh(2\xi_1) - \cosh(2\xi_1\eta)}{4\xi_1^2} \right\} - \left\{ \frac{\cos(2\xi_2) - \cos(2\xi_2\eta)}{4\xi_2^2} \right\} \right], \end{aligned} \quad (4.43)$$

where  $B_r = E_c P_r$  is the Brinkman number.

## 4.4 The force and torque

The components of force on the bottom disk are defined by

$$\begin{aligned} X &= \int_{\lambda} T_{xz}(-h) d\lambda, \\ Y &= \int_{\lambda} T_{yz}(-h) d\lambda, \\ Z &= \int_{\lambda} T_{zz}(-h) d\lambda \end{aligned} \quad (4.44)$$

in which  $\lambda$  is surface of the disk with  $r_0$  being the radius.

The force exerted by the fluid on the bottom disk is equal to that on the top disk. Therefore we have

$$\begin{aligned} X &= \pi r_0^2 S_{xz}(-h), \\ Y &= \pi r_0^2 S_{yz}(-h), \\ Z &= \rho \Omega^2 \pi r_0^4 \bar{Z}, \end{aligned} \quad (4.45)$$

whence

$$\begin{aligned} S_{xz}(-h) &= \frac{\mu}{c} (af' - bg'), \\ S_{yz}(-h) &= \frac{\mu}{c} (bf' + ag'), \\ S_{zz}(-h) &= 0, \end{aligned} \quad (4.46)$$

$$\frac{1}{\Omega l} \frac{df(-h)}{dz} = \frac{\left( \begin{array}{l} 1 + V_1 (\xi_1 \cosh \xi_1 \sinh \xi_1 + \xi_2 \cos \xi_2 \sin \xi_2) \\ -V_2 (\xi_2 \cosh \xi_1 \sinh \xi_1 - \xi_1 \cos \xi_2 \sin \xi_2) \end{array} \right)}{\Delta}, \quad (4.47)$$

$$\frac{1}{\Omega l} \frac{dg(-h)}{dz} = \frac{\left( \begin{array}{l} 1 + V_1 (\xi_2 \cosh \xi_1 \sinh \xi_1 - \xi_1 \cos \xi_2 \sin \xi_2) \\ +V_2 (\xi_1 \cosh \xi_1 \sinh \xi_1 + \xi_2 \cos \xi_2 \sin \xi_2) \end{array} \right)}{\Delta}, \quad (4.48)$$

$$\bar{Z} = - \left( \frac{1}{2} + \frac{\rho_0}{\frac{1}{2} \rho \Omega^2 r_0^2} \right). \quad (4.49)$$

The torque exerted by the fluid on the bottom disk is

$$\varkappa = \int_{\lambda} [xT_{yz}(-h) - yT_{xz}(-h)] d\lambda. \quad (4.50)$$

Since  $T_{yz}(-h) = S_{yz}(-h)$  and  $T_{xz}(-h) = S_{xz}(-h)$  it follows that

$$\varkappa = 0. \quad (4.51)$$

## 4.5 Results and discussion

This section displays the graphical illustration of velocity and temperature profiles. Emphasis has been given to examine the difference between the velocity and temperature profiles for six fluid models: Newtonian fluid ( $D_i = 0$  for  $i = 1 - 4$ ), second grade fluid ( $D_1 = D_2 = D_4 = 0, D_3 \neq 0$ ) and generalized Burgers' fluid ( $D_i \neq 0$  for  $i = 1 - 4$ ). Maxwell fluid, Oldroyd-B fluid ( $D_2 = D_4 = 0, D_1 \neq 0$ , and Burgers' fluid ( $D_i \neq 0$  for  $i = 1 - 3, D_4 = 0$ ) is also given in the form of tables. Graphs are included only for Oldroyd-B and generalized Burgers' fluids. The effects of various emerging parameters especially Hartman number  $M$ , Hall parameter  $\phi$  and the respective rheological parameters  $D_2$  and  $D_4$  of the Burgers' and generalized Burgers' fluids on the velocity and temperature profiles have been investigated.

Table 4.1: A comparison of velocity profiles for various kinds of fluids when  $V_1 = V_2 = R = M = 1$  and  $\eta = 0$ .

| Type of fluid | Rheological parameters                  | $f/\Omega l$ for $\phi = 0$ | $g/\Omega l$ for $\phi = 0$ | $f/\Omega l$ for $\phi = 2$ | $g/\Omega l$ for $\phi = 2$ |
|---------------|-----------------------------------------|-----------------------------|-----------------------------|-----------------------------|-----------------------------|
| Newtonian     | $D_i = 0$ for $i = 1 - 4$               | 1.167471                    | 0.280652                    | 1.252314                    | 0.284636                    |
| Second grade  | $D_1 = D_2 = D_4 = 0, D_3 = 1$          | 0.996644                    | 0.017918                    | 1.206468                    | 0.089889                    |
| Maxwell       | $D_2 = D_3 = D_4 = 0, D_1 = 15$         | 0.000544                    | -0.000544                   | -0.000024                   | 0.000024                    |
| Oldroyd-B     | $D_2 = D_4 = 0, D_1 = 15, D_3 = 1$      | 0.180574                    | -0.178503                   | 0.216435                    | -0.207075                   |
| Burgers'      | $D_1 = 15, D_2 = 5, D_3 = 1, D_4 = 0$   | 0.227338                    | -0.218113                   | 0.323556                    | -0.304419                   |
| G. Burgers'   | $D_1 = 15, D_2 = 5, D_3 = 1, D_4 = 0.5$ | 0.341535                    | -0.317547                   | 0.508019                    | -0.421904                   |

Table 4.2: A comparison of temperature profile for various kinds of fluids when  $V_1 = V_2 = R = M = B_r = 1$  and  $\eta = 0.5$ .

| Type of fluid | Rheological parameters                  | $\theta$ for $\phi = 0$ | $\theta$ for $\phi = 2$ |
|---------------|-----------------------------------------|-------------------------|-------------------------|
| Newtonian     | $D_i = 0$ for $i = 1 - 4$               | 1.978297                | 1.967802                |
| Second grade  | $D_1 = D_2 = D_4 = 0, D_3 = 1$          | 1.939457                | 2.092677                |
| Maxwell       | $D_2 = D_3 = D_4 = 0, D_1 = 15$         | 0.255531                | 0.256146                |
| Oldroyd-B     | $D_2 = D_4 = 0, D_1 = 15, D_3 = 1$      | 0.352216                | 0.399166                |
| Burgers'      | $D_1 = 15, D_2 = 5, D_3 = 1, D_4 = 0$   | 0.390681                | 0.420053                |
| G. Burgers'   | $D_1 = 15, D_2 = 5, D_3 = 1, D_4 = 0.5$ | 0.448159                | 0.547824                |

It is interesting to note that the Newtonian fluid has the maximum velocity profile  $f/\Omega$  in the absence as well as in the presence of Hall parameter when compared with the other fluids while Maxwell fluid has minimum. The velocity profile  $f/\Omega$  in second grade fluid are greater than those for Burgers' and generalized Burgers' fluids for both cases ( $\phi = 0$  and  $\phi \neq 0$ ) whereas Oldroyd-B fluid has smaller than those for Burgers' and generalized Burgers' fluids. Moreover, the Burgers' fluid has smaller velocity profile  $f/\Omega$  in comparison to the generalized Burgers' fluid for both cases.

The velocity profile  $g/\Omega$  in generalized Burgers' fluid is maximum whereas Maxwell fluid has smallest in the absence as well as in the presence of Hall parameter. A comparison between Burgers' and generalized Burgers' fluids reveals that generalized Burgers' fluid has the greater velocity profile  $g/\Omega$  for both cases ( $\phi = 0$  and  $\phi \neq 0$ ).

It is noted that temperature  $\theta$  in case of Newtonian fluid has the greater value when compared with Burgers' and generalized Burgers' fluids. The temperature  $\theta$  for a Burgers' fluid is greater than Oldroyd-B fluid and less than generalized Burgers' fluid.

Figures 4.2(a) – 4.7(b) are prepared to show the effect of increasing Hartman number  $M$  on the velocity profiles  $f/\Omega$  and  $g/\Omega$  of Oldroyd-B fluid and generalized Burgers' fluid in the absence as well as in the presence of Hall parameter  $\phi$  by keeping the values of other parameters fixed i.e.  $V_1 = V_2 = R = M = 1, D_1 = 15, D_2 = 15, D_3 = 1, D_4 = 0.5$ . These Figures depict that an increase in the values of Hartman number  $M$  tend to reduce the velocity profiles monotonically due to the effect of magnetic force against the direction of the flow for both fluids. Moreover, these Figures also elucidate the influence of the Hall parameter  $\phi$  on

the velocity profiles with fixed values of other parameters. As expected, the velocity increases by increasing  $\phi$  for examined fluids. This has the effect of reducing effective conductivity by increasing  $\phi$ . In fact the magnetic damping force on velocity decreases. Also it appears that the velocity is an increasing function of the rheological parameter  $D_2$  of the Burgers' fluid. However, this result cannot be generalized for other chosen values of the rheological parameter  $D_2$  since the behavior of  $D_2$  is non-monotonous. Moreover, it is observed that the velocity is also an increasing function of the rheological parameter  $D_4$  of the generalized Burgers' fluid.

Figures 4.8(a) and 4.9(b) show the variation of dimensionless temperature  $\theta$  for different values of the Brinkman number  $B_r$  for both fluids. It is noted that  $\theta$  is an increasing function of  $B_r$ . It is also observed from these Figures that the temperature profiles for a generalized Burgers' fluid are larger when compared with an Oldroyd-B fluid. The effect of Hall parameter  $\phi$  on the temperature and velocity profiles is qualitatively similar.

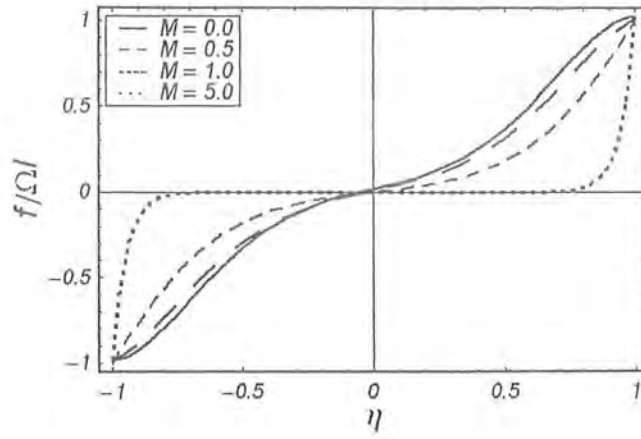


Figure 4.2(a): The variation of velocity profile  $f/\Omega l$  of an Oldroyd-B fluid for various values of Hartman number  $M$  when  $\phi = 0$ .

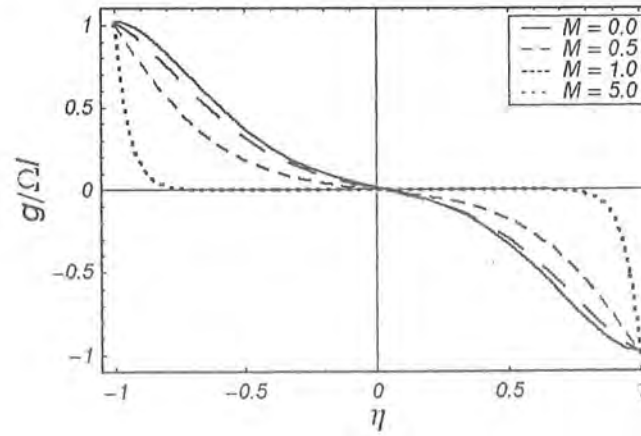


Figure 4.2(b): The variation of velocity profile  $g/\Omega b$  of an Oldroyd-B fluid for various values of Hartman number  $M$  when  $\phi = 0$ .



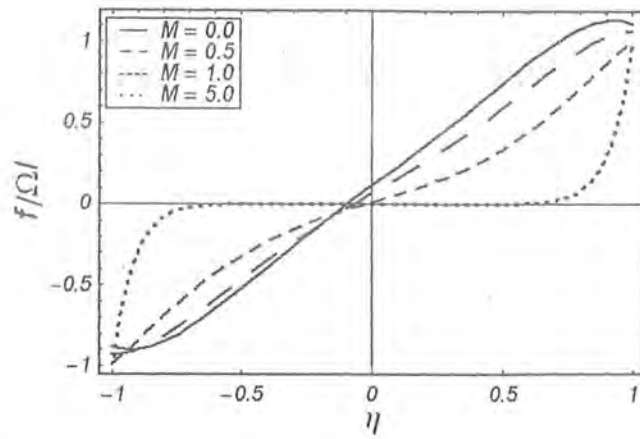


Figure 4.3(a): The variation of velocity profile  $f/\Omega l$  of generalized Burgers' fluid for various values of Hartman number  $M$  when  $\phi = 0$ .

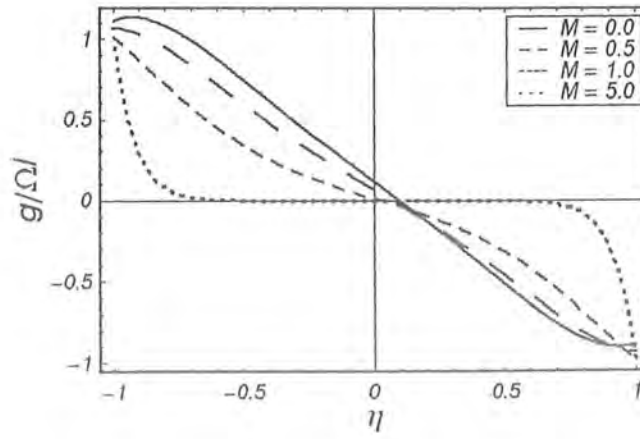


Figure 4.3(b): The variation of velocity profile  $g/\Omega l$  of generalized Burgers' fluid for various values of Hartman number  $M$  when  $\phi = 0$ .

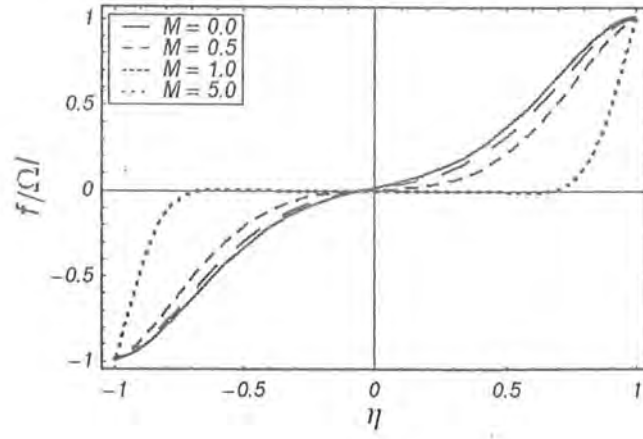


Figure 4.4(a): The variation of velocity profile  $f/\Omega l$  of an Oldroyd-B fluid for various values of Hartman number  $M$  when  $\phi = 2$ .

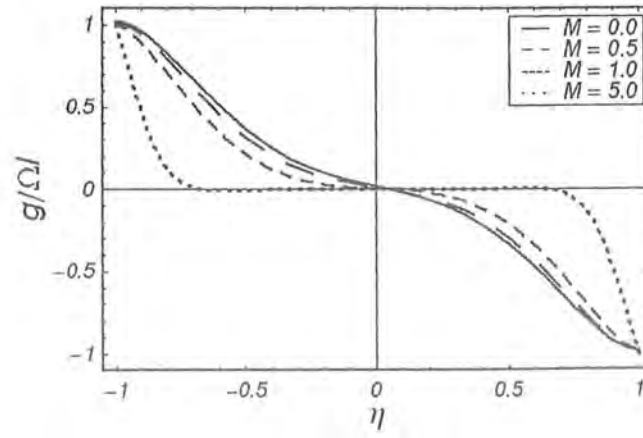


Figure 4.4(b): The variation of velocity profile  $g/\Omega b$  of an Oldroyd-B fluid for various values of Hartman number  $M$  when  $\phi = 2$ .

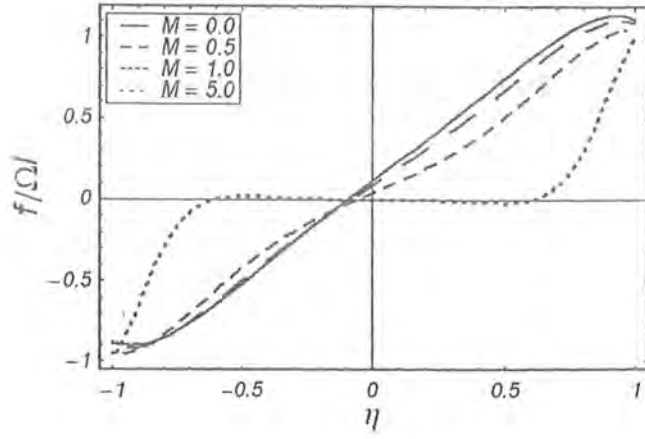


Figure 4.5(a): The variation of velocity profile  $f/\Omega l$  of generalized Burgers' fluid for various values of Hartman number  $M$  when  $\phi = 2$ .

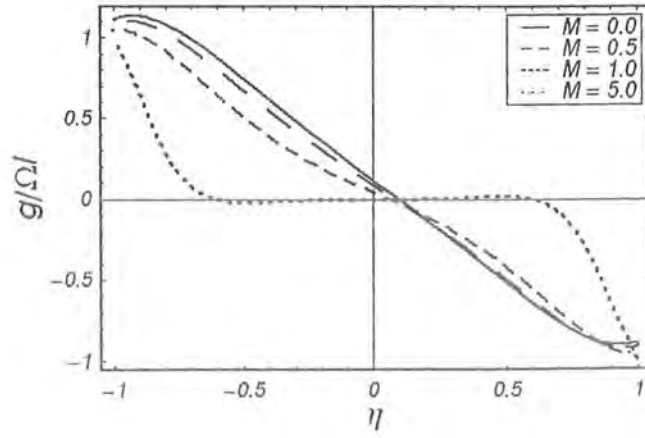


Figure 4.5(b): The variation of velocity profile  $g/\Omega b$  of generalized Burgers' fluid for various values of Hartman number  $M$  when  $\phi = 2$ .

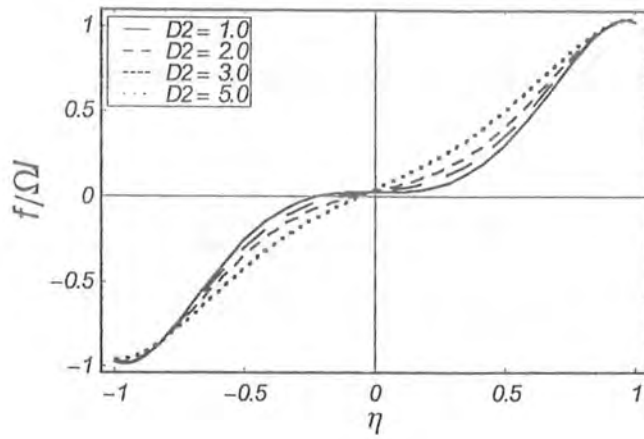


Figure 4.6(a): The variation of velocity profile  $f/\Omega l$  for various values of Burgers' parameter  $D_2$  when  $\phi = 2$ .

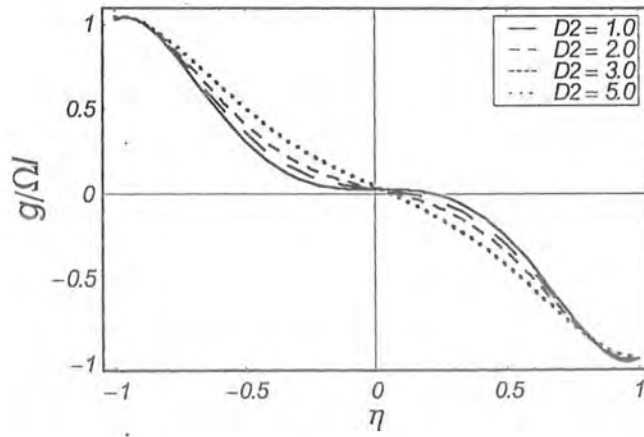


Figure 4.6(b): The variation of velocity profile  $g/\Omega l$  for various values of Burgers' parameter  $D_2$  when  $\phi = 2$ .

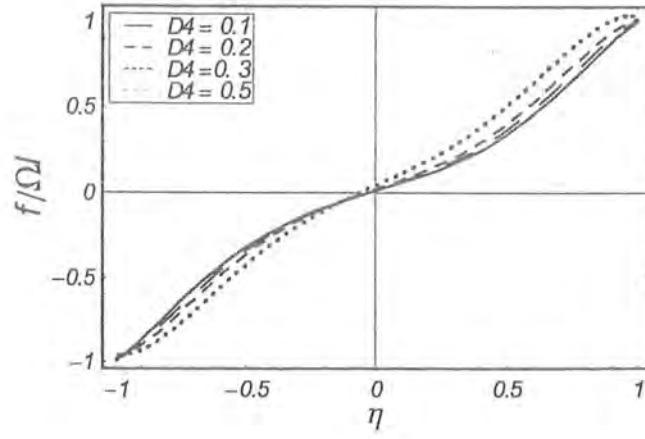


Figure 4.7(a): The variation of velocity profile  $f/\Omega l$  for various values of generalized Burgers' parameter  $D_4$  when  $\phi = 2$ .

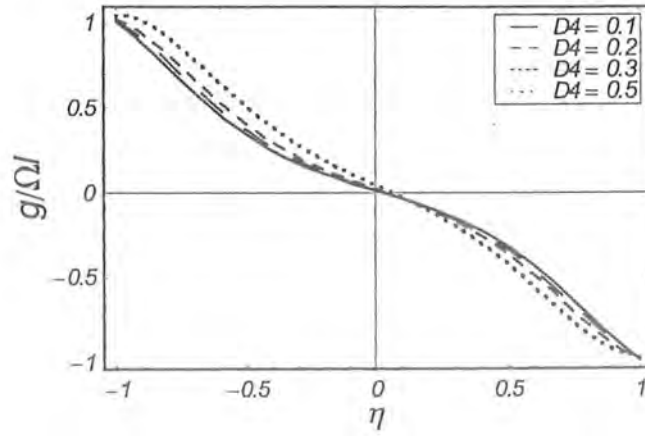


Figure 4.7(b): The variation of velocity profile  $g/\Omega b$  for various values of generalized Burgers' parameter  $D_4$  when  $\phi = 2$ .

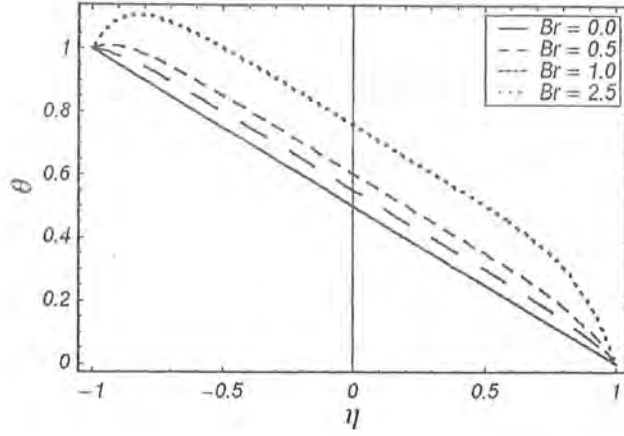


Figure 4.8(a): The variation of temperature profile  $\theta$  of an Oldroyd-B fluid for various values of Brinkman number  $Br$  when  $\phi = 0$ .

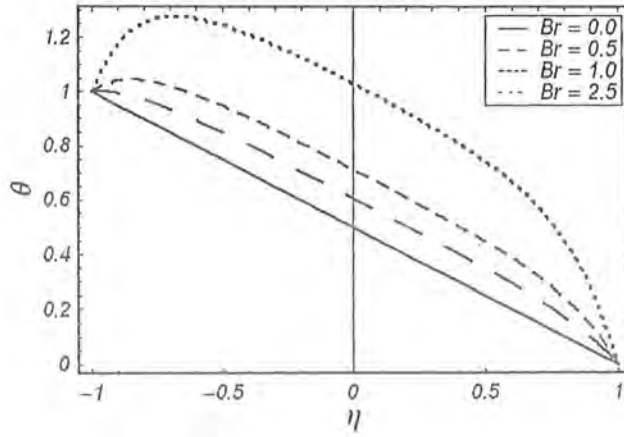


Figure 4.8(b): The variation of temperature profile  $\theta$  of generalized Burgers' fluid for various values of Brinkman number  $Br$  when  $\phi = 0$ .

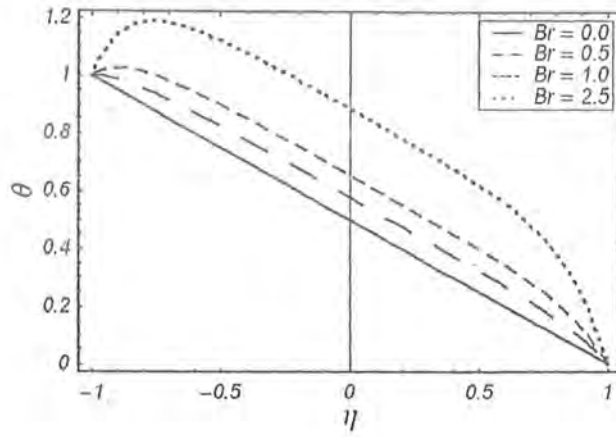


Figure 4.9(a): The variation of temperature profile  $\theta$  of an Oldroyd-B fluid for various values of Brinkman number  $Br$  when  $\phi = 2$ .

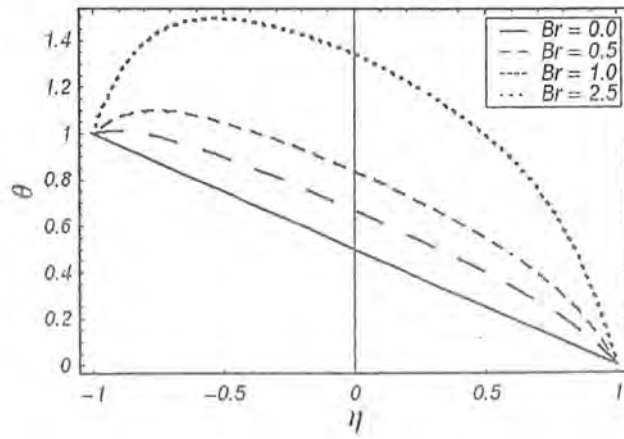


Figure 4.9(b): The variation of temperature profile  $\theta$  of generalized Burgers' fluid for various values of Brinkman number  $Br$  when  $\phi = 2$ .

## Chapter 5

# Effects of Hall current and heat transfer on the steady flow of a fourth grade fluid

The aim of this chapter is to analyze the steady flow of a fourth grade fluid between two eccentric rotating disks of different temperatures. The flow is engendered due to a sudden pull of eccentric disks. Hall effects are retained. Series solutions of the velocity and temperature are derived. A comparative study is made between the results of some subclasses of differential type fluids. Plots are prepared and discussed.

### 5.1 Formulation of the problem

Consider the steady flow of an electrically conducting fourth grade fluid between two infinite disks rotating non-coaxially with constant angular velocity  $\Omega$ . The distance between the axes is  $2l$ . A constant magnetic field of strength  $B_0$  is applied parallel to the  $z$ -axis (chosen normal to the disks). The electric and induced magnetic fields are assumed negligible. However the Hall effect is taken into account. Furthermore, the disks at  $z = h$  and  $z = -h$  are pulled with velocities  $U$  and  $-U$  respectively. The corresponding boundary conditions and velocity field is defined in (4.1) and (4.2).



The constitutive equation for the Cauchy stress tensor  $\mathbf{T}$  in a fourth grade fluid is [121]

$$\begin{aligned}
\mathbf{T} &= -p\mathbf{I} + \mathbf{S}_1 + \mathbf{S}_2 + \mathbf{S}_3 + \mathbf{S}_4, \\
\mathbf{S}_1 &= \mu\mathbf{A}_1, \quad \mathbf{S}_2 = \alpha_1\mathbf{A}_2 + \alpha_2\mathbf{A}_1^2, \\
\mathbf{S}_3 &= \beta_1\mathbf{A}_3 + \beta_2(\mathbf{A}_2\mathbf{A}_1 + \mathbf{A}_1\mathbf{A}_2) + \beta_3(\text{tr}\mathbf{A}_1^2)\mathbf{A}_1, \\
\mathbf{S}_4 &= \gamma_1\mathbf{A}_4 + \gamma_2(\mathbf{A}_3\mathbf{A}_1 + \mathbf{A}_1\mathbf{A}_3) + \gamma_3\mathbf{A}_2^2 + \gamma_4(\mathbf{A}_2\mathbf{A}_1^2 + \mathbf{A}_1^2\mathbf{A}_2) \\
&\quad + \gamma_5(\text{tr}\mathbf{A}_2)\mathbf{A}_2 + \gamma_6(\text{tr}\mathbf{A}_2)\mathbf{A}_1^2 + (\gamma_7\text{tr}\mathbf{A}_3 + \gamma_8\text{tr}(\mathbf{A}_2\mathbf{A}_1))\mathbf{A}_1.
\end{aligned} \tag{5.1}$$

Now using equations (4.2) and above expressions we have

$$\mathbf{A}_1 = \begin{pmatrix} 0 & 0 & \frac{df}{dz} \\ 0 & 0 & \frac{dg}{dz} \\ \frac{df}{dz} & \frac{dg}{dz} & 0 \end{pmatrix}, \tag{5.2}$$

$$\mathbf{A}_2 = \begin{pmatrix} 0 & 0 & \Omega\frac{dg}{dz} \\ 0 & 0 & -\Omega\frac{df}{dz} \\ \Omega\frac{dg}{dz} & -\Omega\frac{df}{dz} & 2\left(\left(\frac{df}{dz}\right)^2 + \left(\frac{dg}{dz}\right)^2\right) \end{pmatrix}, \tag{5.3}$$

$$\mathbf{A}_3 = \begin{pmatrix} 0 & 0 & -\Omega^2\frac{df}{dz} \\ 0 & 0 & -\Omega^2\frac{dg}{dz} \\ -\Omega^2\frac{df}{dz} & -\Omega^2\frac{dg}{dz} & 0 \end{pmatrix}, \tag{5.4}$$

$$\mathbf{S}_1 = \begin{pmatrix} 0 & 0 & \mu\frac{df}{dz} \\ 0 & 0 & \mu\frac{dg}{dz} \\ \mu\frac{df}{dz} & \mu\frac{dg}{dz} & 0 \end{pmatrix}, \tag{5.5}$$

$$\mathbf{S}_2 = \begin{pmatrix} \alpha_2\left(\frac{df}{dz}\right)^2 & \alpha_2\frac{df}{dz}\frac{dg}{dz} & \alpha_1\Omega\frac{dg}{dz} \\ \alpha_2\frac{df}{dz}\frac{dg}{dz} & \alpha_2\left(\frac{dg}{dz}\right)^2 & -\alpha_1\Omega\frac{df}{dz} \\ \alpha_1\Omega\frac{dg}{dz} & -\alpha_1\Omega\frac{df}{dz} & 2(\alpha_1 + \alpha_2)\left(\left(\frac{df}{dz}\right)^2 + \left(\frac{dg}{dz}\right)^2\right) \end{pmatrix}, \tag{5.6}$$

$$\mathbf{S}_3 = \begin{pmatrix} 2\beta_2\Omega \frac{df}{dz} \frac{dg}{dz} & -\Omega\beta_2 \left( \left( \frac{df}{dz} \right)^2 - \left( \frac{dg}{dz} \right)^2 \right) & \begin{pmatrix} 2(\beta_2 + \beta_3) \\ \times \left( \left( \frac{df}{dz} \right)^2 + \left( \frac{dg}{dz} \right)^2 \right) \\ -\beta_1\Omega^2 \end{pmatrix} \frac{df}{dz} \\ -\Omega\beta_2 \left( \left( \frac{df}{dz} \right)^2 - \left( \frac{dg}{dz} \right)^2 \right) & -2\beta_2\Omega \frac{df}{dz} \frac{dg}{dz} & \begin{pmatrix} 2(\beta_2 + \beta_3) \\ \times \left( \left( \frac{df}{dz} \right)^2 + \left( \frac{dg}{dz} \right)^2 \right) \\ -\beta_1\Omega^2 \end{pmatrix} \frac{dg}{dz} \\ \begin{pmatrix} 2(\beta_2 + \beta_3) \\ \times \left( \left( \frac{df}{dz} \right)^2 + \left( \frac{dg}{dz} \right)^2 \right) \\ -\beta_1\Omega^2 \end{pmatrix} \frac{df}{dz} & \begin{pmatrix} 2(\beta_2 + \beta_3) \\ \times \left( \left( \frac{df}{dz} \right)^2 + \left( \frac{dg}{dz} \right)^2 \right) \\ -\beta_1\Omega^2 \end{pmatrix} \frac{dg}{dz} & 0 \end{pmatrix}, \quad (5.7)$$

$$\mathbf{S}_4 = \begin{pmatrix} s_{11} & s_{12} & s_{13} \\ s_{21} & s_{22} & s_{23} \\ s_{31} & s_{32} & s_{33} \end{pmatrix} \quad (5.8)$$

where

$$\begin{aligned}
s_{11} &= \left( \gamma_3 \left( \frac{dg}{dz} \right)^2 - 2\gamma_2 \left( \frac{df}{dz} \right)^2 \right) \Omega^2 + 2 \left( \gamma_6 \left( \left( \frac{df}{dz} \right)^2 + \left( \frac{dg}{dz} \right)^2 \right) \right) \left( \frac{df}{dz} \right)^2, \\
s_{12} = s_{21} &= \left( -(\gamma_3 + 2\gamma_2) \Omega^2 + 2 \left( \gamma_6 \left( \left( \frac{df}{dz} \right)^2 + \left( \frac{dg}{dz} \right)^2 \right) \right) \right) \frac{df}{dz} \frac{dg}{dz}, \\
s_{13} = s_{31} &= \Omega \left( (2(\gamma_3 + \gamma_5) + \gamma_4) \left( \left( \frac{df}{dz} \right)^2 + \left( \frac{dg}{dz} \right)^2 \right) - \gamma_1 \Omega^2 \right) \frac{dg}{dz}, \\
s_{22} &= \left( \gamma_3 \left( \frac{df}{dz} \right)^2 - 2\gamma_2 \left( \frac{dg}{dz} \right)^2 \right) \Omega^2 + 2 \left( \gamma_6 \left( \left( \frac{df}{dz} \right)^2 + \left( \frac{dg}{dz} \right)^2 \right) \right) \left( \frac{dg}{dz} \right)^2, \\
s_{23} = s_{32} &= \Omega \left( -2((\gamma_3 + \gamma_5) - \gamma_4) \left( \left( \frac{df}{dz} \right)^2 + \left( \frac{dg}{dz} \right)^2 \right) + \gamma_1 \Omega^2 \right) \frac{dg}{dz},
\end{aligned}$$

$$s_{33} = \left( \Omega^2 (\gamma_3 - 2(\gamma_1 + \gamma_2)) + 4 \left( (\gamma_3 + \gamma_4 + \gamma_5) + \frac{\gamma_6}{2} \right) \left( \left( \frac{df}{dz} \right)^2 + \left( \frac{dg}{dz} \right)^2 \right) \right) \times \left( \left( \frac{df}{dz} \right)^2 + \left( \frac{dg}{dz} \right)^2 \right)$$

From Eqs. (5.1)- (5.8) we can write

$$T_{xx} = -p + 2\beta_2\Omega \left( \frac{df}{dz} \frac{dg}{dz} \right) + \gamma_3\Omega^2 \left( \frac{dg}{dz} \right)^2 + \left[ \alpha_2 - 2\Omega^2\gamma_2 + 2\gamma_6 \left( \left( \frac{df}{dz} \right)^2 + \left( \frac{dg}{dz} \right)^2 \right) \right] \left( \frac{df}{dz} \right)^2, \quad (5.9)$$

$$T_{yy} = -p + \alpha_2 \left( \frac{dg}{dz} \right)^2 - 2\beta_2\Omega \left( \frac{df}{dz} \frac{dg}{dz} \right) + \left[ \gamma_3\Omega^2 - 2\Omega^2\gamma_2 + 2\gamma_6 \left( \left( \frac{df}{dz} \right)^2 + \left( \frac{dg}{dz} \right)^2 \right) \right] \left( \frac{df}{dz} \right)^2, \quad (5.10)$$

$$T_{zz} = -p + (\alpha_2 + 2\alpha_1) \left( \left( \frac{dg}{dz} \right)^2 + \left( \frac{df}{dz} \right)^2 \right) + \left[ \begin{array}{c} \gamma_3\Omega^2 - 2\Omega^2(\gamma_1 + \gamma_2) \\ + 2(\gamma_6 + 2\gamma_3 + 2\gamma_4 + 2\gamma_5) \left( \left( \frac{df}{dz} \right)^2 + \left( \frac{dg}{dz} \right)^2 \right) \end{array} \right] \times \left( \left( \frac{df}{dz} \right)^2 + \left( \frac{dg}{dz} \right)^2 \right), \quad (5.11)$$

$$T_{xy} = T_{yx} = -\beta_2\Omega \left( \left( \frac{df}{dz} \right)^2 - \left( \frac{dg}{dz} \right)^2 \right) + \left[ \alpha_2 - \gamma_3\Omega^2 - 2\Omega^2\gamma_2 + 2\gamma_6 \left( \left( \frac{\partial f}{\partial z} \right)^2 + \left( \frac{\partial g}{\partial z} \right)^2 \right) \right] \left( \frac{\partial f}{\partial z} \frac{\partial g}{\partial z} \right), \quad (5.12)$$

$$T_{yz} = T_{zy} = \left[ \mu + 2(\beta_2 + \beta_3) \left( \left( \frac{\partial f}{\partial z} \right)^2 + \left( \frac{\partial g}{\partial z} \right)^2 \right) - \beta_1\Omega^2 \right] \frac{\partial g}{\partial z} + \left[ -\alpha_1\Omega + \Omega^3\gamma_1 - \Omega(2\gamma_3 + 2\gamma_5 + \gamma_4) \left( \left( \frac{\partial f}{\partial z} \right)^2 + \left( \frac{\partial g}{\partial z} \right)^2 \right) \right] \frac{\partial f}{\partial z}, \quad (5.13)$$

$$T_{zx} = T_{xz} = \left[ \mu + 2(\beta_2 + \beta_3) \left( \left( \frac{\partial f}{\partial z} \right)^2 + \left( \frac{\partial g}{\partial z} \right)^2 \right) - \beta_1\Omega^2 \right] \frac{\partial f}{\partial z} + \left[ \alpha_1\Omega - \Omega^3\gamma_1 + \Omega(2\gamma_3 + 2\gamma_5 + \gamma_4) \left( \left( \frac{\partial f}{\partial z} \right)^2 + \left( \frac{\partial g}{\partial z} \right)^2 \right) \right] \frac{\partial g}{\partial z}. \quad (5.14)$$

Invoking equations (4.2) and (5.1) into momentum equation one arrives at

$$\frac{\partial p}{\partial x} = \rho\Omega(\Omega x + g(z)) + \frac{\partial T_{xz}}{\partial z} + \frac{\sigma B_0^2(1+i\phi)}{1+\phi^2} \left( \frac{Q}{2h} - f(z) \right), \quad (5.15)$$

$$\frac{\partial p}{\partial y} = -\rho\Omega(-\Omega y + f(z)) + \frac{\partial T_{yz}}{\partial z} + \frac{\sigma B_0^2(1+i\phi)}{1+\phi^2} \left( \frac{P}{2h} - g(z) \right), \quad (5.16)$$

where  $z$ -component of momentum equation indicates that  $p \neq p(z)$ ,  $\phi = \omega_e \tau_e$  is the Hall parameter and  $Q$  and  $P$  are defined in equations (4.19).

Performing integration of equations (5.15) and (5.16) we get

$$p = p_0 + \frac{1}{2}(x^2 + y^2) + \left( C_1 + \frac{HQ}{2h} \right) x + \left( C_2 + \frac{HP}{2h} \right) y, \quad (5.17)$$

in which  $p_0$  is the reference pressure,  $C_i (i = 1, 2)$  are the arbitrary constants defined in equations (4.22) and (4.23) in absence of the pressure gradient

$$C_1 = -\frac{HQ}{2h}, \quad C_2 = -\frac{HP}{2h}, \quad (5.18)$$

$$F = f + ig, \quad \bar{F} = f - ig. \quad (5.19)$$

Substitution of Eqs. (5.13), (5.14) and (5.18) into equations (5.15) and (5.16) and then combining the resulting equations and using the boundary conditions (4.20) and (4.21) we have

$$\begin{aligned} & [\mu - \beta_1 \Omega^2 + i(\Omega^3 \gamma_1 - \alpha_1 \Omega)] \frac{d^2 F}{dz^2} \\ & + [4(\beta_2 + \beta_3) - 2i\Omega(2\gamma_3 + 2\gamma_5 + \gamma_4)] \frac{d^2 F}{dz^2} \frac{dF}{dz} \frac{d\bar{F}}{dz} \\ & + [2(\beta_2 + \beta_3) - i\Omega(2\gamma_3 + 2\gamma_5 + \gamma_4)] \frac{d^2 \bar{F}}{dz^2} \left( \frac{dF}{dz} \right)^2 \\ & - \left( \frac{\sigma B_0^2(1+i\phi)}{1+\phi^2} + i\Omega R \right) F = - \left( \frac{\sigma B_0^2(1+i\phi)}{1+\phi^2} \right) \left( \frac{Q + iP}{2h} \right), \end{aligned} \quad (5.20)$$

$$F(h) = \Omega l + U_1 + iU_2, \quad F(-h) = -(\Omega l + U_1 + iU_2). \quad (5.21)$$

Introducing

$$\begin{aligned}
z^* &= \frac{z}{h}, \quad F^* = \frac{F}{\Omega l}, \quad \alpha_1^* = \frac{\alpha_1 \Omega}{\mu}, \quad \beta_1^* = \frac{\beta_1 \Omega^2}{\mu}, \quad \gamma_1^* = \frac{\gamma_1 \Omega^3}{\mu}, \\
\gamma^* &= \frac{(2\gamma_3 + 2\gamma_5 + \gamma_4) \Omega^3}{\mu}, \quad \beta^* = \frac{2(\beta_2 + \beta_3) \Omega^2}{\mu}, \\
R &= \Omega \rho \frac{h^2}{a}, \quad V_1 = \frac{U_1}{\Omega l}, \quad V_2 = \frac{U_2}{\Omega l}, \quad M^2 = \frac{\sigma B_0^2 h^2}{a},
\end{aligned} \tag{5.22}$$

the governing non-dimensional problem reduces to

$$\begin{aligned}
&(1 - \alpha_1 - \beta_1 + i\gamma_1) \frac{d^2 F}{dz^2} \\
&+ 2(\beta - i\gamma) \left[ \left( \frac{d^2 F}{dz^2} \frac{d\bar{F}}{dz} \frac{dF}{dz} + \left( \frac{dF}{dz} \right)^2 \frac{d^2 \bar{F}}{dz^2} \right) \right] \\
&+ \left( \frac{M^2(1 + i\phi)}{1 + \phi^2} + iR \right) F = \left( \frac{M^2(1 + i\phi)}{1 + \phi^2} \right) \left( \frac{Q + iP}{2h\Omega l} \right),
\end{aligned} \tag{5.23}$$

$$F(1) = 1 + V_1 + iV_2, \quad F(-1) = -(1 + V_1 + iV_2), \tag{5.24}$$

where asteriks have been suppressed for brevity.

## 5.2 Analytic solution by homotopy analysis method

To solve Eq. (5.23) subject to the boundary conditions (5.24) we use homotopy analysis method.

### 5.2.1 Zeroth order deformation problem

For analytic solution we choose the initial guess  $F_0$  and an auxiliary linear operator ( $\mathcal{L}_1$ ) in the following form

$$F_0(z) = (1 + V_1 + iV_2)z, \tag{5.25}$$

$$\mathcal{L}_1 \left[ \hat{F}(z; q) \right] = \frac{d^2 \hat{F}(z; q)}{dz^2}, \tag{5.26}$$

where

$$\mathcal{L}_1 [A_1 + zA_2] = 0 \tag{5.27}$$

and  $A_1$  and  $A_2$  are the arbitrary constants.

Let  $\hbar_1 \neq 0$  be an auxiliary parameter and  $H_1 = 1$  is the base function. Then we form the zeroth order deformation problem as

$$(1 - q)\mathcal{L}_1 [\hat{F}(z; q) - F_0(z)] = q\hbar_1 H_1 \mathcal{N}_1 [\hat{F}(z; q)], \quad (5.28)$$

$$\hat{F}_0(1; q) = 1 + V_1 + iV_2, \quad \hat{F}_0(-1; q) = -(1 + V_1 + iV_2), \quad (5.29)$$

where nonlinear operator is defined by

$$\begin{aligned} \mathcal{N}_1 [\hat{F}(z; q)] &= (1 - \alpha_1 - \beta_1 + i\gamma_1) \frac{\partial^2 \hat{F}}{\partial z^2} \\ &+ 2(\beta - i\gamma) \left[ \left( \frac{\partial^2 \hat{F}}{\partial z^2} \frac{\partial \bar{\hat{F}}}{\partial z} \frac{\partial \hat{F}}{\partial z} + \left( \frac{\partial \hat{F}}{\partial z} \right)^2 \frac{\partial^2 \bar{\hat{F}}}{\partial z^2} \right) \right] \\ &- \left( \frac{M^2(1 + i\phi)}{1 + \phi^2} + iR \right) \hat{F} + \left( \frac{M^2(1 + i\phi)}{1 + \phi^2} \right) \left( \frac{Q + iP}{2\hbar\Omega l} \right). \end{aligned} \quad (5.30)$$

For  $q = 0$  the solution of Eq. (5.28) under the boundary condition (5.29) is

$$\hat{F}(z; 0) = F_0(z),$$

and when  $q = 1$  left hand side of Eq. (5.28) vanishes and problem becomes similar to Eq. (5.20). That is

$$\hat{F}(z; 1) = F(z). \quad (5.31)$$

Note that when  $q$  increases from 0 to 1,  $\hat{F}(z; q)$  varies from the initial guess  $F_0(z)$  to  $F(z)$ . By Taylors' theorem one can easily write

$$\hat{F}(z; q) = F_0(z) + \sum_{m=1}^{\infty} F_m(z) q^m, \quad F_m(z) = \frac{1}{m!} \left. \frac{\partial^m \hat{F}(z, q)}{\partial q^m} \right|_{q=0} \quad (5.32)$$

and convergence of the above series strongly depends upon  $\hbar_1$ . Here  $\hbar_1$  is chosen in such a way that the series (5.32) is convergent at  $q = 1$  then

$$\hat{F}(z) = F_0(z) + \sum_{m=1}^{\infty} F_m(z). \quad (5.33)$$

### 5.2.2 $m$ th-order deformation equation

Differentiating equations (5.28) and (5.29)  $m$  times with respect to  $q$ , dividing by  $m!$  and finally setting  $q = 0$  we get the  $m$ th order deformation problem in the following form

$$\mathcal{L}_1 [F_m(z) - \chi_m F_{m-1}(z)] = \hbar_1 \mathcal{R}_{1m}(z), \quad (5.34)$$

$$F_m(1) = F_m(-1) = 0, \quad (5.35)$$

$$\begin{aligned} \mathcal{R}_{1m}(z) = & (1 - \alpha_1 - \beta_1 + i\gamma_1) F_{m-1}'' - \left( \frac{M^2(1+i\phi)}{1+\phi^2} + iR \right) F_{m-1} \\ & + (1 - \chi_m) \left( \frac{M^2(1+i\phi)}{1+\phi^2} \right) \left( \frac{Q+iP}{2h\Omega l} \right) \\ & + 2(\beta - i\gamma) \sum_{k=0}^{m-1} \sum_{l=0}^k \left[ F_{m-1-k}' \bar{F}'_{k-l} F_l'' + F_{m-1-k}' F_{k-l}' \bar{F}_l'' \right], \end{aligned} \quad (5.36)$$

$$\chi_m = \begin{cases} 0, & m \leq 1, \\ 1, & m > 1. \end{cases}$$

Now the boundary value problem consisting of Eqs. (5.34) with boundary conditions (5.35) has been solved by "MATHEMATICA" up to first few order of approximations. Finally we get

$$F_m(z) = \sum_{t=0}^{2m+1} c_{m,t} z^t, \quad \text{where } c_{m,t} = \text{Re } c_{m,t} + i \text{Im } c_{m,t} \quad m \geq 0, \quad (5.37)$$

and  $m \geq 1$ , and  $0 \leq t \leq 2m+1$ , we have

$$\begin{aligned} F_m'(z) &= \sum_{t=1}^{2m+1} t c_{m,t} z^{t-1} = \sum_{t=0}^{2m+1} c1_{m,t} z^t, \\ F_m''(z) &= \sum_{t=1}^{2m+1} t c1_{m,t} z^{t-1} = \sum_{t=0}^{2m+1} c2_{m,t} z^t, \\ \bar{F}'_{k-l} F_l'' &= \sum_{i=0}^{2k-2l+1} \bar{c}1_{k-l,i} z^i \sum_{j=0}^{2l+1} \bar{c}1_{l,j} z^j, \end{aligned}$$

$$i + j = s, \quad 0 \leq i \leq 2k - 2l + 1, \quad 0 \leq j \leq 2l + 1,$$

$$0 \leq s \leq 2k + 2, \quad 0 \leq s - i \leq 2l + 1,$$

$$s - 2l - 1 \leq i \leq s,$$

$i$  varies from  $\max\{0, s - 1 - 2l\}$  to  $\min\{s, 2k - 2l + 1\}$ .

$$\bar{F}'_{k-l} F''_l = \sum_{s=0}^{2k+2} \sum_{i=\max\{0, s-1-2l\}}^{\min\{s, 2k-2l+1\}} \bar{c}1_{k-l, i} \bar{c}1_{l, s-i} z^s,$$

$$F'_{m-1-k} \bar{F}'_{k-l} F''_l = \sum_{r=0}^{2m-2k-1} c1_{m-1-k, r} z^r \sum_{s=0}^{2k+2} \sum_{i=\max\{0, s-1-2l\}}^{\min\{s, 2k-2l+1\}} \bar{c}1_{k-l, i} \bar{c}1_{l, s-i} z^s,$$

$$s + r = t, \quad 0 \leq s \leq 2k + 2, \quad 0 \leq r \leq 2m - 2k - 1,$$

$$0 \leq t \leq 2m + 1, \quad 0 \leq t - s \leq 2m - 2k - 1,$$

$$t - 2m + 2k + 1 \leq s \leq t,$$

$s$  varies from  $\max\{0, t - 2m + 2k + 1\}$  to  $\min\{t, 2k + 2\}$ .

$$F'_{m-1-k} \bar{F}'_{k-l} F''_l = \sum_{t=0}^{2m+1} \sum_{s=\max\{0, t-2m+2k+1\}}^{\min\{t, 2k+2\}} c1_{m-1-k, t-s} \sum_{i=\max\{0, s-1-2l\}}^{\min\{s, 2k-2l+1\}} \bar{c}1_{k-l, i} \bar{c}1_{l, s-i} z^t,$$

$$F'_{m-1-k} \bar{F}'_{k-l} F''_l = \sum_{t=0}^{2m+1} \alpha 1_{m, t} z^t.$$

Similarly

$$F'_{m-1-k} F'_{k-l} \bar{F}''_l = \sum_{t=0}^{2m+1} \alpha 2_{m, t} z^t$$

and the coefficients  $\alpha 1_{m, t}$  and  $\alpha 2_{m, t}$ , for  $m \geq 1, 0 \leq t \leq 2m + 1$  are

$$\alpha 1_{m, t} = \sum_{k=0}^{m-1} \sum_{l=0}^k \sum_{s=\max\{0, 1+t+2k-2m\}}^{\min\{t, 2k+2\}} c1_{m-1-k, t-s} \sum_{r=\max\{0, s-1-2l\}}^{\min\{s, 2k-2l+1\}} \bar{c}1_{k-l, i} c2_{l, s-i},$$

$$\alpha 2_{m, t} = \sum_{k=0}^{m-1} \sum_{l=0}^k \sum_{s=\max\{0, t-2k-2\}}^{\min\{t, 2k+2\}} c1_{m-1-k, t-s} \sum_{r=\max\{0, s-1-2l\}}^{\min\{s, 2k-2l+1\}} \bar{c}1_{k-l, i} \bar{c}2_{l, s-i}.$$



Now Eq. (5.34) becomes

$$\mathcal{L}_1 [F_m(z) - \chi_m F_{m-1}(z)] = \sum_{t=0}^{2m+1} m,t \Gamma_{m,t} z^t + (1 - \chi_m) \left( \frac{M^2(1+i\phi)}{1+\phi^2} \right) \left( \frac{Q+iP}{2h\Omega l} \right),$$

in which

$$\Gamma_{m,t} = \hbar_1 \left( \begin{array}{c} \chi_{2m-t+1} (1 - \alpha_1 - \beta_1 + i\gamma_1) c_{2m-1,t} \\ -\chi_{2m-t+1} \left( \frac{M^2(1+i\phi)}{1+\phi^2} + iR \right) c_{m-1,t} + 2(\beta - i\gamma) (\alpha_1 c_{m,t} + \alpha_2 c_{m,t}) \end{array} \right).$$

The values of coefficients are

$$\begin{aligned} c_{m,0} &= \chi_m \chi_{2m+1} c_{m-1,0} \left( \frac{A}{2} - \sum_{t=0}^m \frac{\Gamma_{m,2t}}{(2t+1)(2t+2)} \right), \\ c_{m,1} &= \chi_m \chi_{2m} c_{m-1,1} - \sum_{t=0}^m \frac{\Gamma_{m,2t+1}}{(2+2t)(3+2t)}, \\ c_{m,2} &= \chi_m \chi_{2m-1} c_{m-1,2} + \frac{1}{2} (-A + \Gamma_{m,0}), \\ c_{m,t} &= \chi_m \chi_{2m-t+1} c_{m-1,t} + \Gamma_{m,t-2} \frac{1}{(t-1)t}, \quad 3 \leq t \leq 2m+1, \\ A &= -(1 - \chi_m) \left( \frac{M^2(1+i\phi)}{1+\phi^2} \right) \left( \frac{Q+iP}{2h\Omega l} \right), \end{aligned} \quad (5.38)$$

$$\begin{aligned} c_{m,t} &= \text{Re } c_{m,t} + i \text{Im } c_{m,t}, & \bar{c}_{m,t} &= \text{Re } c_{m,t} - i \text{Im } c_{m,t}, \\ c_{1m,t} &= (1+t)c_{m,1+t}, & \bar{c}_{m,t} &= (1+t)\bar{c}_{m,1+t}, \\ c_{2m,t} &= (1+t)c_{1m,1+t}, & \bar{c}_{2m,t} &= (1+t)\bar{c}_{1m,1+t}. \end{aligned}$$

The corresponding  $m$ th order approximation and therefore series solution is expressed by the following equation

$$F(z) = \lim_{M \rightarrow \infty} \left[ \sum_{m=0}^M F_m(z) = \sum_{m=0}^M \left( \sum_{t=0}^{2m+1} c_{m,t} z^t \right) \right]. \quad (5.39)$$

### 5.3 Heat transfer analysis

This section looks at the heat transfer analysis from disk to the fluid. Therefore the law of conservation of energy in the absence of radiation effects is given in equation (4.36). The corresponding temperatures of the disks are given in equations (4.37).

Making use of equations (5.13) and (5.14), the problem under consideration is of the form

$$\frac{d^2\theta}{dz^2} = -Br \left( 1 + \frac{\beta l^2}{h^2} \left( \frac{dF}{dz} \frac{d\bar{F}}{dz} \right) \right) \frac{dF}{dz} \frac{d\bar{F}}{dz}, \quad (5.40)$$

$$\theta(-1) = 1, \quad \theta(1) = 0, \quad (5.41)$$

where  $P_r (= aC_P/K_e)$  is the Prandtl number,  $Br (= E_c P_r)$  is the Brinkman number,  $E_c (= (\Omega l)^2 / (\tau_1 - \tau_2) C_P)$  is the Eckert number and  $T_1 > T_2$  so that  $E_c > 0$  (i.e. heat is transferred from disk to the fluid).

Selecting the initial guess and auxiliary linear operator of the following type

$$\theta_0(z) = \frac{1}{2}(1 - z), \quad (5.42)$$

$$\mathcal{L}_2 [\hat{\theta}(z; q)] = \frac{d^2 \hat{\theta}(z; q)}{dz^2}, \quad (5.43)$$

$$\mathcal{L}_2 [B_1 + zB_2] = 0, \quad (5.44)$$

where  $B_1$  and  $B_2$  are constants.

#### 5.3.1 Zeroth and $m$ th order problem

$$(1 - q)\mathcal{L}_2 [\hat{\theta}(z; q) - \theta_0(z)] = q\hbar_2 H_2 \mathcal{N}_2 [\hat{\theta}(z; q)], \quad (5.45)$$

$$\hat{\theta}_0(-1; q) = 1, \quad \hat{\theta}_0(1; q) = 0, \quad (5.46)$$

$$\mathcal{L}_2 [\theta_m(z) - \chi_m \theta_{m-1}(z)] = \hbar_2 \mathcal{R}_2(z), \quad (5.47)$$

$$\theta_m(1) = \theta_m(-1) = 0, \quad (5.48)$$

whence

$$\mathcal{N}_2 [\hat{\theta}(z; q)] = \frac{\partial^2 \hat{\theta}}{\partial z^2} + Br \left( 1 + \frac{\beta l^2}{h^2} \left( \frac{\partial \hat{F}}{\partial z} \frac{\partial \bar{F}}{\partial z} \right) \right) \frac{\partial \hat{F}}{\partial z} \frac{\partial \bar{F}}{\partial z}, \quad (5.49)$$

$$\mathcal{R}_2(z) = \theta''_{m-1}(z) + Br \sum_{k=0}^{m-1} F'_{m-1-k} \bar{F}'_k + \frac{\beta l^2}{h^2} \sum_{k=0}^{m-1} F'_{m-1-k} \sum_{l=0}^k F'_{k-l} \sum_{a=0}^l \bar{F}'_{l-a} \bar{F}'_a. \quad (5.50)$$

### 5.3.2 Solution of the $m$ th order problem

Here

$$\theta_m(z) = \sum_{t=0}^{2m} b_{m,t} z^t, \quad m \geq 0, \quad (5.51)$$

$$\begin{aligned} b_{2m,t} &= (1+t)b_{1m,t+1}, & b_{1m,t} &= (1+t)b_{m,t+1}, \\ \bar{b}_{2m,t} &= (1+t)\bar{b}_{1m,t+1}, & \bar{b}_{1m,t} &= (1+t)\bar{b}_{m,t+1}, \end{aligned}$$

where for  $m \geq 1$  and  $0 \leq t \leq 2m$ , we have

$$\begin{aligned} b_{m,0} &= \chi_m \chi_{2m} b_{m-1,0} - \sum_{t=0}^m \frac{\Gamma_{m,2t}}{(2t+1)(2t+2)}, \\ b_{m,1} &= \chi_m \chi_{2m-1} b_{m-1,1} - \sum_{t=0}^m \frac{\Gamma_{m,2t+1}}{(2t+3)(2t+2)}, \\ b_{m,2} &= \chi_m \chi_{2m-2} b_{m-1,2} + \frac{1}{2} \Gamma_{m,0}, \\ b_{m,t} &= \chi_m \chi_{2m-t} b_{m-1,t} + \Gamma_{m,t-2} \frac{1}{(t-1)t}, \quad 3 \leq t \leq 2m, \\ \Gamma_{m,t} &= \chi_{2m+1-t} (\chi_{2m-t} b_{2m-1,t} + Br \beta_{1m,t}) + Br \beta_{2m,t} \frac{Bl^2}{h^2} \end{aligned}$$

and the coefficients  $\beta_{1m,t}$  and  $\beta_{2m,t}$  for  $m \geq 1, 0 \leq t \leq 2m$  are

$$\begin{aligned} \beta_{1m,t} &= \sum_{k=0}^{m-1} \sum_{r=\max\{0,1+t+2k-2m\}}^{\min\{t,2k\}} b_{1m-1-k,t-r} \bar{b}_{1k,r}, \\ \beta_{2m,t} &= \sum_{k=0}^{m-1} \sum_{l=0}^k \sum_{a=0}^l \sum_{v=\max\{0,2k+1+t-2m\}}^{\min\{t,2k+3\}} b_{1m-1-k,t-v} \sum_{u=\max\{0,2l+v-1-2k\}}^{\min\{v,2l+2\}} b_{1k-l,t-u} \sum_{r=\max\{0,u-1-2a\}}^{\min\{u,2l-2a+1\}} \bar{b}_{1l-a,r}. \end{aligned}$$

$$\sum_{m=0}^M \theta_m(z) = \sum_{m=0}^M \sum_{t=0}^{2m} b_{m,t} z^t,$$

and the expression of temperature is

$$\theta(z) = \lim_{M \rightarrow \infty} \left[ \sum_{m=0}^M \theta_m(z) = \sum_{m=0}^M \left( \sum_{t=0}^{2m} b_{m,t} z^t \right) \right]. \quad (5.52)$$

## 5.4 Convergence of the homotopy solution

The explicit expressions of the series (5.39) and (5.52) are the solutions of the considered problem if one guarantees the convergence of these series. The convergence of both series strongly depends upon auxiliary parameter  $\hbar_1$  and  $\hbar_2$ . Figures 5.1(a) and 5.1(b) show the residual error of velocity profile versus  $\hbar_1$ . Figures 5.2(a) and 5.2(b) are prepared for the residual error of temperature profile and temperature gradient versus  $\hbar_2$  respectively. Computations are made for 15th order of approximations by fixing  $M$ ,  $\alpha_1$ ,  $\beta_1$ ,  $\gamma$ ,  $\alpha$ ,  $\beta$ ,  $V_1$ ,  $V_2$ ,  $R$  and  $\phi$ . Figures 5.1(a) and 5.2(a) show that the range for the admissible values of  $\hbar_1$  and  $\hbar_2$  are  $-1.65 \leq \hbar_1 \leq -0.25$  and  $-1.45 \leq \hbar_2 \leq -0.4$  respectively.

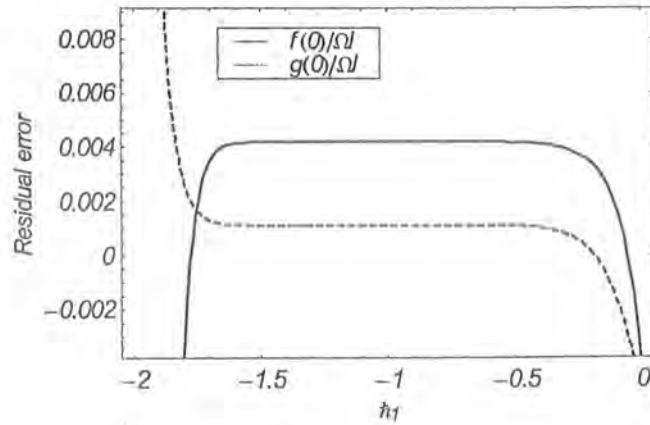


Figure 5.1(a): Residual error of velocity fields  $f/\Omega l$  and  $g/\Omega l$  versus  $\hbar_1$  for the 15th order of approximation.

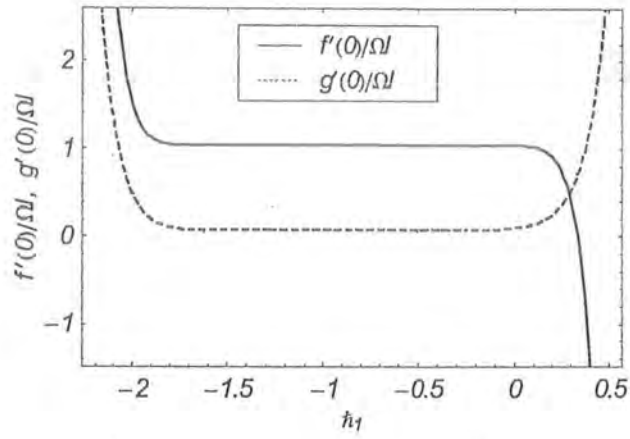


Figure 5.1(b): The graphs of  $f'(0)/\Omega l$  and  $g'(0)/\Omega l$  versus  $h_1$  for the 15th order of approximation.

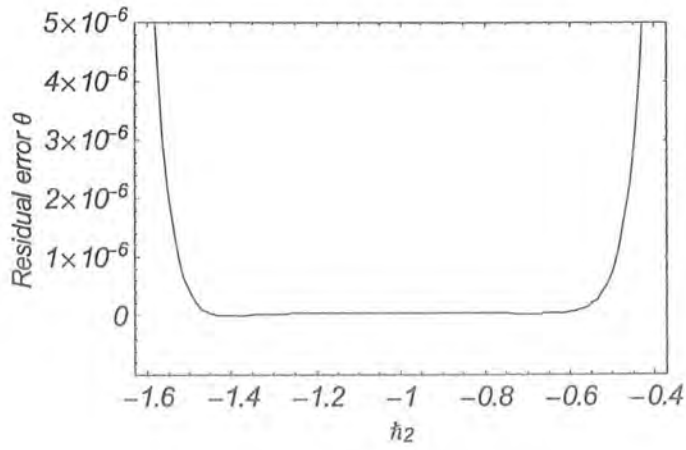


Figure 5.2(a): Residual error of temperature profile versus  $h_2$  for 10th order of approximation.

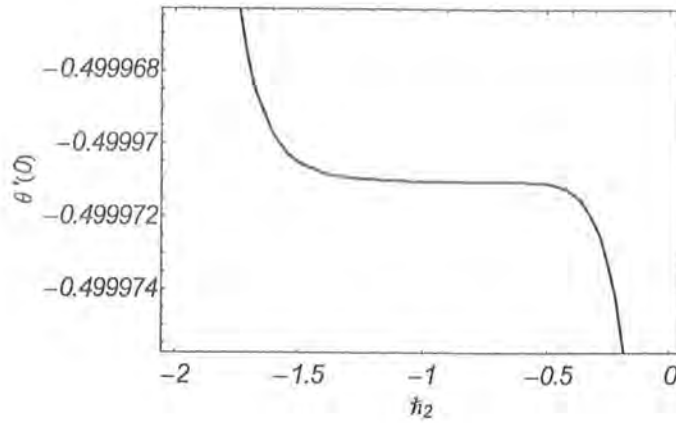


Figure 5.2(b):  $\theta'(0)$  versus  $h_2$  for 10th order approximation.

## 5.5 Numerical results and discussion

The analytic solution of the differential equations (5.23) and (5.40) subject to the boundary conditions (5.24) and (5.41) are obtained in the form of series. A comparison of the velocity profiles and temperature is also given. Special attention has been focused to analyze the effects of various physical parameters like,  $M, \beta, \gamma, \alpha_1, \beta_1$  and  $\gamma_1$ . Further, the effect of Hall parameter  $\phi$  on the velocity field and temperature profile is also shown in Table 5.1.

Table 5.1: Velocity and temperature profiles for different types of the fluid when  $M = \beta = \gamma = \alpha_1 = \beta_1 = \gamma_1 = 0.1$  for the 15th order of approximation.

| Types of the fluid | $\phi = 0$   |              |          | $\phi = 0.1$ |              |          |
|--------------------|--------------|--------------|----------|--------------|--------------|----------|
|                    | $f/\Omega l$ | $g/\Omega l$ | $\theta$ | $f/\Omega l$ | $g/\Omega l$ | $\theta$ |
| Fourth grade fluid | -0.0335821   | -0.0480789   | 0.506262 | -0.0319473   | -0.0515259   | 0.506263 |
| Third grade fluid  | -0.0224848   | -0.0411789   | 0.506195 | -0.0196857   | -0.0451585   | 0.506195 |
| Second grade fluid | -0.0265531   | -0.0291432   | 0.505573 | -0.0233888   | -0.0314923   | 0.505573 |
| Viscous fluid      | -0.0240132   | -0.0261104   | 0.505572 | -0.021174    | -0.0282365   | 0.505572 |

Firstly, numerical results corresponding to the fourth-grade fluid, third grade fluid, second grade fluid and viscous fluid are listed in Table 5.1. From this Table it can be seen that velocity and temperature in the fourth-grade fluid are much greater than the other types of fluid in the presence as well as in the absence of Hall parameter. Velocity along the flow is greater in the absence of Hall parameter in all types of the fluid, whereas the normal component of velocity is smaller in the absence of Hall parameter and increases in the presence of Hall parameter. The temperature in the fourth-grade fluid increases due to the presence of Hall parameter but there is no effect of Hall parameter on the temperature profile in other fluids.

Figures 5.3(a)-5.16(b) show the components of the velocity profile and temperature for different values of  $M, \beta, \gamma, \alpha_1, \beta_1, \gamma_1$  and  $Br$  in the presence and absence of Hall parameter. Figures 5.3(a) - 5.4(b) show that velocities decrease rapidly in the absence of Hall parameter as compared when the Hall parameter is present. Figures 5.5(a)-5.8(b) show that velocity profile increases with the increase of parameter  $\beta$  and  $\gamma$ . Figures 5.9(a)-5.10(b) show that normal component of velocity decreases with the increase in  $\alpha_1$  but the velocity profile parallel to the plate is not effected by increasing  $\alpha_1$  in the absence as well as in the presence of Hall parameter. Figures 5.11(a)-5.14(b) depict that the normal component of velocity effected much when compared with the velocity along the plates when the fourth grade parameters  $\beta_1$  and  $\gamma_1$  are increased. Figures 5.15(a) and 5.15(b) display that temperature profile increases in the presence as well as absence of the Hall parameter when Brinkman number  $Br$  increases. Figures 5.16(a) and 5.16(b) show that temperature profile does not change through the variation of parameter  $\beta$ .

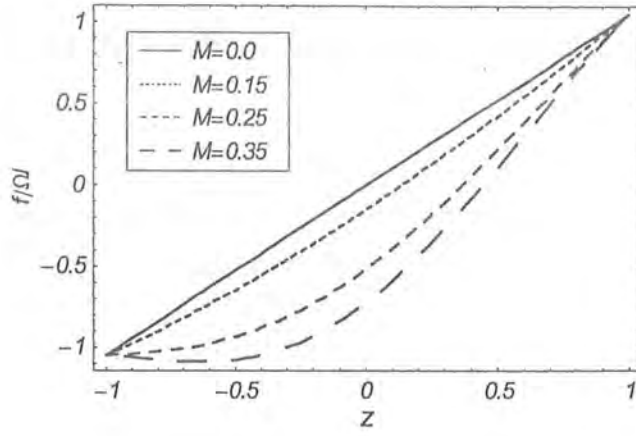


Figure 5.3(a): The variation of velocity profile  $f/\Omega l$  for various values of the Hartman number  $M$  when  $V_1 = 1/20, V_2 = 1/10 = R$  and  $\phi = 1/10$  are fixed.

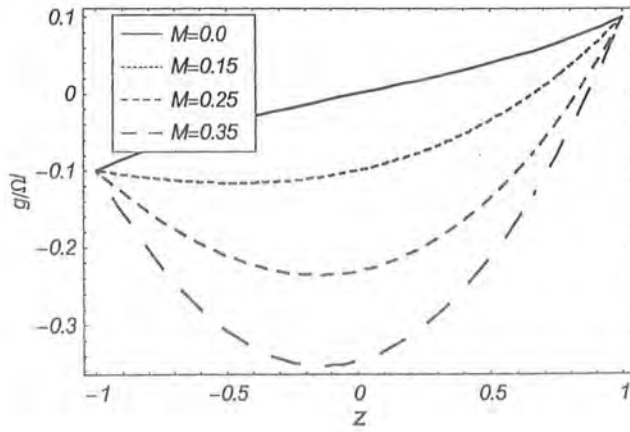


Figure 5.3(b): The variation of velocity profile  $g/\Omega l$  for various values of the Hartman number  $M$  when  $V_1 = 1/20, V_2 = 1/10 = R$  and  $\phi = 1/10$  are fixed.



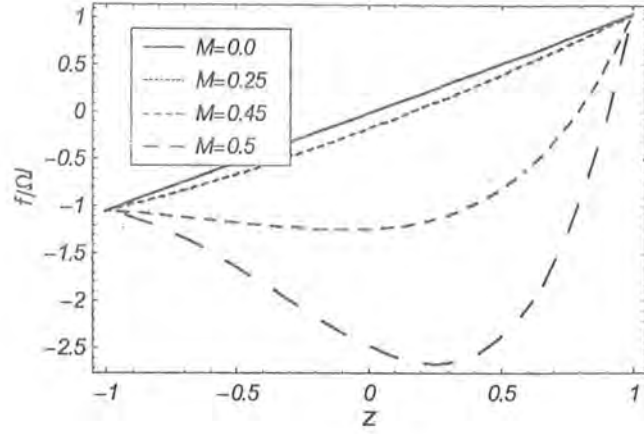


Figure 5.4(a): The variation of velocity profile  $f/\Omega l$  for various values of the Hartman number  $M$  when  $V_1 = 1/20, V_2 = 1/10 = R$  and  $\phi = 0$  are fixed.

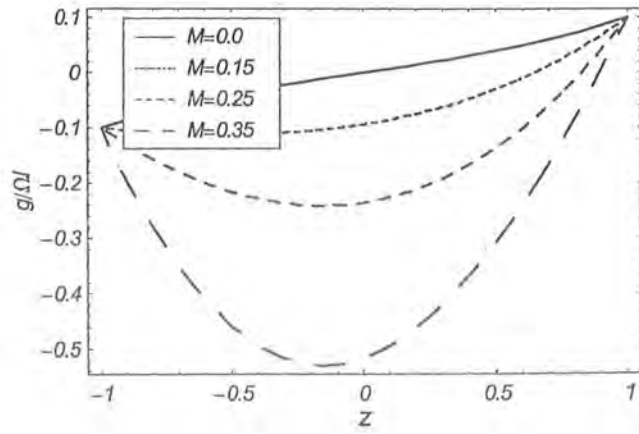


Figure 5.4(b): The variation of velocity profile  $g/\Omega l$  for various values of the Hartman number  $M$  when  $V_1 = 1/20, V_2 = 1/10 = R$  and  $\phi = 0$  are fixed.

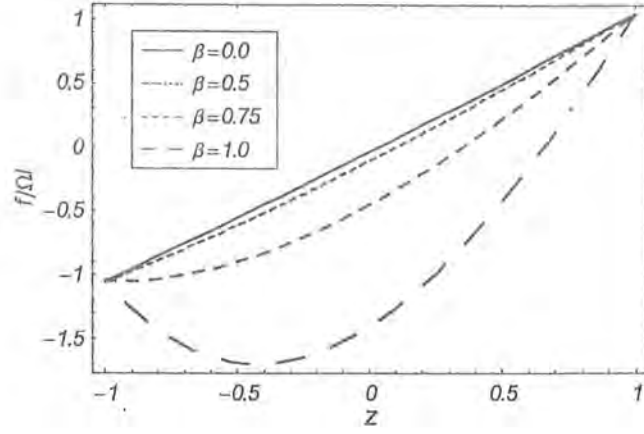


Figure 5.5(a): The variation of velocity profile  $f/\Omega l$  for various values of  $\beta$  when  $V_1 = 1/20$ ,  $V_2 = 1/10 = R$  and  $\phi = 1/10$  are fixed.

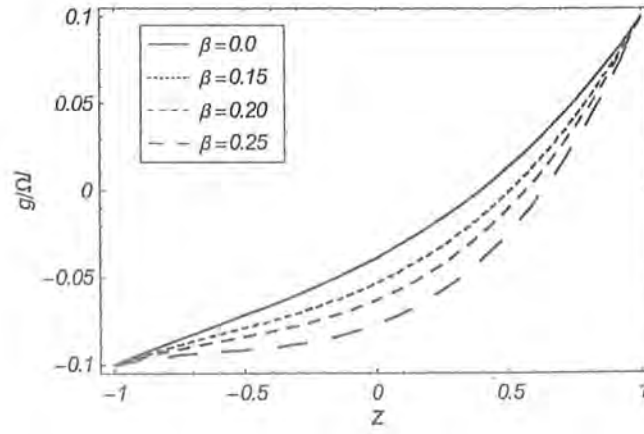


Figure 5.5(b): The variation of velocity profile  $g/\Omega l$  for various values of  $\beta$  when  $V_1 = 1/20$ ,  $V_2 = 1/10 = R$  and  $\phi = 1/10$  are fixed.

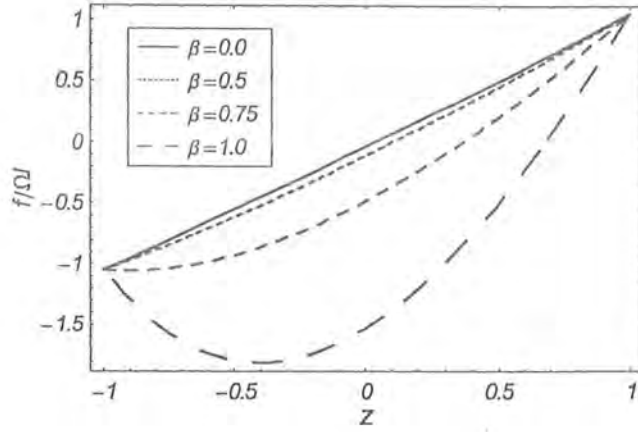


Figure 5.6(a): The variation of velocity profile  $f/\Omega$  for various values of  $\beta$  when  $V_1 = 1/20$ ,  $V_2 = 1/10 = R$  and  $\phi = 0$  are fixed.

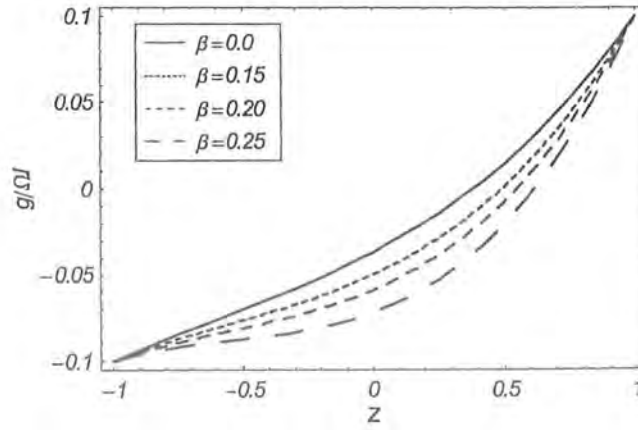


Figure 5.6(b): The variation of velocity profile  $g/\Omega$  for various values of  $\beta$  when  $V_1 = 1/20$ ,  $V_2 = 1/10 = R$  and  $\phi = 0$  are fixed.

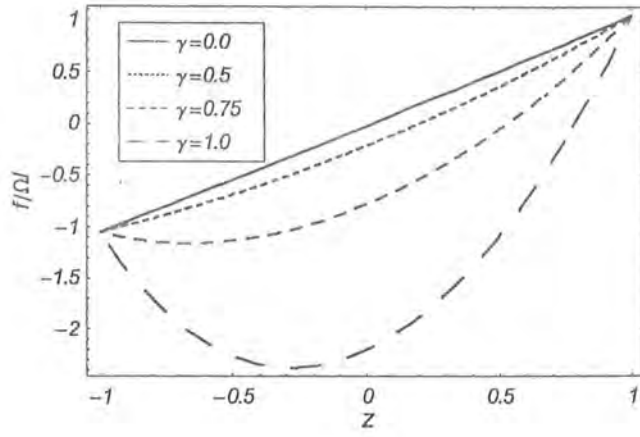


Figure 5.7(a): The variation of velocity profile  $f/\Omega l$  for various values of  $\gamma$  when  $V_1 = 1/20$ ,  $V_2 = 1/10 = R$  and  $\phi = 0$  are fixed.

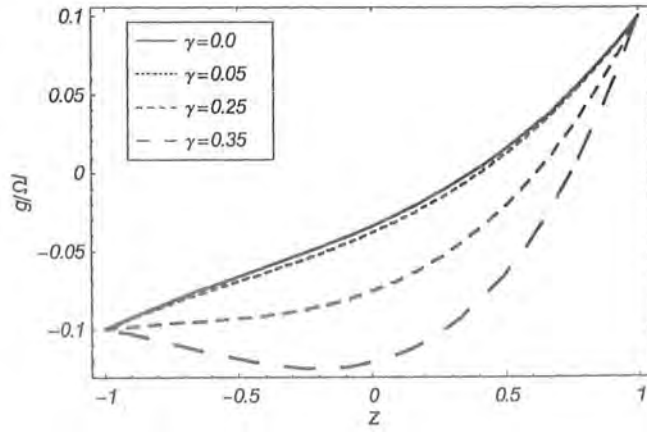


Figure 5.7(b): The variation of velocity profile  $g/\Omega l$  for various values of  $\gamma$  when  $V_1 = 1/20$ ,  $V_2 = 1/10 = R$  and  $\phi = 0$  are fixed.

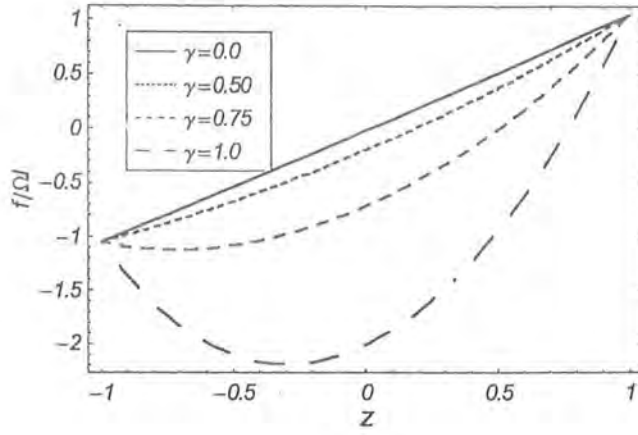


Figure 5.8(a): The variation of velocity profile  $f/\Omega$  for various values of  $\gamma$  when  $V_1 = 1/20$ ,  $V_2 = 1/10 = R$  and  $\phi = 1/10$  are fixed.

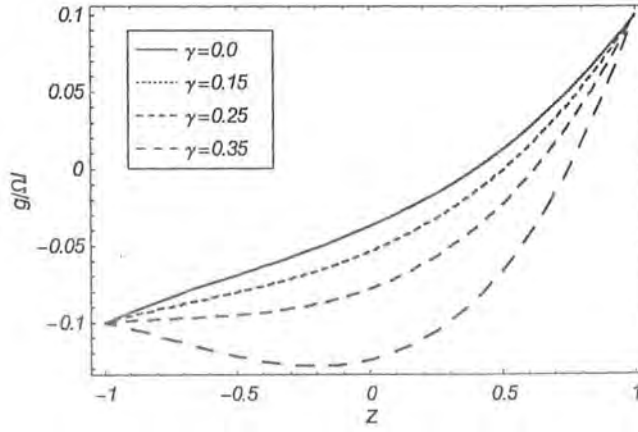


Figure 5.8(b): The variation of velocity profile  $g/\Omega$  for various values of  $\gamma$  when  $V_1 = 1/20$ ,  $V_2 = 1/10 = R$  and  $\phi = 1/10$  are fixed.

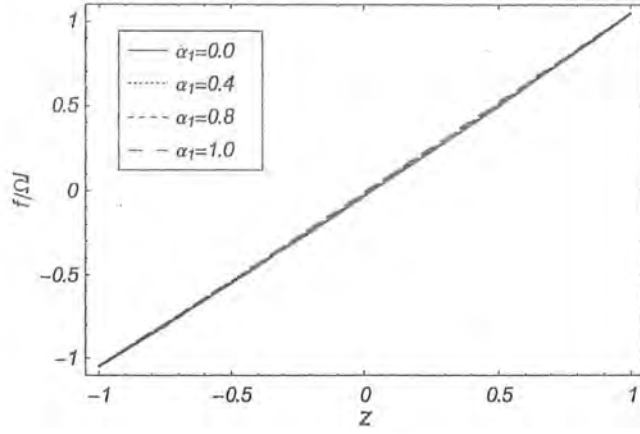


Figure 5.9(a): The variation of velocity profile  $f/\Omega l$  for various values of  $\alpha_1$  when  $V_1 = 1/20, V_2 = 1/10 = R$  and  $\phi = 0$  are fixed.

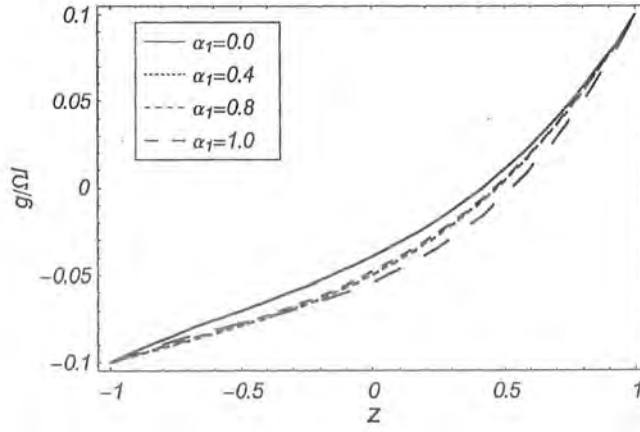


Figure 5.9(b): The variation of velocity profile  $g/\Omega l$  for various values of  $\alpha_1$  when  $V_1 = 1/20, V_2 = 1/10 = R$  and  $\phi = 0$  are fixed.

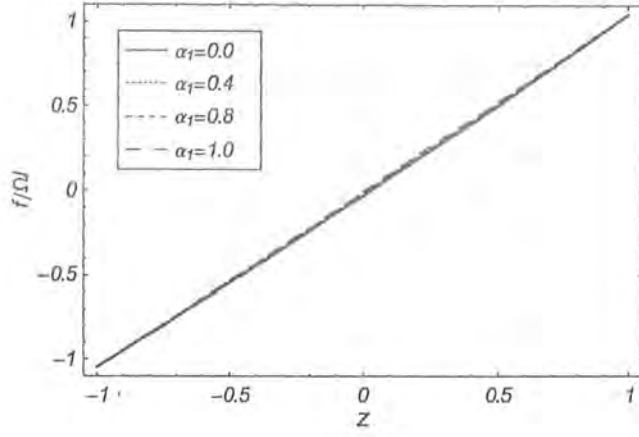


Figure 5.10(a): The variation of velocity profile  $f/\Omega l$  for various values of  $\alpha_1$  when  $V_1 = 1/20, V_2 = 1/10 = R$  and  $\phi = 1/10$  are fixed.

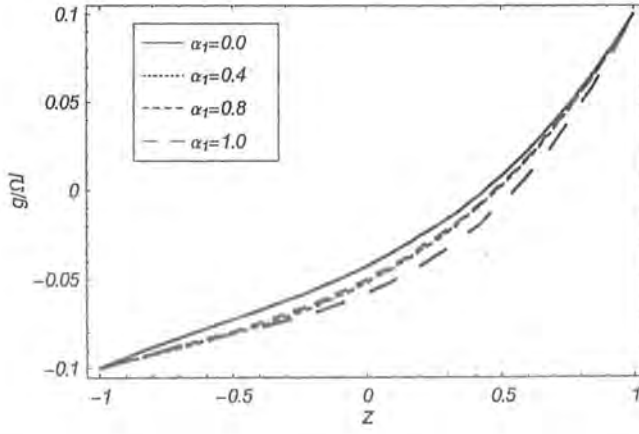


Figure 5.10(b): The variation of velocity profile  $g/\Omega l$  for various values of  $\alpha_1$  when  $V_1 = 1/20, V_2 = 1/10 = R$  and  $\phi = 1/10$  are fixed.

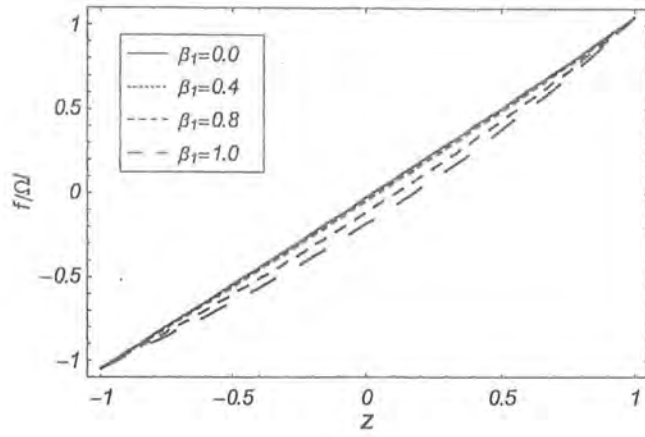


Figure 5.11(a): The variation of velocity profile  $f/\Omega l$  for various values of  $\beta_1$  when  $V_1 = 1/20$ ,  $V_2 = 1/10 = R$  and  $\phi = 0$  are fixed.

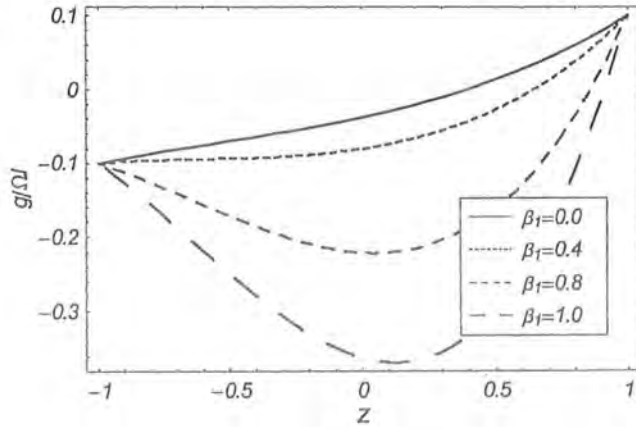


Figure 5.11(b): The variation of velocity profile  $g/\Omega l$  for various values of  $\beta_1$  when  $V_1 = 1/20$ ,  $V_2 = 1/10 = R$  and  $\phi = 0$  are fixed.



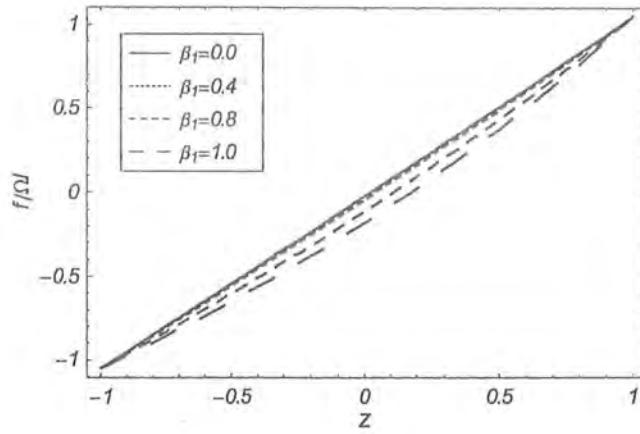


Figure 5.12(a): The variation of velocity profile  $f/\Omega l$  for various values of  $\beta_1$  when  $V_1 = 1/20, V_2 = 1/10 = R$  and  $\phi = 1/10$  are fixed

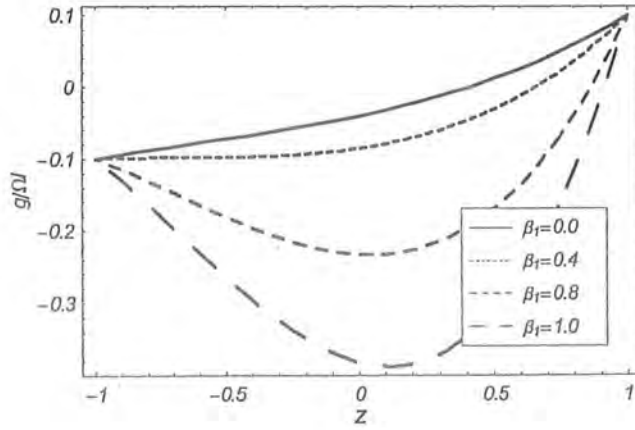


Figure 5.12(b): The variation of velocity profile  $g/\Omega l$  for various values of  $\beta_1$  when  $V_1 = 1/20, V_2 = 1/10 = R$  and  $\phi = 1/10$  are fixed.

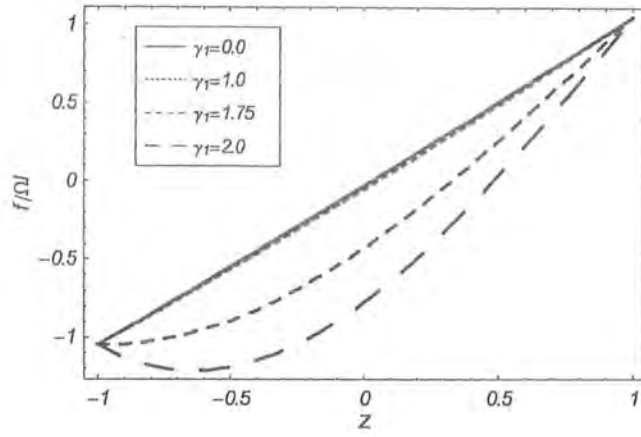


Figure 5.13(a): The variation of velocity profile  $f/\Omega l$  for various values of  $\gamma_1$  when  $V_1 = 1/20$ ,  $V_2 = 1/10 = R$  and  $\phi = 0$  are fixed.

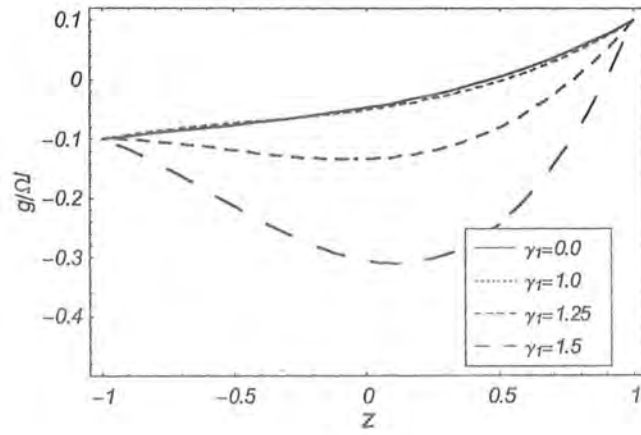


Figure 5.13(b): The variation of velocity profile  $g/\Omega l$  for various values of  $\gamma_1$  when  $V_1 = 1/20$ ,  $V_2 = 1/10 = R$  and  $\phi = 0$  are fixed.

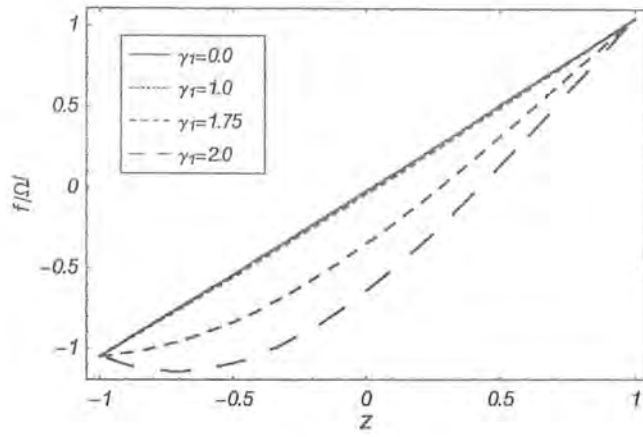


Figure 5.14(a): The variation of velocity profile  $f/\Omega l$  for various values of  $\gamma_1$  when  $V_1 = 1/20$ ,  $V_2 = 1/10 = R$  and  $\phi = 1/10$  are fixed.

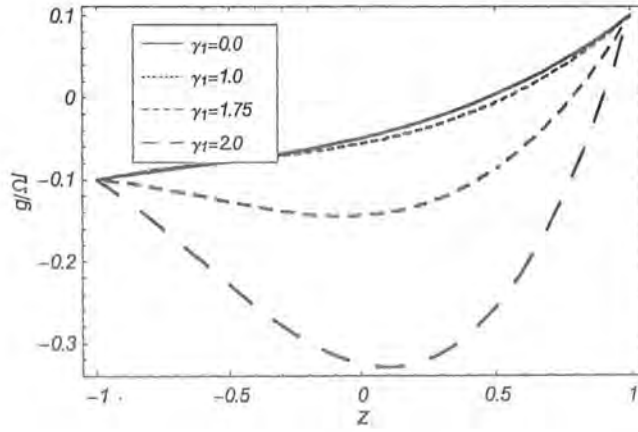


Figure 5.14(b): The variation of velocity profile  $g/\Omega l$  for various values of  $\gamma_1$  when  $V_1 = 1/20$ ,  $V_2 = 1/10 = R$  and  $\phi = 1/10$  are fixed.

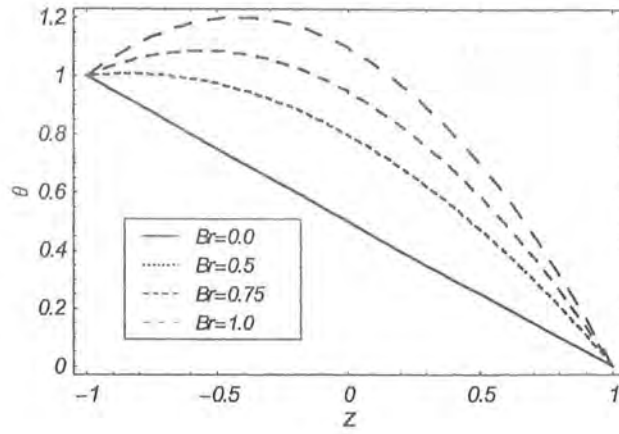


Figure 5.15(a): The variation of temperature  $\theta$  for various values of  $Br = Pr E_c$  when  $V_1 = 1/20, V_2 = R = M = 1/10$  and  $\phi = 0$  are fixed.

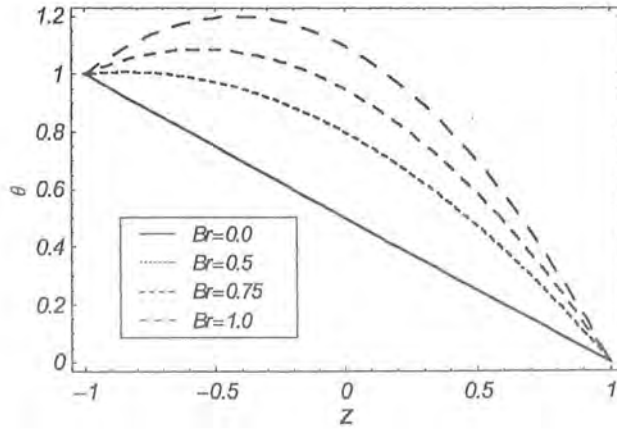


Figure 5.15(b): The variation of temperature for various values of  $Br = Pr E_c$  when  $V_1 = 1/20, V_2 = R = M = 1/10$  and  $\phi = 1/10$  are fixed.

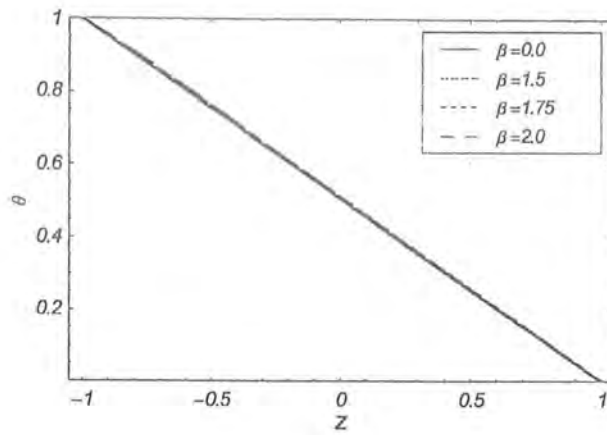


Figure 5.16(a): The variation of temperature for various values of  $\beta$  when  $V_1 = 1/20$ ,  $V_2 = R = M = 1/10$  and  $Br = 1/100$  are fixed and  $\phi = 0$

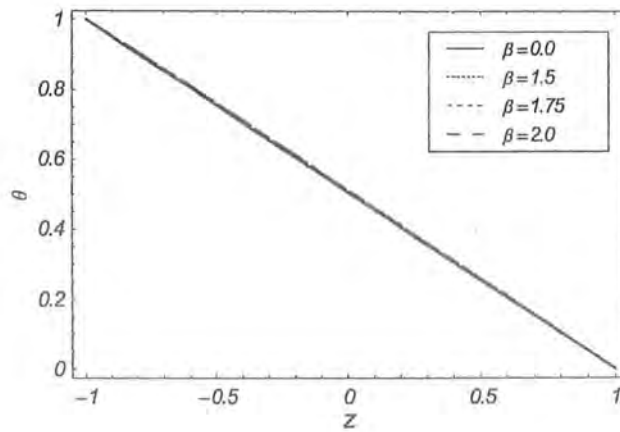


Figure 5.16(b): The variation of temperature for various values of  $\beta$  when  $V_1 = 1/20$ ,  $V_2 = R = M = 1/10$  and  $Br = 1/100$  are fixed and  $\phi = 1/10$ .

## Chapter 6

# Steady flow of a Sisko fluid under the influence of Hall current and heat transfer

This chapter aims to revisit the flow analysis of previous chapter for a Sisko fluid. The governing nonlinear flow problem is first modeled and then solved by a homotopy analysis method. The effects of material parameters associated with Sisko fluid are explained.

### 6.1 Mathematical formulation

Consider an electrically conducting Sisko fluid between two infinite disks rotating with angular velocity  $\Omega$  about two non-coaxial axes distant  $2l$  apart. The  $z$  - axis is chosen normal to the disks. The fluid is electrically conducting in the presence of a constant applied magnetic field. The disks at  $z = h$  and  $z = -h$  are pulled with constant velocities  $U$  and  $-U$  respectively. The appropriate boundary conditions and velocity field is defined in equations (4.1) and (4.2).

The Cauchy stress tensor for the Sisko fluid [129, 130] is

$$\begin{aligned} \mathbf{T} &= -p\mathbf{I} + \mathbf{S}, \\ \mathbf{S} &= \left[ a + b \left| \frac{1}{2} \text{tr}(\mathbf{A}_1^2) \right|^{\frac{n-1}{2}} \right] \mathbf{A}_1. \end{aligned} \tag{6.1}$$

It should be noted that for  $b = 0$  and  $a = \mu$ , Eq. (6.1) reduces to viscous fluid. Invoking Eq. (4.2) into Eq. (6.1) we obtain

$$S_{xx} = S_{yy} = S_{zz} = S_{xy} = S_{yx} = 0, \quad (6.2)$$

$$S_{xz} = S_{zx} = \left( a + b \left( \left( \frac{df}{dz} \right)^2 + \left( \frac{dg}{dz} \right)^2 \right)^{\frac{n-1}{2}} \right) \frac{df}{dz},$$

$$S_{yz} = S_{zy} = \left( a + b \left( \left( \frac{df}{dz} \right)^2 + \left( \frac{dg}{dz} \right)^2 \right)^{\frac{n-1}{2}} \right) \frac{dg}{dz}. \quad (6.3)$$

Invoking equations (4.2) and (6.1) into momentum equation we obtain

$$\frac{\partial p}{\partial x} = \rho \Omega (\Omega x + g(z)) + \frac{\partial S_{xz}}{\partial z} + \frac{\sigma B_0^2 (1 + i\phi)}{1 + \phi^2} \left( \frac{Q}{2h} - f(z) \right), \quad (6.4)$$

$$\frac{\partial p}{\partial y} = -\rho \Omega (-\Omega y + f(z)) + \frac{\partial S_{yz}}{\partial z} + \frac{\sigma B_0^2 (1 + i\phi)}{1 + \phi^2} \left( \frac{P}{2h} - g(z) \right), \quad (6.5)$$

where z-component of momentum equation indicates that  $p \neq p(z)$ ,  $\phi = \omega_e \tau_e$  is the Hall parameter and  $Q$  and  $P$  are defined in the equations (4.19).

Performing integration of equations (6.4) and (6.5) we get

$$p = p_0 + \frac{1}{2} \Omega^2 (x^2 + y^2) + \left[ C_1 + \frac{HQ}{2h} \right] x + \left[ C_2 + \frac{HP}{2h} \right] y, \quad (6.6)$$

in which  $p_0$  is the reference pressure,  $C_i (i = 1, 2)$  are the arbitrary constants defined in equations (4.22) and (4.23). After using equations (6.3) into equations (6.4) and (6.5) we arrive at

$$\frac{d}{dz} \left[ \left\{ a + b \left( \left( \frac{df}{dz} \right)^2 + \left( \frac{dg}{dz} \right)^2 \right)^{\frac{n-1}{2}} \right\} \frac{df}{dz} \right] + \Omega \rho g(z) - H f(z) + \frac{HQ}{2h} = 0, \quad (6.7)$$

$$\frac{d}{dz} \left[ \left\{ a + b \left( \left( \frac{df}{dz} \right)^2 + \left( \frac{dg}{dz} \right)^2 \right)^{\frac{n-1}{2}} \right\} \frac{dg}{dz} \right] - \Omega \rho f(z) - H g(z) + \frac{HP}{2h} = 0. \quad (6.8)$$

The above two equations can be combined as

$$a \frac{d^2 F}{dz^2} + b \left[ \frac{d^2 F}{dz^2} \left( \frac{dF}{dz} \frac{d\bar{F}}{dz} \right)^{\frac{n-1}{2}} + \frac{n-1}{2} \frac{dF}{dz} \left( \frac{dF}{dz} \frac{d\bar{F}}{dz} \right)^{\frac{n-3}{2}} \left( \frac{d^2 F}{dz^2} \frac{d\bar{F}}{dz} + \frac{dF}{dz} \frac{d^2 \bar{F}}{dz^2} \right) \right] - \left( \frac{\sigma B_0^2 (1+i\phi)}{1+\phi^2} + i\Omega\rho \right) F + \left( \frac{\sigma B_0^2 (1+i\phi)}{1+\phi^2} \right) \left( \frac{Q+iP}{2h} \right) = 0, \quad (6.9)$$

where the boundary conditions are

$$F(h) = \Omega l + U_1 + iU_2, \quad F(-h) = -(\Omega l + U_1 + iU_2), \quad (6.10)$$

and

$$F = f + ig, \quad \bar{F} = f - ig.$$

At this stage it is convenient to define the dimensionless quantities as follows

$$z^* = \frac{z}{h}, \quad F^* = \frac{F}{\Omega l}, \quad b_1^* = \frac{b}{a} \left( \frac{\Omega l}{h} \right)^{n-1}, \\ M^2 = \frac{\sigma B_0^2 h^2}{a}, \quad R = \Omega \rho \frac{h^2}{a}, \quad V_1 = \frac{U_1}{\Omega l}, \quad V_2 = \frac{U_2}{\Omega l}.$$

The resulting dimensionless problem becomes

$$\frac{d^2 F}{dz^2} + b_1 \left( \frac{d^2 F}{dz^2} \left( \frac{dF}{dz} \frac{d\bar{F}}{dz} \right)^{\frac{n-1}{2}} + \frac{n-1}{2} \frac{dF}{dz} \left( \frac{dF}{dz} \frac{d\bar{F}}{dz} \right)^{\frac{n-3}{2}} \left( \frac{d^2 F}{dz^2} \frac{d\bar{F}}{dz} + \frac{dF}{dz} \frac{d^2 \bar{F}}{dz^2} \right) \right), \quad (6.11) \\ - \left( \frac{M^2(1+i\phi)}{1+\phi^2} + iR \right) F = - \left( \frac{M^2(1+i\phi)}{1+\phi^2} \right) \left( \frac{Q+iP}{2h\Omega l} \right),$$

$$F(1) = 1 + V_1 + iV_2, \quad F(-1) = -(1 + V_1 + iV_2), \quad (6.12)$$

where asteriks have been suppressed for simplicity.



## 6.2 Analytic solution by homotopy analysis method (HAM)

For series solutions of Eqs. (6.11) and (6.12), the initial guess and linear operator are

$$F_0(z) = (1 + V_1 + iV_2)z, \quad (6.13)$$

$$\mathcal{L}_3(\hat{F}(z; q)) = \frac{\partial^2 \hat{F}}{\partial z^2}, \quad (6.14)$$

$$\mathcal{L}_3 [D_1 + zD_2] = 0. \quad (6.15)$$

where  $D_i$  ( $i = 1, 2$ ) are the arbitrary constants.

Zeroth order deformation problem is written as

$$(1 - q)\mathcal{L}_3 [\hat{F}(z; q) - F_0(z)] = q\hbar_3 \mathcal{N}_3 [\hat{F}(z; q)], \quad (6.16)$$

$$\hat{F}_0(1; q) = 1 + V_1 + iV_2, \quad \hat{F}_0(-1; q) = -(1 + V_1 + iV_2), \quad (6.17)$$

where  $q \in [0, 1]$  is an embedding parameter and  $\hbar_3$  is an auxiliary parameter and the non linear operator  $\mathcal{N}_3$  is

$$\mathcal{N}_3 [\hat{F}(z; q)] = \frac{\partial^2 \hat{F}(z; q)}{\partial z^2} + b_1 \left( \begin{aligned} & \frac{\partial^2 \hat{F}}{\partial z^2} \left( \frac{\partial \hat{F}}{\partial z} \frac{\partial \bar{\hat{F}}}{\partial z} \right)^{\frac{n-1}{2}} \\ & + \frac{n-1}{2} \frac{\partial \hat{F}}{\partial z} \left( \frac{\partial \hat{F}}{\partial z} \frac{\partial \bar{\hat{F}}}{\partial z} \right)^{\frac{n-3}{2}} \left( \frac{\partial^2 \hat{F}}{\partial z^2} \frac{\partial \hat{F}}{\partial z} + \frac{\partial \hat{F}}{\partial z} \frac{\partial^2 \bar{\hat{F}}}{\partial z^2} \right) \\ & - \left( \frac{M^2(1+i\phi)}{1+\phi^2} + iR \right) \hat{F} + \left( \frac{M^2(1+i\phi)}{1+\phi^2} \right) \left( \frac{Q+iP}{2\hbar\Omega} \right). \end{aligned} \right) \quad (6.18)$$

The  $m$ th order deformation problem is

$$\mathcal{L}_3 [F_m(z) - \chi_m F_{m-1}(z)] = \hbar_3 \mathcal{R}_{3m}(z), \quad (6.19)$$

$$F_m(1) = F_m(-1) = 0. \quad (6.20)$$

When  $n = 3$ , nonlinear operator is defined as

$$\begin{aligned} \mathcal{R}_{3m}(z) &= F''_{m-1}(z) - \left( \frac{M^2(1+i\phi)}{1+\phi^2} + iR \right) F_{m-1}(z) \\ &+ (1 - \chi_m) \left( \frac{M^2(1+i\phi)}{1+\phi^2} \right) \left( \frac{Q + iP}{2h\Omega l} \right) \\ &+ b_1 \left( \sum_{k=0}^{m-1} F'_{m-1-k} \sum_{l=0}^k (2\bar{F}'_{k-l} F''_l + F'_{k-l} \bar{F}''_l) \right). \end{aligned} \quad (6.21)$$

For  $n = 5$  nonlinear operator is given by

$$\begin{aligned} \mathcal{R}_{3m}(z) &= F''_{m-1}(z) - \left( \frac{M^2(1+i\phi)}{1+\phi^2} + iR \right) F_{m-1}(z) \\ &+ (1 - \chi_m) \left( \frac{M^2(1+i\phi)}{1+\phi^2} \right) \left( \frac{Q + iP}{2h\Omega l} \right) \\ &+ b_1 \left( \sum_{k=0}^{m-1} F'_{m-1-k} \sum_{l=0}^k F'_{k-l} \sum_{a=0}^l \bar{F}'_{l-a} \sum_{b=0}^a (3\bar{F}'_{b-a} F''_a + 2F'_{b-a} \bar{F}''_a) \right). \end{aligned} \quad (6.22)$$

The  $m$ th order deformation problem has been solved by using "MATHEMATICA" up to first few order of approximations for  $n = 3$  and  $n = 5$ . The solution is expressed by

$$F_m(z) = \sum_{t=0}^{2m+1} d_{m,t} z^t, \quad d_{m,t} = \text{Re } d_{m,t} + i \text{Im } d_{m,t}, \quad m \geq 0, \quad (6.23)$$

in which for  $m \geq 1$  and  $0 \leq t \leq 2m + 1$ , the recurrence formulas are

$$\begin{aligned} d_{m,0} &= \chi_m \chi_{2m+1} d_{m-1,0} - \left( \frac{A}{2} + \sum_{t=0}^{2m+n-2} \frac{\Gamma_{m,t}}{(1+t)(2+t)} \left( \frac{1 - (-1)^{t+2}}{2} \right) \right), \\ d_{m,1} &= \chi_m \chi_{2m} d_{m-1,1} - \sum_{t=0}^{2m+n-2} \frac{\Gamma_{m,t}}{(1+t)(2+t)} \left( \frac{1 + (-1)^{t+2}}{2} \right), \\ d_{m,2} &= \chi_m \chi_{2m-1} d_{m-1,2} + \frac{1}{2} (A + \Gamma_{m,0}), \\ d_{m,t} &= \chi_m \chi_{2m-t+1} d_{m-1,t} + \Gamma_{m,t-2} \frac{1}{(t-1)t}, \quad 3 \leq t \leq 2m + n - 2, \\ \Gamma_{m,t} &= \hbar \left( \chi_{2m-t+n-2} \left( e_{m-1,t} - \left( \frac{M^2(1+i\phi)}{1+\phi^2} + iR \right) c_{m-1,t} \right) + b_1 \Pi(z) \right), \\ \Pi(z) &= 2\delta_{m,t} + \Delta_{m,t} \quad \text{for } n = 3, \\ \Pi(z) &= 3\lambda_{m,t} + 2\gamma_{m,t} \quad \text{for } n = 5, \end{aligned}$$

and the related coefficients  $\delta_{m,t}$ ,  $\Delta_{m,t}$ ,  $\lambda_{m,t}$ ,  $\gamma_{m,t}$  for  $m \geq 1$ ,  $0 \leq t \leq 2m + n - 2$  are

$$\begin{aligned}
\delta_{m,t} &= \sum_{k=0}^{m-1} \sum_{l=0}^k \sum_{q=\max\{0,1+t-2k-2m\}}^{\min\{t,2k+2\}} d1_{m-1-k,t-q} \sum_{u=\max\{0,q-1-2l\}}^{\min\{q,2k-2l+1\}} \bar{d}1_{k-l,u} d2_{l,q-u}, \\
\Delta_{m,t} &= \sum_{k=0}^{m-1} \sum_{l=0}^k \sum_{u=\max\{0,1+t+2k-2m\}}^{\min\{t,2k+2\}} d1_{m-1-k,t-u} \sum_{q=\max\{0,u+1+2l-2k\}}^{\min\{u,2l+1\}} d1_{k-l,u-q} \bar{d}2_{l,q}, \\
\lambda_{m,t} &= \sum_{k=0}^{m-1} \sum_{l=0}^k \sum_{a=0}^l \sum_{b=0}^a \sum_{w=\max\{0,2k+1+t-2m\}}^{\min\{t,2k+4\}} d1_{m-1-k,t-w} \sum_{u=\max\{0,2l+w-1-2k\}}^{\min\{w,2l+3\}} d1_{k-l,w-u} \\
&\quad \sum_{r=\max\{0,2a+u-2l-1\}}^{\min\{u,2a+2\}} \bar{d}1_{l-a,u-r} \sum_{p=\max\{0,r-1-2b\}}^{\min\{r,2b+1\}} \bar{d}1_{a-b,p} d2_{b,r-p}, \\
\gamma_{m,t} &= \sum_{k=0}^{m-1} \sum_{l=0}^k \sum_{a=0}^l \sum_{b=0}^a \sum_{w=\max\{0,2k+2+t-2m\}}^{\min\{t,2k+4\}} d1_{m-1-k,t-w} \sum_{u=\max\{0,2l+w-1-2k\}}^{\min\{w,2k-2l+1\}} d1_{k-l,w-u} \\
&\quad \sum_{r=\max\{0,2a+u-2l-1\}}^{\min\{u,2a+2\}} d1_{l-a,u-r} \sum_{p=\max\{0,r-1-2b\}}^{\min\{r,2b+1\}} \bar{d}1_{a-b,p} \bar{d}2_{b,r-p}, \\
d_{m,t} &= \operatorname{Re} d_{m,t} + i \operatorname{Im} d_{m,t}, & \bar{d}_{m,t} &= \operatorname{Re} d_{m,t} - i \operatorname{Im} d_{m,t}, \\
d1_{m,t} &= (1+t)d_{m,1+t}, & \bar{d}1_{m,t} &= (1+t)\bar{d}_{m,1+t}, \\
d2_{m,t} &= (1+t)d1_{m,1+t}, & \bar{d}2_{m,t} &= (1+t)\bar{d}2_{m,1+t}.
\end{aligned} \tag{6.24}$$

The corresponding  $m$ th order approximation is

$$\sum_{m=0}^M F_m(z) = \sum_{m=0}^M \sum_{t=0}^{2m+1} d_{m,t} z^t \tag{6.25}$$

and the explicit solution is

$$F(z) = \lim_{M \rightarrow \infty} \left( \sum_{m=0}^M F_m(z) \right) = \lim_{M \rightarrow \infty} \left( \sum_{m=0}^M \sum_{t=0}^{2m+1} d_{m,t} z^t \right). \tag{6.26}$$

### 6.3 Heat transfer analysis

This section describes the heat transfer analysis. The corresponding temperature of the upper (at  $z = h$ ) and lower (at  $z = -h$ ) plates are defined in Eq. (4.37)

Non-dimensional form of energy equation for the Sisko fluid is

$$\frac{d^2\theta}{dz^2} = -E_c Pr \left( 1 + b_1 \left\{ \left( \frac{df^*}{dz} \right)^2 + \left( \frac{dg^*}{dz} \right)^2 \right\}^{\frac{n-1}{2}} \right) \left( \left( \frac{df^*}{dz} \right)^2 + \left( \frac{dg^*}{dz} \right)^2 \right), \quad (6.27)$$

where  $f^* = f/\Omega l$ ,  $g^* = g/\Omega l$ ,  $b_1 = (\Omega l)^{n-1} b/a$ .

In terms of  $F$ , Eq. (6.27) is

$$\frac{d^2\theta}{dz^2} = -Br \left( 1 + b_1 \left( \frac{dF}{dz} \frac{d\bar{F}}{dz} \right)^{\frac{n-1}{2}} \right) \frac{dF}{dz} \frac{d\bar{F}}{dz} \quad (6.28)$$

subject to the boundary conditions

$$\theta(-1) = 1, \quad \theta(1) = 0, \quad (6.29)$$

The initial guess  $\theta_0$  and an auxiliary linear operator  $\mathcal{L}_4$  are chosen as

$$\theta_0(z) = \frac{1}{2}(1-z), \quad (6.30)$$

$$\mathcal{L}_4[\hat{\theta}(z; q)] = \frac{\partial^2 \theta(z; q)}{\partial z^2}, \quad (6.31)$$

$$\mathcal{L}_4(E_1 + zE_2) = 0, \quad (6.32)$$

where  $E_i$  ( $i = 1, 2$ ) are the arbitrary constants.

The zeroth order problem becomes

$$(1-q)\mathcal{L}_4[\hat{\theta}(z; q) - \theta_0(z)] = q\hbar_4 \mathcal{N}_4[\hat{F}(z; q), \hat{\theta}(z; q)], \quad (6.33)$$

$$\hat{\theta}_0(-1; q) = 1, \quad \hat{\theta}_0(1; q) = 0, \quad (6.34)$$

$$\mathcal{N}_4 [\hat{F}(z; q)] = \frac{\partial^2 \hat{\theta}}{\partial z^2} + E_c P_r \left( 1 + b_1 \left( \frac{\partial \hat{F}}{\partial z} \frac{\partial \overline{\hat{F}}}{\partial z} \right)^{\frac{n-1}{2}} \right) \frac{\partial \hat{F}}{\partial z} \frac{\partial \overline{\hat{F}}}{\partial z} \quad (6.35)$$

The problem at  $m$ th order satisfies the following equations

$$\mathcal{L}_4 [\theta_m(z) - \chi_m \theta_{m-1}(z)] = \hbar_4 \mathcal{R}_{4m}(z), \quad (6.36)$$

$$\theta_m(-1) = 0, \quad \theta_m(1) = 0, \quad (6.37)$$

$$\mathcal{R}_{4m}(z) = \theta''_{m-1}(z) + E_c P_r \sum_{k=0}^{m-1} F'_{m-1-k} \overline{F}'_k + b_1 \Psi(z), \quad (6.38)$$

$$\begin{aligned} \Psi(z) &= \sum_{k=0}^{m-1} \sum_{l=0}^k \sum_{a=0}^l \left( F'_{m-1-k} F'_{k-l} \overline{F}'_{l-a} \overline{F}'_a \right), \quad \text{for } n = 3, \\ &= \sum_{k=0}^{m-1} \sum_{l=0}^k \sum_{a=0}^l \sum_{b=0}^a \sum_{c=0}^b \left( F'_{m-1-k} F'_{k-l} F'_{1-a} \overline{F}'_{a-b} \overline{F}'_{b-c} \overline{F}'_c \right) \quad \text{for } n = 5. \end{aligned} \quad (6.39)$$

When  $n = 3$  and  $n = 5$  the solution is

$$\theta_m(z) = \sum_{t=0}^{2m} e_{m,t} z^t, \quad m \geq 0, \quad (6.40)$$

in which for  $m \geq 1$  and  $0 \leq t \leq 2m$ , we have

$$\begin{aligned} e_{m,0} &= \chi_m \chi_{2m} e_{m-1,0} - \sum_{t=0}^{2m+n-1} \frac{\zeta_{m,2t}}{(2t+1)(2t+2)}, \\ e_{m,1} &= \chi_m \chi_{2m-1} e_{m-1,1} - \sum_{t=0}^{2m+n-1} \frac{\zeta_{m,2t+1}}{(2t+2)(2t+3)}, \\ e_{m,2} &= \chi_m \chi_{2m-2} e_{m-1,2} + \frac{1}{2} \zeta_{m,0}, \\ e_{m,t} &= \chi_m \chi_{2m-t} e_{m-1,t} + \zeta_{m,t-2} \frac{1}{(t-1)t}, \quad 3 \leq t \leq 2m, \\ \zeta_{m,t} &= \hbar_4 \sum_{t=0}^{2m+n-1} [\chi_{2m+n-1-t} (e_{2m,t} + E_c P_r \alpha_{m,t}) + b_1 E_c P_r \Pi(z)], \\ \Pi(z) &= \sum_{t=0}^{2m+2} \beta_{m,t} \quad \text{for } n = 3, \end{aligned} \quad (6.41)$$

$$\Pi(z) = \sum_{t=0}^{2m+4} \gamma_{m,t} \quad \text{for } n = 5 \quad (6.42)$$

and the coefficients  $\alpha_{m,t}, \beta_{m,t}, \gamma_{m,t}$  for  $m \geq 1, 0 \leq t \leq 2m + n - 1$  are

$$\alpha_{m,t} = \sum_{k=0}^{m-1} \sum_{q=\max\{0,t-1-2k\}}^{\min\{t,2m-2k-1\}} d_{1_{m-1-k,q}} \bar{d}_{1_{k,t-q}}$$

$$\beta_{m,t} = \sum_{k=0}^{m-1} \sum_{l=0}^k \sum_{a=0}^l \sum_{u=\max\{0,1+t+2k-2m\}}^{\min\{t,2k+2\}} d_{1_{m-1-k,t-u}} \sum_{r=\max\{0,u+2l-2k\}}^{\min\{u,2l+2\}} d_{1_{k-l,u-r}} \sum_{p=\max\{0,r-2a-1\}}^{\min\{r,2l-2a+1\}} \bar{d}_{1_{a,r-p}} \bar{d}_{1_{l-a,p}}$$

$$\gamma_{m,t} = \sum_{k=0}^{m-1} \sum_{l=0}^k \sum_{r=0}^l \sum_{s=0}^r \sum_{a=0}^s \sum_{v=\max\{0,2k+1+t-2m\}}^{\min\{t,2k+5\}} d_{1_{m-1-k,t-v}} \sum_{w=\max\{0,2l+v-1-2k\}}^{\min\{v,2l+4\}} d_{1_{k-l,t-w}} \sum_{u_1=\max\{0,2r+w-2l-1\}}^{\min\{w,2r+3\}} d_{1_{l-r,w-u_1}} \sum_{p_1=\max\{0,2s+u_1-2r-1\}}^{\min\{u_1,2s+2\}} \bar{d}_{1_{r-s,u_1-p_1}} \sum_{q=\max\{0,2a+p_1-2s-1\}}^{\min\{p_1,2a+1\}} \bar{d}_{1_{s-a,p_1-q}} \bar{d}_{1_{a,q}}$$

$$e_{2m,p} = (1+p)e_{1m,p+1}, \quad e_{1m,p} = (1+p)e_{m,p+1}. \quad (6.43)$$

The corresponding  $m$ th order approximation is

$$\sum_{m=0}^M \theta_m(z) = \sum_{m=1}^M \sum_{t=0}^{2m} e_{m,t} z^t \quad (6.44)$$

and the explicit expression for the series solution is

$$\theta(z) = \lim_{M \rightarrow \infty} \left( \sum_{m=0}^M \theta_m(z) \right) = \lim_{M \rightarrow \infty} \left( \sum_{m=1}^M \sum_{t=0}^{2m} e_{m,t} z^t \right). \quad (6.45)$$

## 6.4 Convergence of the solution

The convergence of the series solutions (6.26) and (6.45) strongly depends upon the values of  $\bar{h}_3$  and  $\bar{h}_4$ . For this purpose  $\bar{h}_3$  and  $\bar{h}_4$ -curves are drawn in Figures (6.1)-(6.3). It is noted that admissible values of  $\bar{h}_3$  and  $\bar{h}_4$  are  $-0.47 \leq \bar{h}_3 \leq 0.05, -2.5 \leq \bar{h}_4 \leq 0.5$  when  $n = 3$  and  $-0.45 \leq \bar{h}_3 \leq -0.1, -2 \leq \bar{h}_4 \leq 0$  when  $n = 5$ . Figures 6.1 and 6.2 show the residual error for velocity profiles and Figure 6.3 show temperature profiles. From these Figures we choose the values of  $\bar{h}_3$  and  $\bar{h}_4$  i.e.  $\bar{h}_3 = -0.35$  and  $\bar{h}_4 = -1.77$  for  $n = 3$  whereas  $\bar{h}_3 = -0.388$  and

$\tilde{h}_4 = -0.23$  for  $n = 5$ .

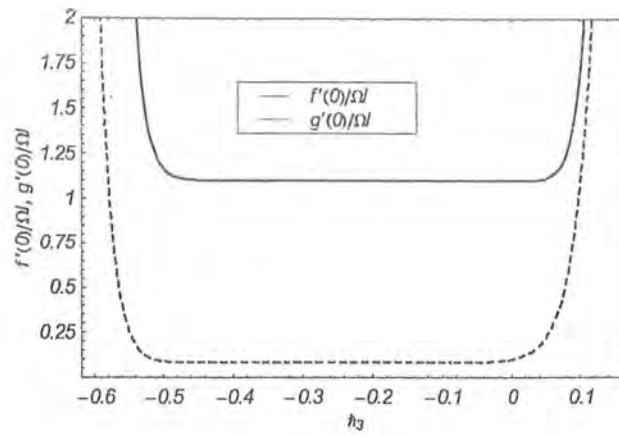


Figure 6.1(a):  $f'/\Omega l$  and  $g'/\Omega l$  versus  $h_3$ -curves for the 25th order approximation when  $n = 3$ .

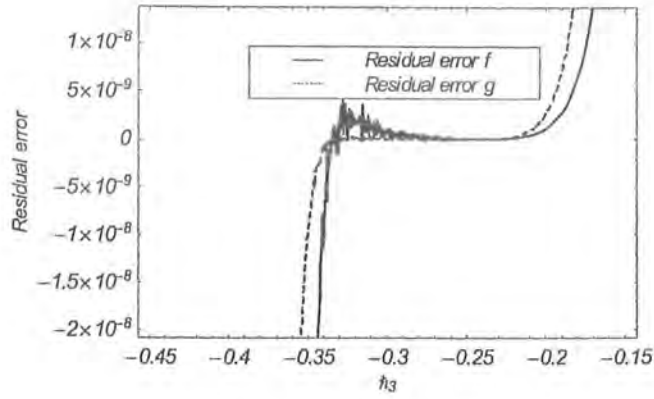


Figure 6.1(b): Residual error versus  $\tilde{h}_3$ -curves of the velocity for the 25th order approximation when  $n = 3$ .

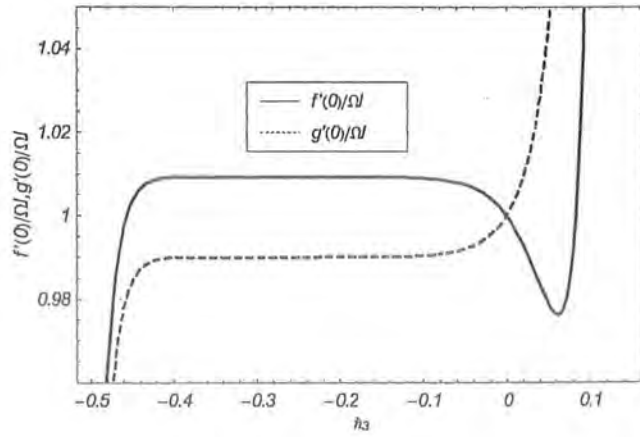


Figure 6.2(a):  $f'/\Omega$  and  $g'/\Omega$  versus  $\tilde{h}_3$ -curves for the 20th order approximation when  $n = 5$ .



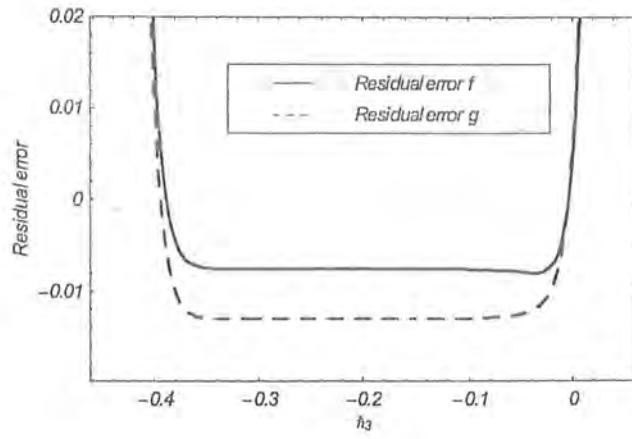


Figure 6.2(b): Residual error versus  $\tilde{h}_3$ -curves of velocity for the 20th order approximation when  $n = 5$ .

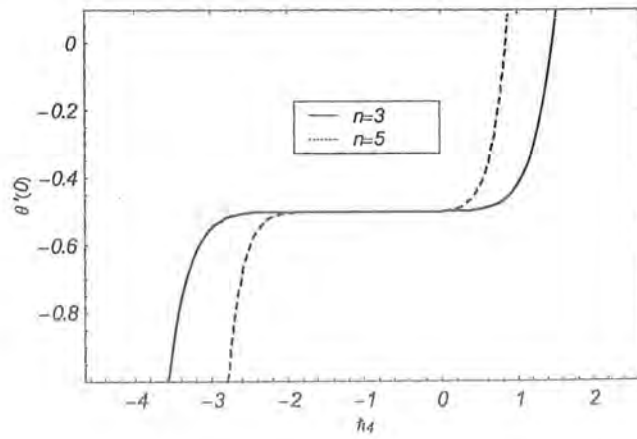


Figure 6.3:  $\theta'(0)$  versus  $\tilde{h}_4$  when  $n = 3$  and  $n = 5$  for 10th order of approximation.

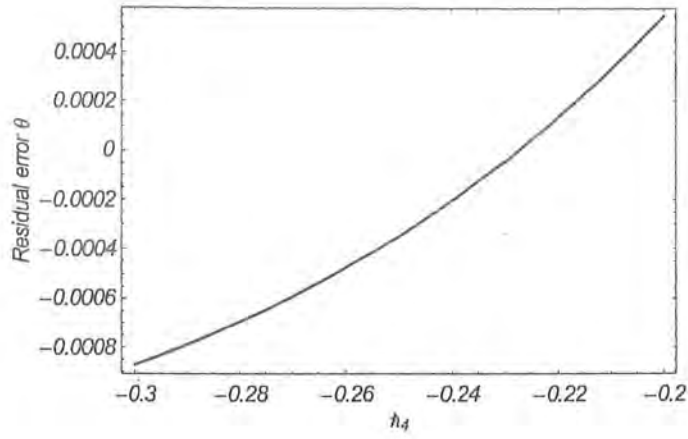


Figure 6.4(a): The graph of residual error of  $\theta$  versus  $h_4$  when  $z = 0$  and  $n = 3$  for 10th order of approximation.

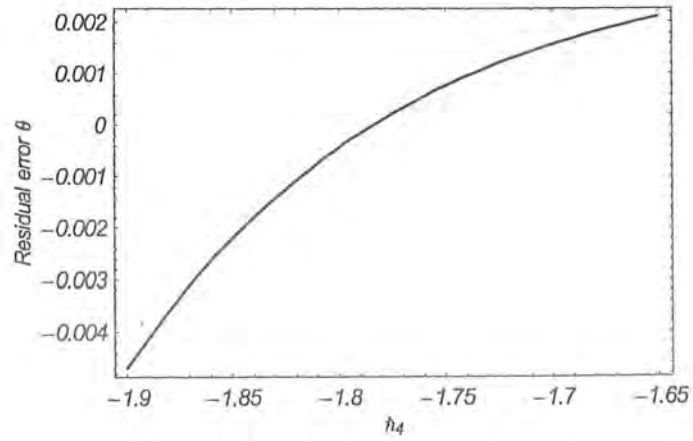


Figure 6.4(b): Residual error of  $\theta$  versus  $h_4$  when  $z = 0$  and  $n = 5$  for 10th order of approximation.

## 6.5 Results and discussion

Figures 6.5(a) – 6.20(b) show the profiles  $f/\Omega l$ ,  $g/\Omega l$  and temperature  $\theta$  for various values of  $b$  and  $M$  with and without Hall effects when  $n = 3$  and  $n = 5$  in viscous and Sisko fluids. We observe that the velocity profiles  $g/\Omega l$  decrease and  $f/\Omega l$  increases by increasing  $b$  when  $n = 3$  and  $\phi = 0$ . Moreover, the same trend of velocity profiles is noted when  $\phi \neq 0$ . However, the behavior of  $b$  on the velocity profiles when  $n = 5$  is quite opposite in Figures 6.11(a) and 6.16(b). It can be seen that velocity profiles are greater for viscous fluid in comparison to the Sisko fluid. Further, the velocities increase for large values of  $M$  when  $\phi = 0$  and  $\phi \neq 0$  in both fluids. The variation of  $b$  and Brinkman number  $Br$  on the temperature when  $\phi = 0$  and  $\phi \neq 0$  is shown in the Figures 6.17(a) – 6.20(b). Here it is evident that temperature increases when  $b$  increases for both cases when  $\phi = 0$  and  $\phi \neq 0$ . Furthermore the variation of  $Br$  on the temperature is qualitatively similar to that of  $b$  in both cases of  $\phi = 0$  and  $\phi \neq 0$  for both fluids. However it is noted that temperature for  $n = 5$  is larger when compared with that of  $n = 3$  for both viscous and Sisko fluids.

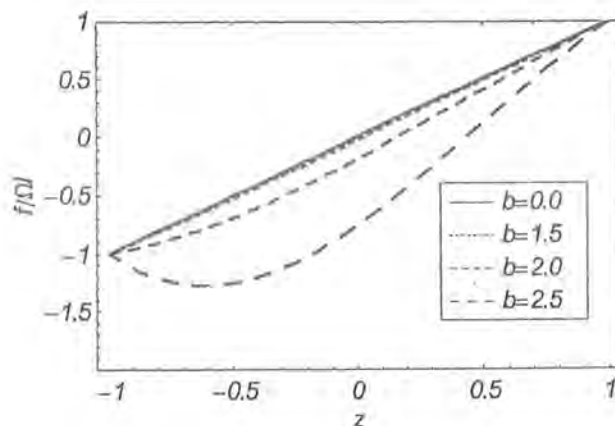


Figure 6.5(a): Velocity profile  $f/\Omega l$  for different values of  $b$  in Sisko fluid when  $\phi = 0$  and  $n = 3$ .

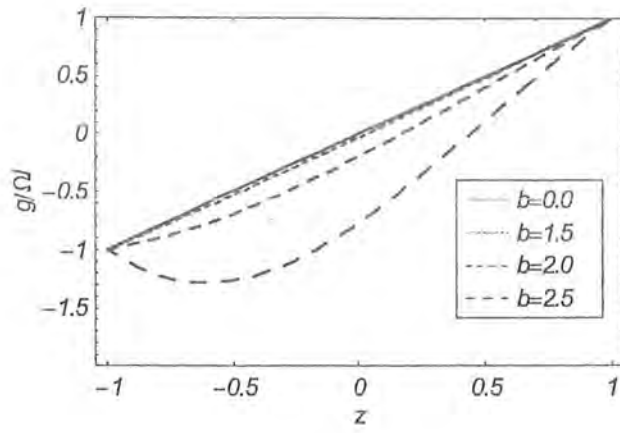


Figure 6.5(b): Velocity profile  $g/\Omega l$  for different values of  $b$  in Sisko fluid when  $\phi = 0$  and  $n = 3$ .

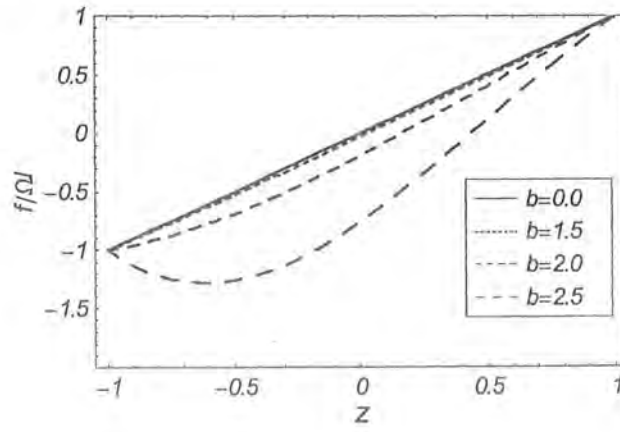


Figure 6.6(a): Velocity profile  $f/\Omega l$  for different values of  $b$  in Sisko fluid when  $\phi = 1/2$  and  $n = 3$ .

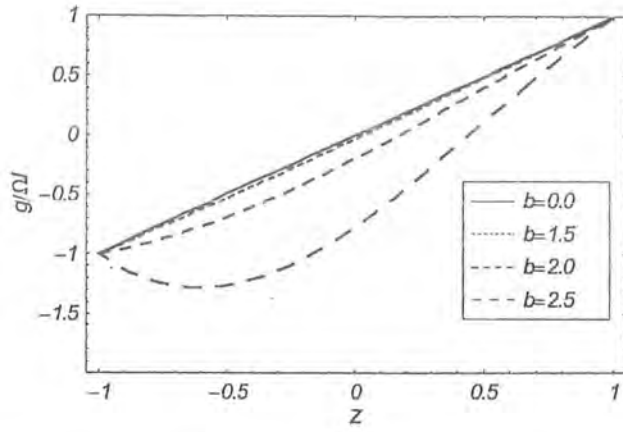


Figure 6.6(b): Velocity profile  $g/\Omega l$  for different values of  $b$  in Sisko fluid when  $\phi = 1/2$  and  $n = 3$ .

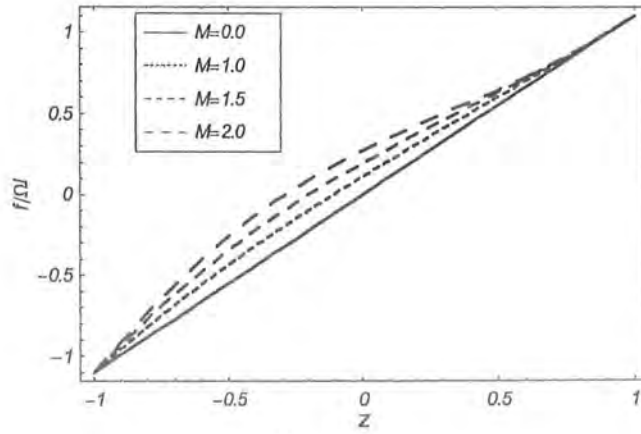


Figure 6.7(a): Velocity profile  $f/\Omega l$  for different values of  $M$  in Sisko fluid when  $\phi = 0$  and  $n = 3$ .

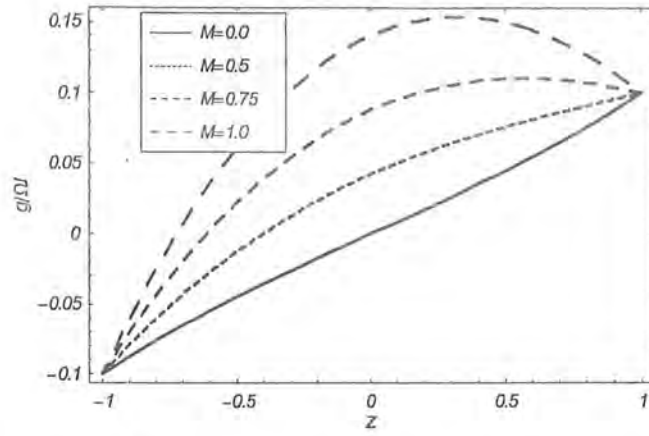


Figure 6.7(b): Velocity profile  $g/\Omega$  for different values of  $M$  in Sisko fluid when  $\phi = 0$  and  $n = 3$ .

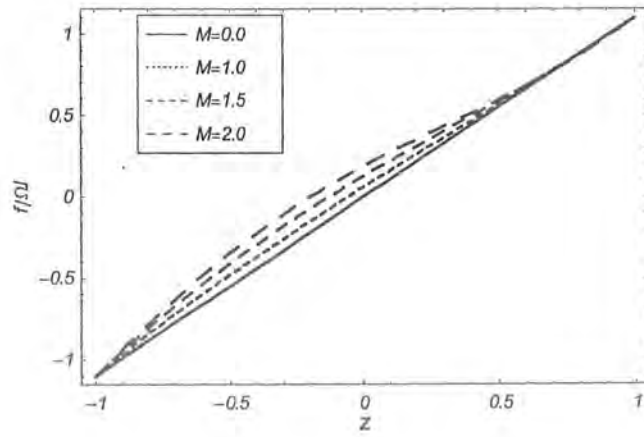


Figure 6.8(a): Velocity profile  $f/\Omega$  for different values of  $M$  in Sisko fluid when  $\phi = 1/2$  and  $n = 3$ .

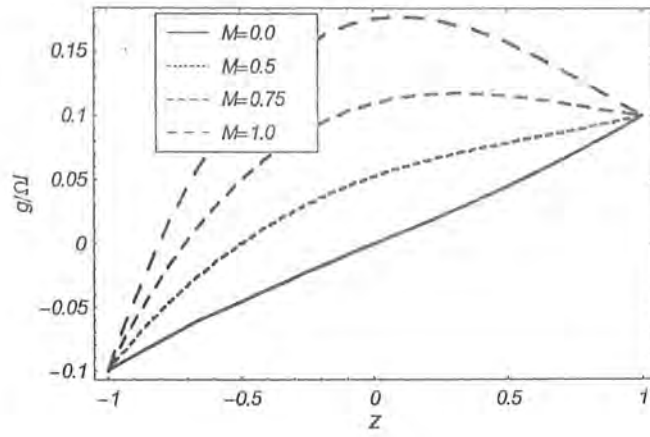


Figure 6.8(b): Velocity profile  $g/\Omega l$  for different values of  $M$  in Sisko fluid when  $\phi = 1/2$  and  $n = 3$ .

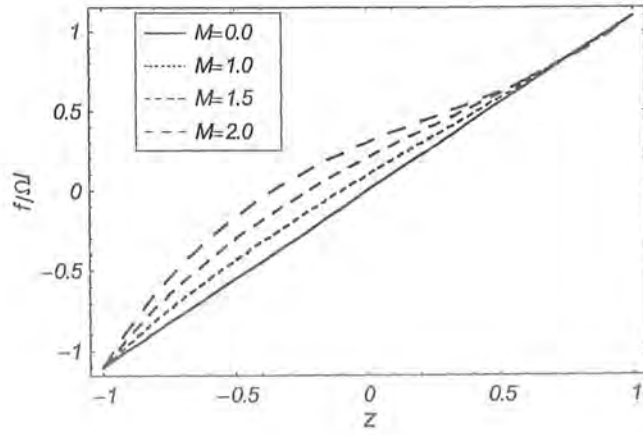


Figure 6.9(a): Velocity profile  $f/\Omega l$  for different values of  $M$  in viscous fluid when  $\phi = 1/2$  and  $n = 3$ .

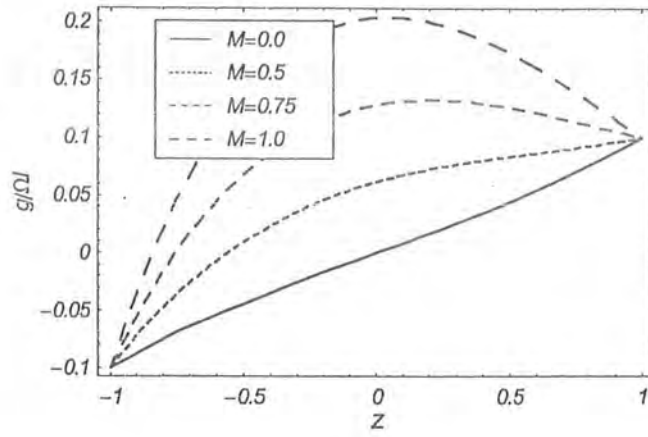


Figure 6.9(b): Velocity profile  $g/\Omega l$  for different values of  $M$  in viscous fluid when  $\phi = 1/2$  and  $n = 3$ .

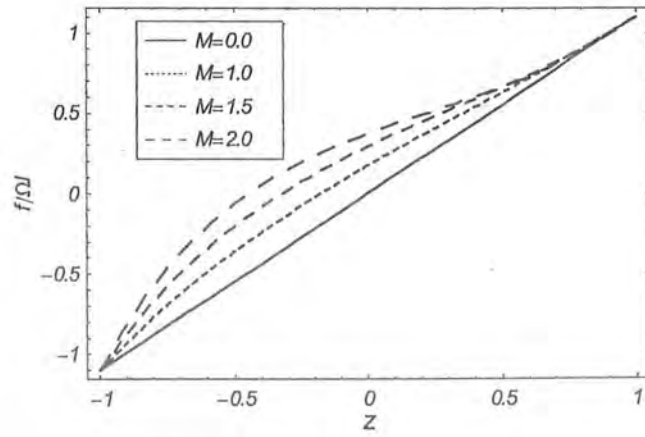


Figure 6.10(a): Velocity profile  $f/\Omega l$  for different values of  $M$  in viscous fluid when  $\phi = 0$  and  $n = 3$ .



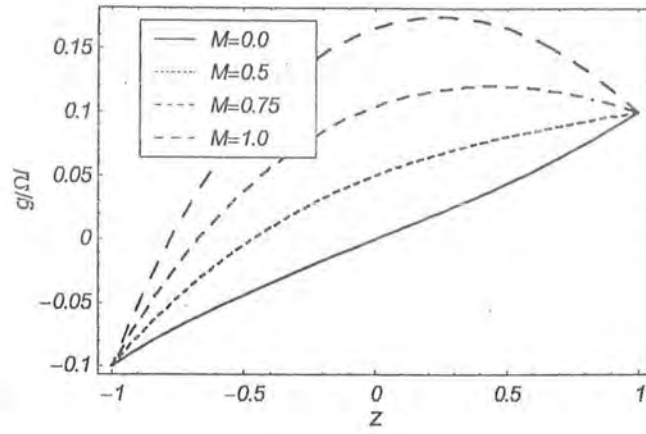


Figure 6.10(b): Velocity profile  $g/\Omega$  for different values of  $M$  in viscous fluid when  $\phi = 0$  and  $n = 3$ .

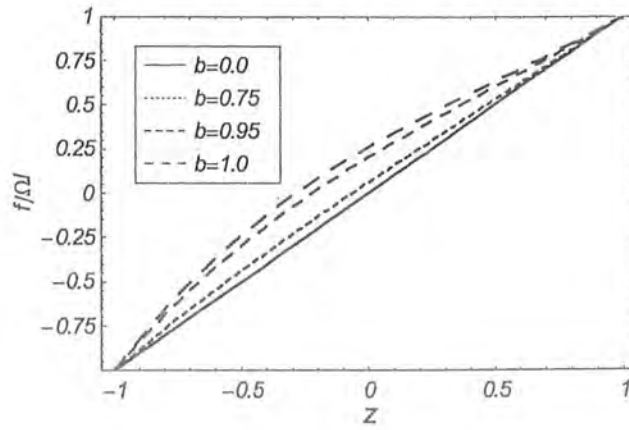


Figure 6.11(a): Velocity profile  $f/\Omega$  for different values of  $b$  in Sisko fluid when  $\phi = 0$  and  $n = 5$ .

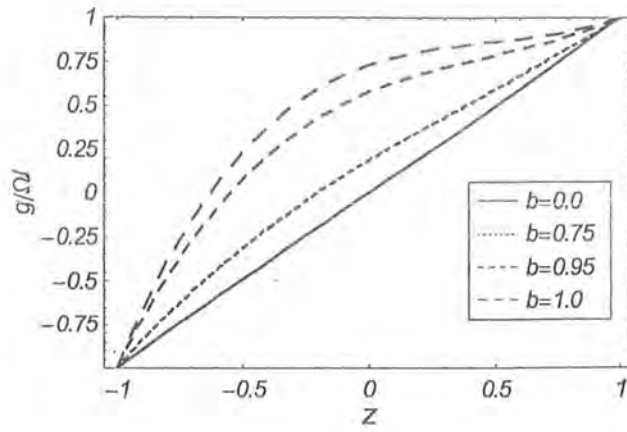


Figure 6.11(b): Velocity profile  $g/\Omega l$  for different values of  $b$  in Sisko fluid when  $\phi = 0$  and  $n = 5$ .

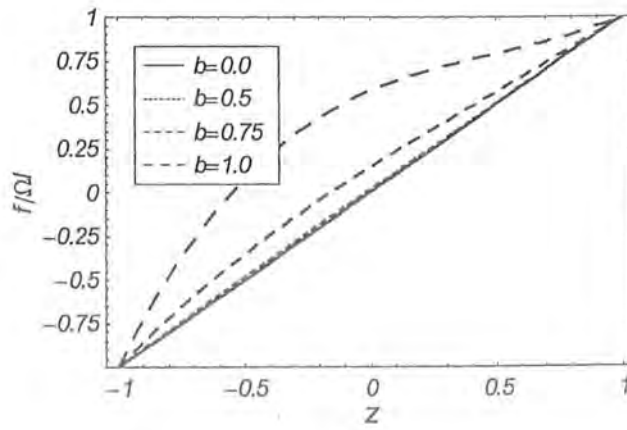


Figure 6.12(a): Velocity profile  $f/\Omega l$  for different values of  $b$  in Sisko fluid when  $\phi = 1/2$  and  $n = 5$ .

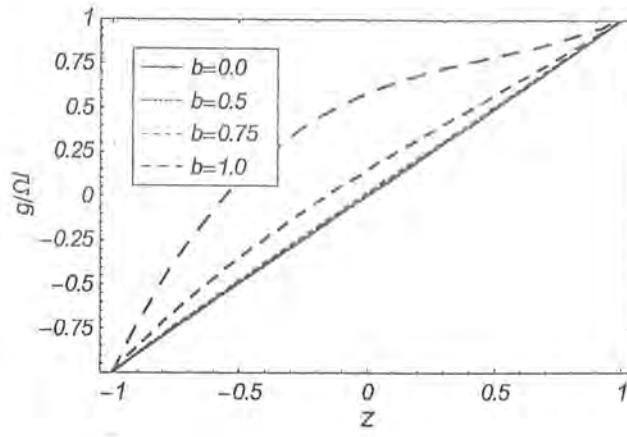


Figure 6.12(b): Velocity profile  $g/\Omega l$  for different values of  $b$  in Sisko fluid when  $\phi = 1/2$  and  $n = 5$ .

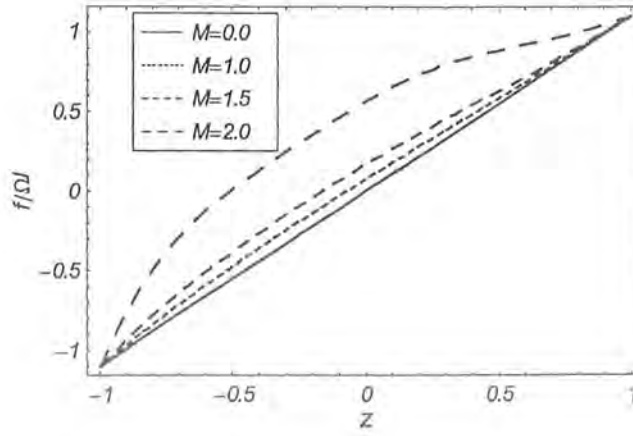


Figure 6.13(a): Velocity profile  $f/\Omega l$  for different values of  $M$  in Sisko fluid when  $\phi = 0$  and  $n = 5$ .

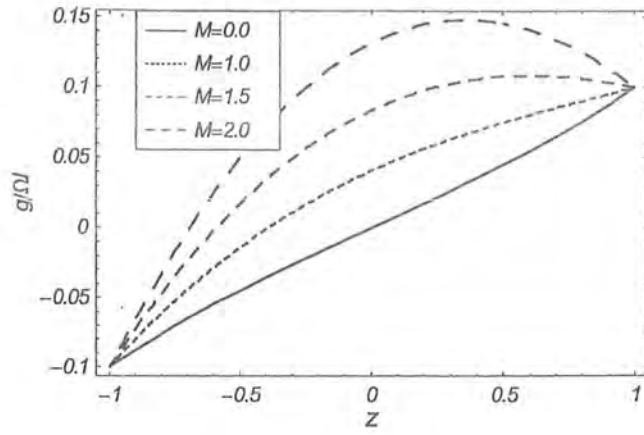


Figure 6.13(b): Velocity profile  $g/\Omega l$  for different values of  $M$  in Sisko fluid when  $\phi = 0$  and  $n = 5$ .

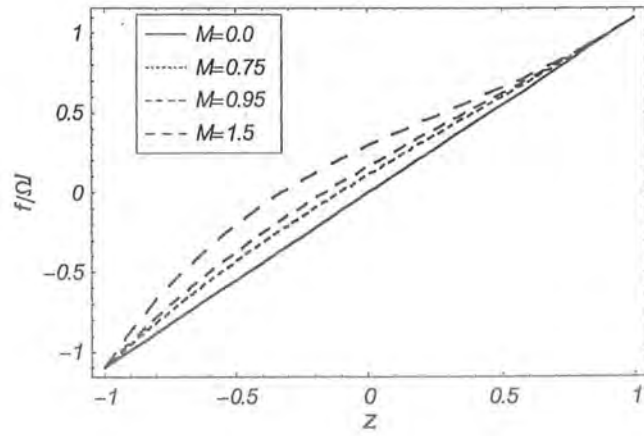


Figure 6.14(a): Velocity profile for different values of  $M$  in viscous fluid when  $\phi = 0$  and  $n = 5$ .

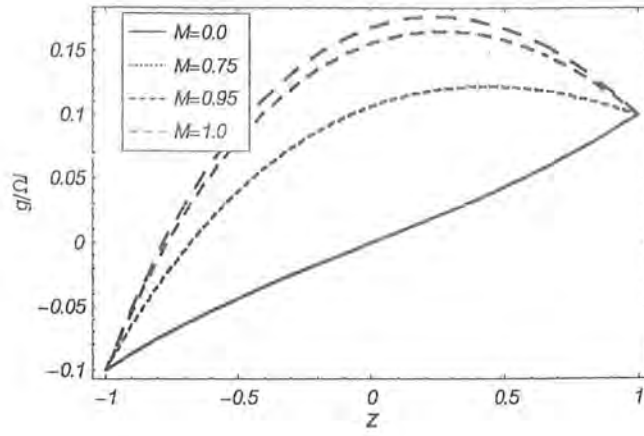


Figure 6.14(b): Velocity profile for different values of  $M$  in viscous fluid when  $\phi = 0$  and  $n = 5$ .

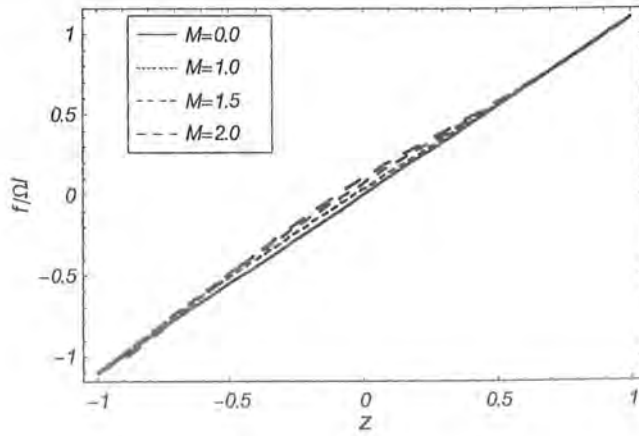


Figure 6.15(a): Velocity profile  $f/\Omega$  for different values of  $M$  in Sisko fluid when  $\phi = 1/2$  and  $n = 5$ .

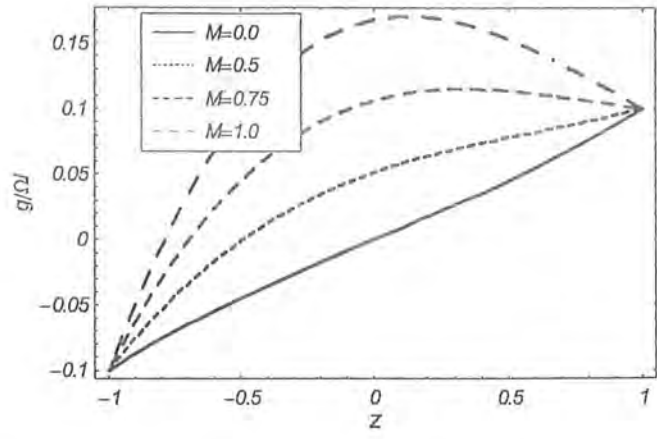


Figure 6.15(b): Velocity profile  $g/\Omega l$  for different values of  $M$  in Sisko fluid when  $\phi = 1/2$  and  $n = 5$ .

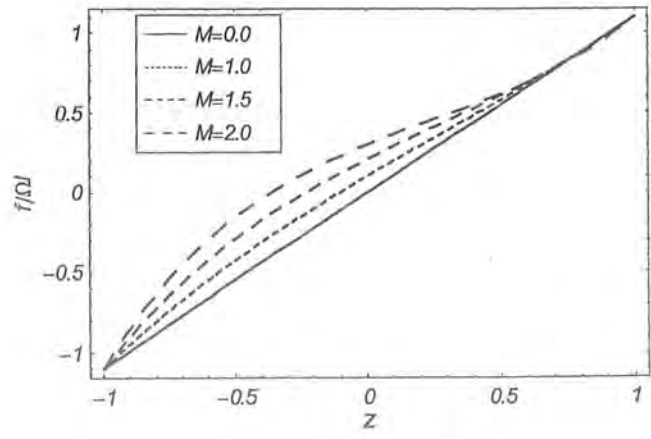


Figure 6.16(a): Velocity profile  $f/\Omega l$  for different values of  $M$  in viscous fluid when  $\phi = 1/2$  and  $n = 5$ .

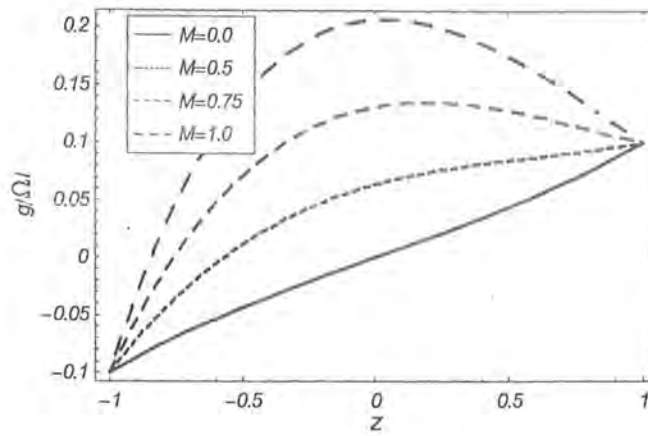


Figure 6.16(b): Velocity profile  $g/\Omega l$  for different values of  $M$  in viscous fluid when  $\phi = 1/2$  and  $n = 5$ .

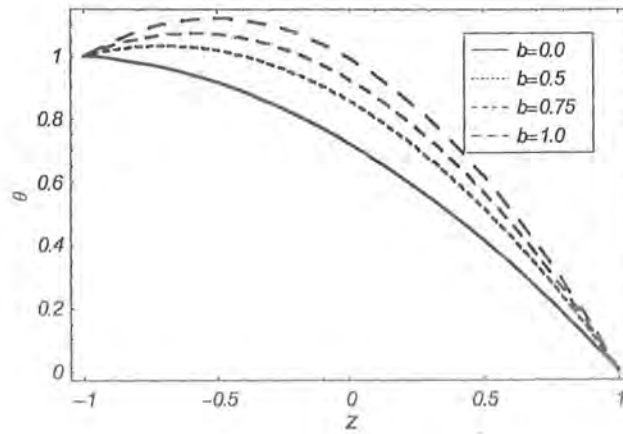


Figure 6.17(a): Temperature profile  $\theta$  for different values of  $b$  in Sisko fluid when  $n = 3$  and  $\phi = 0$ .

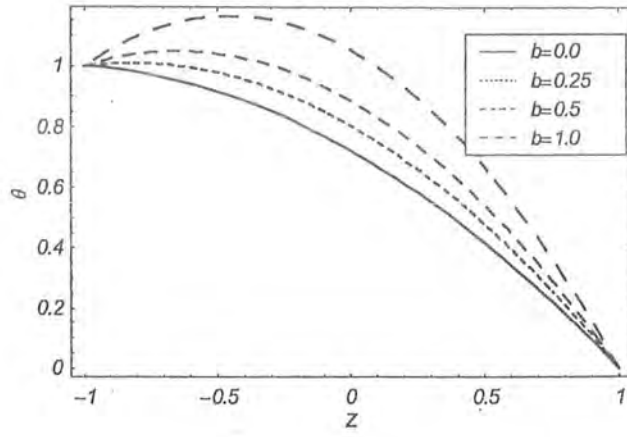


Figure 6.17(b): Temperature profile  $\theta$  for different values of  $b$  in Sisko fluid when  $n = 5$  and  $\phi = 0$ .

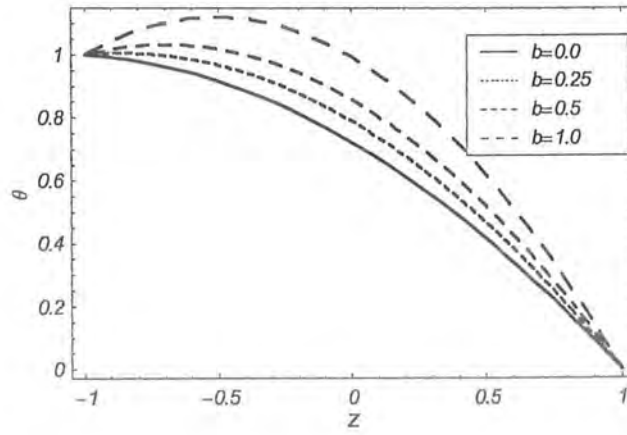


Figure 6.18(a): Temperature profile  $\theta$  for different values of  $b$  in Sisko fluid when  $n = 3$  and  $\phi = 1/2$ .



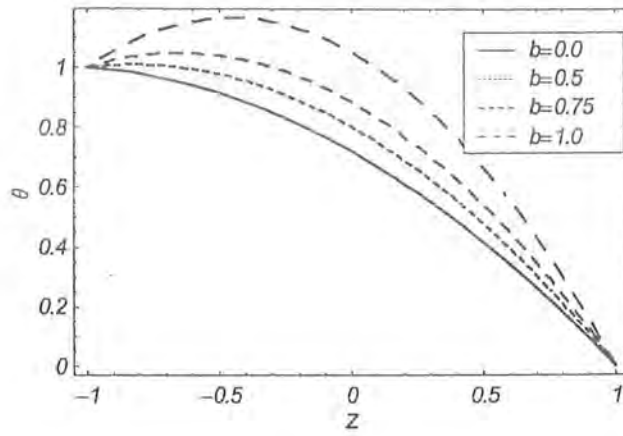


Figure 6.18(b): Temperature profile  $\theta$  for different values of  $b$  in Sisko fluid when  $n = 5$  and  $\phi = 1/2$ .

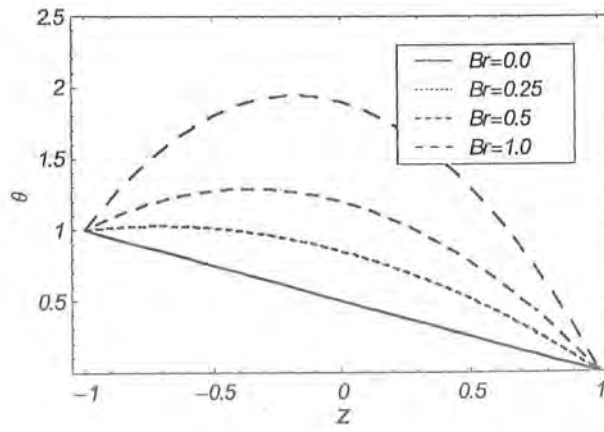


Figure 6.19(a): Temperature profile  $\theta$  for different values of  $Br$  in Sisko fluid when  $n = 3$  and  $\phi = 0$ .

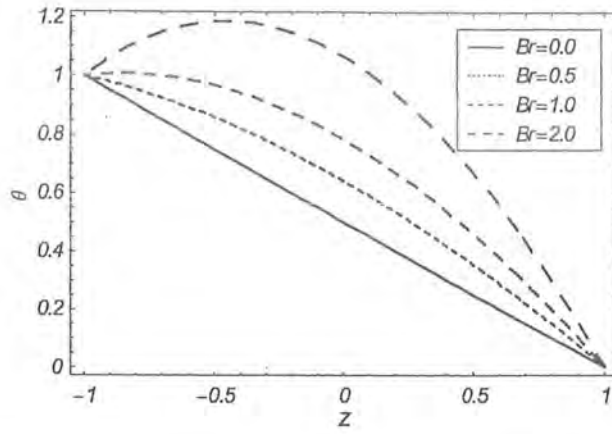


Figure 6.19(b): Temperature profile  $\theta$  for different values of  $Br$  in Sisko fluid when  $n = 5$  and  $\phi = 0$ .

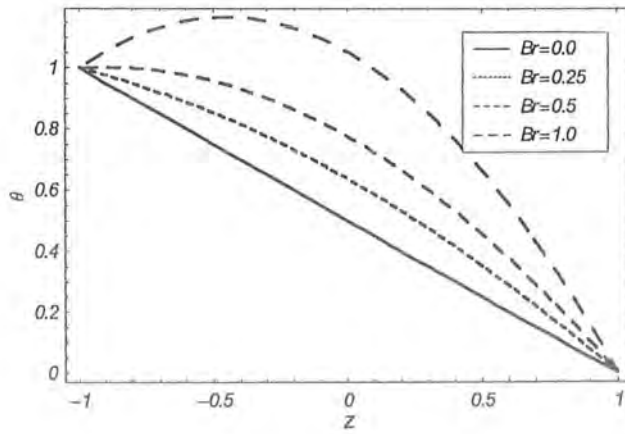


Figure 6.20(a): Temperature profile  $\theta$  for different values of  $Br$  in Sisko fluid when  $n = 3$  and  $\phi = 1/2$ .

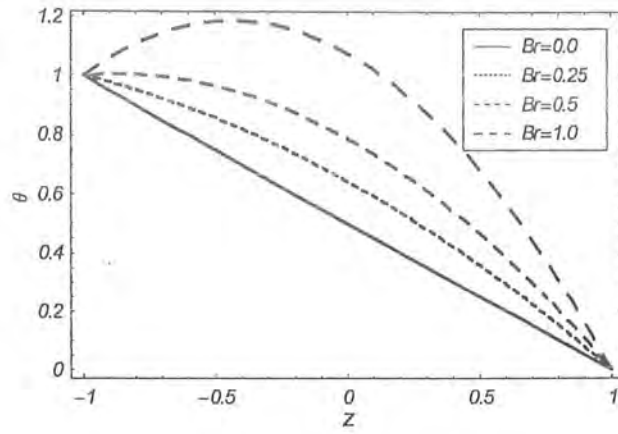


Figure 6.20(b): Temperature profile  $\theta$  for different values of  $Br$  in Sisko fluid when  $n = 5$  and  $\phi = 1/2$ .

## Chapter 7

# Simultaneous effects of heat transfer and Hall current on the flow of a Johnson-Segalman fluid

This chapter is concerned with the steady flow of a Johnson-Segalman fluid between two eccentric rotating and suddenly pulled disks. The flow analysis is conducted in the presence of Hall current. Mathematical modeling is based upon continuity, momentum and energy equations. Homotopy analysis method is utilized in obtaining the series solutions. Convergence of the developed solutions for velocity and temperature are explicitly shown. The influence of involved key parameters in the present analysis is examined carefully.

### 7.1 Mathematical formulation

Here we have an interest in steady flow of a Johnson-Segalman fluid. The flow is considered between two infinite disks rotating with constant angular velocity  $\Omega$  about two non-coaxial axes distant  $2l$  apart. The  $z$  - axis is taken in the transverse direction to the disks. The disks at  $z = h$  and  $z = -h$  are pulled with constant velocities  $U$  and  $-U$  respectively. The Cauchy stress tensor for a Johnson-Segalman fluid is [131] .

The appropriate boundary conditions and velocity field are defined in equations (4.1) and (4.2)

$$\mathbf{T} = 2\mu\mathbf{D} + \mathbf{S} \quad (7.1)$$

$$\mathbf{S} + \lambda_s \left( \frac{d\mathbf{S}}{dt} + \mathbf{S}(\mathbf{W} - a\mathbf{D}) + (\mathbf{W} - a\mathbf{D})^T \mathbf{S} \right) = 2\xi\mathbf{D}, \quad (7.2)$$

$$\mathbf{W} = \frac{1}{2}(\mathbf{L} - \mathbf{L}^T), \quad \mathbf{D} = \frac{1}{2}(\mathbf{L} + \mathbf{L}^T), \quad \mathbf{L} = \text{grad } \mathbf{V}. \quad (7.3)$$

where  $d/dt$  is the material time derivative,  $D$  is the symmetric part of the velocity gradient and  $W$  is the skew symmetric part of the velocity gradient,  $\mu$  and  $\xi$  are the viscosities,  $\lambda_s$  is called the relaxation time and  $a$  is the slip parameter. For  $\mu = 0$  and  $a = 1$ , the Johnson -Segalman fluid model reduces to the Maxwell fluid model and when  $\lambda_s = 0$  this model reduces to the classical Naiver -Stokes model.

Using equations (4.2) and (7.2) we get the following expressions

$$S_{xx} + \lambda_s \{2\Omega S_{xy} - (1+a) f' S_{xz}\} = 0, \quad (7.4)$$

$$S_{xy} + \frac{\lambda_s}{2} \{-2\Omega S_{xx} + 2\Omega S_{yy} - (1+a) g' S_{xz} - (1+a) f' S_{yz}\} = 0, \quad (7.5)$$

$$S_{xz} + \frac{\lambda_s}{2} \{2\Omega S_{xy} + (1-a) g' S_{xy} - (1+a) f' S_{zz} + (1-a) f' S_{xx}\} = \xi f', \quad (7.6)$$

$$S_{yy} + \lambda_s \{-2\Omega S_{xy} - (1+a) g' S_{yz}\} = 0, \quad (7.7)$$

$$S_{yz} + \frac{\lambda_s}{2} \{-2\Omega S_{xz} + (1-a) g' S_{yy} + (1-a) f' S_{xy} - (1+a) g' S_{zz}\} = \xi g', \quad (7.8)$$

$$S_{zz} + \lambda_s \{(1-a) f' S_{xz} + (1-a) g' S_{yz}\} = 0. \quad (7.9)$$

Using equations (7.4), (7.7) and (7.9) into equations (7.5), (7.6) and (7.8) we obtain

$$(1 + 4\Omega^2 \lambda_s^2) S_{xy} - \frac{\lambda_s}{2} (1+a) (g' + 2\Omega \lambda_s f') S_{xz} + \frac{\lambda_s}{2} (1+a) (-f' + 2\Omega \lambda_s g') S_{yz} = 0, \quad (7.10)$$

$$\frac{\lambda_s}{2} (1-a) (g' - 2\Omega \lambda_s f') S_{xy} + (1 + (f')^2 \lambda_s^2 (1-a^2)) S_{xz} + \left( \Omega \lambda_s + f' g' \frac{\lambda_s^2}{2} (1-a^2) \right) S_{yz} = \xi f', \quad (7.11)$$

$$\frac{\lambda_s}{2} (1-a) (f' + 2\Omega \lambda_s g') S_{xy} + (1 + (g')^2 \lambda_s^2 (1-a^2)) S_{yz} + \left( -\Omega \lambda_s + f' g' \frac{\lambda_s^2}{2} (1-a^2) \right) S_{xz} = \xi g'. \quad (7.12)$$

Solving equations (7.10), (7.11), and (7.12) we can write

$$S_{xz} = \frac{D_1}{D}, \quad (7.13)$$

$$S_{yz} = \frac{D_2}{D}, \quad (7.14)$$

where

$$D = (1 + 4\Omega^2\lambda_s^2)(1 + \Omega^2\lambda_s^2) + \frac{\lambda_s^2}{4}(1 - a^2) \left( \frac{5 + 8\Omega^2\lambda_s^2}{+ \lambda_s^2(1 - a^2)((f')^2 + (g')^2)} \right) ((f')^2 + (g')^2), \quad (7.15)$$

$$D_1 = \xi \left( \frac{(1 + 4\Omega^2\lambda_s^2)(f' - \Omega\lambda_s g')}{+ \frac{\lambda_s^2}{4}(1 - a^2)((f')^3 + 2\Omega\lambda_s g'(f')^2 + 2\Omega\lambda_s (g')^3 + f'(g')^2)} \right), \quad (7.16)$$

$$D_2 = \xi \left( \frac{(1 + 4\Omega^2\lambda_s^2)(g' + \Omega\lambda_s f')}{+ \frac{\lambda_s^2}{4}(1 - a^2)((g')^3 - 2\Omega\lambda_s f'(g')^2 - 2\Omega\lambda_s (f')^3 + g'(f')^2)} \right). \quad (7.17)$$

With the help of Eqs. (4.2) and (7.1) one obtains

$$\frac{dp}{dx} = \rho\Omega [\Omega x + g(z)] + \frac{dS_{xz}}{dz} + \mu \frac{d^2 f}{dz^2} + \frac{\sigma B_0^2(1 + i\phi)}{1 + \phi^2} \left( \frac{Q}{2h} - f(z) \right), \quad (7.18)$$

$$\frac{dp}{dy} = \rho\Omega [\Omega y - f(z)] + \frac{dS_{yz}}{dz} + \mu \frac{d^2 g}{dz^2} + \frac{\sigma B_0^2(1 + i\phi)}{1 + \phi^2} \left( \frac{P}{2h} - g(z) \right), \quad (7.19)$$

$$\frac{dp}{dz} = \frac{dS_{zz}}{dz}, \quad (7.20)$$

where  $P$  and  $Q$  are defined in Eq. (4.19) and

$$\hat{p} = p + \frac{\rho}{2}\Omega^2(x^2 + y^2) + \lambda_s \left( (1 - a) f' S_{xz} + (1 - a) g' S_{yz} \right). \quad (7.21)$$

Adopting the same procedure as employed in chapter four we have

$$\mu \frac{df^2}{dz^2} + \frac{dS_{xz}}{dz} + \rho\Omega g - Hf = -\frac{HQ}{2h}, \quad (7.22)$$

$$\mu \frac{dg^2}{dz^2} + \frac{dS_{yz}}{dz} - \rho\Omega f - Hg = -\frac{HP}{2h} \quad (7.23)$$

$$\mu \frac{dF^2}{dz^2} + \frac{d(S_{xz} + iS_{xz})}{dz} - i\rho\Omega F - HF = -\frac{H(Q + iP)}{2h} \quad (7.24)$$

where

$$F = f + ig, \quad \bar{F} = f - ig, \quad H = \frac{\sigma B_0^2}{1 - i\phi},$$

and boundary conditions are

$$F(h) = \Omega l + U_1 + iU_2, \quad F(-h) = -(\Omega l + U_1 + iU_2). \quad (7.25)$$

Introducing

$$\begin{aligned} z^* &= \frac{z}{h}, \quad F^* = \frac{F}{\Omega l}, \quad S_{xz}^* = \frac{hS_{xz}}{\mu\Omega l}, \quad S_{yz}^* = \frac{hS_{yz}}{\mu\Omega l}, \quad \frac{1}{K} = \frac{h^2\phi_1}{k_1}, \\ M^2 &= \frac{\sigma B_0^2 h^2}{\mu}, \quad R = \Omega\rho \frac{h^2}{\mu}, \quad L = \frac{h^2\lambda_s^2(1-a^2)}{(\Omega l)^2}, \quad V_1 = \frac{U_1}{\Omega l}, \quad V_2 = \frac{U_2}{\Omega l}. \end{aligned} \quad (7.26)$$

The dimensionless problem reduces to

$$\begin{aligned} &\left[ \frac{d^2 F}{dz^2} + \frac{d}{dz} \left[ \frac{\left( A_1 + \frac{L(1-2i\Omega\lambda_s)}{4} \frac{dF}{dz} \frac{d\bar{F}}{dz} \right) \frac{dF}{dz}}{A_2 + \frac{L}{4} (A_3 + L \frac{dF}{dz} \frac{d\bar{F}}{dz}) \frac{dF}{dz} \frac{d\bar{F}}{dz}} \right] - \left( \frac{M^2(1-i\phi)}{1+\phi^2} + iR \right) F \right. \\ &= \left. - \left( \frac{M^2(1+i\phi)}{1+\phi^2} \right) \left( \frac{Q+iP}{2h\Omega l} \right) \right], \end{aligned} \quad (7.27)$$

$$F(1) = 1 + V_1 + iV_2, \quad F(-1) = -(1 + V_1 + iV_2), \quad (7.28)$$

where

$$A_1 = (1 + 4\Omega^2\lambda_s^2)(1 + i\Omega\lambda_s), \quad A_2 = (1 + 4\Omega^2\lambda_s^2)(1 + \Omega^2\lambda_s^2), \quad A_3 = 5 + 8\Omega^2\lambda_s^2 \quad (7.29)$$

and asteriks have been omitted.

### 7.1.1 Analytic solution

For series solution of Eq. (7.27) together with the boundary condition (7.28). We solve the nonlinear problem with the help of homotopy analysis method. For that

$$F_0(z) = (1 + V_1 + iV_2)z, \quad (7.30)$$

$$\mathcal{L}_5[\hat{F}(z; q)] = \frac{\partial^2 \hat{F}}{\partial z^2}, \quad (7.31)$$

$$\mathcal{L}_5[M_1 + zM_2] = 0. \quad (7.32)$$

are chosen as the initial guess and auxiliary linear operator respectively and  $M_i$  ( $i = 1, 2$ ) are the arbitrary constants.

The zeroth order deformation problem is

$$(1 - q)\mathcal{L}_5[\hat{F}(z; q) - F_0(z)] = q\hbar_5\mathcal{N}_5[\hat{F}(z; q)], \quad (7.33)$$

$$\hat{F}_0(1; q) = 1 + V_1 + iV_2, \quad \hat{F}_0(-1; q) = -(1 + V_1 + iV_2), \quad (7.34)$$

where  $q \in [0, 1]$  is an embedding parameter and  $\hbar_5$  is the auxiliary parameter and the non linear operator  $\mathcal{N}_5$  is

$$\begin{aligned} \mathcal{N}_5[\hat{F}(z; q)] = & \left[ \frac{d^2 \hat{F}}{dz^2} - \left( \frac{M^2}{1-i\phi} + iR \right) \hat{F} + \frac{M^2}{1-i\phi} \frac{Q+iP}{2\hbar\Omega l} \right] \left[ A_2 + \frac{L}{4} \left( A_3 + L \frac{d\hat{F}}{dz} \frac{d\bar{\hat{F}}}{dz} \right) \frac{d\hat{F}}{dz} \frac{d\bar{\hat{F}}}{dz} \right]^2 \\ & + \left[ A_2 + \frac{L}{4} \left( A_3 + L \frac{d\hat{F}}{dz} \frac{d\bar{\hat{F}}}{dz} \right) \frac{d\hat{F}}{dz} \frac{d\bar{\hat{F}}}{dz} \right] \left[ A_1 \frac{d^2 \hat{F}}{dz^2} + \frac{L(1-2i\Omega\lambda_s)}{4} \left( 2 \frac{d\hat{F}}{dz} \frac{d^2 \hat{F}}{dz^2} + \frac{d\hat{F}}{dz} \frac{d^2 \bar{\hat{F}}}{dz^2} \right) \frac{d\hat{F}}{dz} \right] \\ & - \frac{L}{4} \left( A_1 + \frac{L(1-2i\Omega\lambda_s)}{4} \frac{d\hat{F}}{dz} \frac{d\bar{\hat{F}}}{dz} \right) \frac{d\hat{F}}{dz} \left( A_3 + 2L \frac{d\hat{F}}{dz} \frac{d\bar{\hat{F}}}{dz} \right) \left( \frac{d\hat{F}}{dz} \frac{d^2 \bar{\hat{F}}}{dz^2} + \frac{d\bar{\hat{F}}}{dz} \frac{d^2 \hat{F}}{dz^2} \right). \end{aligned} \quad (7.35)$$

For  $q = 0$  and  $q = 1$  we write

$$\hat{F}(z, 0) = F_0(z), \quad \hat{F}(z, 1) = F(z). \quad (7.36)$$

As  $q$  increases from 0 to 1,  $\hat{F}(z; q)$  varies from  $F_0(z)$  to the solution  $F(z)$ . By Taylors' series and Eq. (7.35), we get

$$\hat{F}(z; q) = F_0(z) + \sum_{m=1}^{\infty} F_m(z) q^m, \quad (7.37)$$

$$F_m(z) = \frac{1}{m!} \left. \frac{\partial^m \hat{F}(z, q)}{\partial q^m} \right|_{q=0}$$



Choosing  $\hbar_5$  properly so that the above series is convergent at  $q = 1$ , one can write

$$\hat{F}(z) = F_0(z) + \sum_{m=1}^{\infty} F_m(z). \quad (7.38)$$

The  $m$ th order deformation problem is

$$\mathcal{L}_5 [F_m(z) - \chi_m F_{m-1}(z)] = \hbar_5 \mathcal{R}_{5m}(z), \quad (7.39)$$

$$F_m(1) = F_m(-1) = 0, \quad (7.40)$$

$$\begin{aligned}
\mathcal{R}_{5m}(z) = & A_1(A_1 + A_2)F''_{m-1} - A_2^2 R_1 F_{m-1} - M_1 A_2 A_3 \frac{L}{2} \sum_{k=0}^{m-1} F'_{m-1-k} \bar{F}'_k \\
& + \frac{L}{4} \left[ \sum_{k=0}^{m-1} F'_{m-1-k} \sum_{l=0}^k \left\{ \bar{F}'_{k-l} (A_2 ((2A_3 + 1 - 2i\lambda_s \Omega) F''_l - 2A_3 R_1 F_l)) \right. \right. \\
& \quad \left. \left. + (A_2(1 - 2i\lambda_s \Omega) - A_1 A_3) F'_{k-l} \bar{F}''_l \right\} \right] \\
& - M_1 \frac{L^2 (8A_2 + A_3^2)}{16} \sum_{k=0}^{m-1} F'_{m-1-k} \sum_{l=0}^k F'_{k-l} \sum_{p=0}^l \bar{F}'_{l-p} \bar{F}'_p \\
& + \frac{L^2}{16} \left[ \sum_{k=0}^{m-1} F'_{m-1-k} \sum_{l=0}^k F'_{k-l} \sum_{p=0}^l \bar{F}'_{l-p} \right. \\
& \quad \left. \times \sum_{q=0}^p \left[ \begin{aligned} & -R_1 (8A_2 + A_3^2) \bar{F}'_{p-q} F_q \\ & (8A_2 - 4A_1 + A_3^2) \bar{F}'_{p-q} F''_q - 8A_1 F'_{p-q} \bar{F}''_q \end{aligned} \right] \right] \\
& - \frac{L^3}{8} M_1 A_3 \sum_{k=0}^{m-1} F'_{m-1-k} \sum_{l=0}^k F'_{k-l} \sum_{p=0}^l F'_{l-p} \sum_{q=0}^p \bar{F}_{p-q} \sum_{r=0}^q \bar{F}'_{q-r} \bar{F}'_r \\
& + \frac{L^3}{16} \left[ \sum_{k=0}^{m-1} F'_{m-1-k} \sum_{l=0}^k F'_{k-l} \sum_{p=0}^l F'_{l-p} \sum_{q=0}^p \bar{F}_{p-q} \sum_{r=0}^q \bar{F}'_{q-r} \right. \\
& \quad \left. \sum_{s=0}^r \left\{ \bar{F}'_{r-s} ((2A_3 - (1 - 2i\Omega\lambda_s)) F''_s + F_s) - (1 - 2i\Omega\lambda_s) F'_{r-s} \bar{F}''_s \right\} \right] \\
& - \frac{M_1 L^4}{16} \sum_{k=0}^{m-1} F'_{m-1-k} \sum_{l=0}^k F'_{k-l} \sum_{p=0}^l F'_{l-p} \sum_{q=0}^p F'_{p-q} \sum_{r=0}^q \bar{F}'_{q-r} \sum_{s=0}^r \bar{F}_{r-s} \sum_{t=0}^s \bar{F}_{s-t} \bar{F}_t \\
& + \frac{L^4}{16} \sum_{k=0}^{m-1} F'_{m-1-k} \sum_{l=0}^k F'_{k-l} \sum_{p=0}^l F'_{l-p} \sum_{q=0}^p F'_{p-q} \sum_{r=0}^q \bar{F}'_{q-r} \sum_{s=0}^r \bar{F}_{r-s} \sum_{t=0}^s \bar{F}_{s-t} \\
& \sum_{u=0}^t \bar{F}_{t-u} (F''_u - R_1 F_u) + (1 - \chi_m) A_2^2 M_1
\end{aligned}$$

or

$$\begin{aligned}
\mathcal{R}_{5m}(z) = & A_2(A_1 + A_2) \sum_{t=0}^{2m-1} C_{m-1,t} z^t - A_2^2 R_1 \sum_{t=0}^{2m-1} C_{m-1,t} z^t - M_1 A_2 A_3 \frac{L}{2} \sum_{t=0}^{2m} \alpha_{m,t}^1 z^t \\
& + \frac{L}{4} \sum_{t=0}^{2m+1} \alpha_{m,t}^2 z^t - M_1 \frac{L^2 (8A_2 + A_3^2)}{4} \sum_{t=0}^{2m+2} \alpha_{m,t}^3 z^t \\
& + \frac{L^2}{16} \sum_{t=0}^{2m+3} \alpha_{m,t}^4 z^t - \frac{L^3}{8} M_1 A_3 \sum_{t=0}^{2m+4} \alpha_{m,t}^5 z^t + \frac{L^3}{16} \sum_{t=0}^{2m+5} \alpha_{m,t}^6 z^t \\
& - \frac{M_1 L^4}{16} \sum_{t=0}^{2m+6} \alpha_{m,t}^7 z^t + \frac{L^4}{16} \sum_{t=0}^{2m+7} \alpha_{m,t}^8 z^t - (1 - \chi_m) A_2^2 M_1
\end{aligned} \tag{7.41}$$

$$M_1 = \frac{M^2}{1 + i\phi} \frac{Q + iP}{2h\Omega l}, \quad R_1 = \frac{M^2}{1 + i\phi} + iR$$

The  $m$ th order deformation problem has been solved by using "MATHEMATICA" up to first few order of approximations. The solution is expressed by

$$F_m(z) = \sum_{t=0}^{2m+1} C_{m,t} z^t, \quad C_{m,t} = a_{m,t} + ib_{m,t}, \quad m \geq 0, \tag{7.42}$$

in which for  $m \geq 1$  and  $0 \leq t \leq 2m + 1$ , the recurrence formulas are

$$\begin{aligned}
C_{m,0} &= \chi_m \chi_{2m+1} C_{m-1,0} - \sum_{t=0}^{2m+7} \frac{\Gamma_{m,t}}{(x+1)(x+2)} \left( \frac{1 + (-1)^{t+2}}{2} \right) - \frac{(1 - \chi_m) M_1 A_2^2}{2}, \\
C_{m,1} &= \chi_m \chi_{2m} C_{m-1,1} - \sum_{t=0}^{2m+7} \frac{\Gamma_{m,t}}{(x+1)(x+2)} \left( \frac{1 - (-1)^{t+2}}{2} \right), \\
C_{m,2} &= \chi_m \chi_{2m-1} C_{m-1,2} + \frac{\Gamma_{m,0}}{2}, \\
C_{m,t} &= \chi_m \chi_{2m-t+1} C_{m-1,t} + \Gamma_{m,t-2} \frac{1}{(t-1)t}, \quad 2 \leq t \leq 2m + 1,
\end{aligned}$$

$$\Gamma_{m,t} = \tilde{h}_5 \left( \begin{aligned} & \frac{L^4}{16} \alpha_{m,t}^8 - \frac{M_1 L^4}{16} \alpha_{m,t}^7 \chi_{2m+8-t} \\ & + \frac{L^3}{16} \alpha_{m,t}^6 \chi_{2m+7-x} - \frac{L^3 A_3 M_1}{8} \alpha_{m,t}^5 \chi_{2m+7-x} \chi_{2m+6-x} \\ & \quad + \frac{L^2}{16} \alpha_{m,t}^4 \chi_{2m+7-x} \chi_{2m+6-x} \chi_{2m+5-x} \\ & - \frac{L^2 (8A_2 + A_3^2) M_1}{16} \alpha_{m,t}^3 \chi_{2m+7-x} \chi_{2m+6-x} \chi_{2m+5-x} \chi_{2m+4-x} \\ & \quad + \frac{L}{4} \alpha_{m,t}^2 \chi_{2m+7-x} \chi_{2m+6-x} \chi_{2m+5-x} \chi_{2m+4-x} \chi_{2m+3-x} \\ & - \frac{L(A_2 A_3) M_1}{2} \alpha_{m,t}^1 \chi_{2m+7-x} \chi_{2m+6-x} \chi_{2m+5-x} \chi_{2m+4-x} \chi_{2m+3-x} \chi_{2m+2-x} \\ & + \alpha_{m,t}^0 \chi_{2m+7-x} \chi_{2m+6-x} \chi_{2m+5-x} \chi_{2m+4-x} \chi_{2m+3-x} \chi_{2m+2-x} \chi_{2m+1-x} \end{aligned} \right) \quad (7.43)$$

and the related coefficients  $\alpha_{m,t}^8, \alpha_{m,t}^7, \alpha_{m,t}^6, \alpha_{m,t}^5, \alpha_{m,t}^4, \alpha_{m,t}^3, \alpha_{m,t}^2, \alpha_{m,t}^1$  and  $\alpha_{m,t}^0$  for  $m \geq 1, 0 \leq t \leq 2m+1$  are

$$\alpha_{m,t}^0 = A_2 (A_1 + A_2) C_{m-1,t}^2 - R_1 A_2^2 C_{m-1,t}$$

$$\alpha_{m,t}^1 = \sum_{k=0}^{m-1} \sum_{a_1=\max\{0,t+2k-2m+1\}}^{\min\{t,2k+1\}} C_{m-1-k,t-a_1}^1 \bar{C}_{k,a_1}^1,$$

$$\alpha_{m,t}^2 = \sum_{k=0}^{m-1} \sum_{l=0}^k \sum_{a_1=\max\{0,t+2k-2m+1\}}^{\min\{l,2k+2\}} C_{m-1-k,t-a_1}^1 \left[ \sum_{a_2=\max\{0,a_1+2l-2k-1\}}^{\min\{a_1,2l+1\}} \left\{ \bar{C}_{k-l,a_1-a_2}^1 \left( A_2 (1 - 2i\lambda_s \Omega + 2A_3) C_{l,a_2}^2 - 2A_2 A_3 R_1 C_{l,a_2} \right) + (A_2 (1 - 2i\lambda_s \Omega) + A_1 A_3) C_{k-l,a_1-a_2}^1 \bar{C}_{l,a_2}^2 \right\} \right],$$

$$\alpha_{m,t}^3 = \sum_{k=0}^{m-1} \sum_{l=0}^k \sum_{p=0}^l \sum_{a_1=\max\{0,t+2k-2m+1\}}^{\min\{t,2k+3\}} C_{m-1-k,t-a_1}^1 \sum_{a_2=\max\{0,a_1+2l-2k-1\}}^{\min\{a_1,2l+2\}} C_{k-l,a_1-a_2}^1 \sum_{a_3=\max\{0,a_2,2p-2l-1\}}^{\min\{a_2,2p+1\}} \bar{C}_{l-p,a_2-a_3}^1 \bar{C}_{p,a_3}^1,$$

$$\begin{aligned}
\alpha_{m,t}^4 = & \sum_{k=0}^{m-1} \sum_{l=0}^k \sum_{p=0}^l \sum_{q=0}^p \sum_{a_1=\max\{0,t+2k-2m+1\}}^{\min\{t,2k+4\}} C_{m-1-k,t-a_1}^1 \\
& \sum_{a_2=\max\{0,a_1+2l-2k-1\}}^{\min\{a_1,2l+3\}} C_{k-l,a_1-a_2}^1 \sum_{a_3=\max\{0,a_2+2p-2l-1\}}^{\min\{a_2,2p+2\}} \bar{C}_{l-p,a_2-a_3}^1 \\
& \sum_{a_4=\max\{0,a_3+2q-2p-1\}}^{\min\{a_3,2q+1\}} \left( \bar{C}_{p-q,a_3-a_4}^1 \begin{pmatrix} -R_1(8A_2 + A_3^2) C_{q,a_4} \\ (8A_2 - 4A_1 + A_3^2) C_{q,a_4}^2 \\ -8A_1 C_{p-q,a_3-a_4}^1 \bar{C}_{q,a_4}^2 \end{pmatrix} \right),
\end{aligned}$$

$$\begin{aligned}
\alpha_{m,t}^5 = & \sum_{k=0}^{m-1} \sum_{l=0}^k \sum_{p=0}^l \sum_{q=0}^p \sum_{r=0}^q \sum_{a_1=\max\{0,t+2k-2m+1\}}^{\min\{t,2k+5\}} C_{m-1-k,t-a_1}^1 \\
& \sum_{a_2=\max\{0,a_1+2l-2k-1\}}^{\min\{a_1,2l+4\}} C_{k-l,a_1-a_2}^1 \sum_{a_3=\max\{0,a_2+2p-2l-1\}}^{\min\{a_2,2p+3\}} C_{l-p,a_2-a_3}^1 \\
& \sum_{a_4=\max\{0,a_3+2q-2p-1\}}^{\min\{a_3,2q+2\}} \bar{C}_{p-q,a_3-a_4}^1 \sum_{a_5=\max\{0,a_4+2r-2q-1\}}^{\min\{a_4,2r+1\}} \bar{C}_{q-r,a_4-a_5}^1 \bar{C}_{r,a_5}^1,
\end{aligned}$$

$$\begin{aligned}
\alpha_{m,t}^6 = & \sum_{k=0}^{m-1} \sum_{l=0}^k \sum_{p=0}^l \sum_{q=0}^p \sum_{r=0}^q \sum_{s=0}^r \sum_{a_1=\max\{0,t+2k-2m+1\}}^{\min\{t,2k+6\}} C_{m-1-k,t-a_1}^1 \\
& \sum_{a_2=\max\{0,a_1+2l-2k-1\}}^{\min\{a_1,2l+5\}} C_{k-l,a_1-a_2}^1 \sum_{a_3=\max\{0,a_2+2p-2l-1\}}^{\min\{a_2,2p+4\}} C_{l-p,a_2-a_3}^1 \\
& \sum_{a_4=\max\{0,a_3+2q-2p-1\}}^{\min\{a_3,2q+3\}} \bar{C}_{p-q,a_3-a_4}^1 \sum_{a_5=\max\{0,a_4+2r-2q-1\}}^{\min\{a_4,2r+2\}} \bar{C}_{q-r,a_4-a_5}^1 \\
& \sum_{a_6=\max\{0,a_5+2s-2r-1\}}^{\min\{a_5,2s+1\}} \left( \bar{C}_{r-s,a_5-a_6}^1 \left( (2A_3 - 1 + 2i\lambda_s\Omega) C_{s,a_6}^2 - 2A_3 R_1 C_{s,a_6} \right) \right. \\
& \quad \left. - (1 - 2i\lambda_s\Omega) C_{r-s,a_5-a_6}^1 \bar{C}_{s,a_6}^2 \right),
\end{aligned}$$

$$\begin{aligned}
\alpha_{m,t}^7 = & \sum_{k=0}^{m-1} \sum_{l=0}^k \sum_{p=0}^l \sum_{q=0}^p \sum_{r=0}^q \sum_{s=0}^r \sum_{u=0}^s \sum_{a_1=\max\{0,t+2k-2m+1\}}^{\min\{t,2k+7\}} C_{m-1-k,t-a_1}^1 \\
& \sum_{a_2=\max\{0,a_1+2l-2k-1\}}^{\min\{a_1,2l+6\}} C_{k-l,a_1-a_2}^1 \sum_{a_3=\max\{0,a_2+2p-2l-1\}}^{\min\{a_2,2p+5\}} C_{l-p,a_2-a_3}^1 \\
& \sum_{a_4=\max\{0,a_3+2q-2p-1\}}^{\min\{a_3,2q+4\}} C_{p-q,a_3-a_4}^1 \sum_{a_5=\max\{0,a_4+2r-2q-1\}}^{\min\{a_4,2r+3\}} \bar{C}_{q-r,a_4-a_5}^1 \\
& \sum_{a_6=\max\{0,a_5+2s-2r-1\}}^{\min\{a_5,2s+2\}} \bar{C}_{r-s,a_5-a_6}^1 \sum_{a_7=\max\{0,a_6+2t-2s-1\}}^{\min\{a_6,2u+1\}} \bar{C}_{s-u,a_6-a_7}^1 \bar{C}_{u,a_7}^1,
\end{aligned}$$

$$\begin{aligned}
\alpha_{m,t}^8 = & \sum_{k=0}^{m-1} \sum_{l=0}^k \sum_{p=0}^l \sum_{q=0}^p \sum_{r=0}^q \sum_{s=0}^r \sum_{u=0}^s \sum_{v=0}^u \sum_{a_1=\max\{0,t+2k-2m+1\}}^{\min\{t,2k+8\}} C_{m-1-k,t-a_1}^1 \\
& \sum_{a_2=\max\{0,a_1+2l-2k-1\}}^{\min\{a_1,2l+7\}} C_{k-l,a_1-a_2}^1 \sum_{a_3=\max\{0,a_2+2p-2l-1\}}^{\min\{a_2,2p+6\}} C_{l-p,a_2-a_3}^1 \\
& \sum_{a_4=\max\{0,a_3+2q-2p-1\}}^{\min\{a_3,2q+5\}} C_{p-q,a_3-a_4}^1 \sum_{a_5=\max\{0,a_4+2r-2q-1\}}^{\min\{a_4,2r+4\}} \bar{C}_{q-r,a_4-a_5}^1 \\
& \sum_{a_6=\max\{0,a_5+2s-2r-1\}}^{\min\{a_5,2s+3\}} \bar{C}_{r-s,a_5-a_6}^1 \sum_{a_7=\max\{0,a_6+2u-2s-1\}}^{\min\{a_6,2u+2\}} \bar{C}_{s-u,a_6-a_7}^1 \\
& \times \sum_{a_7=\max\{0,a_6+2v-2u-1\}}^{\min\{a_7,2v+1\}} \bar{C}_{u-v,a_7-a_8}^1 (C_{v,a_8}^2 - R_1 C_{v,a_8}),
\end{aligned}$$

$$\begin{aligned}
C_{m,t} &= \operatorname{Re} C_{m,t} + i \operatorname{Im} C_{m,t}, & \bar{C}_{m,t} &= \operatorname{Re} C_{m,t} - i \operatorname{Im} C_{m,t}, \\
C_{m,t}^1 &= (1+t)C_{m,1+t}, & \bar{C}_{m,t}^1 &= (1+t)\bar{C}_{m,1+t}, \\
C_{m,t}^2 &= (1+t)C_{m,1+t}^1, & \bar{C}_{m,t}^2 &= (1+t)\bar{C}_{m,1+t}^1.
\end{aligned} \tag{7.44}$$

The corresponding  $m$ th order approximation is

$$F_m(z) = \sum_{t=0}^{2m+1} C_{m,t} z^t, \tag{7.45}$$

and the explicit solution is

$$F(z) = \lim_{M \rightarrow \infty} \left( \sum_{m=0}^M F_m(z) \right) = \lim_{M \rightarrow \infty} \left( \sum_{m=0}^M C_{m,0} + \sum_{m=0}^M \sum_{t=1}^{2m+1} C_{m,t} z^t \right). \quad (7.46)$$

## 7.2 Heat transfer analysis

In this section we investigated the heat transfer analysis between two heated disks. The corresponding temperatures of the lower at ( $z = -h$ ) and upper at ( $z = h$ ) disks are defined in Eq. (4.37). For the convenience of readers these are

$$\begin{aligned} \tau &= \tau_1 & \text{at } z = -h, \\ \tau &= \tau_2 & \text{at } z = h. \end{aligned} \quad (7.47)$$

The dimensionless form of resulting energy equation takes the following form

$$\begin{aligned} \frac{d^2\theta}{dz^2} &= -E_c P_r \left[ \frac{A + \frac{L}{4} \left( \left( \frac{df^*}{dz} \right)^2 + \left( \frac{dg^*}{dz} \right)^2 \right)}{A_2 + \frac{L}{4} \left( A_3 + L \left( \left( \frac{df^*}{dz} \right)^2 + \left( \frac{dg^*}{dz} \right)^2 \right) \right) \left( \left( \frac{df^*}{dz} \right)^2 + \left( \frac{dg^*}{dz} \right)^2 \right)} \right] \\ &\times \left( \left( \frac{df^*}{dz} \right)^2 + \left( \frac{dg^*}{dz} \right)^2 \right), \end{aligned} \quad (7.48)$$

where  $f^* = f/\Omega l$ ,  $g^* = g/\Omega l$ ,  $C_p$  is the specific heat,  $P_r = \xi/K$  is the Prandtl number,  $E_c = (\Omega l)^2 / (\tau_1 - \tau_2)$  is the Eckert number and  $\theta = \frac{\tau - \tau_2}{\tau_1 - \tau_2}$ . Here  $\tau_1 > \tau_2$ , so that  $E_c > 0$ .

Equation (7.48) in notation of  $F$  becomes

$$\frac{d^2\theta}{dz^2} = -Br \left[ \frac{A + \frac{L}{4} \frac{dF}{dz} \frac{d\bar{F}}{dz}}{A_2 + \frac{L}{4} \left( A_3 + L \frac{dF}{dz} \frac{d\bar{F}}{dz} \right) \frac{dF}{dz} \frac{d\bar{F}}{dz}} \right] \frac{dF}{dz} \frac{d\bar{F}}{dz} \quad (7.49)$$

subject to the boundary conditions

$$\theta(-1) = 1, \quad \theta(1) = 0, \quad (7.50)$$

where  $Br = E_c P_r$  is the Brinkman number

The initial guess  $\theta_0$  and the auxiliary linear operator  $\mathcal{L}_6$  are selected in the following forms

$$\theta_0(z) = \frac{1}{2}(1-z), \quad (7.51)$$

$$\mathcal{L}_6[\hat{\theta}(z; q)] = \frac{\partial^2 \hat{\theta}(z; q)}{\partial z^2}, \quad (7.52)$$

$$\mathcal{L}_6 [N_1 + zN_2] = 0, \quad (7.53)$$

in which  $N_i$  ( $i = 1, 2$ ) are the arbitrary constants.

Zeroth order problem is

$$(1-q)\mathcal{L}_6 [\hat{\theta}(z; q) - \theta_0(z)] = q\hbar_6 \mathcal{N}_6 [\hat{F}(z; q), \hat{\theta}(z; q)], \quad (7.54)$$

$$\hat{\theta}(-1; q) = 1, \quad \hat{\theta}(1; q) = 0, \quad (7.55)$$

$$\mathcal{N}_6 [\hat{F}(z; q)] = A_2 \frac{\partial^2 \hat{\theta}}{\partial z^2} + \left( AB r + LA_3 \frac{\partial^2 \hat{\theta}}{\partial z^2} \right) \frac{\partial \hat{F}}{\partial z} \frac{\partial \bar{F}}{\partial z} + \left( \frac{L}{4} Br + \frac{L^2}{4} \frac{\partial^2 \hat{\theta}}{\partial z^2} \right) \left( \frac{\partial \hat{F}}{\partial z} \frac{\partial \bar{F}}{\partial z} \right)^2 \quad (7.56)$$

The problem at the  $m$ th order yields

$$\mathcal{L}_6 [\theta_m(z) - \chi_m \theta_{m-1}(z)] = \hbar_6 \mathcal{R}_{6m}(z), \quad (7.57)$$

$$\theta_m(-1) = 1, \theta_m(1) = 0, \quad (7.58)$$

$$\begin{aligned} \mathcal{R}_{6m}(z) = & A_2 \theta_{m-1}''(z) + AB r \sum_{k=0}^{m-1} F_{m-1-k}' \bar{F}'_k + LA_3 \sum_{k=0}^{m-1} F_{m-1-k}' \sum_{l=0}^k \bar{F}'_{k-l} \theta_l'' \\ & \frac{L}{4} Br \sum_{k=0}^{m-1} F_{m-1-k}' \sum_{l=0}^k F'_{k-l} \sum_{p=0}^l \bar{F}'_{l-p} \bar{F}'_p \\ & + \frac{L^2}{4} \sum_{k=0}^{m-1} F_{m-1-k}' \sum_{l=0}^k F'_{k-l} \sum_{p=0}^l \bar{F}'_{l-p} \sum_{q=0}^p \bar{F}'_{p-q} \theta_q'', \end{aligned} \quad (7.59)$$

and the solution is

$$\theta_m(z) = \sum_{t=0}^{2m} A_{m,t} z^t, \quad m \geq 0, \quad (7.60)$$



in which for  $m \geq 1$  and  $0 \leq t \leq 2m$ , we have

$$\begin{aligned}
A_{m,0} &= \chi_m \chi_{2m} A_{m-1,0} - \sum_{t=0}^{2m+3} \frac{\gamma_{m,t} \left(1 + (-1)^{t+2}\right)}{2(t+1)(t+2)}, \\
A_{m,1} &= \chi_m \chi_{2m-1} A_{m-1,1} - \sum_{t=0}^{2m+3} \frac{\gamma_{m,t} \left(1 - (-1)^{t+2}\right)}{2(t+2)(t+1)}, \\
A_{m,2} &= \chi_m \chi_{2m-2} A_{m-1,2} + \frac{1}{2} \gamma_{m,0}, \\
A_{m,t} &= \chi_m \chi_{2m-t} A_{m-1,t} + \gamma_{m,t-2} \frac{1}{(t-1)t}, \quad 2 \leq t \leq 2m,
\end{aligned} \tag{7.61}$$

$$\mathcal{L}_6 [\theta_m(z) - \chi_m \theta_{m-1}(z)] = \hbar_6 \sum_{t=0}^{2m+3} \left[ \begin{aligned} &\frac{L^2}{4} \beta_{m,t}^1 + \frac{LB_{rk}}{4} \chi_{2m+3-t} \beta_{m,t}^2 + LA_3 \chi_{2m+3-t} \chi_{2m+2-t} \beta_{m,t}^3 \\ &+ AB_{rk} \beta_{m,t}^4 \chi_{2m+3-t} \chi_{2m+2-t} \chi_{2m+1-t} \\ &+ A_2 A_{m-1,t}^3 \chi_{2m+3-t} \chi_{2m+2-t} \chi_{2m+1-t} \chi_{2m-t} \chi_{2m-1-t} \end{aligned} \right] z^t$$

and the coefficients  $\beta_{m,t}^1, \beta_{m,t}^2, \beta_{m,t}^3$  and  $\beta_{m,t}^4$  for  $m \geq 1, 0 \leq t \leq 2m$  are

$$\begin{aligned}
\beta_{m,t}^1 &= \sum_{k=0}^{m-1} \sum_{l=0}^k \sum_{p=0}^l \sum_{q=0}^p \sum_{a_1=\max\{0,t+2k-2m+1\}}^{\min\{t,2k+4\}} C_{m-1-k,x-a_1}^1 \sum_{a_2=\max\{0,a_1+2l-2k-1\}}^{\min\{a_1,2l+3\}} C_{k-l,a_1-a_2}^1 \\ &\quad \sum_{a_3=\max\{0,a_2+2p-2l-1\}}^{\min\{a_2,2p+2\}} \bar{C}_{l-p,a_2-a_3}^1 \sum_{a_4=\max\{0,a_3+2q-2p-1\}}^{\min\{a_3,2q+1\}} \bar{C}_{p-q,a_3-a_4}^1 A_{q,a_4}^3, \\
\beta_{m,t}^2 &= \sum_{k=0}^{m-1} \sum_{l=0}^k \sum_{p=0}^l \sum_{a_1=\max\{0,t+2k-2m+1\}}^{\min\{t,2k+3\}} C_{m-1-k,x-a_1}^1 \sum_{a_2=\max\{0,a_1+2l-2k-1\}}^{\min\{a_1,2l+2\}} C_{k-l,a_1-a_2}^1 \\ &\quad \sum_{a_3=\max\{0,a_2+2p-2l-1\}}^{\min\{a_2,2p+1\}} \bar{C}_{l-p,a_2-a_3}^1 \bar{C}_{p-q,a_3-a_4}^1, \\
\beta_{m,t}^3 &= \sum_{k=0}^{m-1} \sum_{l=0}^k \sum_{a_1=\max\{0,t+2k-2m+1\}}^{\min\{t,2k+2\}} C_{m-1-k,x-a_1}^1 \sum_{a_2=\max\{0,a_1+2l-2k-1\}}^{\min\{a_1,2l+1\}} \bar{C}_{k-l,a_1-a_2}^1 \theta''_{l,a_2}, \\
\beta_{m,t}^4 &= \sum_{k=0}^{m-1} \sum_{a_1=\max\{0,t+2k-2m+1\}}^{\min\{t,2k+2\}} C_{m-1-k,x-a_1}^1 \bar{C}_{k,a_1}^1.
\end{aligned} \tag{7.62}$$

$$\begin{aligned}
A_{m,t} &= \operatorname{Re} A_{m,t} + i \operatorname{Im} A_{m,t}, & A1_{m,t} &= (1+p)A_{m,p+1}, \\
A2_{m,p} &= (1+p)A1_{m,p+1}, & A3_{m,p} &= (1+p)A2_{m,p+1}, \\
A2_{m,p} &= (1+p)A_{m,p+1}, & A3_{m,p} &= (1+p)A2_{m,p+1}.
\end{aligned} \tag{7.63}$$

The corresponding  $m$ th order approximation is

$$\sum_{m=0}^M \theta_m(z) = \sum_{m=0}^M \sum_{t=0}^{2m} A3_{m,t} z^t \tag{7.64}$$

and the series solution is

$$\theta(z) = \lim_{M \rightarrow \infty} \left( \sum_{m=0}^M \theta_m(z) \right) = \lim_{M \rightarrow \infty} \left( \sum_{m=0}^M \sum_{t=0}^{2m} A_{m,t} z^t \right). \tag{7.65}$$

### 7.3 Convergence of the solution

Now we have an interest to show the convergence of the series solutions (7.46) and (7.65). Therefore  $\bar{h}_5$  and  $\bar{h}_6$ -curves are plotted when  $V_1 = 1/2$ ,  $V_2 = 1/3$ ,  $M = R = L = 1/10$  in Figures 7.1(a) and 7.2. These show that the admissible values of  $\bar{h}_5$  and  $\bar{h}_6$  are  $-0.75 \leq \bar{h}_5 \leq 0.1$  and  $-0.8 \leq \bar{h}_6 \leq 0$  for the velocity gradient and temperature gradient respectively. Moreover, the series solutions (7.46) and (7.65) converge in the whole region of  $z$  when  $\bar{h}_5 = -0.35$  and  $\bar{h}_6 = -0.8$ .

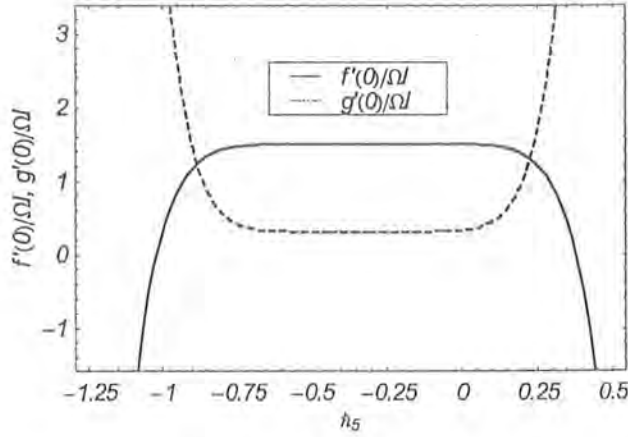


Figure 7.1(a): Plots of  $f'(0)$ ,  $g'(0)$  versus  $\bar{h}_5$  when  $\phi = 2$ .

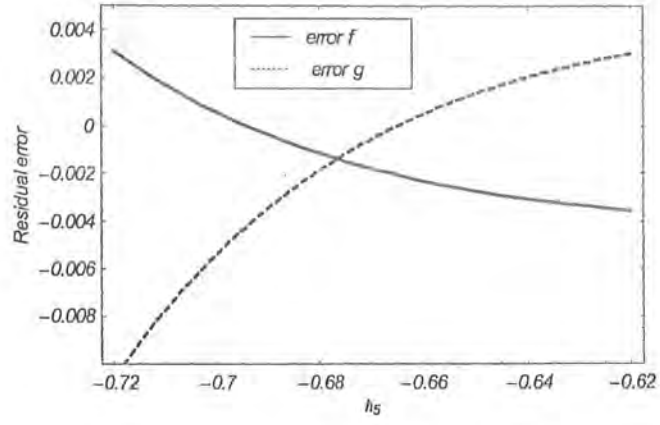


Figure 7.1(b): The graph of residual error versus  $h_5$  when  $\phi = 2$ .

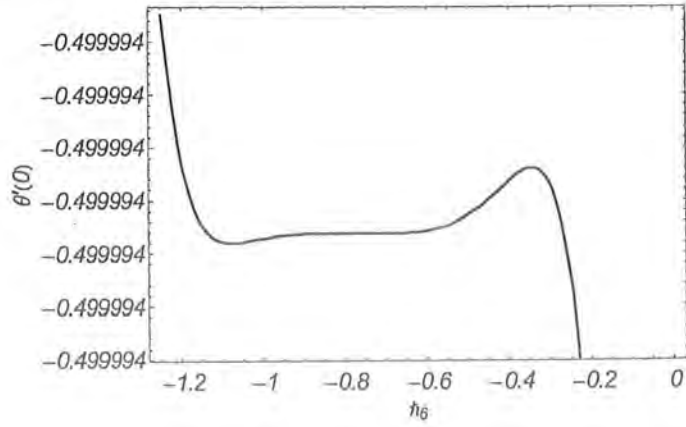


Figure 7.2: The graph of  $\theta'(0)$  versus  $h_6$  when  $\phi = 2$ .

## 7.4 Results and discussion

Here we examined the graphical representations of velocity and temperature profiles for the Johnson-Segalman and Newtonian fluids. The analysis is made for the emerging parameter for instance Hartman number  $M$ , viscoelastic parameter of Johnson-Segalman fluid  $\lambda_s$ , Hall parameter  $\phi$  and angular velocity of non-coaxial rotation  $R$  when  $V_1 = 1/2, V_2 = 1/3$  and  $M = R = L = 1/10$ .

Figures 7.3(a)-7.8(b) show the variation in the velocity field for the Hartman number  $M$ , rotation parameter  $R$  and viscoelastic parameter  $\lambda_s$  in the presence and absence of Hall parameter  $\phi$ . Figures 7.9(a)-7.11 show the variation in temperature profile for the Brinkman number  $Br$ , Hartman number  $M$ , and viscoelastic parameter  $\lambda_s$  in both situation when  $\phi = 0$  and  $\phi = 1$ . Figures 7.12(a)-7.14 show the analysis of velocity field and temperature profile for the Newtonian fluid for the embedded parameters  $M$ ,  $R$  and  $Br$ .

In Figures 7.3(a)-7.8(b) the velocity profile increases monotonically when there is an increase in the parameters  $M$ ,  $R$  and  $\lambda_s$ . Figures 7.9(a)-7.11 depict that temperature profile increases with an increase in Hartman number  $M$  and Brinkman number  $Br$ . However it decreases when viscoelastic parameter  $\lambda_s$  is increased.

Figures 7.12-7.14 elucidate that  $y$ -component of velocity for the Newtonian fluid increases if we increase the Hartman number  $M$ . This velocity decreases if we increase rotation parameter  $R$ . The temperature profile increases by increasing the Brinkman number  $Br$ .

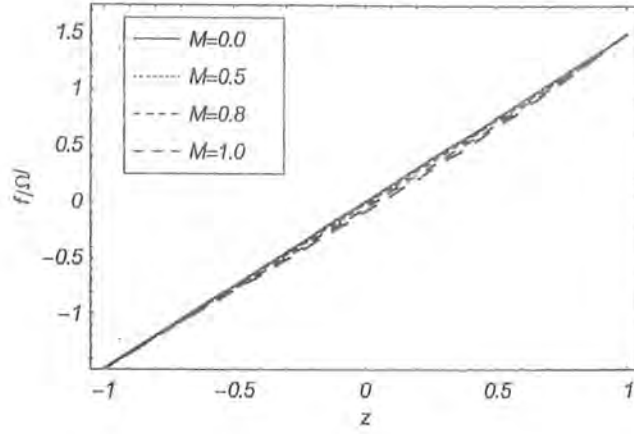


Figure 7.3(a): Variation of  $f/\Omega l$  for different values of Hartman number  $M$  in Johnson-Segalman fluid when  $\phi = 2$ .

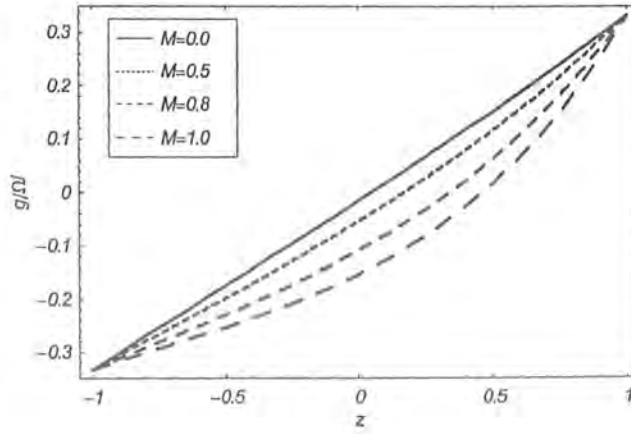


Figure 7.3(b): Variation of  $g/\Omega l$  for different values of Hartman number  $M$  in Johnson-Segalman fluid when  $\phi = 2$ .

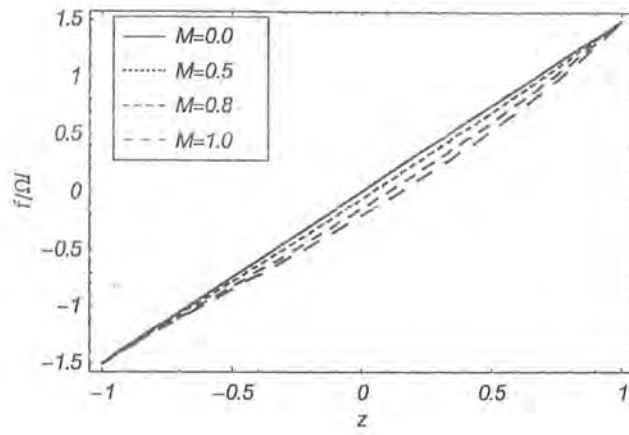


Figure 7.4(a): Variation of  $f/\Omega$  for different values of Hartman number  $M$  in Johnson-Segalman fluid when  $\phi = 0$ .

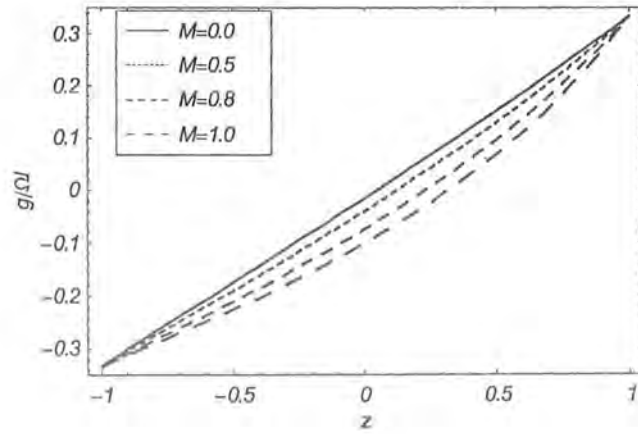


Figure 7.4(b): Variation of  $g/\Omega$  for different values of Hartman number  $M$  in Johnson-Segalman fluid when  $\phi = 0$ .

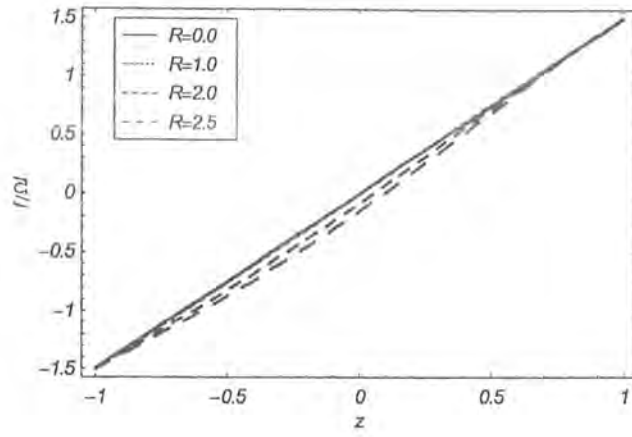


Figure 7.5(a): Variation of  $f/\Omega l$  for different values of rotation parameter  $R$  in Johnson-Segalman fluid when  $\phi = 1$ .

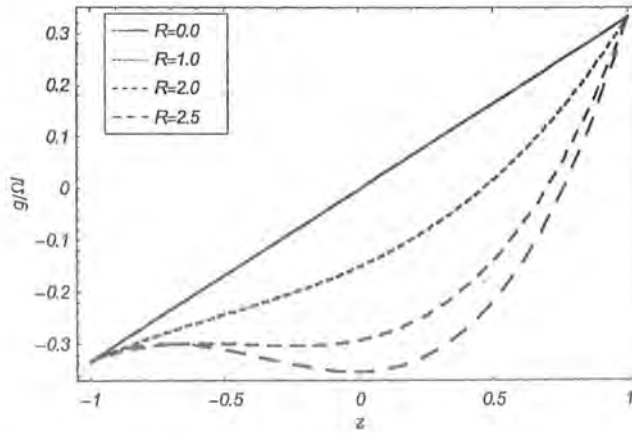


Figure 7.5(b): Variation of  $g/\Omega l$  for different values of rotation parameter  $R$  in Johnson-Segalman fluid when  $\phi = 1$ .

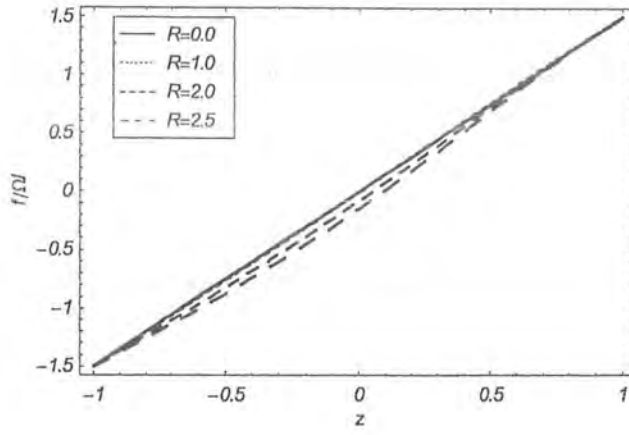


Figure 7.6(a): Variation of  $f/\Omega l$  for different values of rotation parameter  $R$  in Johnson-Segalman fluid when  $\phi = 0$ .

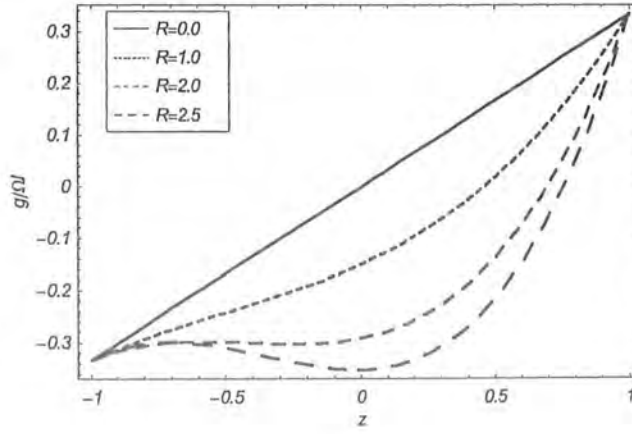


Figure 7.6(b): Variation of  $g/\Omega l$  for different values of rotation parameter  $R$  in Johnson-Segalman fluid when  $\phi = 0$ .



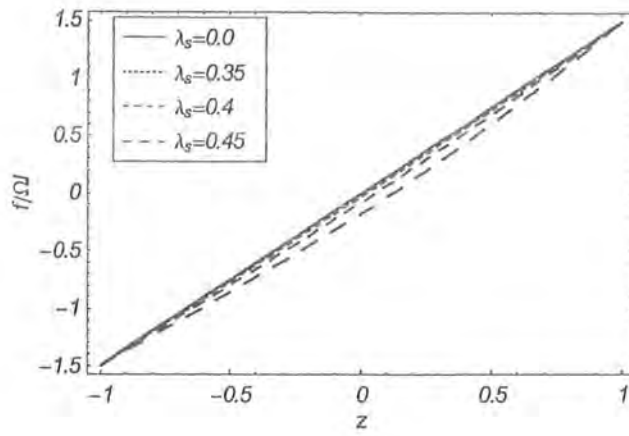


Figure 7.7(a): Variation of  $f/\Omega l$  for different values of Johnson-Segalman fluid parameter  $\lambda_s$  when  $\phi = 1$ .

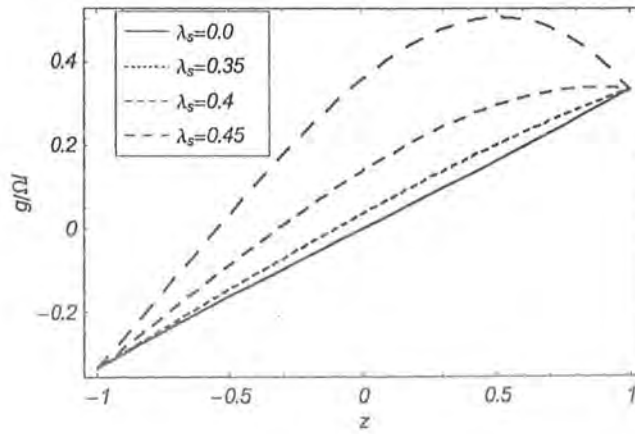


Figure 7.7(b): Variation of  $g/\Omega l$  for different values of Johnson-Segalman fluid parameter  $\lambda_s$  when  $\phi = 1$ .

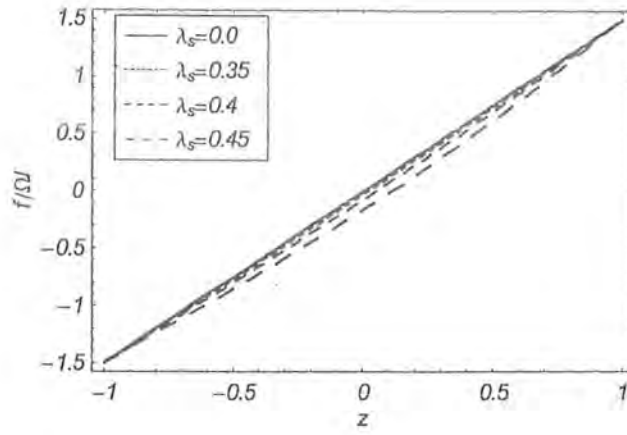


Figure 7.8(a): Variation of  $f/\Omega l$  for different values of Johnson-Segalman fluid parameter  $\lambda_s$  when  $\phi = 0$ .

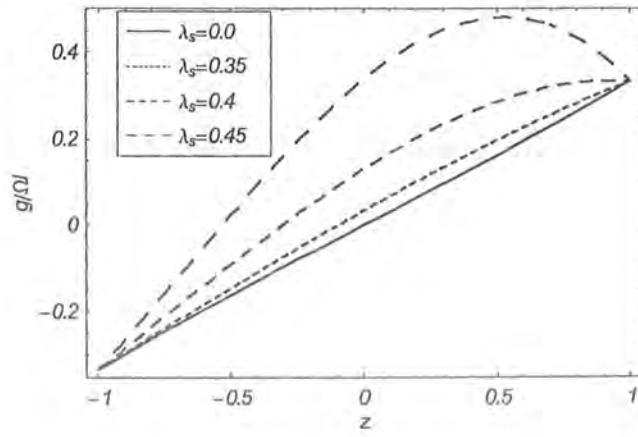


Figure 7.8(b): Variation of  $g/\Omega l$  for different values of Johnson-Segalman fluid parameter  $\lambda_s$  when  $\phi = 0$ .

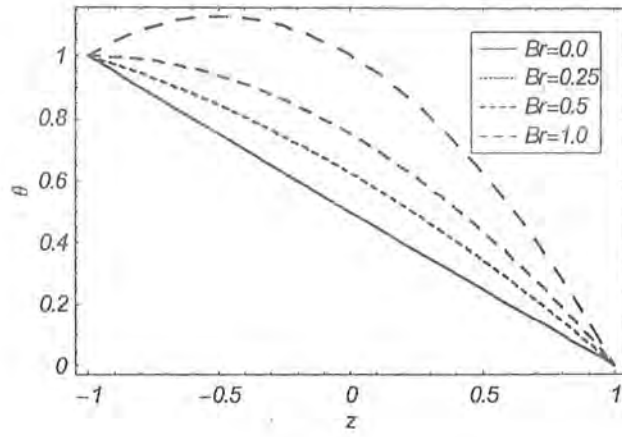


Figure 7.9(a): Variation of the temperature profile for different values of Brinkman number  $Br$  when  $\phi = 1$ .

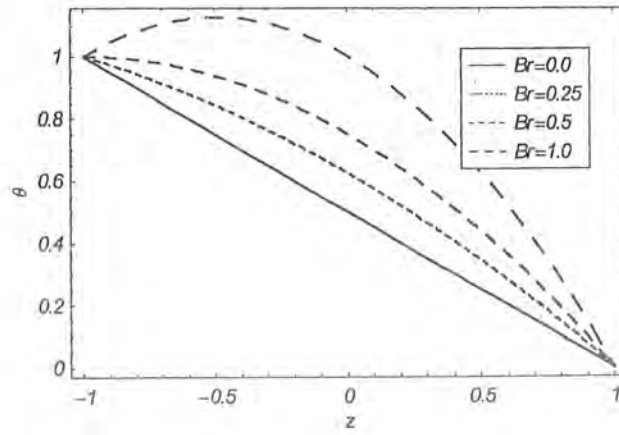


Figure 7.9(b): Variation of the temperature profile for different values of Brinkman number  $Br$  when  $\phi = 0$ .

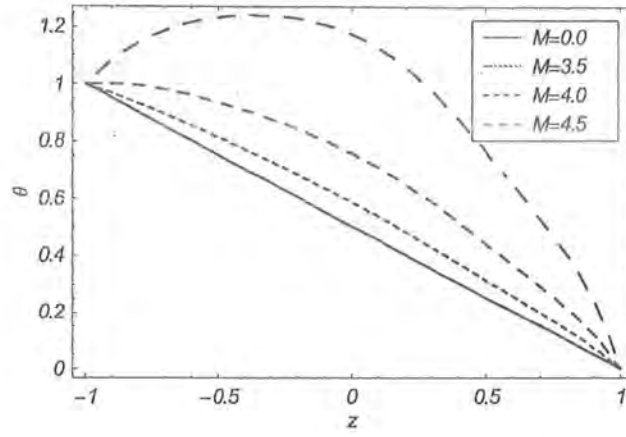


Figure 7.10(a): Variation of the temperature profile for different values of Hartman number  $M$  when  $\phi = 1$ .

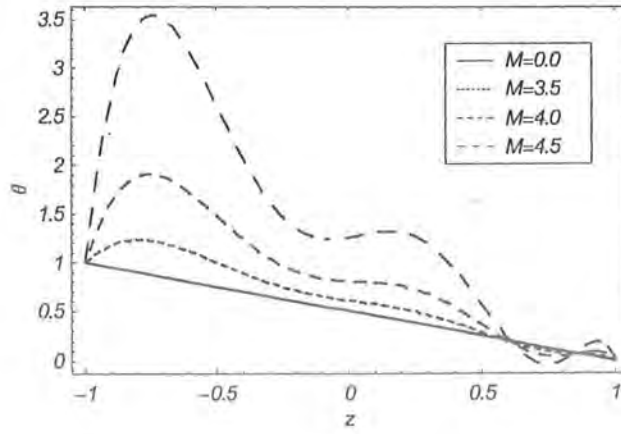


Figure 7.10(b): Variation of the temperature profile for different values of Hartman number  $M$  when  $\phi = 0$ .

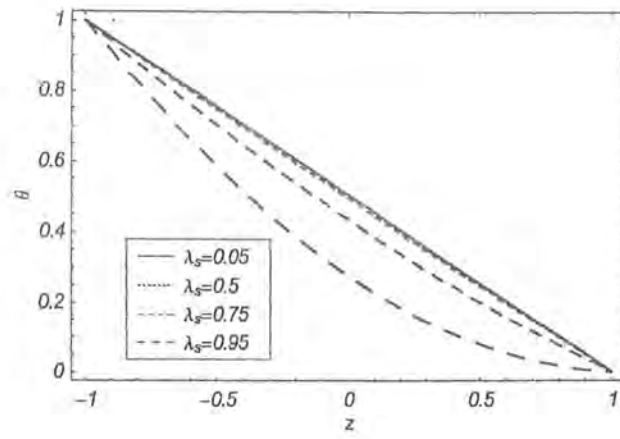


Figure 7.11: Variation of the temperature profile for different values of viscoelastic parameter  $\lambda_s$  when  $\phi = 1$ .

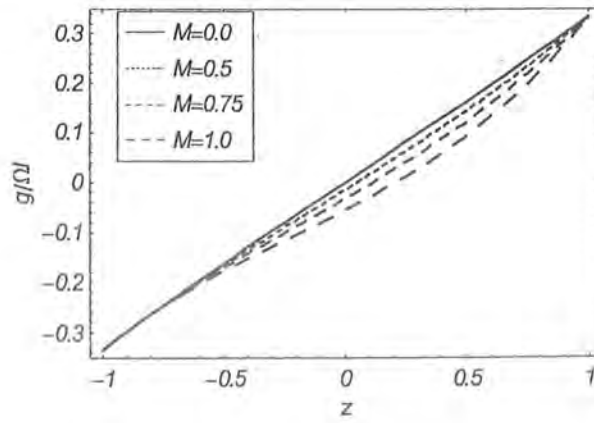


Figure 7.12: Variation of the velocity field for different values of Hartman number  $M$  for Newtonian fluid ( $\lambda_s = 0$ ) when  $\phi = 1$ .

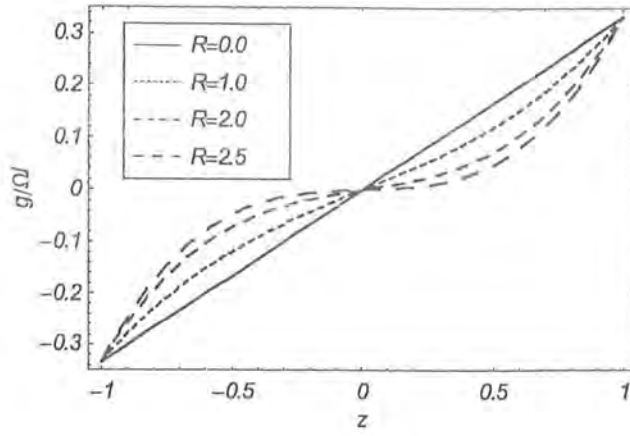


Figure 7.13: Variation of the velocity field for different values of rotation parameter  $R$  for Newtonian fluid ( $\lambda_s = 0$ ) when  $\phi = 1$ .

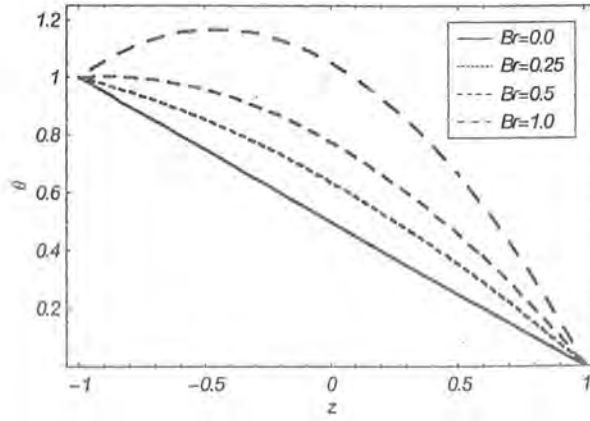


Figure 7.14: Variation of the temperature profile for different values of Brinkman number  $Br$  for Newtonian fluid when  $\phi = 1$ .

## Chapter 8

# Analytic solution for MHD plane and axisymmetric flow near a stagnation point

This chapter provides the mathematical model describing the momentum, heat and mass transfer characteristics of MHD flow and heat generating /absorbing fluid near a stagnation point of an isothermal two-dimensional axisymmetric body. Analytic solution of the non-linear problem is found with the help of homotopy analysis method. Numerical values of wall heat transfer coefficient and graphical results for velocity and heat transfer are also presented and examined.

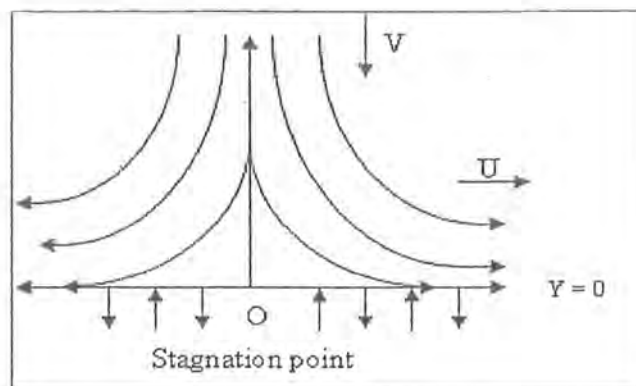


Fig. 8.1: Plane flow when  $U = ax, V = -ay$  and axisymmetric flow when  $U = ax, V = -2ay$ .

## 8.1 Mathematical formulation

Here we consider the steady and MHD stagnation point flow impinging on a horizontal surface. The considered viscous fluid generates or absorbs heat at uniform rate. The  $x$  and  $y$  axes are chosen along and normal to the plate. A uniform magnetic field is applied transversely to the flow. The induced magnetic field is negligible by choosing small magnetic Reynolds number. The governing equations are [132]

$$\frac{\partial}{\partial x}(x^{n-2}u) + \frac{\partial}{\partial y}(x^{n-2}v) = 0, \quad (8.1)$$

$$u \frac{\partial u}{\partial x} + v \frac{\partial u}{\partial y} = -\frac{1}{\rho} \frac{\partial P}{\partial x} + \zeta \left( \frac{\partial^2 u}{\partial x^2} + \frac{\partial}{\partial x} \left( \frac{u^{n-2}}{x^{n-2}} \right) + \frac{\partial^2 u}{\partial y^2} \right) - \frac{\sigma B_0^2}{\rho} u, \quad (8.2)$$

$$u \frac{\partial v}{\partial x} + v \frac{\partial v}{\partial y} = -\frac{1}{\rho} \frac{\partial P}{\partial y} + \zeta \left( x^{1-n} \frac{\partial}{\partial x} (x^{n-1}v) + \frac{\partial^2 v}{\partial y^2} \right), \quad (8.3)$$

$$\rho C_P \left( u \frac{\partial T}{\partial x} + v \frac{\partial T}{\partial y} \right) = K_e \left( x^{2-n} \frac{\partial}{\partial x} (x^{n-2}T) + \frac{\partial^2 T}{\partial y^2} \right) + Q_0(T - T_w), \quad (8.4)$$

where  $u$ ,  $v$ ,  $P$  and  $T$  are the velocity components, pressure and temperature, respectively.  $\rho$ ,  $\zeta$ ,  $K_e$ ,  $C_P$  and  $\sigma$  the fluid density, kinematic viscosity, thermal conductivity, specific heat at constant pressure and electrical conductivity, respectively.  $B_0$ ,  $Q_0$ ,  $T_w$  and  $n$  are the respective magnetic induction, heat generation/absorption coefficient, wall temperature and the dimensionality index such that  $n = 2$  corresponding to plane flow and  $n = 3$  corresponding to axisymmetric flow.

The boundary conditions for the problem under consideration are

$$u(X, 0) = 0, \quad v(X, 0) = -v_0, \quad T(X, 0) = T_w, \quad u(X, \infty) = U_\infty, \quad T(X, \infty) = T_\infty, \quad (8.5)$$

in which  $v_0$  indicates the suction or injection velocity, and  $U_\infty$  and  $T_\infty$  are the free stream velocity and temperature, respectively.

Writing

$$\eta = y \sqrt{\frac{B}{\zeta}}, \quad \psi = \frac{x^{n-1}}{n-1} \sqrt{B\zeta} f(\eta), \quad \theta(\eta) = \frac{T - T_w}{T_\infty - T_w}, \quad (8.6)$$

$$u = \frac{Bx}{n-1} \sqrt{f'(\eta)}, \quad v = -\sqrt{B\zeta} f(\eta), \quad (8.7)$$



where the constant  $B$  is a sort of a velocity gradient parallel to the wall and prime denotes ordinary differentiation with respect to  $\eta$ .

Invoking Eq. (8.6), Eq. (8.1) is identically satisfied, and equations (8.2)-(8.4) yield

$$f'''(\eta) + f(\eta)f''(\eta) + \frac{1}{n-1}(1-f'^2(\eta)) - M^2 f'(\eta) = 0, \quad (8.8)$$

$$\theta''(\eta) + Pr f(\eta)\theta'(\eta) + Pr \alpha \theta(\eta) = 0, \quad (8.9)$$

where  $M^2 = \sigma B_0^2(\rho B)^{-1}$ ,  $Pr = \mu C_P/K_e$  ( $\mu$  is the dynamic viscosity of the fluid) and  $\alpha = Q_0(\rho C_P B)^{-1}$  are the square of the Hartman number, the Prandtl number and the dimensionless heat generation/absorption coefficient, respectively.

The boundary conditions (8.5) now become

$$f(0) = f_w, \quad f'(0) = 0, \quad f'(\infty) = 1, \quad \theta(0) = 0, \quad \theta(\infty) = 1, \quad (8.10)$$

in which  $f_w$  is the suction/injection parameter.

The expressions of skin friction coefficient  $C$  and the wall heat transfer coefficient  $H$  are

$$C = \frac{2\sqrt{n-1}f''(0)}{\sqrt{Re_x}}, \quad (8.11)$$

$$H = \frac{\sqrt{n-1}\theta'(0)}{Pr\sqrt{Re_x}}. \quad (8.12)$$

In above equations  $Re_x = U_\infty x/\zeta$  and  $U_\infty = Bx/(n-1)$  are the Reynolds number and the free stream velocity.

## 8.2 Solution by homotopy analysis method

According to equations (8.8) and (8.9) and the boundary conditions (8.10), solution can be expressed in the form

$$f(\eta) = a_0 + \eta + \sum_{m=1}^{+\infty} \sum_{q=0}^{\infty} a_{q,m} \eta^q e^{-m\eta}, \quad (8.13)$$

$$\theta(\eta) = 1 + \sum_{m=1}^{+\infty} \sum_{q=0}^{\infty} b_{q,m} \eta^q e^{-m\eta}, \quad (8.14)$$

where  $a_0$ ,  $a_{q,m}$  and  $b_{q,m}$  are coefficients to be determined. According to the *rule of solution expression* denoted by equations (8.13) and (8.14) and the boundary conditions (8.10), it is natural to choose

$$f_0(\eta) = f_w + \eta - (1 - e^{-\eta}), \quad (8.15)$$

$$\theta_0(\eta) = (1 - e^{-\eta}) - \frac{1}{2} \eta e^{-\eta}, \quad (8.16)$$

as the initial approximation to  $f(\eta)$  and  $\theta(\eta)$ , respectively. We define an auxiliary linear operator  $\mathcal{L}_7$  and  $\mathcal{L}_8$  by

$$\mathcal{L}_7[\phi(\eta; q)] = \left( \frac{\partial^3}{\partial \eta^3} + \frac{\partial^2}{\partial \eta^2} \right) \phi(\eta; q), \quad (8.17)$$

$$\mathcal{L}_8[\psi(\eta; q)] = \left( \frac{\partial^2}{\partial \eta^2} - 1 \right) \psi(\eta; q), \quad (8.18)$$

with the property

$$\mathcal{L}_7[C_1 + C_2\eta + C_3e^{-\eta}] = 0, \quad \mathcal{L}_8[C_4e^{\eta} + C_5e^{-\eta}] = 0, \quad (8.19)$$

where  $C_i$ ,  $i = 1, 2, \dots, 5$  are constants. This choice of  $\mathcal{L}_7$  and  $\mathcal{L}_8$  is motivated by equations (8.13) and (8.14), respectively, and from boundary conditions (8.10), we have  $C_2 = C_4 = 0$ .

From Eqs. (8.8) and (8.9) we define nonlinear operators

$$\mathcal{N}_7[\phi(\eta; q), \psi(\eta; q)] = \frac{\partial^3 \phi}{\partial \eta^3} + \phi \frac{\partial^2 \phi}{\partial \eta^2} + \frac{1}{n-1} \left( 1 - \left( \frac{\partial \phi}{\partial \eta} \right)^2 \right) - M^2 \frac{\partial \phi}{\partial \eta}, \quad (8.20)$$

$$\mathcal{N}_8[\phi(\eta; q), \psi(\eta; q)] = \frac{\partial^2 \psi}{\partial \eta^2} + Pr \phi \frac{\partial \psi}{\partial \eta} + Pr \alpha \psi. \quad (8.21)$$

Zero-order deformation problems are as follows:

$$(1 - q)\mathcal{L}_7[\phi(\eta; q) - f_0(\eta)] = \hbar_7 q H_7(\eta) \mathcal{N}_7[\phi(\eta; q), \psi(\eta; q)], \quad (8.22)$$

and

$$(1 - q)\mathcal{L}_8[\psi(\eta; q) - \theta_0(\eta)] = \hbar_8 q H_8(\eta) \mathcal{N}_8[\phi(\eta; q), \psi(\eta; q)], \quad (8.23)$$

subject to conditions

$$\begin{aligned} \phi(0; q) = f_w, \quad \left. \frac{\partial \phi(\eta; q)}{\partial \eta} \right|_{\eta=0} = 0, \quad \left. \frac{\partial \phi(\eta; q)}{\partial \eta} \right|_{\eta=\infty} = 1, \\ \psi(0; q) = 0, \quad \psi(\infty; q) = 1, \end{aligned}$$

where  $q \in [0, 1]$  is an embedding parameter. When the parameter  $q$  increases from 0 to 1, the solution  $\phi(\eta; q)$  varies from  $f_0(\eta)$  to  $f(\eta)$  and the solution  $\psi(\eta; q)$  varies from  $\theta_0(\eta)$  to  $\theta(\eta)$ . If these continuous variation are smooth enough, the Maclaurin's series with respect to  $q$  can be constructed for  $\phi(\eta; q)$  and  $\psi(\eta; q)$ , respectively, and further, if these series are convergent at  $q = 1$ , we have

$$f(\eta) = f_0(\eta) + \sum_{m=1}^{+\infty} f_m(\eta) = \sum_{m=0}^{+\infty} \phi_m(\eta, \hbar_7), \quad (8.24)$$

and

$$\theta(\eta) = \theta_0(\eta) + \sum_{m=1}^{+\infty} \theta_m(\eta) = \sum_{m=0}^{+\infty} \psi_m(\eta, \hbar_8), \quad (8.25)$$

where

$$f_m(\eta) = \frac{1}{m!} \left. \frac{\partial^m \phi(\eta; q)}{\partial q^m} \right|_{q=0}, \quad \theta_m(\eta) = \frac{1}{m!} \left. \frac{\partial^m \psi(\eta; q)}{\partial q^m} \right|_{q=0}.$$

Differentiating Eqs. (8.22) and (8.23) and related conditions  $m$  times with respect to  $q$ , then setting  $q = 0$ , and finally dividing by  $m!$ , we obtain the  $m$ th order deformation problems as

$$\mathcal{L}_7[f_m(\eta) - \chi_m f_{m-1}(\eta)] = \hbar_7 H_7(\eta) R_{7m}(\eta), \quad (8.26)$$

$$\mathcal{L}_8[\theta_m(\eta) - \chi_m \theta_{m-1}(\eta)] = \hbar_8 H_8(\eta) R_{8m}(\eta), \quad (8.27)$$

subject to conditions

$$f_m(0) = 0, \quad f'_m(0) = 0, \quad f'_m(\infty) = 0, \quad \theta_m(0) = 0, \quad \theta_m(\infty) = 0, \quad (8.28)$$

where  $R_{7m}(\eta)$  and  $R_{8m}(\eta)$  are defined as

$$R_{7m}(\eta) = f_{m-1}''' + \sum_{i=0}^{m-1} f_i f_{m-i-1}'' - \frac{1}{n-1} \sum_{i=0}^{m-1} f_i' f_{m-i-1}' - M^2 f_{m-1}' + \frac{1}{n-1} (1 - \chi_m),$$

$$R_{3m}(\eta) = \theta''_{m-1} + Pr \sum_{i=0}^{m-1} f_i \theta'_{m-i-1} + Pr \alpha \theta_{m-1},$$

where prime denotes differentiation with respect to  $\eta$  and

$$\chi_m = \begin{cases} 0, & m \leq 1, \\ 1, & m > 1. \end{cases}$$

The general solutions of Eqs. (8.26) and (8.27) are

$$f_m(\eta) = \hat{f}_m(\eta) + C_1 + C_2\eta + C_3e^{-\eta}, \quad (8.29)$$

$$\theta_m(\eta) = \hat{\theta}_m(\eta) + C_4e^\eta + C_5e^{-\eta}, \quad (8.30)$$

where  $C_i$  for  $i = 1, \dots, 5$  are constants,  $\hat{f}_m(\eta)$  and  $\hat{\theta}_m(\eta)$  are particular solutions of equations (8.26) and (8.27), respectively.

According to the rule of solution expression denoted by equations (8.13) and (8.14),  $C_2 = C_4 = 0$ . The other unknowns are governed by

$$\hat{f}_m(0) + C_1 + C_3 = 0, \quad \hat{f}'_m(0) - C_3 = 0, \quad \hat{\theta}_m(0) + C_5 = 0,$$

and according to our algorithm, the another boundary conditions are fulfilled. In this way, we derive  $f_m(\eta)$  and  $\theta_m(\eta)$  for  $m = 1, 2, 3, \dots$ , successively.

For simplicity, here we take  $H_7(\eta) = H_8(\eta) = H(\eta)$ . According to the third rule of solution expression denoted by (8.24) and (8.25) and from equations (8.26) and (8.27), the auxiliary function  $H(\tau)$  should be in the form

$$H(\eta) = e^{-\kappa\eta},$$

where  $\kappa$  is an integer. To ensure that each coefficients  $a_{q,m}$  in (8.13) and  $b_{q,m}$  in (8.14) can be modified as the order of approximation tends to infinity, we set  $\kappa = 1$ .

At the  $m$ th-order approximation, we have the analytic solution of equations (8.8) and (8.9),

namely

$$f(\eta) \approx F_m(\eta) = \sum_{i=0}^m f_i(\eta), \quad \theta(\eta) \approx \Theta_m(\eta) = \sum_{i=0}^m \theta_i(\eta). \quad (8.31)$$

For simplicity, here we take  $\hbar_7 = \hbar_8 = \hbar$ . The auxiliary parameter  $\hbar$  can be employed to adjust the convergence region of the series (8.31) in the homotopy analysis solution. By means of the so-called  $\hbar$ -curve, it is straightforward to choose an appropriate range for  $\hbar$  which ensures the convergence of the solution series. As pointed out by Liao the appropriate region for  $\hbar$  is a horizontal line segment.

### 8.3 Numerical results

We use the widely applied symbolic computation software "MATHEMATICA" to solve equations (8.26) and (8.27) and find that  $\phi_m(\eta, \hbar)$  and  $\psi_m(\eta, \hbar)$  have the following structure:

$$\phi_m(\eta, \hbar) = \sum_{i=0}^{2m+n-2} \Phi_{m,i}(\eta, \hbar) \exp(-i\eta), \quad m \geq 0,$$

$$\psi_m(\eta, \hbar) = \sum_{i=0}^{2m+1} \Psi_{m,i}(\eta, \hbar) \exp(-i\eta), \quad m \geq 0,$$

By means of the so-called  $\hbar$ -curve, it is straightforward to choose an appropriate range for  $\hbar_7$  and  $\hbar_8$  which ensures the convergence of the solution series. We can investigate the influence of  $\hbar_7$  and  $\hbar_8$  the convergence of  $f''(0)$  and  $\theta'(0)$ , by plotting the curve of it versus  $\hbar_7$  and  $\hbar_8$ , as shown in Figure 8.2 for some examples in plane flow ( $n = 2$ ). Also, Figure. 8.3 shows the  $\hbar$ -curve in axisymmetric flow ( $n = 3$ ). By considering the  $\hbar$ -curve we can obtain the reasonable interval for  $\hbar_7$  and  $\hbar_8$  in each case.

Also, by computing the error for two successive approximation of  $F_m(\eta)$  or  $\Theta_m(\eta)$ , in each case, we can obtain the best value for  $\hbar_7$  and  $\hbar_8$ . Figure. 8.4 shows this error for  $F_{10}(\eta)$  with  $\alpha = 0.1$ ,  $M = 1$  and  $Pr = 0.7$  in axisymmetric flow and  $f_w = -0.1$  and  $0.1$  for  $\eta \in [0, 5]$ . One can compute easily that, in case  $f_w = -0.1$ , we have  $\hbar_7 = -1.056$ ,  $f_w = 0.1$ ,  $\hbar_7 = -1.095$  and for  $f_w = 0$ ,  $\hbar_8 = -1.095$  and these values match with  $\hbar$ -curve (in Figures 8.2 and 8.3).

Figure 8.5 presents representative profiles for the normal velocity  $f$  of both plane and axisymmetric flows for various values of Hartman number  $M$  and in each case the value of  $\hbar$

computed by rule of minimizing the error. Figures 8.6 and 8.7 show the respective effects of the Prandtl number  $Pr$  and the heat generation/absorption coefficient  $\alpha$  on the temperature profiles for both plane and axisymmetric stagnation point flows. As pointed by Chamkha [133], for heat-generation case ( $\alpha = 0.1$ ) in Figure 8.7 a sharp peak exists in the layer close the wall.

The so-called homotopy-Padé technique [135] is employed, which greatly accelerates the convergence. The  $[r, s]$  homotopy-Padé approximations of  $f''(0)$ , or  $C$  in (8.11) and  $\theta'(0)$ , or  $H$  in (8.12) according to (8.24) and (8.25) are formulated by

$$\frac{\sum_{k=0}^r \phi_k''(0, \hbar_7)}{1 + \sum_{k=1}^s \phi_{r+k+1}''(0, \hbar_7)}, \quad \frac{\sum_{k=0}^r \psi_k'(0, \hbar_8)}{1 + \sum_{k=1}^s \psi_{r+k+1}'(0, \hbar_8)},$$

respectively. In many cases, the  $[r, r]$  homotopy-Padé approximation does not depend upon the auxiliary parameter  $\hbar_7$  and  $\hbar_8$ . To verify the accuracy of HAM, a comparison of wall heat transfer coefficient  $C_h = H \sqrt{Re_x}$  with those reported by White [132], Chamkha [133], and Abdelkhalek [134] is given in Table 8.1 for  $M = 0$  and  $\alpha = 0$ . The values of  $C_f = C \sqrt{Re_x}$  also compare well since the obtained values for  $n = 2$  and  $n = 3$  by [15, 15] Homotopy-Padé method are 2.4652 and 2.6239, while the values reported by Chamkha [133] are 2.4695 and 2.6240 and based on White's correlations  $C_f \approx 2Pr^{2/3}C_h$  are 2.4782 and 2.6275, respectively.

Table 8.1: Results for [15, 15] Homotopy-Padé approach for  $C_h$

| $Pr$  | $n = 2$ |        |             |         | $n = 3$ |        |             |         |
|-------|---------|--------|-------------|---------|---------|--------|-------------|---------|
|       | White   | Chamka | Abdelkhalek | HAM     | White   | Chamka | Abdelkhalek | HAM     |
| 0.7   | 0.7060  | 0.7080 | 0.7054      | 0.70812 | 0.9438  | 0.9507 | 0.95421     | 0.95036 |
| 1.0   | 0.5700  | 0.5705 | 0.57235     | 0.56963 | 0.7620  | 0.7624 | 0.76421     | 0.76154 |
| 10.0  | 0.1432  | 0.1339 | 0.1446      | 0.13377 | 0.1914  | 0.1752 | 0.1925      | 0.13868 |
| 100.0 | 0.0360  | 0.0299 | 0.0381      | 0.02477 | 0.0481  | 0.0387 | 0.04923     | 0.02767 |

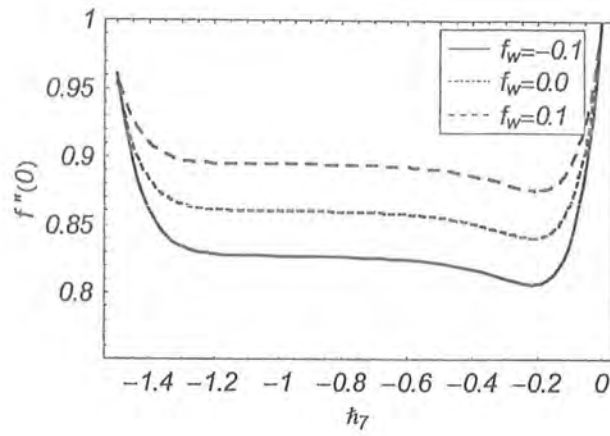


Figure 8.2(a): The  $h_7$ -curves for the 10th-order approximation and  $n = 2$ .

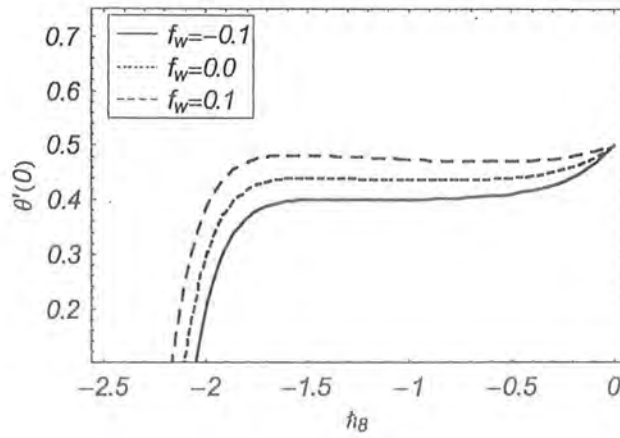


Figure 8.2(b): The  $h_8$ -curves for the 10th-order approximation and  $n = 2$ .

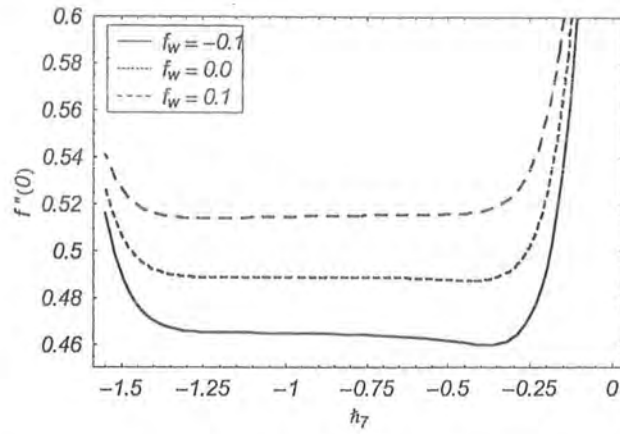


Figure 8.3(a): The  $\tilde{h}_7$ -curves for the 10th-order approximation and  $n = 3$ .

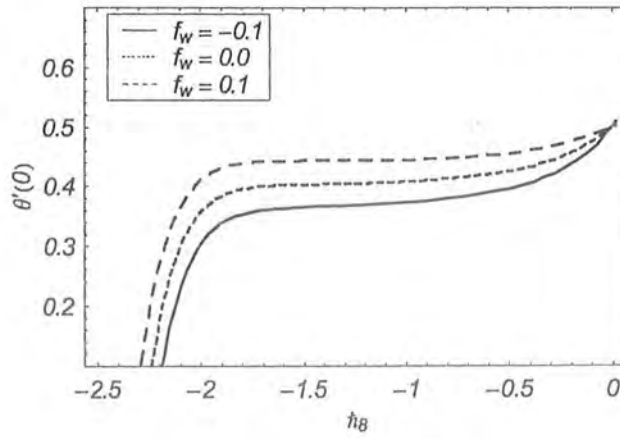


Figure 8.3(b): The  $\tilde{h}_8$ -curves for the 10th-order approximation and  $n = 3$ .



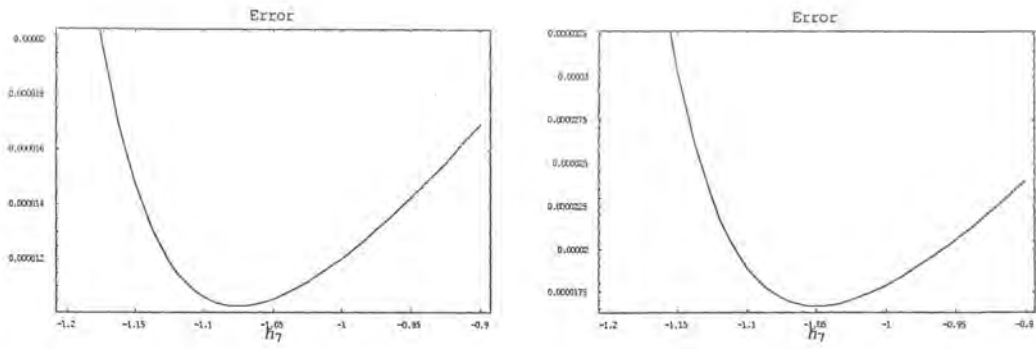


Figure 8.4(a): The error of  $F_{10}(\eta)$  versus  $h_7$ ; in left:  $f_w = 0.1$ , in right:  $f_w = -0.1$ .

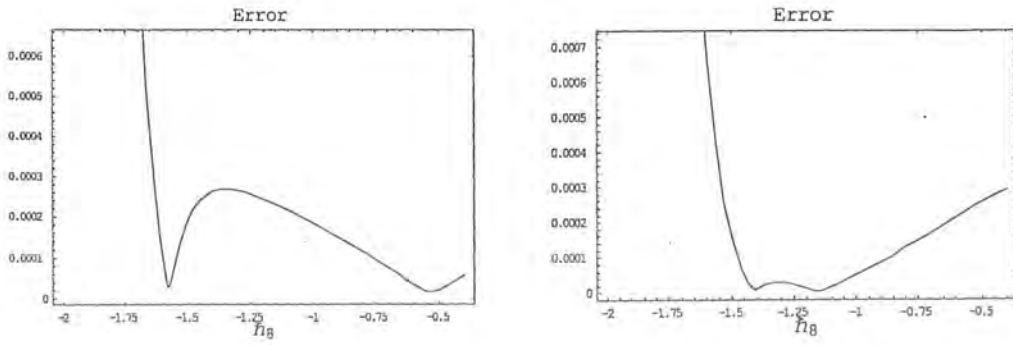


Figure 8.4(b): The error of  $\theta_{10}(\eta)$  versus  $h_8$ ; in left:  $f_w = 0.1$ , in right:  $f_w = -0.1$ .

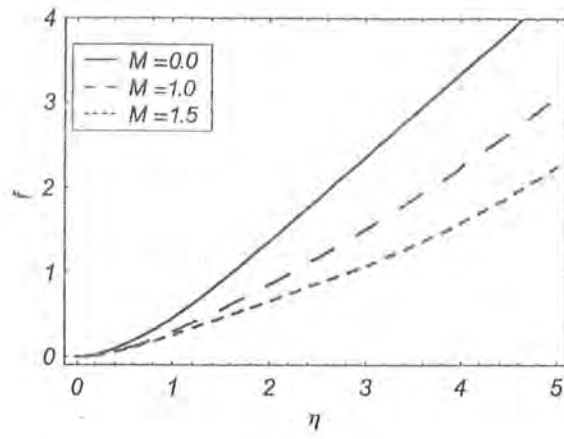


Figure 8.5(a): Effect of  $M$  on normal velocity profiles in 10th-order approximation when  $n = 2$ .

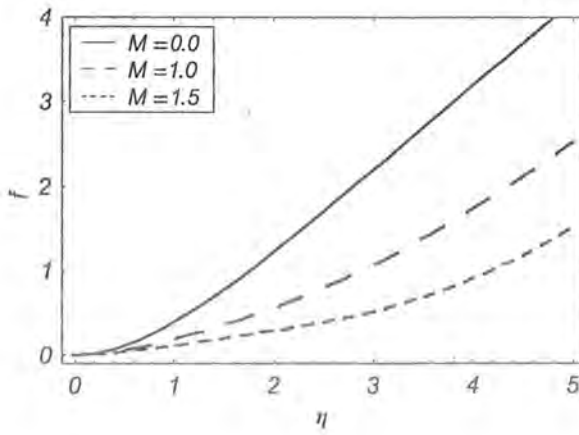


Figure 8.5(b): Effect of  $M$  on normal velocity profiles in 10th-order approximation when  $n = 3$ .

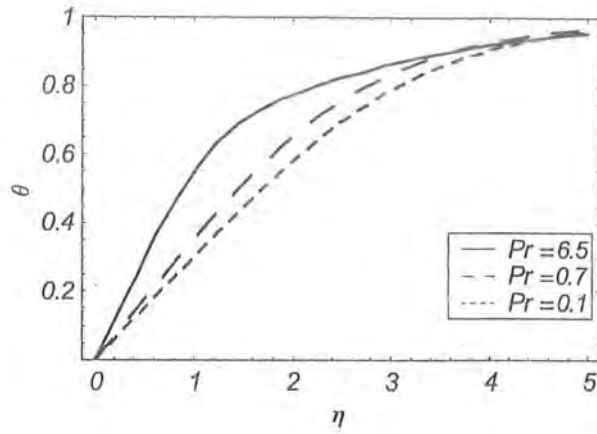


Figure 8.6(a): Effect of  $Pr$  on temperature profiles in 10th-order approximation when  $n = 2$ .

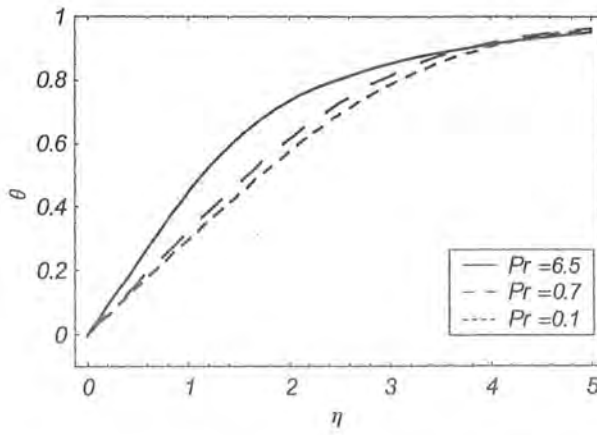


Figure 8.6(b): Effect of  $Pr$  on temperature profiles in 10th-order approximation when  $n = 3$ .

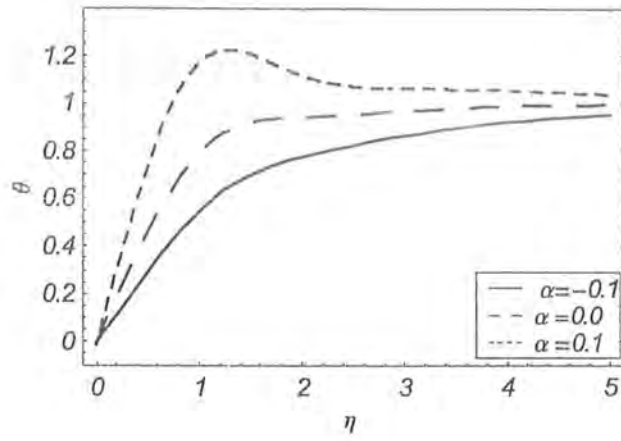


Figure 8.7(a): Effect of  $\alpha$  on temperature profiles in 10th-order approximation when  $n = 2$ .

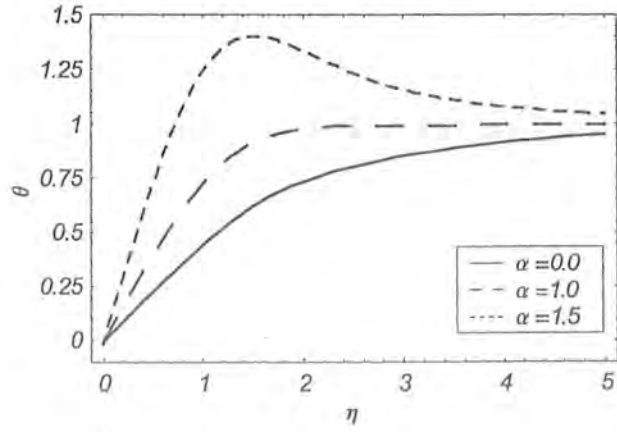


Figure 8.7(b): Effect of  $\alpha$  on temperature profiles in 10th-order approximation when  $n = 3$ .

## Chapter 9

# Series solution for the Falkner Skan flow of the FENE-P model

This chapter reports the Falkner Skan flow of FENE-P (finitely extensible nonlinear elastic Peterlin) fluid. The governing equations in the regime of boundary layer are utilized. Series solution is constructed by employing a homotopy analysis method. Numerical values of the skin friction coefficients are computed by using the Crocco's transformation, HAM and other existing methods in the literature.

### 9.1 Mathematical formulation

Consider the steady boundary layer flow of a viscoelastic fluid governed by the FENE-P model when Reynolds number  $Re$  number is very large ( $Re = O(1/\delta)$ ) and Weissenberg number  $We$  is very small ( $We = O(\delta)$ ). The viscoelastic fluid is bounded by a semi infinite porous plate and flow is produced by the pressure gradient when fluid is flowing with the free stream velocity

$u_e$  far away from the plate.

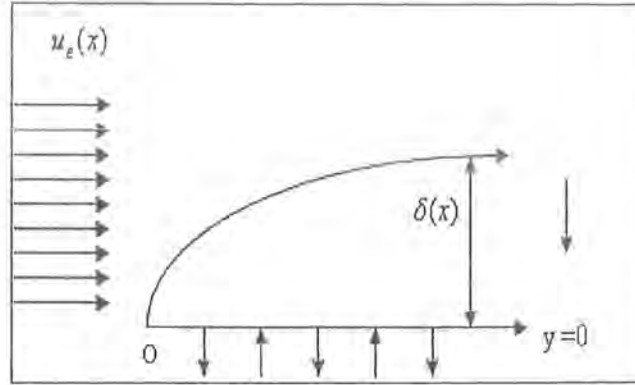


Fig. 9.1: Flow description.

The appropriate boundary conditions are

$$\begin{aligned} u &= 0, \quad v = v_w \quad \text{when } y = 0, \\ u &= u_e(x), \quad v = 0 \quad \text{as } y \rightarrow \infty. \end{aligned} \quad (9.1)$$

The velocity field for the two-dimensional flow is

$$\mathbf{V} = (u(x, y), v(x, y), 0). \quad (9.2)$$

The Cauchy stress tensor of viscoelastic fluid described by the FENE-P model is [136]

$$\mathbf{T} = -p\mathbf{I} + \tau_p + \tau_s, \quad (9.3)$$

where  $\tau_p$  and  $\tau_s$  represents the contribution from the polymer molecules and solvent respectively, which follow the relations

$$\tau_s = \eta_s \mathbf{A}_1, \quad (9.4)$$

and

$$\tau_p = \frac{\eta_p}{\lambda} Z^{-1} \mathbf{S} - \mathbf{I}, \quad (9.5)$$

where  $Z$  and configuration tensor  $S$  satisfy the following relation

$$Z = 1 - \frac{\text{tr}S}{b}, \quad (9.6)$$

$$Z^{-1}S + \lambda \frac{\bar{D}S}{\bar{D}t} = \mathbf{I}, \quad (9.7)$$

$$\frac{\bar{D}S}{\bar{D}t} = \frac{\partial S}{\partial t} - (\nabla V)S - S(\nabla V)^T.$$

Here  $\text{tr}S$  is the trace of  $S$ ,  $\mathbf{I}$  is the identity matrix. The parameter  $\lambda$  is the fluid relaxation time,  $b$  is the extensibility parameter of polymer which is modelled by two beads connected by a nonlinear spring.  $\eta_s$  and  $\eta_p$  are the viscosities of solvent and polymer respectively.

$$\mathbf{A}_1 = \begin{pmatrix} 2\frac{\partial u}{\partial x} & \frac{\partial u}{\partial y} + \frac{\partial v}{\partial x} & 0 \\ \frac{\partial u}{\partial y} + \frac{\partial v}{\partial x} & 2\frac{\partial v}{\partial y} & 0 \\ 0 & 0 & 0 \end{pmatrix},$$

$$\tau_p = \tau(x, y). \quad (9.8)$$

Invoking equations (9.2)-(9.8), the continuity and momentum equations give

$$\frac{\partial u}{\partial x} + \frac{\partial v}{\partial y} = 0, \quad (9.9)$$

$$u \frac{\partial u}{\partial x} + v \frac{\partial u}{\partial y} = -\frac{1}{\rho} \frac{\partial p}{\partial x} + \nu_s \left( \frac{\partial^2 u}{\partial x^2} + \frac{\partial^2 u}{\partial y^2} \right) + \frac{1}{\rho} \left( \frac{\partial \tau_{xx}}{\partial x} + \frac{\partial \tau_{xy}}{\partial y} \right), \quad (9.10)$$

$$u \frac{\partial v}{\partial x} + v \frac{\partial v}{\partial y} = -\frac{1}{\rho} \frac{\partial p}{\partial y} + \nu_s \left( \frac{\partial^2 v}{\partial x^2} + \frac{\partial^2 v}{\partial y^2} \right) + \frac{1}{\rho} \left( \frac{\partial \tau_{xy}}{\partial x} + \frac{\partial \tau_{yy}}{\partial y} \right), \quad (9.11)$$

$$Z^{-1}S_{xx} + \lambda \left( u \frac{\partial S_{xx}}{\partial x} + v \frac{\partial S_{xx}}{\partial y} - 2 \left( S_{xx} \frac{\partial u}{\partial x} + S_{xy} \frac{\partial u}{\partial y} \right) \right) = 1, \quad (9.12)$$

$$Z^{-1}S_{yy} + \lambda \left( u \frac{\partial S_{yy}}{\partial x} + v \frac{\partial S_{yy}}{\partial y} - 2 \left( S_{xy} \frac{\partial v}{\partial x} + S_{yy} \frac{\partial v}{\partial y} \right) \right) = 1, \quad (9.13)$$

$$Z^{-1}S_{zz} + \lambda \left( u \frac{\partial S_{zz}}{\partial x} + v \frac{\partial S_{zz}}{\partial y} \right) = 1, \quad (9.14)$$

$$Z^{-1}S_{xy} + \lambda \left( u \frac{\partial S_{xy}}{\partial x} + v \frac{\partial S_{xy}}{\partial y} - \left( S_{yy} \frac{\partial u}{\partial y} + S_{xx} \frac{\partial v}{\partial x} \right) \right) = 0. \quad (9.15)$$

### 9.1.1 Boundary layer equations

To find the boundary layer equations [137] we use the following assumptions

$$\begin{aligned} u &= O(1), \quad x = O(1), \quad v = O(\delta), \quad y = O(\delta), \quad \lambda = O(1), \\ v_s &= v_p = O(\delta^2), \quad \tau_{xx} = \tau_{yy} = O(\delta^2), \quad \tau_{xy} = O(\delta). \end{aligned}$$

Neglecting higher order terms in  $\delta$ , equations (9.10)-(9.15) reduce to

$$u \frac{\partial u}{\partial x} + v \frac{\partial u}{\partial y} = -\frac{1}{\rho} \frac{\partial p}{\partial x} + v_s \frac{\partial^2 u}{\partial y^2} + \frac{1}{\rho} \frac{\partial \tau_{xy}}{\partial y}, \quad (9.16)$$

$$Z^{-1} S_{xx} - 2\lambda S_{xy} \frac{\partial u}{\partial y} = 1, \quad (9.17)$$

$$Z^{-1} S_{xy} - \lambda S_{yy} \frac{\partial u}{\partial y} = 0, \quad (9.18)$$

$$Z^{-1} S_{yy} = 1, \quad Z^{-1} S_{zz} = 1. \quad (9.19)$$

Through Eqs. (9.17)-(9.19), Eqs. (9.5) and (9.6) become

$$\tau_{xy} = \eta_p Z \frac{\partial u}{\partial y}, \quad (9.20)$$

$$\kappa \left( \frac{\partial u}{\partial y} \right)^2 Z^3 + Z - \gamma = 0, \quad (9.21)$$

where

$$\kappa = \frac{2\lambda^2}{b+3}, \quad \gamma = \frac{b}{b+3},$$

Introducing the stream function  $\chi$  such that

$$u = \frac{\partial \chi}{\partial y}, \quad v = -\frac{\partial \chi}{\partial x}$$

equations (9.16) and (9.21) become

$$\frac{\partial \chi}{\partial y} \frac{\partial^2 \chi}{\partial x \partial y} - \frac{\partial \chi}{\partial x} \frac{\partial^2 \chi}{\partial y^2} = u_e \frac{du_e}{dx} + v_s \frac{\partial^2}{\partial y^2} \left( \frac{\partial \chi}{\partial y} \right) + v_p \frac{\partial}{\partial y} \left( Z \frac{\partial \chi}{\partial y} \right)$$



or

$$\frac{\partial \chi}{\partial y} \frac{\partial^2 \chi}{\partial x \partial y} - \frac{\partial \chi}{\partial x} \frac{\partial^2 \chi}{\partial^2 y} = u_\epsilon \frac{du_\epsilon}{dx} + v \frac{\partial}{\partial y} \left( (1 - \beta + \beta z) \frac{\partial^2 \chi}{\partial y^2} \right), \quad (9.22)$$

where  $v = v_s + v_p$  and  $\beta = v_p/v$  and hence

$$\kappa \left( \frac{\partial^2 \chi}{\partial^2 y} \right)^2 Z^3 + Z - \gamma = 0, \quad (9.23)$$

For similarity solution we introduce the following transformation and write  $u_\epsilon = U_0 X^n$ , (where  $X = x/L$  is dimensionless)

$$\eta = \sqrt{\frac{(n+1)u_\epsilon}{2\nu x}} y, \quad \chi = \sqrt{\frac{2\nu x u_\epsilon}{(n+1)}} f(\eta), \quad Z = g(\eta).$$

Now problem statement becomes

$$(Hf'')' + ff'' + \frac{2n}{n+1} (1 - (f')^2) = 0, \quad (9.24)$$

$$f(0) = f_w, \quad f'(0) = 0, \quad f'(\infty) = 1. \quad (9.25)$$

where  $f = f(\eta)$  satisfies

$$\Lambda g^3(\eta)(f'')^2 + g(\eta) - \gamma = 0. \quad (9.26)$$

Here  $\eta$  is the dimensionless variable, and  $v_w = -f_w \sqrt{(n+1)u_\epsilon \nu / 2x}$  where  $f_w$  is a constant that corresponds to blowing/injection or suction and

$$\Lambda = \frac{(n+1)\epsilon}{3+b},$$

where  $\epsilon = We^2 Re$ . The constant  $We$  is the well known Weissenberg number which is the measure of the fluid elasticity and  $Re$  is the Reynolds number.

As in this study we consider the case where  $We \rightarrow 0$  and  $Re \rightarrow \infty$ . Also, the variable  $H$  in Eq. (9.24) is given by

$$H = 1 - \beta + \beta g.$$

By these assumptions, in Eq. (9.26), it is proved that  $H \neq 0$  is constant and we have the

following generalized Falkner-Skan equation

$$Hf''' + ff'' + \frac{2n}{n+1}(1-f'^2) = 0. \quad (9.27)$$

Now, by introducing the transformations

$$f(\eta) = \sqrt{H}F(\xi), \quad \xi = \frac{\eta}{\sqrt{H}}, \quad (9.28)$$

we have the following problem

$$F'''(\xi) + F(\xi)F''(\xi) + \alpha(1-F'^2) = 0, \quad (9.29)$$

$$F(0) = \frac{f_w}{\sqrt{H}}, \quad F'(0) = 0, \quad F'(\infty) = 1, \quad (9.30)$$

where  $\alpha = \frac{2n}{n+1}$ .

## 9.2 Crocco's transformation

A direct solution of equation (9.29) with boundary conditions (9.30) can be obtained by a shooting method using Runge-Kutta algorithm or other iterative numerical methods [138]. The arising difficulty is that we have to make an initial guess for the value  $F''(0)$  to initiate the shooting process and this guess is very important to obtain a good solution. Unfortunately, the process is very sensitive to this starting value and the problem is made worse by the values of  $\alpha$  and  $F(0)$  in the problem.

Crocco's transformation can be used in calculating  $F''(0)$ . The idea is to transform the equation and boundary conditions into another set of variables that reduces the order of differential equation. Choose a suitable profile for the unknown function and then integrate over the complete range of the independent variable. We first introduce the transformations

$$\lambda = F'(\xi), \quad \psi = F'^2, \quad (9.31)$$

which convert equation (9.29) into the following second order differential equation

$$\psi \frac{d^2\psi}{d\lambda^2} - \frac{1}{2} \left( \frac{d\psi}{d\lambda} \right)^2 + \alpha (\lambda^2 - 1) \frac{d\psi}{d\lambda} - (4\alpha - 2)\lambda\psi = 0. \quad (9.32)$$

The boundary conditions (9.30) together with the fact that  $F''(+\infty) = 0$  give the following conditions for the equation (9.32):

$$\lambda = 0; \quad \frac{d\psi}{d\lambda} = -2(aM + \alpha), \quad (9.33)$$

$$\lambda = 1; \quad \frac{d\psi}{d\lambda} = 0, \quad (9.34)$$

where  $a = F(0) = \frac{f_w}{\sqrt{H}}$  and  $M = F''(0)$ . Further, from equations (9.32)-(9.34) we obtain the so-called supplementary boundary conditions:

$$\lambda = 1; \quad \psi = 0, \quad (9.35)$$

$$\lambda = 0; \quad \psi = M^2. \quad (9.36)$$

To solve equation (9.32) subject to the conditions (9.33)-(9.36), we choose the following profile for  $\psi$ :

$$\psi(\lambda) = (aM + \alpha)(-2\lambda^3 + 4\lambda^2 - 2\lambda) + M^2(2\lambda^3 - 3\lambda^2 + 1), \quad (9.37)$$

which satisfies (9.33)-(9.36). Substituting equation (9.37) into equation (9.32) and integrating with respect to  $\lambda$  from  $\lambda = 0$  to  $\lambda = 1$ , we obtain a four order polynomial for  $M$ .

$$\frac{2\alpha}{5} \left( \alpha + \frac{1}{3} \right) + \frac{2aM}{5} \left( 3\alpha + \frac{1}{3} \right) - \frac{M^2}{5} \left( \frac{3}{2}(1 + 9\alpha) - 4a^2 - \frac{13a}{5}M^3 + \frac{9}{5}M^4 \right) = 0$$

We take the algebraically larger root as the other root does not give realistic results. Hence, in this method, calculating  $M = F''(0)$  for various values of  $\alpha$  and  $a = F(0)$  is very easy and indeed we can find that the problem for which values of these parameters are realistic.

### 9.3 Solution by homotopy analysis method (HAM)

According to equation (9.24) and the boundary conditions (9.25), solution can be expressed in the form

$$F(\xi) = \sum_{k,m=0}^{+\infty} c_{k,m} \xi^k e^{-m\delta\xi}, \quad (9.38)$$

where the  $c_{k,m}$  ( $q, m = 0, 1, \dots$ ) are coefficients to be determined and  $\delta > 0$  is a spatial-scale parameter. According to the *rule of solution expression* denoted by equation (9.38) and the boundary conditions (9.25), it is natural to choose

$$F_0(\xi) = a + \xi - \frac{1 - \exp(-\delta\xi)}{\delta}, \quad (9.39)$$

as the initial approximation to  $F(\xi)$ , where  $a = F(0) = \frac{J_\omega}{\sqrt{H}}$ . We define an auxiliary linear operator  $\mathcal{L}_9$  by

$$\mathcal{L}_9[\phi(\xi, \delta; q)] = \left( \frac{\partial^3}{\partial \xi^3} + \delta \frac{\partial^2}{\partial \xi^2} \right) \phi(\xi, \delta; q), \quad (9.40)$$

with the property

$$\mathcal{L}_9[D_1 + D_2\xi + D_3e^{-\delta\xi}] = 0, \quad (9.41)$$

where  $D_1$ ,  $D_2$  and  $D_3$  are constants. This choice of  $\mathcal{L}_9$  is motivated by equation (9.38) and the later requirement that (9.49) should contain only two non-zero constants, namely  $D_1$  and  $D_3$ .

From (9.29) we define a nonlinear operator

$$\mathcal{N}_9[\phi(\xi, \delta; q)] = \left( \frac{\partial^3 \phi}{\partial \xi^3} \right) + \phi \left( \frac{\partial^2 \phi}{\partial \xi^2} \right) + \alpha \left( 1 - \left( \frac{\partial \phi}{\partial \xi} \right)^2 \right), \quad (9.42)$$

and then construct the homotopy

$$\mathcal{H}_9[\phi(\xi, \delta; q)] = (1 - q)\mathcal{L}_9[\phi(\xi, \delta; q) - F_0(\xi)] - \mathcal{N}_9\hbar_9q[\phi(\xi, \delta; q)], \quad (9.43)$$

where  $\hbar_9 \neq 0$  is the convergence-control parameter. Setting  $\mathcal{H}_9[\phi(\xi, \delta; q)] = 0$ , we have the zero-order deformation problem as follows:

$$(1 - q)\mathcal{L}_9[\phi(\xi, \delta; q) - F_0(\xi)] = \hbar_9q\mathcal{N}_9[\phi(\xi, \delta; q)], \quad (9.44)$$

$$\phi(0, \delta; q) = a, \quad \left. \frac{\partial \phi(\xi, \delta; q)}{\partial \xi} \right|_{\xi=0} = 0, \quad \left. \frac{\partial \phi(\xi, \delta; q)}{\partial \xi} \right|_{\xi=+\infty} = 1, \quad (9.45)$$

where  $q \in [0, 1]$  is an embedding parameter. When the parameter  $q$  increases from 0 to 1, the solution  $\phi(\xi, \delta; q)$  varies from  $F_0(\xi)$  to  $F(\xi)$ . If this continuous variation is smooth enough, the Maclaurin's series with respect to  $q$  can be constructed for  $\phi(\xi, \delta; q)$ , and further, if this series is convergent at  $q = 1$ , we have

$$F(\xi) = F_0(\xi) + \sum_{m=1}^{+\infty} F_m(\xi) = \sum_{m=0}^{+\infty} \varphi_m(\xi, \hbar_9, \delta), \quad (9.46)$$

where

$$F_m(\xi) = \frac{1}{m!} \left. \frac{\partial^m \phi(\xi, \delta; q)}{\partial q^m} \right|_{q=0}.$$

Differentiating equations (9.44) and (9.45)  $m$  times with respect to  $q$ , then setting  $q = 0$ , and finally dividing by  $m!$ , we obtain the  $m$ th-order deformation problem

$$\mathcal{L}_9[F_m(\xi) - \chi_m F_{m-1}(\xi)] = \hbar_9 \mathcal{R}_{9m}(\xi), \quad (m = 1, 2, 3, \dots), \quad (9.47)$$

$$F_m(0) = 0, \quad F'_m(0) = 0, \quad F'_m(+\infty) = 0, \quad (9.48)$$

where  $\mathcal{R}_{9m}$  is defined as

$$\mathcal{R}_{9m}(\xi) = F'''_{m-1} + \sum_{i=0}^{m-1} F_i F''_{m-i-1} - \alpha \sum_{i=0}^{m-1} F'_i F'_{m-i-1} + \alpha(1 - \chi_m),$$

with

$$\chi_m = \begin{cases} 0, & m \leq 1, \\ 1, & m > 1. \end{cases}$$

The general solution of Eq. (9.47) is

$$F_m(\xi) = \hat{F}_m(\xi) + D_1 + D_2 \xi + D_3 e^{-\delta \xi}, \quad (9.49)$$

where  $D_1$ ,  $D_2$  and  $D_3$  are constants and  $\hat{F}_m(\xi)$  is a particular solution of Eq. (9.47).

Using  $F'_m(+\infty) = 0$ , we have  $D_2 = 0$ . The unknowns  $D_1$  and  $D_3$  are governed by

$$\hat{F}'_m(0) + D_1 + D_3 = 0, \quad \hat{F}'_m(0) - \delta D_3 = 0.$$

In this way, we derive  $F_m(\xi)$  for  $m = 1, 2, 3, \dots$ , successively. At the  $M$ th-order approximation, we have the analytic solution of Eq.(9.24), namely

$$F(\xi) \approx \sum_{m=0}^M F_m(\xi). \quad (9.50)$$

The auxiliary parameter  $\hbar_g$  can be employed to adjust the convergence region of the series (9.50) in the homotopy analysis solution. By means of the so-called  $\hbar_g$ -curve, it is straightforward to choose an appropriate range for  $\hbar_g$  which ensures the convergence of the solution series.

## 9.4 Numerical results

We use the widely applied symbolic computation software "MATHEMATICA" to solve equations (9.47) and find that  $\varphi_n(\xi, \hbar, \delta)$  has the following structure:

$$\varphi_n(\xi, \hbar_g, \delta) = \sum_{k=0}^{m+1} \Psi_{m,k}(\xi, \hbar_g, \delta) \exp(-k\delta\xi), \quad m \geq 0,$$

where the function  $\Psi_{m,k}(\xi, \hbar_g, \delta)$  is defined by

$$\begin{aligned} \Psi_{0,0}(\xi, \hbar_g, \delta) &= b_{0,0}^0 + b_{0,0}^1 \xi, \\ \Psi_{0,1}(\xi, \hbar_g, \delta) &= b_{0,1}^0, \\ \Psi_{n,0}(\xi, \hbar_g, \delta) &= b_{n,0}^0, \quad n \geq 1, \\ \Psi_{n,k}(\xi, \hbar_g, \delta) &= \sum_{i=0}^{2(m+1-k)} b_{m,k}^i \xi^i, \quad m \geq 1, \quad 1 \leq k \leq m+1, \end{aligned}$$

and the related coefficients are

$$\begin{aligned}
b_{0,0}^0 &= a - \frac{1}{\delta}, \quad b_{0,0}^1 = 1, \quad b_{0,1}^0 = \frac{1}{\delta}, \\
b_{1,0}^0 &= \hbar_9 \left( \frac{-5}{4\delta^3} - \frac{7\alpha}{4\delta^3} - \frac{a}{\delta^2} + \frac{1}{\delta} \right), \\
b_{1,1}^0 &= \hbar_9 \left( \frac{3}{2\delta^3} + \frac{3\alpha}{2\delta^3} + \frac{a}{\delta^2} - \frac{1}{\delta} \right), \\
b_{1,1}^1 &= \hbar_9 \left( -1 + \frac{a}{\delta} + \frac{1}{\delta^2} + \frac{2\alpha}{\delta^2} \right), \\
b_{1,1}^2 &= \frac{\hbar_9}{2\delta}, \\
b_{1,2}^0 &= \hbar_9 \left( \frac{-1}{4\delta^3} + \frac{\alpha}{4\delta^3} \right),
\end{aligned}$$

and so on. Note that the infinite series (9.46) gives a family of explicit analytic solutions in two parameters  $\delta$  ( $\delta > 0$ ) and  $\hbar_9$  ( $\hbar_9 \neq 0$ ). Note that the HAM provides us with great freedom and large flexibility to select better values of  $\delta$  and  $\hbar_9$  so as to ensure that the related series (9.46) converges to  $F(\xi)$ . Certainly, if Eq. (9.46) converges, its second-order derivative with respect to  $\xi$  at  $\xi = 0$  say

$$\sum_{k=0}^{+\infty} \varphi_k''(0, \hbar_9, \delta) = \lim_{m \rightarrow +\infty} \left( \sigma_m = \sum_{k=0}^m \varphi_k''(0, \hbar_9, \delta) \right) \quad (9.51)$$

must converge too. We can see

$$\begin{aligned}
\sigma_1 &= a + (\delta - a)(1 + \hbar_9) - \frac{\hbar_9}{2\delta} - \frac{3\hbar_9\alpha}{2\delta}, \\
\sigma_2 &= a + (\delta - a)(1 + \hbar_9)^2 - \frac{5\hbar_9^2}{6\delta^3} - \frac{3\hbar_9^2\alpha}{\delta^3} - \frac{8\hbar_9^2\alpha^2}{3\delta^3} - \frac{a\hbar_9^2}{2\delta^2} - \frac{3a\hbar_9^2\alpha}{2\delta^2} - \frac{\hbar_9}{\delta} - \frac{3\hbar_9\alpha}{\delta}, \\
\sigma_3 &= a + (\delta - a)(1 + \hbar_9)^3 - \frac{275\hbar_9^3}{72\delta^5} - \frac{2303\hbar_9^3\alpha}{144\delta^5} - \frac{1549\hbar_9^3\alpha^2}{72\delta^5} - \frac{1417\hbar_9^3\alpha^3}{144\delta^5} \\
&\quad - \frac{5a\hbar_9^3}{2\delta^4} - \frac{9a\hbar_9^3\alpha}{\delta^4} - \frac{8a\hbar_9^3\alpha^2}{\delta^4} - \frac{5\hbar_9^2}{2\delta^3} + \frac{5\hbar_9^3}{6\delta^3} - \frac{9\hbar_9^2\alpha}{\delta^3} + \frac{3\hbar_9^3\alpha}{\delta^3} - \frac{8\hbar_9^2\alpha^2}{\delta^3} \\
&\quad - \frac{a^2\hbar_9^3}{2\delta^3} - \frac{3a^2\hbar_9^3\alpha}{2\delta^3} - \frac{3a\hbar_9^2}{2\delta^2} - \frac{9a\hbar_9^2\alpha}{2\delta^2} + \frac{8\hbar_9^3\alpha^2}{3\delta^3} - \frac{3\hbar_9}{2\delta} - \frac{9\hbar_9\alpha}{2\delta}.
\end{aligned}$$

Note that  $\sigma_m$  contains the term  $(\delta - a)(1 + \hbar_9)^m$ . Thus,  $\hbar_9$  must belong to a subset of the region  $|1 + \hbar| \leq 1$ . Note that in equations (9.44) and (9.45) we have defined  $\hbar_9 \neq 0$ . Our calculations

indicate that the series (9.51) converges if

$$-2 < \hbar < 0, \quad \delta \geq 2. \quad (9.52)$$

By means of the so-called  $\hbar$ -curve, it is straightforward to choose an appropriate range for  $\hbar_0$  which ensures the convergence of the solution series. Our solution series contain the auxiliary parameter  $\hbar_0$ . We can choose an appropriate value of  $\hbar_0$  to ensure that the solution series converge. We can investigate the influence of  $\hbar_0$  on the convergence of  $F''(0)$ , by plotting the curve of it versus  $\hbar_0$ , as shown in Figure 9.2 for some examples by  $\delta = 3$ .



Figure 9.3 shows the residual error of equation (9.24) for  $\xi = 0$  and  $\delta = 3$ . It can be found that the best value for  $\hbar_9$  is -0.475 when  $a = 0$ ,  $\alpha = 0.5$  and is -0.55 when  $a = 0.05$ ,  $\alpha = 0.25$ . Graphs of  $F(\xi)$ ,  $F'(\xi)$  and  $F''(\xi)$  for selected values of the parameters and  $\delta = 3$  are shown in Figures 9.4 and 9.5. The values of  $F''(0)$  obtained by HAM with minimum residual error of Eq. (9.24) with best value for  $\hbar_9$  are shown in Table 9.1 for  $\delta = 3$ . First column shows the value of  $F''(0)$  which obtained before by Anabtawi and Khuri with four terms of Adomian decomposition method [139]. Third column shows the same values which obtained by shooting method described in [141] and fourth column gives the values calculated by Crocco's transformation. The second column gives these values by numerical method employed in [140] for the Falkner-Skan equation. In this method, we obtain  $F''(0)$  by solving

$$\begin{aligned} \frac{dF}{d\xi} &= \eta_\infty U, \\ \frac{dU}{d\xi} &= \eta_\infty V, \\ \frac{dV}{d\xi} &= -\eta_\infty (FV + \alpha(1 - U^2)), \end{aligned}$$

subject to

$$F(0) = a, \quad U(0) = 0, \quad V(0) = \beta,$$

with Runge-Kutta method. Note that  $\beta$  and  $\eta_\infty$  are obtained by using the boundary conditions

$$\begin{aligned} U(1) &= 1, \\ V(1) &= 0, \end{aligned}$$

with nested secant iterative method. In this method, the last boundary condition is obtained by using the asymptotic condition  $F''(+\infty) = 0$ .

Table 9.1: Results for 20th-order of homotopy analysis method for  $\delta = 3$

| $a$   | $\alpha$ | ADM      | Asaithambi   | Shooting     | Crocco's  | HAM      | $\hbar_9$ |
|-------|----------|----------|--------------|--------------|-----------|----------|-----------|
|       |          | [139]    | Method [140] | Method [141] | Trans.    |          |           |
| 0     | 0.5      | 0.955076 | 0.92768      | 0.92772      | 0.89503   | 0.928403 | -0.475    |
| 0.05  | 0.25     | 0.849058 | 0.796295     | 0.7963       | 0.74422   | 0.796528 | -0.55     |
| 0.02  | 0.5      | 0.857887 | 0.97637      | 0.976375     | 0.9395875 | 0.976905 | -0.476    |
| 0.01  | 0.5      | 0.798723 | 0.939715     | 0.93972      | 0.90602   | 0.940406 | -0.4723   |
| -0.5  | 0.25     | 0.354134 | 0.269049     | 0.274784     | 0.306938  | 0.294572 | -0.51     |
| -0.25 | 0.5      | 0.491415 | 0.460428     | 0.461925     | 0.478145  | 0.485848 | -0.415    |
| -0.15 | 0.25     | 0.380547 | 0.409882     | 0.410658     | 0.420888  | 0.415261 | -0.5242   |

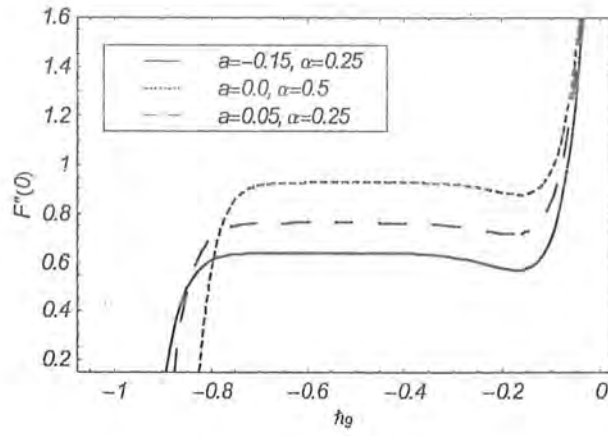


Figure 9.2: The curves of the  $F''(0)$  versus  $h_9$  for the 20th-order approximation.

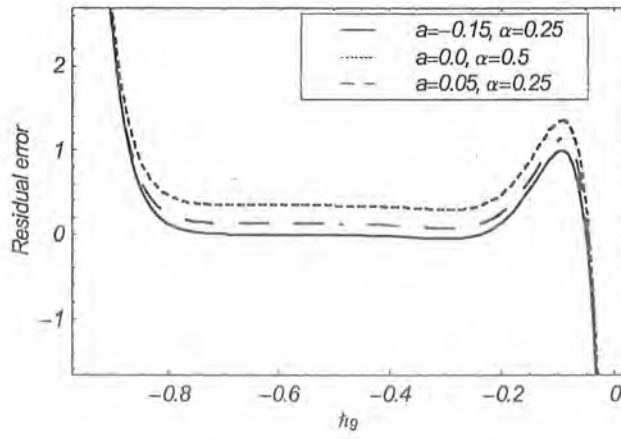


Figure 9.3: Residual error of Eq. (9.24) versus  $h_9$  for the 20th-order approximation.

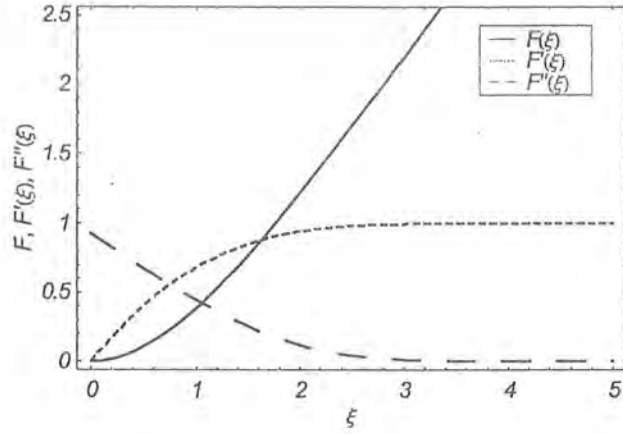


Figure 9.4: Plot of  $F(\xi)$ ,  $F'(\xi)$  and  $F''(\xi)$  for the 20th-order approximation when:  $a = 0$ ,  $\alpha = 0.5$ ,  $h_0 = -0.475$ .

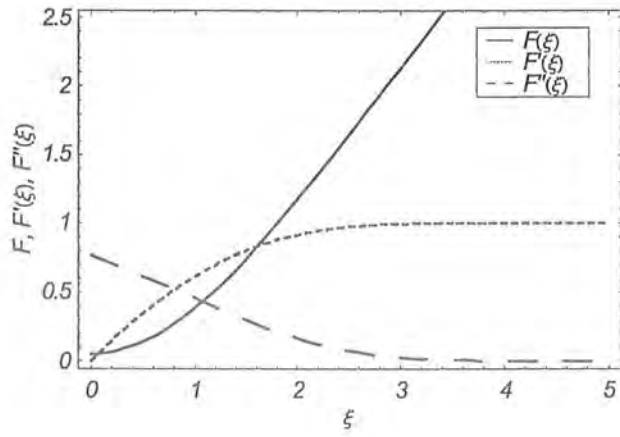


Figure 9.5: Plot of  $F(\xi)$ ,  $F'(\xi)$  and  $F''(\xi)$  for the 20th-order approximation when:  $a = 0.05$ ,  $\alpha = 0.25$ ,  $h_0 = -0.55$ .

# Bibliography

- [1] R. Berker, Hand book of fluid Dynamics, Springer, Berlin, 8 (1962)
- [2] R. Berker, Integration des equations mouvement d'un fluid visqueux incompressible, Hand book of fluid Dynamics, Springer, Berlin, 8 (1962) pp. 87.
- [3] T. N. G. Abbott and K. Walters, Rheometrical flow systems: part 2. Theory for the orthogonal rheometer including an exact solution of the Navier-Stokes equation, J. Fluid Mech. 40 (1970) 205-213.
- [4] H. K. Mohanty, Hydromagnetic flow between two rotating disks with non-coincident parallel axis of rotation, Phys. Fluids 15 (1972) 1456-1458.
- [5] J. Coirier, Rotations non-coaxiales d'un disque et d'un fluid a l' infini, J. Mec. 11 (1972) 317-340.
- [6] M. E. Erdogan, Flow due to eccentric rotating a porous disk and a fluid at infinity, ASME J. Appl. Mech. 43 (1976) 203-204.
- [7] M. E. Erdogan, Flow due to non-coaxially rotations of a porous disk and a fluid at infinity, Rev. Roum. Mec. Appl. 22 (1977) 171-178.
- [8] M. E. Erdogan, Non-Newtonian flow due to non-coaxially rotations of a disk and a fluid at infinity, Z. Angew. Math. Mech. 56 (1976) 141-146.
- [9] S. N. Murthy and R. K. P. Ram, MHD flow and heat transfer due to eccentric rotations of a porous disk and a fluid at infinity, Int. J. Eng. Sci. 16 (1978) 943-949.

- [10] K. R. Rajagopal, On the flow of a simple fluid in an orthogonal rheometer, *Arch. Rational Mech. Anal.* 79 (1982) 39-47.
- [11] R. J. Lingwood, Absolute instability of the Ekman layer and related rotating flows, *J. Fluid. Mech.* 331 (1997) 405-428.
- [12] K. R. Rajagopal, The flow of a second order fluid between rotating parallel plates. *J. Non-Newtonian Fluid Mech.* 9 (1981) 185-190.
- [13] R. Berker, A new solution of the Navier-Stokes equation for the motion of a fluid contained between two parallel plates rotating about the same axis, *Arch. Mech.* 31 (1979) 265-280.
- [14] R. Berker, An exact solution of the Navier-Stokes equation: The vortex with curvilinear axis, *Int. J. Eng. Sci.* 20 (1981) 217-230.
- [15] K. R. Rajagopal and A. S. Gupta, Flow and stability of a second grade fluid between two parallel plates rotating about non-coincident axis, *Int. J. Eng. Sci.* 19 (1981) 1401-1409.
- [16] A. R. Rao and S. R. Kasiviswanathan, A class of exact solutions for the flow of a micropolar fluid, *Int. J. Eng. Sci.* 25 (1987) 443-453.
- [17] K. R. Rajagopal, On an exact solution for the flow of an Oldroyd-B fluid, *Bull. Tech. Univ. Inst.* 49 (1996) 617-623.
- [18] D. G. Knight, Flow between eccentric disks rotating at different speeds: inertia effects, *ZAMP (J. Appl. Math. Phys.)* 31 (1980) 309-317.
- [19] C. Y. Lai and K. R. Rajagopal, Asymmetric flow between parallel rotating disks. *J. Fluid. Mech.* 146 (1984) 203-225.
- [20] S. V. Parter and K. R. Rajagopal, Swirling flow between rotating plates, *Arch. Rational Mech. Anal.* 86 (1984) 305-315.
- [21] A. R. Rao and S. R. Kasiviswanathan, On exact solutions of the unsteady Navier-Stokes equations- The vortex with curvilinear axis, *Int. J. Eng. Sci.* 25 (1987) 337-349.
- [22] S. H. Smith, Eccentric rotating flows: exact unsteady solutions of the Navier-Stokes equations. *ZAMP (J. Appl. Math. Phys.)* 38 (1987) 573-579.

- [23] A. R. Rao and S. R. Kasiviswanathan, An unsteady flow due to eccentrically rotating porous disk and a fluid at infinity, *Int. J. Eng. Sci.* 25 (1987) 1419-1425.
- [24] I. Pop, Unsteady flow due to non-coaxially rotating disk and fluid at infinity, *Bull. Tech. Univ. Inst.* 32 (1979) 14-18.
- [25] M. E. Erdogan, Unsteady viscous flow between eccentric rotating disks, *Int. J. Nonlinear. Mech.* 30 (1995) 711-717.
- [26] M. E. Erdogan, Unsteady viscous flow due to non-coaxial rotations of a disk and a fluid at infinity, *Int. J. Nonlinear. Mech.* 32 (1997) 285-290.
- [27] M. E. Erdogan, Unsteady flow between two eccentric rotating disks executing non-torsional oscillations, *Int. J. Nonlinear. Mech.* 35 (2000) 691-699.
- [28] M. E. Erdogan, Flow induced by non-coaxial rotation of a disk executing non-torsional oscillations and a fluid at infinity, *Int. J. Eng. Sci.* 38 (2000) 175-196.
- [29] T. Hayat, M. Zamurad, S. Asghar and A. M. Siddiqui, Magnetohydrodynamic flow due to non-coaxial rotations of a porous disk and a fluid at infinity, *Int. J. Eng. Sci.* 41 (2003) 1177-1196.
- [30] T. Hayat, T. Haroon, S. Asghar and A. M. Siddiqui, Unsteady MHD flow of a non-Newtonian fluid due to eccentric rotations of a porous disk and fluid at infinity, *Acta Mech.* 147 (2001) 99-109.
- [31] T. Hayat, R. Ellahi and S. Asghar, Unsteady periodic flows of a magnetohydrodynamic disk and a fluid at infinity, *Math. Comp. Modell.* 40 (2004) 173-179.
- [32] A. C. Srivastava, The effect of magnetic field on the flow between two non-parallel planes, *Quart. J. Math. Mech.* 14 (1961) 353-359.
- [33] R. K. Bhatnagar, Flow of visco-elastic Maxwell fluid between torsionally oscillating discs, *Proc. Indian Acad. Sci.* 58 (1967) 279-289.
- [34] M. Reiner, A mathematical theory of dilatancy, *Amer. J. Math.* 67 (1945) 350-354.

- [35] R. K. Bhatnagar and V. J. Zago, Numerical investigations of flow of a viscoelastic fluid between rotating coaxial disks, *Rheol. Acta.* 17 (1978) 557-569.
- [36] P. N. Kaloni and A. M. Siddiqui, A note on the flow of a viscoelastic fluid between eccentric disks, *J. Non-Newtonian Fluid Mech.* 26 (1987)125-133.
- [37] S. Dupont and M. Crochet, The vortex growth of a KBK-Z fluid in an abrupt correction, *J. Non-Newtonian Fluid Mech.* 29 (1988) 81-91.
- [38] K. R. Rajagopal and M. Renardy, Flow of viscoelastic fluids between plates rotating about different axis, *Rheol. Acta.* 25 (1986) 459-467.
- [39] K. Zhang and J. D. Goddard, Inertial and elastic effects in circular shear flow of viscoelastic fluids, *J. Non-Newtonian Fluid Mech.* 33 (1989) 233-255.
- [40] M. V. Bower and K. R. Rajagopal, Flow of KBK-Z fluids between parallel plates rotating about distinct axes: shear thinning and inertial effects, *J. Non-Newtonian Fluid Mech.* 22 (1987) 289-307.
- [41] K. R. Rajagopal and R. X. Dai, A numerical study of the flow of a K-BKZ fluid between plates rotating between non-coincident axes, *J. Non-Newtonian Fluid Mech.* 38 (1991) 289-312.
- [42] K. R. Rajagopal, Hydromagnetic flow between two porous disks rotating about non-coincident axes, *Bull. Tech. Univ. Inst.* 49 (1996) 617-623.
- [43] M. S. Gogus, The steady flow of a binary mixture between two rotating parallel non-coaxial disks, *Int. J. Eng. Sci.* 32 (1992) 665-677.
- [44] K. R. Rajagopal and A. Massoudi, Flow of granular materials between rotating disks, *Mech. Res. Commun.* 21(1994)629-634.
- [45] K. R. Rajagopal, Flow of electrorheological materials, *Acta Mech.* 91 (1992) 57-71.
- [46] A. S. Gupta, Magnetohydrodynamic Ekman layer, *Acta Mech.* 13 (1972) 155-160.
- [47] C. S. Erkman, Magnetohydrodynamic flow of a viscous incompressible fluid between rotating parallel plates, *Lett. Appl. Eng. Sci.* 3 (1975) 51-59.



- [48] A. R. Rao and P. R. Rao, MHD flow of a second grade fluid in an orthogonal rheometer, *Int. J. Eng. Sci.* 23 (1985) 1387-1395.
- [49] H. V. Ersoy, MHD flow of an Oldroyd-B fluid between eccentric rotating disks, *Int. J. Eng. Sci.* 37 (1999) 1973-1984.
- [50] S. R. Kasiviswanathan and M. V. Gandhi, A class of exact solutions for the magnetohydrodynamic flow of a micropolar fluid, *Int. J. Eng. Sci.* 30 (1992) 409-417.
- [51] T. Hayat, T. Haroon, A. M. Siddiqui and S. Asghar, MHD flow of a third grade fluid due to eccentric rotations of a porous disk and a fluid at infinity, *Int. J. Non-Linear Mech.* 38 (2003) 501-511.
- [52] H. V. Ersoy, Unsteady flow due to a sudden pull of eccentric rotating disks, *Int. J. Eng. Sci.* 39 (2001) 343-354.
- [53] K. R. Rajagopal, Flow of viscoelastic fluids between rotating disks, *Theor. Comput. Fluid Dynamics.* 3 (1992) 185-206.
- [54] K. R. Cramer and S. I. Pai, *Magneto fluid dynamics for engineers and applied physicists*, McGraw-Hill, New York, USA (1973).
- [55] A. G. Rao, Hydromagnetic flow and heat transfer in a saturated porous medium between two parallel porous wall in a rotating system, In proceedings of the eighth national heat and mass transfer conference, Assam, India; 1985.
- [56] P. C. Ram, Unsteady MHD free-convective flow through a porous medium with Hall currents, *Astrophys Space Sci.* 149 (1988) 171-174.
- [57] P. C. Ram, Hall effects on the hydromagnetic free convective flow and mass transfer through a porous medium bounded by an infinite vertical porous plate with constant heat flux, *Int. J. Energy Res.* 12 (1988) 227-231.
- [58] H. S. Takhar and P.C. Ram, Effects of Hall currents on hydromagnetic free convective flow through a porous medium, *Astrophys Space Sci. J.* 192 (1992) 45-51.

- [59] N. G. Kafoussias, MHD free convection flow through a nonhomogeneous porous medium over an isothermal cone surface, *Mech. Res. Commun.* 19 (1992) 89–94.
- [60] H. S. Takhar, P. C. Ram, E. J. D. Garba and J. K. Bitok, Hydromagnetic convective flow of heat generating fluid past a vertical plate with Hall currents and constant heat flux through a porous medium, *Magnetohydrodynamic Plasma Res. J.* 5 (1995) 185–195.
- [61] M. Ezzat and M. Zakaria, State space approach to viscoelastic fluid flow of hydromagnetic fluctuating boundary-layer through a porous medium, *Z. Angew. Math. Mech.* 3 (1997) 197–203.
- [62] M. H. Kamal, Unsteady MHD convection through porous medium with combined heat and mass transfer with heat source/sink, *Energy Convers Manage.* 42 (2001) 393–405.
- [63] D. V. Krishna, D. R. V. P. Rao and A. S. R. Murthy, Hydromagnetic convection flow through a porous medium in a rotating channel, *Inzhenerno-Fizicheskii Zhurnal* 75 (2002) 12–21.
- [64] M. Zakaria, Magnetohydrodynamic unsteady free convection flow of a couple stress fluid with one relaxation time through a porous medium, *Appl. Math. Comput.* 146 (2003) 469–494.
- [65] O. A. Bég, H. S. Takhar and A. K. Singh, Multi-parameter perturbation analysis of unsteady, oscillatory magnetoconvection in porous media with heat source effects, *Int. J. Fluid Mech. Res.* 32 (2005) 635–661.
- [66] S. M. M. El-Kabeir, A. M. Rashad and R. S. R. Gorla, Unsteady MHD combined convection over a moving vertical sheet in a fluid saturated porous medium with uniform surface heat flux, *Math. Comput. Model.* 46 (2007) 384–397.
- [67] M. F. El-Amin, Combined effect of viscous dissipation and Joule heating on MHD forced convection over a non-isothermal horizontal cylinder embedded in a fluid saturated porous medium, *J. Magn. Mater.* 263 (2003) 337–343.
- [68] C. H. Chen, Combined heat and mass transfer in MHD free convection from a vertical surface with Ohmic heating and viscous dissipation, *Int. J. Eng. Sci.* 42 (2004) 699–713.

- [69] V. M. Soundalgekar, N. V. Vighnesam and H. S. Takhar, Hall and ion-slip effects in the MHD Couette flow with heat transfer, *IEEE Trans. Plasma Sci.* 7 (1979) 178-182.
- [70] H. A. Attia, Unsteady Couette flow with heat transfer considering ion-slip, *Turkish J. Phys.* 29 (2005) 379-388.
- [71] O. A. Beg, J. Zueco and H. S. Takhar, Unsteady magnetohydrodynamic Hartman Couette flow and heat transfer in a Darcian channel with Hall current, viscous and Joule heating effects: Network numerical solutions. *Comm. Nonlinear Sci. Numer. Simul.* 14 (2009) 1082-1097.
- [72] V. M. Soundalgekar and A. G. Uplekar, Hall effect in MHD flow with Heat transfer, *IEEE Trans. Plasma Sci. PS.* 14 (1986) 579-583.
- [73] A. K. Singh and A. Raptis, Finite difference analysis of unsteady free convection flow through a porous medium, *Model. Simul. & control. B.* 8 (1987) 9-16.
- [74] A. Sherman and G. W. Sutton, *Engineering Magnetohydrodynamics*, McGraw-Hill, (1965) New York.
- [75] D. V. Krishna and D. R. V. P. Rao, Hall effects on the unsteady hydromagnetic boundary layer flow, *Acta Mech.* 31 (1981) 303-309.
- [76] T. Nagy and Z. Demendy, Effects of Hall currents and coriolis force on Hartman flow under general wall conditions, *Acta Mech.* 113 (1995) 77-91.
- [77] R. N. Ray and B. S. Mazumder, Hall effect on hydromagnetic falling liquid film, *Int. J. Non-Linear Mech.* 36 (2001) 1263-1267.
- [78] H. S. Takhar and A. J. Chamkha, MHD flow over a moving plate in a rotating fluid with magnetic field, Hall currents and free stream velocity, *Int. J. Eng. Sci.* 40 (2002) 1511-1527.
- [79] A. A. Megahed and A. Afify, Similarity analysis in MHD: Hall effects on free convection flow and mass transfer past a semi-infinite vertical flate plate, *Int. J. Non-Linear Mech.* 38 (2003) 513-520.

- [80] T. Hayat and S. Asghar, Effects of Hall current on unsteady flow of second grade fluid in a rotating system, *Chem. Eng. Comm.* 192 (2005) 1272-1284.
- [81] M. A. Sattar, Unsteady hydromagnetic free convection flow with Hall current mass transfer and variable suction through a porous medium near an infinite vertical porous plate with constant heat flux, *Int. J. Energy Res.* 18 (1994) 771-775.
- [82] T. Watanabe, Molten carbonate fuel cell stack performance with gas recycling, *Acta Mech.* 108 (1994) 35-47.
- [83] A. L. Aboul -Hassan and H. A. Attia, Flow due to a rotating disk with Hall effect, *Phys. Lett. A* 228 (1997) 286-290.
- [84] T. Hayat, Y. Wang and K. Hutter, Hall effects on the unsteady hydromagnetic oscillating flow of a second grade fluid, *Int. J. Nonlinear Mech.* 39 (2004)1027-1037.
- [85] S. Asghar, R. Mohyuddin and T. Hayat, Effects of Hall current and heat transfer on flow due to a pull of eccentric rotating disks, *Int. J. Heat Mass Trans.* 48 (2005) 599-607.
- [86] K. R. Rajagopal, On the boundary conditions for fluids of the differential type. In: A. Sequeira, Editor, *Navier-Stokes Equation and Related Non-linear Problems*, Plenum Press, New York. (1995) 273-278.
- [87] K. R. Rajagopal and A. S. Gupta , An exact solution for the flow of a non-Newtonian fluid past an infinite plate, *Meccanica* 19 (1984) 158-160.
- [88] K. R. Rajagopal and P. N. Kaloni , Some remarks on boundary conditions for fluids of differential type, In: G. A. C. Gram and S. K. Malik, Editors, *Continuum Mechanics and its Applications*, Hemisphere, Washington, DC (1989) 935-941.
- [89] R. L. Fosdick and B. Berstein , Non-uniqueness of second order fluid under steady radial flow in annuli, *Int. J. Eng. Sci.* 7 (1969)555-569.
- [90] K. R. Frater , On the solution of some boundary value problems arising in elastico-viscous fluid mechanics, *ZAMP* 21 (1970) 134-137.

- [91] T. W. Ting , Certain Unsteady flows of second-order fluids, *Arch. Ration. Mech. Anal.* 14 (1963) 1–26.
- [92] K. R. Rajagopal , A note on unsteady unidirectional flows of a non-Newtonian fluid, *Int. J. Non-Linear Mech.* 17 (1982) 169–173.
- [93] P. D. Ariel, Three dimensional stagnation point flow of a viscoelastic fluid, *Mech. Res. Commun.* 21 (1994) 389-396.
- [94] P. D. Ariel, Stagnation point flow of a viscoelastic fluid towards a moving plate, *Int. J. Eng. Sci.* 33(1995) 1679-1687.
- [95] P. D. Ariel, Axisymmetric flow of a second grade fluid past a stretching sheet, *Int. J. Eng. Sci.* 39 (2001) 529-553.
- [96] P. D. Ariel, Flow of a viscoelastic fluids through a porous channel, *Int. J. Num. Methods in Fluids.* 17(2005) 605-633.
- [97] M. E. Erdoğan and C. E. İmrak, On the steady flow of a second-grade fluid between two coaxial porous cylinders, *Math. Prob. Eng.* 2007 (2007) 42651-42662.
- [98] M. E. Erdoğan and C. E. İmrak, The effects of the side walls on the flow of a second grade fluid in ducts with suction and injection, *Int. J. Non-Linear Mech.* 42(2007) 765–772.
- [99] M. E. Erdoğan and C. E. İmrak, An exact solution of the governing equation of a fluid of second-grade for three-dimensional vortex flow, *Int. J. Eng. Sci.* 43(2005) 721–7295.
- [100] K. Vajravelu and S. J. Liao, A new method for homoclinic solutions in ordinary differential equations, *Chaos, Solutions and Fractals*, (in press).
- [101] K. Vajravelu and F. T. Akyildiz, Orthogonal cubic spline collocation method for the nonlinear parabolic equation arising in non-Newtonian fluid flow, 189 (2007) 462-471.
- [102] K. Vajravelu and F. T. Akyildiz, Diffusion of chemically reactive species in a porous medium over a stretching Sheet, *J. Math. Anal & Appl.* 320 (2006)322-339.
- [103] K. Vajravelu and F. T. Akyildiz, An exact solution for the second grade fluid between eccentric cylinders, *Int. J. Non-Linear Mech.* 39 (2004) 1571-1578.

- [104] C. Fetecau, T. Hayat, and C. Fetecau, Unsteady flow of a second grade fluid between two side walls perpendicular to a plate, *Nonlinear Anal. Ser. B: Real World Applications*.
- [105] C. Fetecau and C. Fetecau, Decay of potential vortex in a Maxwell fluid, *Int. J. Linear Mech.* 38 (2003) 985-990.
- [106] C. Fetecau and C. Fetecau, Starting solutions for the motion of a second grade fluid due to longitudinal and torsional oscillations of a circular cylinder, *Int. J. Eng. Sci.* 44. 788-796.
- [107] C. Fetecau and C. Fetecau, Starting solutions for some unsteady unidirectional flows of a second grade fluid, *Int. J. Eng. Sci.* 43. 781-789
- [108] C. Fetecau and C. Fetecau, A new solution for the flow of a Maxwell fluid, *Int. J. Non-Linear Mech.* 38 (2003) 427-431.
- [109] C. Fetecau and C. Fetecau, On the uniqueness of some helical flows of second grade fluid, *Acta Mech.* 57 (1985) 247-252.
- [110] T. Hayat and F. M. Mahomed, Note on an exact solution for the pipe flow of a third grade fluid, *Acta Mechanica.* 190 (2007) 233-236.
- [111] T. Hayat, M. Hussain and M. Khan, Effects of Hall current on flows of a Burgers' fluid through a porous medium, *Transport in porous media.* 68 (2007) 249-263.
- [112] T. Hayat, S. B. Khan, M. Sajid and S. Asghar, Rotating flow of a third grade fluid in a porous space with Hall current, *Nonlinear Dynamics.* 49 (2007) 83-91.
- [113] M. Khan, T. Hayat and M. Ayub, Numerical study of partial slip on the MHD flow of an Oldroyd 8-constant fluid, *Computers and Mathematics with applications.* 53 (2007) 1088-1097.
- [114] M. Khan, S. B. Khan and T. Hayat, Exact solution for the magnetohydrodynamic flows of an Oldroyd-B fluid through a porous medium, *J. Porous Media.* 10 (2007) 31-399.
- [115] T. Hayat, M. R. Mohyuddin and S. Asghar, Some inverse solutions for unsteady flows of a non-Newtonian fluid, *Tamsui Oxford J. Mathematics.* 21 (2005) 1-20.



- [116] T. Hayat, Oscillatory flow of a Johnson-Segalman fluid in a rotating system, *J. Appl. Math. Mech. (ZAMM)* 85 (2005) 449-456.
- [117] T. Hayat, M. R. Mohyuddin and S. Asghar, Note on non-Newtonian flow due to a variable shear stress, *Far East J. Appl. Maths.* 18 (2005) 313-321.
- [118] S. Asghar, M. Gulzar and T. Hayat, Rotating flow of a third grade fluid past a porous plate using homotopy analysis method, *Appl. Math. Computation.* 165(2005) 213-221.
- [119] T. Hayat, M. Hussain and M. Khan, Hall effect on flows of an Oldroyd-B fluid through porous medium for cylindrical geometries, *Computers and Mathematics with applications.* 52 (2006) 269-282.
- [120] T. Hayat, C. Fetecau and S. Asghar, Some simple flows of a Burgers' fluid, *Int. J. Eng. Sci.* 44 (2006) 1423-1431.
- [121] M. Sajid, T. Hayat and S. Asghar, On the analytic solution for steady flow of a fourth order fluid, *Phys. Lett. A* 355 (2006) 18-26.
- [122] S. Asghar, M. R. Mohyuddin, P. D. Ariel and T. Hayat, On Stokes' problem for the flow of a third grade fluid induced by a variable shear stress, *Can. J. Phys.* 84 (2006) 945-958.
- [123] T. Hayat, Exact solution to rotating flows of a Burgers' fluid, *Computers and Mathematics with applications.* 52 (2006) 1413-1424.
- [124] R. Hilfer, *Application of fractional calculus in physics.* World Scientific Press: Singapore (2000).
- [125] O. P. Agrawal, A general solution for a fourth-order fractional diffusion-wave equation defined in a bounded domain, *Comput. Struct.* 79 (2001) 1497-1501.
- [126] I. Podlubny, *Fractional differential equations.* Acad. Press: New York (1999).
- [127] T. Hayat, S. B. Khan and M. Khan, Exact solution for rotating flows of a generalized Burgers' fluid in a porous space, *Appl. Math. Modell.* 32 (2008) 749-760.

- [128] C. I. Chen, T. Hayat and J. L. Chen, Exact solutions for the unsteady flow of a Burgers' fluid in a duct induced by time-dependent prescribed volume flow rate, *Heat and Mass Trans.* 43 (2006) 85-90.
- [129] A. W. Sisko, The flow of lubricating greases, *Ind. Eng. Chem.* 50 (1958) 1789-1792.
- [130] M. Khan, Z. Abbas and T. Hayat, Analytic solution for flow of Sisko fluid through porous medium, *Transport in Porous Media.* 71 (2008) 23-37.
- [131] Y. Wang, T. Hayat and K. Hutter, Peristaltic flow of a Johnson-Segalman fluid in a deformable tube, *Theoretical and Computational Fluid Dynamics* 21 (2007) 369-380.
- [132] F. White, *Viscous fluid flow*, McGraw-Hill Book Company, New York, (1974) 173-183.
- [133] A. J. Chamkha, Hydromagnetic plane and axisymmetric flow near a stagnation point with heat generation, *Int. Comm. Heat Mass Transf.* 25 (1998) 269-278.
- [134] M. M. Abdelkhalek, Hydromagnetic stagnation point flow by a perturbation technique, *Comp. Mater. Sci.* 42 (2008) 497-503.
- [135] S. J. Liao, *Beyond perturbation: Introduction to the homotopy analysis method*. Boca Raton: Chapman & Hall/CRC Press; 2003.
- [136] A. Asaithambi, Numerical solution of the Falkner-Skan equation using piecewise linear function, *Applied Mathematics and Computation* 159 (2004) 267-273.
- [137] DO. Olagunju, A self-similar solution for forced convection boundary layer flow of a FENE-P fluid, *Appl. Math. Lett.* 19 (2006) 432-436.
- [138] TC. Chiam, Hydromagnetic flow over a surface stretching with a power-law velocity, *Int. J. Eng. Sci.* 33 (1995) 429-435.
- [139] M. Anabtawi, S. Khuri, On the generalized Falkner-Skan equation governing boundary layer flow of a FENE-P fluid, *Applied Mathematics Letters.* 20 (2006) 1211-1215.
- [140] N. S. Asaithambi, A numerical method for the solution of the Falkner-Skan equation, *Appl. Math. Comp.* 81 (1997) 259-264.



[141] T.Y. Na, Computational methods in engineering: Boundary value problems. Academic Press, New York, (1979).